frontiers | Research Topics

Advances in treatment planning, optimization and delivery for radiotherapy of breast cancer

Edited by
Nisha Ohri, Vishruta Dumane, Haibo Lin and Arpit Chhabra

Coordinated by
Jehee Isabelle Choi and Zahra Ghiassi-Nejad

Published in
Frontiers in Oncology

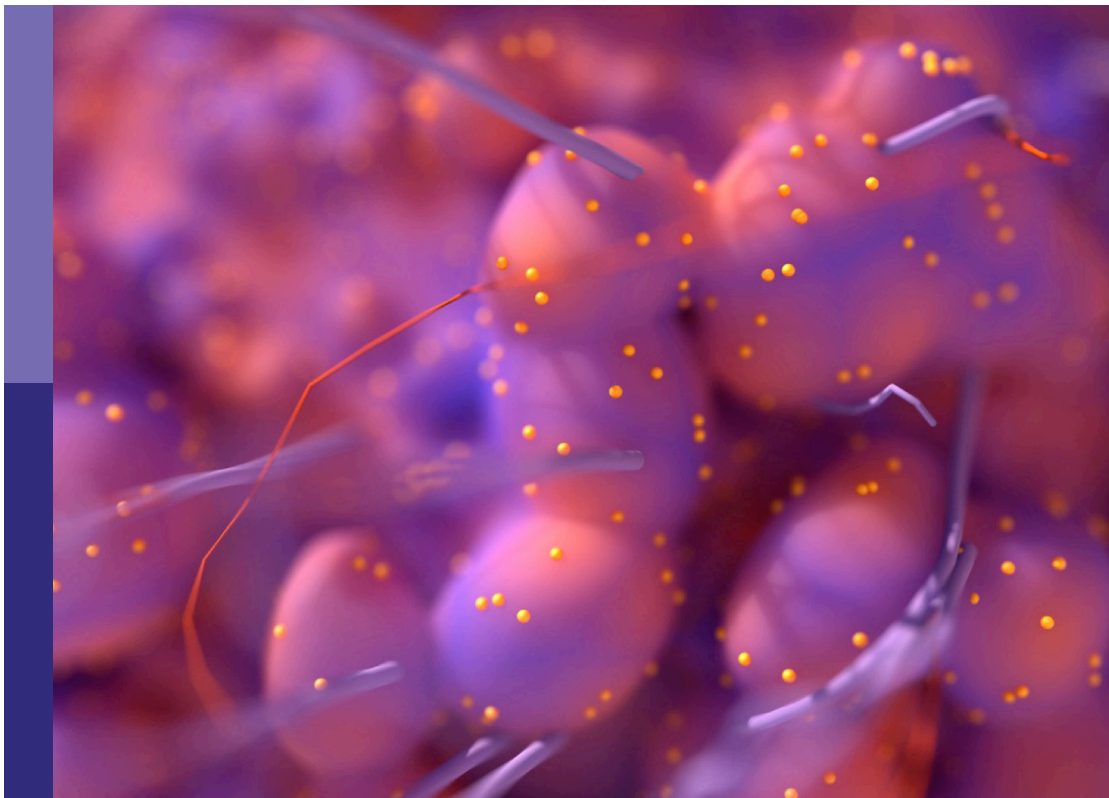

ISSN 1664-8714
ISBN 978-2-8325-4321-4
DOI 10.3389/978-2-8325-4321-4

About Frontiers

Frontiers is more than just an open access publisher of scholarly articles: it is a pioneering approach to the world of academia, radically improving the way scholarly research is managed. The grand vision of Frontiers is a world where all people have an equal opportunity to seek, share and generate knowledge. Frontiers provides immediate and permanent online open access to all its publications, but this alone is not enough to realize our grand goals.

Frontiers journal series

The Frontiers journal series is a multi-tier and interdisciplinary set of open-access, online journals, promising a paradigm shift from the current review, selection and dissemination processes in academic publishing. All Frontiers journals are driven by researchers for researchers; therefore, they constitute a service to the scholarly community. At the same time, the *Frontiers journal series* operates on a revolutionary invention, the tiered publishing system, initially addressing specific communities of scholars, and gradually climbing up to broader public understanding, thus serving the interests of the lay society, too.

Dedication to quality

Each Frontiers article is a landmark of the highest quality, thanks to genuinely collaborative interactions between authors and review editors, who include some of the world's best academicians. Research must be certified by peers before entering a stream of knowledge that may eventually reach the public - and shape society; therefore, Frontiers only applies the most rigorous and unbiased reviews. Frontiers revolutionizes research publishing by freely delivering the most outstanding research, evaluated with no bias from both the academic and social point of view. By applying the most advanced information technologies, Frontiers is catapulting scholarly publishing into a new generation.

What are Frontiers Research Topics?

Frontiers Research Topics are very popular trademarks of the *Frontiers journals series*: they are collections of at least ten articles, all centered on a particular subject. With their unique mix of varied contributions from Original Research to Review Articles, Frontiers Research Topics unify the most influential researchers, the latest key findings and historical advances in a hot research area.

Find out more on how to host your own Frontiers Research Topic or contribute to one as an author by contacting the Frontiers editorial office: frontiersin.org/about/contact

Advances in treatment planning, optimization and delivery for radiotherapy of breast cancer

Topic editors

Nisha Ohri — Rutgers, The State University of New Jersey, United States
Vishruta Dumane — Icahn School of Medicine at Mount Sinai, United States
Haibo Lin — New York Proton Center, United States
Arpit Chhabra — New York Proton Center, United States

Topic Coordinators

Jehee Isabelle Choi — Memorial Sloan Kettering Cancer Center, United States
Zahra Ghiassi-Nejad — Mount Sinai Hospital, United States

Citation

Ohri, N., Dumane, V., Lin, H., Chhabra, A., Choi, J. I., Ghiassi-Nejad, Z., eds. (2024). *Advances in treatment planning, optimization and delivery for radiotherapy of breast cancer*. Lausanne: Frontiers Media SA. doi: 10.3389/978-2-8325-4321-4

Table of contents

frontiers | Frontiers in Oncology

TYPE Editorial
PUBLISHED 08 January 2024
DOI 10.3389/fonc.2023.1354731

OPEN ACCESS

EDITED AND REVIEWED BY
Timothy James Kinsella,
Brown University, United States

*CORRESPONDENCE
Vishruta Dumane
vishruta.dumane@mountsinai.org

RECEIVED 12 December 2023
ACCEPTED 19 December 2023
PUBLISHED 08 January 2024

CITATION
Dumane V, Ohri N, Choi JI, Chhabra A and Lin H (2024) Editorial: Advances in treatment planning, optimization and delivery for radiotherapy of breast cancer.
Front. Oncol. 13:1354731.
doi: 10.3389/fonc.2023.1354731

Editorial: Advances in treatment planning, optimization and delivery for radiotherapy of breast cancer

Vishruta Dumane[1]*, Nisha Ohri[2], Jehee Isabelle Choi[3], Arpit Chhabra[3] and Haibo Lin[3]

[1]Department of Radiation Oncology, Icahn School of Medicine at Mount Sinai, New York, NY, United States, [2]Department of Radiation Oncology, Rutgers Cancer Institute of New Jersey, New Brunswick, NJ, United States, [3]Department of Radiation Oncology, New York Proton Center, New York, NY, United States

KEYWORDS

breast cancer, hypo-fractionation, partial breast irradiation, post-mastectomy radiation therapy, deep inspiration breath-hold, knowledge-based planning, volumetric modulated arc therapy, proton therapy

Editorial on the Research Topic
Advances in treatment planning, optimization and delivery for radiotherapy of breast cancer

Introduction

Various planning, optimization, delivery, and treatment modalities, as well as their fractionations, are constantly being investigated or updated to improve the therapeutic ratio for breast cancer patient care. Advanced treatment planning and delivery methods, such as volumetric modulated arc therapy (VMAT), have been applied in complex anatomical scenarios where standard 3D conformal planning techniques have failed (1). Although VMAT is useful in these situations, long-term follow-up data on toxicity due to low-dose exposure to VMAT is relatively scarce. Knowledge-based planning (KBP) has been applied to predict optimally achievable dose distributions in a given patient anatomy and to determine if a specific delivery technique is suitable for a patient, minimizing the likelihood of toxicity (2). Moderate hypofractionation decreases the logistic burden and cost to patients and healthcare systems, making it the standard of care for whole breast irradiation (WBI) (3–5). However, there is a paucity of data on toxicity when using moderate hypofractionation for regional nodal irradiation (RNI). Minimizing treatment volume from whole breast to partial breast irradiation (PBI), in appropriately selected patients, has further helped improve patient outcomes, thus supporting its use (6, 7). However, deploying PBI among a larger patient population that can benefit from it is an area of active investigation in the community. The dosimetric advantages of proton radiation for breast cancer are well established (8), and its use in the postmastectomy radiation therapy (PMRT) setting with either tissue expander or implant reconstruction is increasing. However, more data are needed when it comes to implant safety and toxicity

with proton therapy. The potential application of MR-guided radiation therapy (MRgRT) as a neoadjuvant therapy to shrink tumor volume has been discussed for PBI (9). An improved understanding of the quantification and dosimetric impact of the electron stream effect (ESE) will only help increase its use for WBI and PMRT with RNI while simultaneously improving tumor visualization. Our Research Topic titled "*Advances in Treatment Planning, Optimization, and Delivery for Radiotherapy of Breast Cancer*" is dedicated to featuring original research and review articles addressing some of these topics and the potential paucity of data in these areas.

Topics covered in this editorial

Knowledge-based planning, delivery, and dosimetry for breast cancer: Phurailatpam et al., Quesada et al., Li et al., Prunaretty et al., and Ramos-Mendez et al.

Hypofractionation and axillary nodal irradiation in breast cancer: Chitapanarux et al. and Elumalai et al.

Partial breast radiation: Le et al., Rhome et al., and Galavis et al.

Proton therapy for breast cancer: Chen et al. and Sayan et al.

MRI-guided radiotherapy for breast cancer: Lee et al.

Articles included in this Research Topic

Many patients in low- and middle-income countries (LMICs) present with locally advanced disease, requiring PMRT and RNI as part of their adjuvant treatment. Phurailatpam et al. designed an efficient workflow using VMAT and KBP for moderate and ultra-hypofractionation for these patients. The automated plans were less complex, improving the efficiency of treatment delivery and impacting the workflow in a busy clinic, thus amalgamating KBP in a decreasing treatment planning burden while planning for patients requiring RNI with hypofractionation.

The need to irradiate IMNs increases heart and lung exposure, and VMAT is known to reduce the dose for these while generating more conformal isodose distributions (1, 10). Quesada et al. addressed the feasibility of VMAT in the treatment of bilateral breast with regional nodes. They reported on long-term follow-up concerning the toxicity and safety of VMAT for the largest cohort of patients in this setting.

Deep inspiration breath-hold (DIBH) reduces the extent of low-dose exposure to normal tissue (10). Li et al. investigated tangent-based arcs to further improve dosimetry over partial VMAT using DIBH. This significantly reduced treatment time, making the treatment more clinically viable.

During treatment planning, factoring surrogates that are predictors of late toxicity is essential. Although such surrogates are reliable for cardiac toxicities in conventional planning, their understanding of advanced planning such as VMAT is scarce. Prunaretty et al. investigated this for left-sided breast cancer patients with unfavorable cardiac anatomy requiring IMRT/VMAT for improved sparing, and they concluded that a heart volume receiving dose ≥ 40 Gy is a better surrogate.

With the increasing use of tissue expanders in the postmastectomy setting, the safety and accuracy of dose calculation in these cases cannot be overemphasized. Ramos-Mendez et al. presented the first comprehensive evaluation of treatment planning strategies accounting for artifacts introduced by tissue expanders and verified it via Monte Carlo calculations, the collapsed cone dose calculation algorithm, and measurement with film. The highest discrepancies in the calculations in their study were noted when artifacts were assumed to have the dosimetric properties of water. These errors could be reduced if the tissue expander geometry and materials were used instead.

Patient eligibility to safely receive PBI is sensitive to when the CT scan is performed for treatment planning. Le et al. first reported the impact of factors other than time post-surgery on the healing of the cavity in the postoperative period, such as body mass index, receipt of neoadjuvant chemotherapy, hypertension, and patient positioning, serving as a reference for safe delivery of PBI.

Triple-negative breast cancer (TNBC) has inferior overall survival, disease-free survival, and local control. The use of PBI can potentially help reduce toxicity over WBI (current standard of care for TNBC) in the concurrent setting while improving logistics. Rhome et al. reported on the outcomes of patients with TNBC treated prospectively with post-lumpectomy PBI and concurrent chemotherapy compared with a matched WBI cohort. The promising results presented in this study are hypothesis generating for prospective clinical trials.

Galavis et al. discussed the PBI delivery technique and the current trends in research to help better define patient selection, treatment delivery, treatment planning dosimetry, and outcomes with respect to toxicity.

There is a relative paucity of data on toxicity profiles for patients receiving regional nodal irradiation (RNI) with hypofractionation and simultaneous integrated boost (SIB). Chitapanarux et al. reported acute toxicities with respect to skin and hematologic function for patients receiving hypofractionation prospectively with helical tomotherapy to the intact breast and regional lymph nodes after BCS and adjuvant chemotherapy. The results were acceptable in both endpoints.

With studies maturing on the use of hypofractionation in the RNI setting, Elumalai et al. presented the latest guidelines and evidence on the management of the axilla with surgery versus radiation.

Chen et al. presented a case study to show the dosimetric impact of a dislocated metallic port of a breast tissue expander while receiving proton therapy and its impact on cumulative dose due to its potential dislocations during treatment.

With the increasing use of proton therapy in post-mastectomy, more data are needed on its use in the reconstruction setting. Sayan et al. presented a retrospective comparison of acute toxicities and reconstructive complications in patients treated with proton-based and photon-based PMRT. They concluded that acute skin toxicity was the most frequent adverse event in PMRT for both modalities. Reconstructive complications were not significantly higher with proton therapy.

Lee et al. quantified the dosimetric impact of the electron stream effect (ESE) during 0.35T MRgRT, along with a discussion on how these excess doses due to ESE can be reduced and the implications for treatment planning after BCS or mastectomy.

Conclusions and future outlook

As results from randomized clinical trials such FABREC are being reported, while the RT CHARM is to arrive within the next year, there are likely to be more and more patients receiving RNI in the PMRT setting, increasing the likelihood of complex anatomies treated with hypofractionation. The need to meet coverage constraints, conformity, and homogeneity while sparing normal tissue from low doses will necessitate deploying these advanced planning, optimization, and delivery methods, such as VMAT and DIBH, while emphasizing new treatment modalities, such as protons. The SHARE trial being made available, which confirms the non-inferiority of APBI to WBI, will also encourage the increased use of the former in the treatment of select patients. With improved image guidance and real-time tumor visualization with MRgRT, the therapeutic ratio is likely to be further enhanced. We hope that through these diverse arrays of topics covering original research and review articles, we have addressed some of the scarcity in the data in a way that could potentially be supplementary and useful in further supporting the safe and efficacious use of these treatments and planning and delivery methods.

Author contributions

VD: Writing – original draft, Writing – review & editing. NO: Writing – review & editing. JC: Writing – review & editing. AC: Writing – review & editing. HL: Writing – review & editing.

Conflict of interest

The authors declare that the research was conducted in the absence of any commercial or financial relationships that could be construed as a potential conflict of interest.

Publisher's note

References

1. Kuo L, Ballangrud AM, Ho AY, Mechalakos JG, Li G, Hong L. A VMAT planning technique for locally advanced breast cancer patients with expander or implant reconstructions requiring comprehensive postmastectomy radiation therapy. *Med Dosim* (2019) 44:150–4. doi: 10.1016/j.meddos.2018.04.006

2. Rice A, Zoller I, Kocos K, Weller D, DiCostanzo D, Hunzeker A, et al. The implementation of RapidPlan in predicting deep inspiration breath-hold candidates with left-sided breast cancer. *Med Dosim* (2019) 44:210–8. doi: 10.1016/j.meddos.2018.06.007

3. Whelan TJ, Pignol JP, Levine MN, Julian JA, MacKenzie R, Parparia S, et al. Long-term results of hypofractionated radiation therapy for breast cancer. *N Engl J Med* (2010) 362:513–20. doi: 10.1056/NEJMoa0906260

4. Haviland JS, Owen JR, Dewar JA, Agrawal RK, Barrett J, Barrett-Lee PJ, et al. The UK standardization of breast radiotherapy (START) trials of radiotherapy hypofractionation for treatment of early breast cancer: 10-year follow-up results of two randomized controlled trials. *Lancet Oncol* (2013) 14:1086–94. doi: 10.1016/S1470-2045(13)70386-3

5. Smith BD, Bellon JR, Blitzblau R, Freedman G, Haffty B, Hahn C, et al. Radiation therapy for the whole breast: Executive summary of an American Society for Radiation Oncology (ASTRO) evidence-based guideline. *Pract Radiat Oncol* (2018) 8:145–52. doi: 10.1016/j.prro.2018.01.012

6. Coles CE, Griffin CL, Kirby AM, Titley J, Agrawal RK, Alhasso A, et al. Partial-breast radiotherapy after breast conservation surgery for patients with early breast cancer (UK IMPORT LOW trial): 5-year results from a multicenter, randomized, controlled, phase 3, non-inferiority trial. *Lancet* (2017) 390:1048–60. doi: 10.1016/S0140-6736(17)31145-5

7. Correa C, Harris EE, Leonardi MC, Smith BD, Taghian AG, Thompson AM, et al. Accelerated partial breast irradiation: Executive summary for update of an ASTRO evidence-based consensus statement. *Pract Radiat Oncol* (2017) 7:73–9. doi: 10.1016/j.prro.2016.09.007

8. Bekelman JE, Lu H, Pugh S, Baker K, Berg CD, Berrington de Gonzalez A, et al. Pragmatic randomized clinical trial of proton versus photon therapy for patients with non-metastatic breast cancer: the radiotherapy comparative effectiveness (RADCOMP) consortium trial protocol. *Br J Radiol* (2019) 9:1–10. doi: 10.1136/bmjopen-2018-025556

9. Koerkamp MLG, Vasmel JE, Russell NS, Shaitelman SF, Anandadas CN, Currey A, et al. Optimizing MR-guided radiotherapy for breast cancer patients. *Fron Oncol* (2020) 10:1107–20. doi: 10.3389/fonc.2020.01107

10. Dumane VA, Saksornchai K, Zhou Y, Hong L, Powell S, Ho AY. Reduction in low-dose to normal tissue with the addition of deep inspiration breath hold (DIBH) to volumetric modulated arc therapy (VMAT) in breast cancer patients with implant reconstruction receiving regional nodal irradiation. *Radiat Oncol* (2018) 13:187–94. doi: 10.1186/s13014-018-1132-9

frontiers | Frontiers in Oncology

TYPE Original Research
PUBLISHED 18 August 2022
DOI 10.3389/fonc.2022.967479

OPEN ACCESS

EDITED BY
Vishruta Dumane,
Icahn School of Medicine at Mount Sinai, United States

REVIEWED BY
Chenbin Liu,
Chinese Academy of Medical Sciences and Peking Union Medical College, China
Linda Rossi,
Erasmus Medical Center, Netherlands

*CORRESPONDENCE
Céline Bourgier
celine.bourgier@icm.unicancer.fr

SPECIALTY SECTION
This article was submitted to Radiation Oncology, a section of the journal Frontiers in Oncology

RECEIVED 12 June 2022
ACCEPTED 02 August 2022
PUBLISHED 18 August 2022

CITATION
Quesada S, Fenoglietto P, Gourgou S, Lemanski C, Draghici R, Ailleres N, Prunaretty J, Azria D and Bourgier C (2022) Efficacy, safety, and feasibility of volumetric modulated arc therapy for synchronous bilateral breast cancer management.
Front. Oncol. 12:967479.
doi: 10.3389/fonc.2022.967479

Efficacy, safety, and feasibility of volumetric modulated arc therapy for synchronous bilateral breast cancer management

Stanislas Quesada[1,2], Pascal Fenoglietto[2], Sophie Gourgou[3], Claire Lemanski[2], Roxana Draghici[2], Norbert Ailleres[2], Jessica Prunaretty[2], David Azria[1,2,3] and Céline Bourgier[1,2,3]*

[1]Faculty of Medicine, University of Montpellier, Montpellier, France, [2]Department of Radiation Oncology, Montpellier Cancer Institute (ICM), Montpellier, France, [3]Institute of Cancer Research of Montpellier (IRCM), Montpellier, France

Purpose: Volumetric Modulated Arc Therapy (VMAT) exhibits potent advantages regarding target volume coverage and protection of organs at risk, notably in the context of anatomical constraints. Nevertheless, reports concerning VMAT for the treatment of synchronous bilateral breast cancers (SBBC) have been scarce to date. As such, we conducted this observational study to assess efficacy, safety and feasibility of VMAT in SBBC.

Materials and Methods: From August 2011 to December 2017, 54 consecutive patients with SBBC with or without axillary nodes involvement underwent a treatment protocol containing radiotherapy using VMAT. A total dose (TD) of 52.2Gy in 29 fractions was delivered to breast and internal mammary chain (IMC) nodes Planning Target Volume (PTV) plus, if applicable, a TD of 49.3Gy in 29 fractions to the supra- and infra-clavicular nodes PTV and a TD of 63.22Gy in 29 fractions to tumor boost PTV. Lungs, heart, esophagus, trachea, liver, thyroid and spinal cord were considered as organs at risk. VMAT feasibility and organ at risk sparing were evaluated by treatments planning of the 20 first enrolled patients. Tolerance and patients' outcome were prospectively monitored by acute/late toxicities records and by the analysis of overall survival (OS), locoregional recurrence-free survival (LRFS) and recurrence-free survival (RFS).

Results: Breast, supraclavicular nodes and boost PTV coverage was adequate with at least 98% of PTV encompassed by more than 95% of the prescribed dose. Less than 90% of IMC PTV was encompassed by 95% of the prescribed dose. Mean lung dose was 12.3Gy (range: 7.7 – 18.7); mean heart dose was 10.7Gy (range: 6.2 – 22.3). Concerning acute toxicities, only 2 patients experienced grade 3 skin toxicity (3.7%) and only 1 patient developed grade 1 pneumonitis. After a median follow-up of 5.3 years, grade 2 fibrosis and/or shrinking was observed in 5 patients (10%), and grade 3 fibrosis in 1 patients

(2%). The 5-year LRFS-rate, RFS-rate and OS were 98% [95% CI= 86.12-99.70%], 96% [95% CI= 84.63-98.96%] and 100%, respectively.

KEYWORDS

bilateral breast cancer, radiotherapy, VMAT, treatment planning, cancer care, dosimetric analysis, treatment outcome

Introduction

Breast cancer (BC) is the most frequently diagnosed cancer worldwide (more than 2 million cases diagnosed in women worldwide in 2018), and also the most frequent cause of cancer-related death in women (1). Synchronous bilateral breast cancer (SBBC), defined as the presence of at least two malignant lesions occurring simultaneously in both breasts, accounts for ≈2% of all BC. Although SBBC represents only a small percentage of all BC, due to the high BC incidence, every year approximately 40,000 new cases of SBBC are detected (2). BC multimodal management includes surgery, systemic therapies, and radiation therapy (RT). RT is mandatory after breast-conserving surgery, and indicated after mastectomy in patients with locally advanced BC (3–5). However, currently, there is no specific recommendation for SBBC that is managed by following the guidelines for unilateral BC. In SBBC, Intensity Modulated Radiation Therapy (IMRT), either through fixed-field or preferably with volumetric modulated arc therapy (VMAT) represents a relevant alternative to 3D-conformal RT (6, 7). Indeed, VMAT has been shown to provide adequate target volume coverage while sparing the organs at risk (OAR) (8, 9). Some reports described the use of VMAT for SBBC and other complex situations (10–12). Nevertheless, only a few small retrospective cohorts (*i.e.* less than 25 patients) reported their experience on VMAT use in patients with SBBC (13–15). At our center, VMAT is used for the management of complex BC and for SBBC. The aim of this monocentric observational study was to assess the dosimetric feasibility, efficacy, safety and long-term outcome of VMAT for SBBC management.

Materials and methods

Patients and treatment protocol

From August 2011 to December 2017, all consecutive patients which received VMAT (Varian Medical systems, Palo Alto, USA) for SBBC at the Institut Regional du Cancer de (Montpellier, France) were included. During this period, VMAT and 3D RT were used in our center. VMAT was indicated over 3D because of node irradiation necessity and/or anatomical constraints (*e.g.*, *pectus excavatum*). This retrospective observational study was approved by the local Ethics Committee. The inclusion criteria were as follows: older than 18 years of age, Eastern Cooperative Oncology Group (ECOG) score ≤2, and histologically confirmed SBBC. Breast surgery (either mastectomy or breast conserving surgery), neoadjuvant or adjuvant chemotherapy, targeted therapies and endocrine therapies were delivered according to the clinical practice guidelines.

Radiation therapy process

Patient positioning/immobilization for VMAT, anatomy data acquisition, target volume definition, organs at risk evaluation, dose prescription, treatment planning and dosimetric analysis are reported in Supplementary Data. Treatment plans of the first 20 patients were used for dosimetric analysis (*i.e.*, dose volume distribution for breasts, nodes and organs at risk) as an evaluation of feasibility of VMAT for SBBC.

Radiation-related toxicities

Acute radiation-related toxicities were recorded every week during VMAT and late toxicities were recorded every 6 months after RT completion. Between end of VMAT and medical consultation at 6-month, supplementary medical evaluation was performed upon patient's request. Both acute and late toxicities were clinically assessed and graded according to the Common Terminology Criteria for Adverse Events (CTCAE) v4.0; respiratory, cardiac, esophageal and cutaneous toxicities were systematically evaluated. For each patient, the highest toxicity score reached was retained. Cardiac toxicity was defined as any cardiac event such as ischemia, arrhythmia or heart failure. Late cutaneous toxicities were subdivided according to the following subscales: fibrosis, hyperpigmentation, shrinking, telangiectasia and breast edema. Skin toxicities were evaluated both at patient and breast scales, as two distinct protocols (*i.e.*, surgery and radiation therapy) were possible for a given patient, with possible impacts on sequelae. Data on the patients' outcome and late toxicities were collected up to December 2020.

Statistical analysis

The median follow-up was estimated using the inverse Kaplan-Meier method. The Kaplan-Meier method was used for estimating recurrence-free survival (RFS: calculated from the beginning of treatment until recurrence or death), locoregional-free survival (LRFS: calculated from the beginning of treatment until locoregional recurrence or death), and overall survival (OS: calculated from the beginning of treatment until the date of death). For patients with metastatic SBBC at diagnosis, RFS corresponded to the progression-free survival (PFS). Data were analyzed both at the patient (n=54) and at the tumor (n=108) levels.

To identify predictive factors of skin toxicities (acute or late), patient and tumor characteristics [age, tumor stage (according to the TNM classification), Scaff-Bloom-Richardson (SBR) grade, hormonal receptor positivity, HER2 amplification, histology] and treatment characteristics [surgery (lumpectomy or mastectomy), systemic therapies, total irradiated volume, PTV, boost volume/PTV ratio] were analyzed. The Chi-square test was used to determine the correlation between categorical variables (or the Fisher's exact test if the expected frequencies were lower than 5). The Spearman's correlation test was used to assess the correlation between ordinal variables. The Wilcoxon test was used to study the correlation between nominal qualitative variables and continuous quantitative variables. Logistic regression was performed to identify factors related to skin toxicity; the p-values of the logistic regression were computed with the likelihood ratio test. Each Odd Ratio (OR) is presented with its 95% confidence interval (CI). For multivariate analysis, variables were selected using the backward method: variables with the largest p-value were removed one by one until only significant variables (at the 5% level) remained. All statistical tests were two-sided and the significance level was set at 5% ($p < 0.05$).

Results

Patients and treatment characteristics

From August 2011 to December 2017, 54 consecutive patients were prospectively enrolled and followed (median follow-up = 5.3 years [min-max=0.46-8.74]). Characteristics of patients/tumors and treatments provided are listed in Tables 1, 2, respectively. Briefly, 39 patients (72.1%) had early bilateral BC (EBC), 1 (1.8%) locally advanced bilateral BC (LABC), and 10 (18.5%) both LABC and EBC. Four patients (7.4%) had at least one metastasis at diagnosis. More than half of patients received neo-adjuvant or adjuvant chemotherapy.

Bilateral and unilateral breast conserving surgeries were performed in 43 and in 6 patients, respectively (n=92 breasts). Regarding treatment planning, 47 patients (n=83 breasts) received mammary gland irradiation with simultaneous integrated boost (SIB) in at least one breast, and 22 patients (n=32 breasts) received also regional node irradiation in at least one breast. The mean PTV was 945 cm^3 (range, 262 – 2421); when SIB was performed, the mean SIB/PTV_SIB ratio was 12% (range, 4 – 32).

The analysis of the first 20 treatment plans (Supplementary Data, Table 1) showed adequate PTV coverage: V95%=98.9% for both breast sides, and >98% for regional nodes (Supplementary Data, Figure 1). The mean lung doses were 12.0 Gy (left lung) and 12.7 Gy (right lung). The mean heart dose was 10.7 Gy for the entire cohort: 8.8Gy with only breast irradiation and 12.5Gy with associated IMC node irradiation (Supplementary Data, Figure 2).

Acute and late toxicities

Acute toxicities: 35 (64.8%) patients had grade 1-2 skin toxicities and only 2 patients had grade 3 skin toxicity (3.7%). One patient developed pneumonitis and none had cardiac or esophageal toxicity (Table 3). Regarding late toxicities, we did not observe non-cutaneous toxicities. Grade 0 and grade 1 cutaneous toxicities were observed in 28 and 16 patients (56% and 32%), respectively. Grade ≥2 toxicities concerned only skin (n=6 patients for any late skin toxicity; 12%) (Table 3). The main grade 3 toxicities were fibrosis and shrinking.

Both neoadjuvant and adjuvant chemotherapy protocols were not associated with higher risk of acute and late toxicities (p=NS). Univariate analyses showed that PTV volume was associated with grade ≥2 acute skin toxicities (OR 1.0015 [95% CI 1.001-1.002]; p-value <0.05). Multivariate analysis performed with surgery type, HER2 amplification, SBR grade, histology and PTV as variables confirmed the association between grade ≥2 acute skin toxicities and PTV (OR 1.01 [95% CI 1.001-1.02]; p-value <0.05) and HER2 amplification (OR 4.22 [95% CI 1.012-17.65]; p-value <0.05).

Similarly, univariate analysis showed a significate association between PTV and grade ≥2 late skin toxicities (OR 1.001 [95% CI 1.0002-1.003]; p-value <0.05). Multivariate analysis could not be performed because of the small number of patients with grade ≥2 late skin toxicity. By matching follow-up data, no significant association was found between acute and late skin toxicities (p-value = 0.12).

Outcomes and survival

When considering the cohort of patients in the curative setting (n=50), the median LRFS, RFS and OS were not reached at the endpoint date. The 5-year LRFS, RFS, and OS rates were 98% [95% CI 86.12-99.70%], 96% [95% CI 84.63-98.96%], and

TABLE 1 Characteristics of patients (n=54) and breast cancer lesions (n=108).

Age (years), median (range)	63 (35-82)
Histological type, breast cancer lesions' number (%)	
Invasive ductal carcinoma	79 (73.1%)
Invasive lobular carcinoma	11 (10.2%)
Other types	6 (5.6%)
In situ carcinoma	12 (11.1%)
Scarff-Bloom-Richardson grade, breast cancer lesions' number (%)	
I	27 (27.8%)
II	53 (54.6%)
III	17 (17.6%)
Missing	11
Hormone receptor expression, breast cancer lesions' number (%)	
Negative	7 (7.2%)
Positive	90 (92.8%)
Missing	11
HER2 amplification (breast cancer lesions' number, %)	
Negative	87 (89.7%)
Positive	10 (10.3%)
Missing	11
Pathological T stage (breast cancer lesions' number, %)	
pT0/ypT0	14 (13.2%)
pT1/ypT1	66 (62.3%)
pT2/ypT2	25 (18.9%)
pT3/ypT3	5 (4.7%)
pT4/ypT4	1 (0.9%)
Unknown	2
Pathological nodes status, breast cancer lesions' number (%)	
Negative (pN0/ypTN0)	75 (79.8%)
Positive (pN+/ypTN+)	19 (20.2%)
Unknown	14
Metastases at diagnosis, patients' number (%)	4 (7.4%)

100%, respectively (Figure 1). Two patients had disease recurrence: one developed pleural metastases and one nodal disease (one positive axillary node at 1 year after the initial treatment). The patient with nodal recurrence had multifocal right breast cancer (pT2N2M0) and underwent lumpectomy - axillary node dissection followed by adjuvant chemotherapy, VMAT (breast/SIB + regional lymph nodes), and hormone therapy. The nodal recurrence was managed by lymph node excision. These two local recurrences occurred outside the VMAT irradiation field, showing a good local control.

In the whole cohort (n=54), the median RFS and OS were not reached at the endpoint date. The 5-year RFS and OS rates were 88.5% [95% CI 76.12-94.66%] and 93.54% [95% CI 81.16%-97.89%], respectively (Supplementary Data, Figure 3). Noteworthy, metastatic progression occurred in four patients, of whom three already had metastases at diagnosis. Among these four metastatic patients, three died because of BC progression.

Discussion

To the best of our knowledge, this is the largest (n=54 patients) and longest study (median follow-up = 63 months) to evaluate VMAT efficiency and tolerance in patients with SBBC. This cohort included all consecutive patients, regardless of the presence of metastases, to reach a higher number of patients.

Firstly, our dosimetric data -performed on the 20 first patients included- confirmed that VMAT for SBBC is technically feasible, with at least 98% of PTV encompassed by more than 95% of the prescribed dose for breast, supraclavicular lymph nodes and boost PTV coverage, in agreement with the study by Nicolini et al. (7). Target volume coverage, planning objectives, and constraints differ among centers. In our study, target volumes were outlined according to the RTOG definition to use breast PTV-eval for the dosimetry study. This definition allows an inter-patient comparison of breast dose distribution regardless of the patients' anatomy. When locoregional lymph nodes were not irradiated, the lung volume encompassed by the isodoses 5Gy and 20Gy was lower in the study by Nicolini et al. than in our study (SBBC with locoregional lymph node irradiation): 58% versus 77-79% (V5Gy) and 9.7–10.3% versus 17-18% (V20Gy) and the mean heart dose was slightly higher in our study (8.8Gy *versus* 6.0Gy in the study by Nicolini et al.) (7). While mean heart dose is reported to be around 8 Gy with IMC irradiation for unilateral BC (*versus* 12.5Gy in our study), we obtained lower values than what described in the literature for similar patients with SBBC (16). This indicates that adequate target volume coverage is possible with reduced heart (10.7Gy in our study *versus* 16.5Gy in the study by Lee et al.) and lung exposure (V20Gy and V30Gy of 17% and 8-9% in our study *versus* 23% and 12% in the study by Lee et al.) (6).

Secondly, regarding safety, VMAT exhibits an interesting safety profile. Indeed, only two (3.7%) patients had acute grade 3 skin toxicity and only one patient (2%) developed late grade 3 skin toxicity (breast fibrosis). Although heart and lungs are exposed to non-negligible dose of radiation, we did not observe all along the follow-up (with a median of 63 months) any clinical cardiac, esophageal or respiratory consequences in our cohort, even in the context of IMC irradiation. Interestingly, grade ≥2 acute skin toxicity occurrence was associated with PTV (volume), in accordance with previous VMAT data in patients with unilateral BC (17, 18). However, compared with the study by Fiorentino et al. (n=16 patients and 24 months of follow-up) (13), we observed fewer acute grade 1 and 2 skin toxicities (33.3% and 31.5% in our study *versus* 72% and 24% in the study by Fiorentino et al.). Furthermore, Fiorentino *el at.* determined late lung toxicity (*i.e.* lung fibrosis) by CT imaging (allowing the detection of subclinical toxicity), but did not record any late cardiac toxicity event, at least clinically (14). We found an association between PTV and acute and late grade ≥2 skin

TABLE 2 Treatment characteristics of patients (n=54) and breast cancer lesions (n=108).

Primary surgery, breast cancer lesions' number (%)	
Breast conserving surgery	92 (85.2%)
Mastectomy	14 (13%)
No surgery	2 (1.8%)
Axillary lymph node staging	
Sentinel node biopsy	66 (61.1%)
Axillary node dissection	30 (27.8%)
None	12 (11.1%)
Radiotherapy radiation fields, breast number (%)	
Exclusive mammary gland	15 (13.9%)
Mammary gland and simultaneous integrated tumor boost (SIB)	83 (76.8%)
Regional lymph nodes	32 (29.6%)
Chest wall	10 (9.3%)
Irradiated volumes (cm^3), mean value (range)	
Planning Target Volume (PTV)	945 (262-2421)
SIB volume	113 (11-288)
SIB/PTV ratio in %	12 (4-32)
Total irradiated volume per patient (cm^3), mean value (range)	1880 (544-4811)
Neoadjuvant chemotherapy, patients' number (%)	
Yes	10 (18.5%)
No	44 (81.5%)
Adjuvant chemotherapy, patients' number (%)	
Yes	18 (33.4%)
No	36 (66.6%)
Post-radiotherapy systemic therapy patients' number (%)	
Endocrine therapy (tamoxifen and/or aromatase inhibitor)	51 (94.4%)
Trastuzumab	6 (11.2%)

toxicities, but the odds ratio values were close to 1, suggesting a low clinical significance. Regarding the higher risk of skin toxicity associated with HER-2 amplification, one of the hypotheses is the confounding effect of trastuzumab, which has been proposed to promote radiosensitization (19).

Thirdly, VMAT for SBBC exhibits relevant treatment efficiency. In patients with local/locoregional SBBC at diagnosis (n=50), the 5-year OS rate was 100%. Furthermore, although two recurrences were recorded, none was in the irradiation field, showing that multimodal treatment with VMAT allows complete local disease control, as reported by Fiorentino et al. (100% survival and 100% local disease control at 24 months of follow-up) (14). Interestingly, although IMC PTV coverage could appear as suboptimal, we did not observe any difference regarding PFS and OS in patients with and without IMC node irradiation. This is probably due to the CBCT-based repositioning of patients at each session. Furthermore, although the dose volume distribution profiles were different between patients with and without IMC node irradiation, PFS and OS were not different between these patients. While consistent with the literature, it is important to point out that the present study included 50 patients (*versus* 9 to 25 in previous studies) and had a longer follow-up (63 months *versus* 10 to 36 months in previous studies) (13–15).

The main limitation of our study is its monocentric design. However, as SBBC is a rare event and as dosimetric parameters, target volume coverage, planning objectives and constraints differ according to the center, this monocentric study allowed collecting homogeneous data and obtaining a more reliable analysis. Another limitation is its retrospective design; nevertheless, data were prospectively collected, thus reducing

TABLE 3 Acute and late radiation-related toxicities.

CTCAE grade		**Per patient (n=54), number (%)**				**Per breast (n=108), number (%)**			
		0	**1**	**2**	**3**	**0**	**1**	**2**	**3**
Acute toxicities	Skin	17 (31.5%)	18 (33.3%)	17 (31.5%)	2 (3.7%)	34 (31.5%)	36 (33.3%)	34 (31.5%)	4 (3.7%)
	Lung	53 (98.1%)	1 (1.9%)	–	–	na	na	na	na
	Esophagus	45 (83.3%)	6 (11.1%)	3 (5.6%)	–	na	na	na	na
	Heart	54 (100%)	–	–	–	na	na	na	na
Late Toxicities*	Skin	28 (56%)	16 (32%)	5 (10%)	1 (2%)	59 (59%)	31 (31%)	9 (9%)	1 (1%)
	Fibrosis	32 (64%)	2 (4%)	4 (8%)	1 (2%)	66 (66%)	26 (26%)	7 (7%)	1 (1%)
	Hyperpigmentation	48 (96%)	2 (4%)	–	–	94 (94%)	6 (6%)	–	–
	Shrinking	44 (88%)	2 (4%)	4 (8%)	–	91 (91%)	3 (3%)	6 (6%)	–
	Telangiectasia	49 (98%)	1 (2%)	–	–	99 (99%)	1 (1%)	–	–
	Breast edema	46 (92%)	4 (8%)	–	–	92 (92%)	8 (8%)	–	–
	Lung	50 (100%)	–	–	–	na	na	na	na
	Esophagus	50 (100%)	–	–	–	na	na	na	na
	Heart	50 (100%)	–	–	–	na	na	na	na

na, not applicable. *Late toxicities were performed on 50 patients and 100 breasts, as 4 patients died or were lost to follow-up within 6 months after radiation therapy protocol.

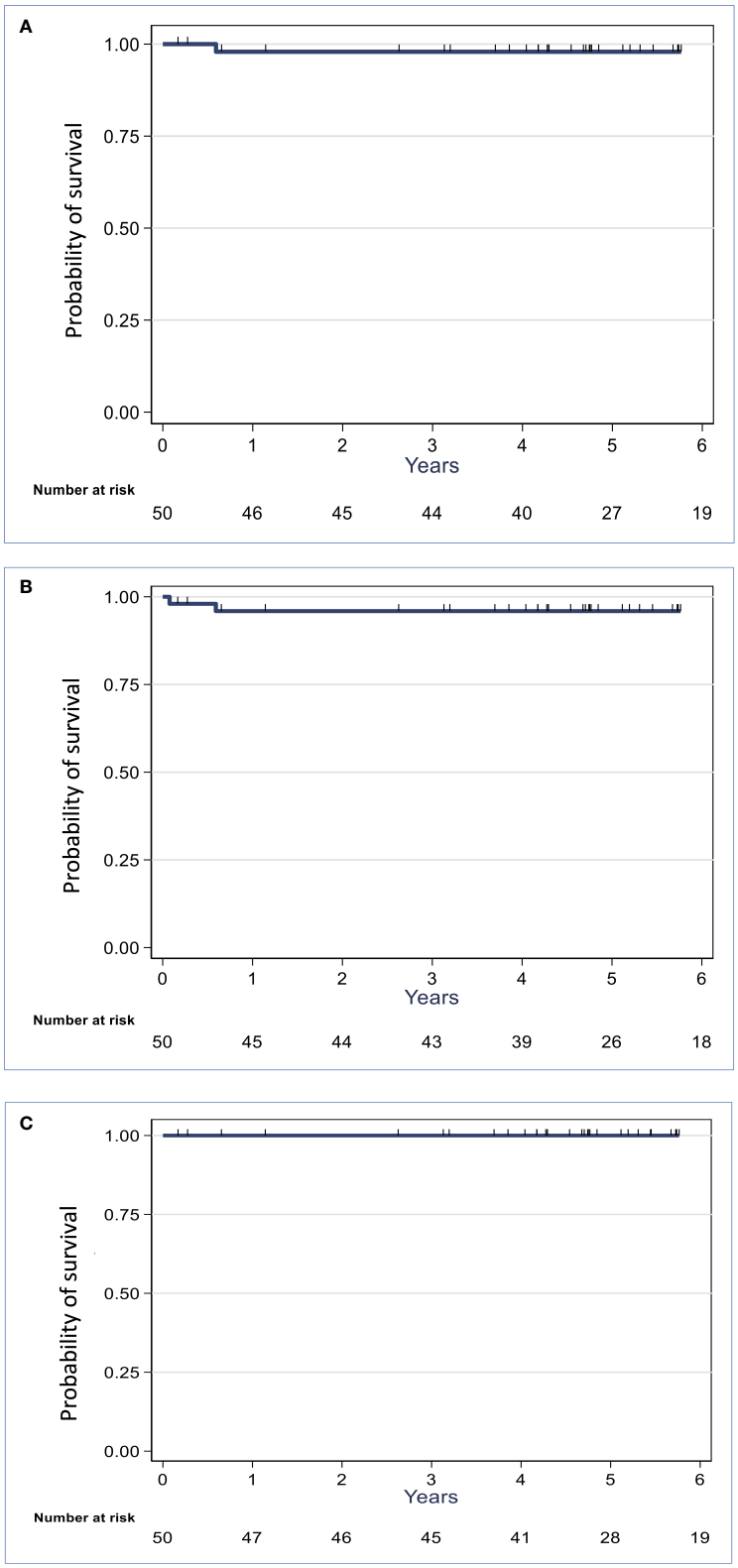

FIGURE 1
Kaplan-Meier locoregional-free **(A)**, recurrence-free **(B)** and overall **(C)** survival curves for the patients with initially non-metastatic synchronous bilateral breast cancer (n=50).

the putative bias. On the other hand, SBBC rarity and the relatively large cohort of patients allow considering the findings of some value.

In conclusion, this study confirmed that VMAT for SBBC is technically feasible and exhibits an interesting efficiency/tolerance profile. Furthermore, the large size of our cohort and the longer follow-up compared to previous studies allowed showing that VMAT has favorable safety and efficiency profiles, and thus is suitable for SBBC management.

Data availability statement

The raw data supporting the conclusions of this article will be made available by the authors, without undue reservation.

Ethics statement

The studies involving human participants were reviewed and approved by Institut régional du Cancer de Montpellier local Ethics Committee. Written informed consent for participation was not required for this study in accordance with the national legislation and the institutional requirements.

Author contributions

All the authors were involved in the conception/design of the work and provide approval for publication of the content more specifically. SQ, PF and CB contributed to drafting the work. All authors contributed to the article and approved the submitted version.

Funding

Institut régional du Cancer de Montpellier, France.

Acknowledgments

The authors thank Elisabetta Andermarcher for English editing and Océane Massot for assistance in statistical programming.

Conflict of interest

The authors declare that the research was conducted in the absence of any commercial or financial relationships that could be construed as a potential conflict of interest.

Publisher's note

All claims expressed in this article are solely those of the authors and do not necessarily represent those of their affiliated organizations, or those of the publisher, the editors and the reviewers. Any product that may be evaluated in this article, or claim that may be made by its manufacturer, is not guaranteed or endorsed by the publisher.

Supplementary material

The Supplementary Material for this article can be found online at: https://www.frontiersin.org/articles/10.3389/fonc.2022.967479/full#supplementary-material

References

1. Sung H, Ferlay J, Siegel RL, Laversanne M, Soerjomataram I, Jemal A, et al. Global cancer statistics 2020: GLOBOCAN estimates of incidence and mortality worldwide for 36 cancers in 185 countries. *CA A Cancer J Clin* (2021) 71:209–49. doi: 10.3322/caac.21660

2. Kheirelseid EAH, Jumustafa H, Miller N, Curran C, Sweeney K, Malone C, et al. Bilateral breast cancer: analysis of incidence, outcome, survival and disease characteristics. *Breast Cancer Res Treat* (2011) 126:131–40. doi: 10.1007/s10549-010-1057-y

3. Haussmann J, Corradini S, Nestle-Kraemling C, Bölke E, Njanang FJD, Tamaskovics B, et al. Recent advances in radiotherapy of breast cancer. *Radiat Oncol* (2020) 15:71. doi: 10.1186/s13014-020-01501-x

4. Early Breast Cancer Trialists' Collaborative Group (EBCTCG). Effect of radiotherapy after breast-conserving surgery on 10-year recurrence and 15-year breast cancer death: meta-analysis of individual patient data for 10 801 women in 17 randomised trials. *Lancet* (2011) 378:1707–16. doi: 10.1016/S0140-6736(11)61629-2

5. van Maaren MC, de Munck L, de Bock GH, Jobsen JJ, van Dalen T, Linn SC, et al. 10 year survival after breast-conserving surgery plus radiotherapy compared with mastectomy in early breast cancer in the Netherlands: a population-based study. *Lancet Oncol* (2016) 17:1158–70. doi: 10.1016/S1470-2045(16)30067-5

6. Lee T-F, Ting H-M, Chao P-J, Wang H-Y, Shieh C-S, Horng M-F, et al. Dosimetric advantages of generalised equivalent uniform dose-based optimisation on dose-volume objectives in intensity-modulated radiotherapy planning for bilateral breast cancer. *Br J Radiol* (2012) 85:1499–506. doi: 10.1259/bjr/24112047

7. Nicolini G, Clivio A, Fogliata A, Vanetti E, Cozzi L. Simultaneous integrated boost radiotherapy for bilateral breast: a treatment planning and dosimetric comparison for volumetric modulated arc and fixed field intensity modulated therapy. *Radiat Oncol* (2009) 4:27. doi: 10.1186/1748-717X-4-27

8. Kim SJ, Lee MJ, Youn SM. Radiation therapy of synchronous bilateral breast carcinoma (SBBC) using multiple techniques. *Med Dosim* (2018) 43:55–68. doi: 10.1016/j.meddos.2017.08.003

9. Cheng H-W, Chang C-C, Shiau A-C, Wang M-H, Tsai J-T. Dosimetric comparison of helical tomotherapy, volumetric-modulated arc therapy, intensity-modulated radiotherapy, and field-in-field technique for synchronous bilateral breast cancer. *Med Dosim* (2020) 45:271–7. doi: 10.1016/j.meddos.2020.01.006

10. Seppälä J, Heikkilä J, Myllyoja K, Koskela K. Volumetric modulated arc therapy for synchronous bilateral whole breast irradiation - a case study. *Rep Pract Oncol Radiother* (2015) 20:398–402. doi: 10.1016/j.rpor.2015.05.011

11. Scorsetti M, Alongi F, Fogliata A, Pentimalli S, Navarria P, Lobefalo F, et al. Phase I-II study of hypofractionated simultaneous integrated boost using volumetric modulated arc therapy for adjuvant radiation therapy in breast

cancer patients: a report of feasibility and early toxicity results in the first 50 treatments. *Radiat Oncol* (2012) 7:145. doi: 10.1186/1748-717X-7-145

12. Cendales R, Schiappacasse L, Schnitman F, García G, Marsiglia H. Helical tomotherapy in patients with breast cancer and complex treatment volumes. *Clin Transl Oncol* (2011) 13:268–74. doi: 10.1007/s12094-011-0652-7

13. Kaidar-Person O, Kostich M, Zagar TM, Jones E, Gupta G, Mavroidis P, et al. Helical tomotherapy for bilateral breast cancer: Clinical experience. *Breast* (2016) 28:79–83. doi: 10.1016/j.breast.2016.05.004

14. Fiorentino A, Mazzola R, Naccarato S, Giaj-Levra N, Fersino S, Sicignano G, et al. Synchronous bilateral breast cancer irradiation: clinical and dosimetrical issues using volumetric modulated arc therapy and simultaneous integrated boost. *Radiol Med* (2017) 122:464–71. doi: 10.1007/s11547-017-0741-y

15. Valli M, Cima S, Gaudino D, Cartolari R, Deantonio L, Frapolli M, et al. Skin and lung toxicity in synchronous bilateral breast cancer treated with volumetric-modulated arc radiotherapy: a mono-institutional experience. *Clin Transl Oncol* (2019) 21:1492–8. doi: 10.1007/s12094-019-02077-z

16. Taylor CW, Wang Z, Macaulay E, Jagsi R, Duane F, Darby SC. Exposure of the heart in breast cancer radiation therapy: A systematic review of heart doses published during 2003 to 2013. *Int J Radiat Oncol Biol Phys* (2015) 93:845–53. doi: 10.1016/j.ijrobp.2015.07.2292

17. Pasquier D, Bataille B, Le Tinier F, Bennadji R, Langin H, Escande A, et al. Correlation between toxicity and dosimetric parameters for adjuvant intensity modulated radiation therapy of breast cancer: a prospective study. *Sci Rep* (2021) 11:3626. doi: 10.1038/s41598-021-83159-3

18. Freedman GM, Anderson PR, Li J, Eisenberg DF, Hanlon AL, Wang L, et al. Intensity modulated radiation therapy (IMRT) decreases acute skin toxicity for women receiving radiation for breast cancer. *Am J Clin Oncol* (2006) 29:66–70. doi: 10.1097/01.coc.0000197661.09628.03

19. Horton JK, Halle J, Ferraro M, Carey L, Moore DT, Ollila D, et al. Radiosensitization of chemotherapy-refractory, locally advanced or locally recurrent breast cancer with trastuzumab: a phase II trial. *Int J Radiat Oncol Biol Phys* (2010) 76:998–1004. doi: 10.1016/j.ijrobp.2009.03.027

frontiers | Frontiers in Oncology

TYPE Review
PUBLISHED 10 November 2022
DOI 10.3389/fonc.2022.1049704

OPEN ACCESS

EDITED BY
Vishruta Dumane,
Icahn School of Medicine at Mount Sinai, United States

REVIEWED BY
Kathryn Huber,
Tufts University, United States
Christin A. Knowlton,
Yale University, United States

*CORRESPONDENCE
Naamit K. Gerber
naamit.gerber@nyulangone.org

†These authors have contributed equally to this work and share first authorship

SPECIALTY SECTION
This article was submitted to Radiation Oncology, a section of the journal Frontiers in Oncology

RECEIVED 20 September 2022
ACCEPTED 25 October 2022
PUBLISHED 10 November 2022

CITATION
Galavis PE, Abeloos CH, Cheng PC, Hitchen C, McCarthy A, Purswani JM, Shah B, Taneja S and Gerber NK (2022) Accelerated partial breast irradiation in early stage breast cancer. *Front. Oncol.* 12:1049704. doi: 10.3389/fonc.2022.1049704

Accelerated partial breast irradiation in early stage breast cancer

Paulina E. Galavis†, Camille Hardy Abeloos†, Pine C. Cheng, Christine Hitchen, Allison McCarthy, Juhi M. Purswani, Bhartesh Shah, Sameer Taneja and Naamit K. Gerber*

Department of Radiation Oncology, New York University (NYU) Langone Health, School of Medicine, New York, NY, United States

Accelerated partial breast irradiation (APBI) is increasingly used to treat select patients with early stage breast cancer. However, radiation technique, dose and fractionation as well as eligibility criteria differ between studies. This has led to controversy surrounding appropriate patients for APBI and an assessment of the toxicity and cosmetic outcomes of APBI as compared to whole breast irradiation (WBI). This paper reviews existing data for APBI, APBI delivery at our institution, and ongoing research to better define patient selection, treatment delivery, dosimetric considerations and toxicity outcomes.

KEYWORDS

early stage breast cancer, accelerated partial breast irradiation, dosimetric considerations, treatment planning, toxicity outcomes

Introduction

Breast cancer is the most common cancer in American women with more than 250,000 invasive breast cancer diagnosed in the United States in 2021 (1). Since 2007, breast cancer mortality rates have continued to decrease in women over 50 years old with more than 3.8 million survivors in the United States (1). Standard of care for patients with early stage breast cancer after breast conserving surgery is radiation and endocrine therapy. As patients with breast cancer live longer, it is increasingly important to improve radiation delivery in order to minimize radiation sequelae.

Accelerated partial breast irradiation (APBI) focuses higher doses of radiation during a shorter time interval to the lumpectomy cavity rather than the whole breast. Different radiation techniques have been studied in phase III trials including multicatheter interstitial brachytherapy, balloon catheter intracavitary brachytherapy, external beam radiation therapy and intra-operative radiation therapy (2–5). Table 1 summarizes these key trials (2–5, 7–14).

10.3389/fonc.2022.1049704

TABLE 1 Summary of key APBI trials.

Study	Years of enrollment	No patients/ FU	Eligibility invasive	Eligibility DCIS	Dose Fractionation	IBTR	Toxicity
Hungary Polgar 2013 (3)	1998-2004	*N* = 258 10.2 yrs	pT1 (≤ 2), pN0–1mi, negative margins, age >40	Excluded	36.4 Gy/7 fx (brachytherapy) or 50 Gy/25 fx (electrons) vs 50 Gy/25 fx WBI	5.9% vs. 5.1%	PBI had higher excellent-good cosmetic score (81% vs. 63%)
Barcelona Rodriguez 2013 (4)		*N* = 102 5.0 yrs	pT1–2 (≤3 cm), pN0, margins ≥ 2 mm, age ≥ 60	Excluded	37.5 Gy/10 fx vs 48 Gy/24 fx WBI	0% Vs 0%	No difference in late skin toxicity or cosmesis
GEC-ESTRO Strnad 2016 (6)	2004-2009	*N* = 1,184 6.6 yrs	pT1–2 (<3 cm), pN0–1mi, margins ≥ 2 mm, age ≥ 40	Included with margin pure DCIS ≱ 5 mm	32 Gy/8 fx or 30.2 Gy/7 fx (HDR) or 50 Gy (PDR) Vs 50 Gy/25 fx WBI	1.4 vs. 0.9%	Reduced breast pain, less late grade 2–3 skin toxicity in APBI arm
IMPORT LOW Coles 2017 (7)	2007-2016	*N* = 2,018 6.0 yrs	pT1-2 (<3 cm), N0–1, margins ≥ 2 mm, age ≥ 50	Excluded	40 Gy/15 fx WBRT vs. 36 Gy WBRT+40 Gy APBI vs. 40 Gy/15 APBI	1.1% vs. 0.2% vs. 0.5%	Reduced toxicity in both experimental arms
NSABP B-39 Vicini 2019 (5)	2005-2018	*N* = 4,216 10.2 yrs	pT1–2 (<3 cm), pN0–1 (1-3), negative margins, age ≥ 18	Included	38.5 Gy/10 fx BID (3D), 34 Gy/10 fx BID (brachy) Vs 50 Gy/25 fx WBI	3.9% vs. 4.6%	APBI: grade 3: 10%, no grade 4–5 WBI: grade 3: 7%, no grade 4 or 5
RAPID Whelan 2019 (8)	2006-2018	*N* = 2,135 8.6 yrs	pT1–2 (≤ 2 cm), pN0-1mic, negative margins, age ≥ 40	Included	38.5 Gy/10 fx BID Vs 50 Gy/25 fx WBI	3% vs. 2.8%	Reduced acute and more late toxicity (grade 2+), similar patient rated cosmetic outcome in APBI arm
Florence Meattini 2020 (9)	2005-2013	N = 520 10.7 yrs	pT1–2 (< 2.5 cm), negative margins, age > 40	extensive DCIS excluded	30 Gy/5 fx QOD Vs 50 Gy/25 fx WBI	2.5% vs. 3.7%	Reduced acute and late toxicity and improved patient and physician rated cosmetic outcome in APBI arm
ELIOT Veronesi 2013 (10) Orecchia 2021 (11)	2000-2007	N = 1305 12.4 yrs	Age 48–75, pT1-2 (≤2.5 cm)	Excluded	21 Gy/1 fx IORT (prescribed to 90% IDL using 3–12 MeV electrons) Vs 50 Gy/25 fx WBI	11% Vs 2%	Reduced acute skin toxicity in IORT arm
TARGIT-A Vaidya 2020 (12)	2000-2012	N = 2298 5 yrs	Age ≥45, ≤3.5 cm, cN0-N1,	Included	20 Gy/1 fx IORT (o cavity surface (~5–7 Gy at 1 cm) with 50 kV photons) Vs WBI 3-6 weeks	2.1% Vs 0.95%	Reduced radiotherapy toxicity in IORT arm
ASTRO guidelines 2017 (13, 14)			pT1 (≤ 2 cm), pN0–1mi, margins ≥ 2 mm, age ≥ 50	screen-detected, 1-2 nuclear grade, ≤ 2.5 cm size, margins ≥ 3 mm			

NSABP B-39/RTOG 0413 is the largest prospective randomized trial completed to date, with over 4,300 patients with stage 0–II (≤3 cm) breast cancer or ductal carcinoma *in situ* (DCIS) status post lumpectomy with negative margins and 0–3 positive lymph nodes randomized to whole breast irradiation (WBI) (50 Gy with optional 10 Gy tumor bed boost) vs. APBI *via* either multicatheter brachytherapy (34 Gy in 10 fractions BID), intracavity brachytherapy (MammoSite 34 Gy in10 fractions BID), or 3D conformal radiation (3D-CRT) (38.5 Gy in10 fractions BID) (5). The 10-year cumulative incidence of in

breast tumor recurrence (IBTR) was 4·6% (95% CI 3·7-5·7) in the APBI group versus 3·9% (3·1-5·0) in the WBI group. While APBI did not meet the criteria for equivalence to WBI, the absolute difference in IBTR was < 1%. Furthermore, the trial had broad eligibility criteria with a heterogeneous pool of patients and APBI techniques and was not designed to test equivalence in patient subgroups or outcomes from different APBI techniques.

The GEC-ESTRO trial randomized 1,184 patients to interstitial brachytherapy (32 Gy in 8 fractions or 30.2 Gy in 7 fractions) or WBI (50 Gy) and showed no difference in IBTR, 0.9% vs 1.4% respectively (6). Two large trials randomized patients to intraoperative radiation therapy (IORT) or WBI (10–12). In a cohort of 1,305 patients aged 48 to 75 y/o with unicentric tumors <2.5 cm s/p quadrantectomy the ELIOT trial showed higher rates of IBRT with IORT vs WBI: 11% vs 2% at median follow up of 12.4 years ($p < 0.0001$) (11). In the IORT arm, patients received 21 Gy/1 fx prescribed to 90% IDL using 3–12 MeV electrons). In a cohort of 2,298 patients ≤45 y/o with clinically unifocal IDC, the TARGIT-A trial showed no statistically significant difference between WBI and immediate IORT for local recurrence (12). In the IORT arm, patients received 20 Gy to cavity surface (~5–7 Gy at 1 cm) with 50 kV photons. Current ASTRO guidelines do not recommend low-energy IORT outside of prospective studies, while electron beam IORT is restricted to suitable risk patients.

The RAPID trial utilized APBI by 3D-CRT (38.5 Gy in 10 fractions BID), and found no difference in IBRT but an increase in moderate late toxicity and adverse cosmesis with APBI compared to WBI (8). However, the Barcelona trial using 3D-CRT and similar fractionation to the RAPID trial showed > 75% of patients in the APBI arm had excellent or good cosmesis and these outcomes were stable over time at a median follow up of 5 years (4). The Florence trial, which randomized patients to WBI vs. APBI using intensity modulated radiation therapy (IMRT) with 30 Gy in 5 every other day fractions, showed equivalent outcomes with APBI as compared to WBI and statistically significant less acute and late toxicity and improved cosmetic outcomes with APBI (vs. WBI) at a median follow up of 10 years (9). The IMPORT LOW trial randomized over 2000 patients to WBI, reduced-dose WBI with partial breast boost, and partial breast irradiation, all over 15 fractions, and showed no difference in IBTR with reduced toxicity with partial breast irradiation (7). Of note, in contrast to the other trials discussed, the IMPORT LOW trial was not an accelerated regimen as the fractionation was identical in the whole breast and partial breast arms.

APBI at NYU

Patients have received APBI since 2000 at our institution (Table 2). The first patients at NYU treated with APBI were based on a pilot study conducted at the University of Southern California published in 2002 by Formenti et al. in which nine post-menopausal patients with pT1N0 breast cancer were treated in the prone position to 25 to 30 Gy in 5 fractions over 10 days using 5-7 horizontal photon treatment fields with couch rotations. Fractionation was based on biologically equivalent dose (BED) calculation for normal tissue (fibrosis, cosmesis) and tumor control (15). All patients were alive and disease free with good to excellent cosmetic results at follow up (median 41 months, range 36-53 months). Given the outcome of the USC pilot study, NYU 00-23 Hypo-Fractionated Conformal Radiation Therapy to the Tumor Bed after Segmental Mastectomy Phase I/II study was conducted between June 2000 and September 2007 (16, 17). 99 patients were treated in the prone position to 30 Gy in 5 fractions over 10 days using opposed mini-tangent photon fields (≥ 4MV). Treatment late toxicity assessment as per LENT (late effect of normal tissue)/SOMA (Subjective, Objective, Management, Analytics) showed low (1%) grade 2-3 toxicities (17) and reduced toxicity to organs at risk (16). Also, at 5 year follow up [95% level of confidence] the reported overall disease-free survival was 95% [87-98%] (17).

NYU 07-582 Image guided Radiotherapy (IGRT) For Prone Partial Breast Irradiation (PBI) study was conducted between 2007 and 2014. 297 post-menopausal patients with pT1 breast cancer excised with negative margins were treated in the prone position to 30 Gy in 5 fractions over 5 consecutive days using 3D or IMRT fields. Wen et al. compared patients treated between 2003-2009 under NYU 0023 and NYU 07-582 with RTOG-0413 (5, 18). In RTOG 0413, patients were treated supine, CTV was defined as the cavity plus 1.5 cm expansion and PTV was defined as CTV plus 1.0 cm expansion (5). In NYU 00-23, patients were treated prone with the CTV defined as the lumpectomy cavity with no expansion and the PTV defined as CTV plus 2.0 cm expansion (16, 17). In NYU 07-582, patients were treated prone with CTV defined as the lumpectomy cavity with no expansion and the PTV defined as CTV plus 1.5 cm expansion (18). The main observation was that even though our PTV was 1 to 1.5 cm smaller than that of RTOG 0413 and our patients were treated prone as opposed to patients treated supine in RTOG 0413, our dosimetric results complied with the RTOG constraints for partial breast irradiation (18). A retrospective analysis of setup variations for 70 patients treated under NYU 07-582 confirmed adequacy of our CTV defined as lumpectomy cavity only and PTV defined as CTV plus 1.5 cm (19).

NYU 14-01306 Prone Partial Breast Irradiation (PBI): Prospective Randomized Controlled Non-inferiority Trial to Compare Radiation Fibrosis with Five Versus Three Fractions study was conducted between 2014 and 2021. 284 post-menopausal patients with pT1 breast cancer excised with negative margins received either 30 Gy in 5 fractions over 5

10.3389/fonc.2022.1049704

TABLE 2 NYU Partial Breast Development.

Study	Years of enrollment	No. Patients/ FU	Target Definition	Dose Fractionation	Target Dose Constraints	OARs Dose Constraints	Planning	Imaging
USC Feasibility Pilot Study (15)	1997 - 1998	N = 9 41 months	PTV= lumpectomy cavity + 2 cm	25 - 30 Gy in 5 fxs over 10 days	D95% = 100% Dmax ≤ 110%	None reported	5-7 fixed horizontal 4 MV beams with couch rotations, avoiding non-breast tissue	Daily portal orthogonal images + two treatment fields
NYU 00-23 Hypo-Fractionated Conformal Radiation Therapy to the Tumor Bed After Segmental Mastectomy (Phase I/II Study) (16, 17)	2000 - 2007	N = 98 64 mos	CTV= lumpectomy cavity PTV= CTV + 2 cm limited anteriorly by skin and posteriorly by chest wall PTV Eval = PTV cropped 0.5 cm from skin surface and excluding chest wall	30 Gy in 5 fxs over 10 days (Mon, Wed, Fri, Mon, Wed)	PTV Eval: Covered by 95% of Rx dose (minimally 90%) Dmax ≤ 110%	Ipsilateral Breast: D50% < 50% of Rx dose Heart: no beam directed at heart Ipsilateral Lung: no beam directed at ipsilateral lung Contralateral Breast: no beam directed at contralateral breast	Opposed mini-tangents ≥ 4 MV	Daily portal images of each treatment field
NYU 07-582 Image Guided Radiotherapy (IGRT) For Prone Partial Breast Irradiation (PBI) (18, 19)	2007 - 2014	N = 297	CTV= lumpectomy cavity PTV = CTV + 1.5cm PTV Eval = PTV cropped to be within ipsilateral breast tissue, excluding first 0.5 cm of tissue under the skin, and tissue beyond the chest wall, pectoralis muscles, and lung	30 Gy in 5 fxs over 5 consecutive days	PTV Eval: D95% = 100% of Rx dose	Ipsilateral breast: V50% <60%; V100% < 35% Ipsilateral lung: V30% < 15% Contralateral lung: V5% < 15% Heart: V5% < 5%	3D or IMRT ≥ 4 MV No beam directed towards contralateral breast, heart or lung Non-coplanar beams encouraged, but not required	Day 1: CBCT and portal images Days 2-4: daily portal images Day 5: CBCT and portal images
NYU 14-01306 Prone Partial Breast Irradiation (PBI): Prospective Randomized Controlled Non-inferiority Trial To Compare Radiation Fibrosis With Five Versus Three Fractions	2014 - 2021	N = 284	CTV = lumpectomy cavity PTV = CTV + 1.5 cm PTV Eval = PTV cropped to be within ipsilateral breast tissue, excluding first 0.5 cm of tissue under the skin, and tissue beyond the chest wall, pectoralis muscles, and lung	Arm 1: 30 Gy in 5 fxs over 5 consecutive days Arm 2: 24 Gy in 3 fxs every other day	D95% = 100% of Rx dose	Ipsilateral breast: V50% < 60%; V100% < 35% Ipsilateral lung: V30% < 15% Contralateral lung: V5% < 15% Heart: V5% < 5%	3D or IMRT > 4 MV No beam directed towards contralateral breast, heart or lung Non-coplanar beams encouraged, but not required	Day 1: CBCT and portal images Subsequent days portal images kV images may be used to verify setup

consecutive days (Arm 1) or 24 Gy in 3 fractions given every other day (Arm 2), using 3D-CRT or IMRT fields. Patients with lobular histology, Estrogen-receptor (ER) negative disease, and lymphovascular invasion (LVI) were included whereas those with an extensive intraductal component (EIC) were excluded. Pure DCIS was initially excluded but the trial eligibility criteria were later amended to include low risk DCIS as defined by the ASTRO APBI guidelines (13, 14).

APBI at NYU – CT simulation, contours, beams, planning constraints and imaging

CT simulation

Most of our APBI patients are simulated and treated in the prone position. We use the ClearVue™ prone breast board overlay (placed on sim and linac couch tops) which allows 18 cm free vertical hang space between board surface and base, and requires the head turned to the side. The kVue™ prone breast board (inserted into linac couch top) is selected for patients with pendulous breasts exceeding 18 cm vertical hang and/or for patients who prefer a neutral head position.

The patient is positioned prone on the breast board with the entire targeted breast hanging within the opening of the board. The sternal marker is palpated to ensure it is at the edge of the opening of the breast board. The contralateral breast is moved away from the targeted breast. A foam wedge is placed under the ankles for comfort.

Triangulation and lower alignment BBs and tattoos are placed. An additional mark on the lateral aspect of the breast in the axial plane of triangulation and a lower alignment mark on the lower back in the sagittal plane of posterior triangulation are used for isocenter location and alignment, respectively. The surgical scars are marked with radiopaque wire.

CT scan is acquired using 3 mm slice thickness, with upper and lower scan limits approximately at mastoid process/base of skull and 8 cm below the inframammary fold, respectively.

The simulation documentation includes the longitudinal scale value corresponding to the plane of triangulation, as well as the sagittal laser position corresponding to the posterior triangulation mark

When we simulate a patient prone for APBI, markers (Beekley RT-SPOT® and CT SPOT®) are placed on the skin corresponding to midline along the sternum, lumpectomy incision, 2 cm inferior to the inframammary fold, and nipple (Figure 1).

Contours

The tumor bed volume for each patient is drawn by the physician to include the resection cavity and any surgical clips (if placed). Pre-surgical imaging such as mammography and MRI is used to help delineate the tumor bed and attention is also given to the location of the scars marked at time of simulation. This volume is expanded to planning target volume (PTV) using a 1.5 cm uniform margin. The planning target volume evaluation (PTV_Eval) is the planning target volume (PTV) limited to be within the defined ipsilateral breast tissue, specifically excluding the 1st 5 mm of tissue under the skin and tissue beyond the chest wall, pectoralis muscles and lung. For all cases, the tumor bed volume, ipsilateral and contralateral breast are contoured by a physician. The other normal structures and OARs, including the ipsilateral and contralateral lung, heart and skin, are contoured by the dosimetry staff and reviewed by a physician.

Beams

Treatment plans are generated in the Eclipse planning system (Varian Medical Systems) by a dosimetrist and reviewed by a physicist and physician. All patients are primarily treated using opposed photon tangents (3D-CRT or IMRT) in the prone position using a prone breast board with right- or left-sided apertures. The gantry and table angle combinations are selected to not enter or exit through other organs of the body. Figure 2 includes a representation of a typical external beam APBI plan in the prone position. Patients treated in the supine position were planned using a similar technique with the possible addition of enface electrons.

Constraints

The ipsilateral breast is constrained to V50% (V15 Gy) < 50-60% and V100% (V30 Gy) < 35%. Other constraints include heart V5% < 5%, ipsilateral lung V30% < 15%, contralateral lung V5% < 15%, PTV_Eval D95% > 100% and D99.5%>90%, Tumor Bed D98%>100%, and Body D0.03cc<110% (Table 3).

Imaging

On day 1: Cone-beam computed tomography (CBCT) image align to cavity, or breast if cavity is not visualized, then followed by MV portal images (no shifts are made based on MV images). For subsequent fractions only CBCT.

Toxicity, dosimetry and outcomes of NYU patients 2010-2019

A retrospective study of 345 patients treated with APBI between 2010-2019 was performed, with 14 excluded due to APBI given for ipsilateral breast tumor recurrence (n=3), palliation (n=9), and incomplete RT course (n=2) (20). All patients being treated on NYU S14 01306, which was accruing at the time were also excluded. We did include patients who were on NYU 07-582 (60% of patients). Of the 331 total patients, the

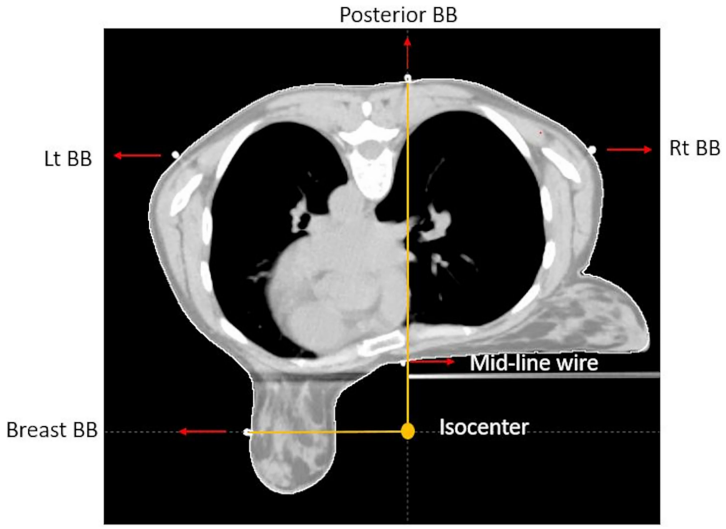

FIGURE 1
CT axial view of prone breast, showing isocenter location, triangulation point, lateral aspect of the breast marker, and midline marker.

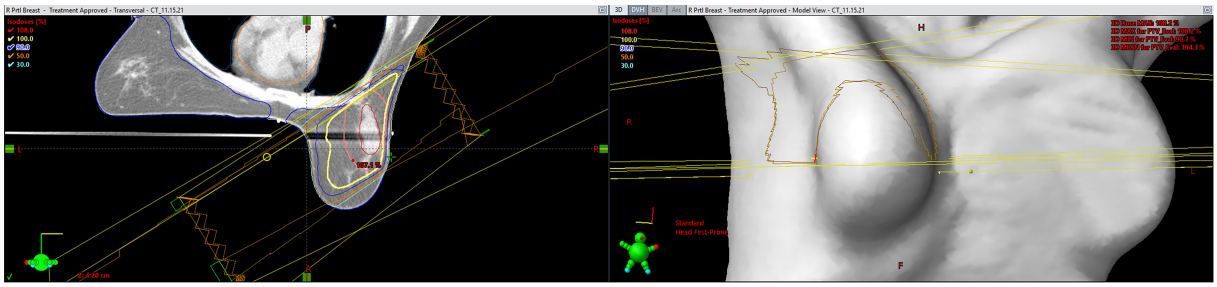

FIGURE 2
A representation of a typical external beam accelerated partial breast irradiation (APBI) plan in the prone position (Eclipse; Varian Medical Systems, Palo Alto, CA).

TABLE 3 Dose constraints for our APBI approach.

Structure	Constraint
Tumor Bed	D98% > 100%
PTV_Eval	PTV D95% > 100%.
	D99.5% > 90%
Body	D0.03cc < 110%
Breast – Ipsilateral	V50% (V15Gy) <50-60%
	V100% (V30 Gy) < 35%
Heart	V5% < 5%
Lung - Ipsilateral	V30% < 15%
Lung - Contralateral	V5% < 15%

median age was 70 and 7.2% had DCIS. Of the 93% with invasive cancer, 9.8% had lobular histology, 2.3% were ≥ T2 stage, 0.9% were estrogen receptor negative, 1.3% had EIC, 2.6% had LVI, 0.3% were node positive, and 3.6% were multifocal. Margins were negative (using consensus criteria) in 67% of DCIS and 90% of invasive patients. In terms of RT delivery, 94% of patients were treated prone, with 32% treated every other day and 68% on consecutive days.

At a median follow-up of 5 years, there were 7 (2.1%) IBTR, 9 (2.7%) contralateral recurrences, and 1 (0.3%) distant metastasis. Five-year locoregional free survival was 99.5%, disease free survival was 96.7%, and overall survival was 98.1% (Figure 2). The 7 patients who experienced IBTR had unifocal pT1 tumors that were ER-strongly positive without EIC, LVI, or

positive margins. When comparing those with IBTR (n=7) to those without (n=324), a higher proportion did not receive endocrine therapy (71.4% vs. 26.2%, p = 0.018). No differences were observed in other factors such as lobular histology (p = 0.49), margin status (p = 0.60), EIC (p = 1.0), LVI (p = 1.0), or ER negative disease (p = 1.0).

Rates of acute grade 1-2 dermatitis, fatigue and pain were 35.4%, 21.8% and 9.4% respectively, with no grade 3 toxicity (Table 2). The rate of good-excellent physician- and patient-rated cosmesis (n=199, median follow-up 2.8 years) was 92.5% and 89.4%, respectively. Patients experienced low rates of telangiectasia (4.5% grade 1 & 1.5% grade 2), fibrosis (17.6% grade 1 & 3.0% grade 2), and retraction/atrophy (24.1% grade 1, 2.5% grade 2, and 0.5% grade 3).

The mean PTV D95% was 100.0%. With regard to organs at risk, the average mean heart dose was 23.8 cGy for left-sided breast cancers and 12.7 cGy for right-sided breast cancers. Average ipsilateral lung V10% was 1.0% and V30% was 0.4%. In patients whose ipsilateral breast dose volume histogram (DVH) data were available (n=111), the mean ipsilateral breast V50% and V100% were 40.4% and 20.7%, respectively. These are further detailed in Table 4.

Future directions

Given the variability in APBI technique, dose and fractionation, cosmetic outcome compared to WBI remains controversial. At a median follow-up of 10 years, NSABP-B39 reported higher grade 3 common toxicity criteria for adverse events in WBI arm vs APBI arm, 7% vs 10% respectively (5). Patient-rated cosmesis was equivalent but physician rated cosmesis was worse with APBI (21). We await more detailed publication of the toxicity, cosmesis and quality of life from this trial. The Canadian RAPID trial showed a statistically significant increase in late radiation toxicity in the APBI group primarily due to an increase in grade 2-3 breast fibrosis or induration (22.9% grade 2-3 induration or fibrosis in APBI group vs 4.6% in WBI) (8). However, the Barcelona trial using 3D-CRT and similar fractionation to the RAPID trial showed > 75% of patients in the APBI arm had excellent or good cosmesis and these outcomes were stable over time at a median follow up of 5 years (4). The Florence trial showed statistically significant less acute and late toxicity and improved cosmetic outcomes with APBI at a median follow-up of 10 years (9). We await the results of NYU S14 01306 which will report a 2 year rate of grade ≥ 2 fibrosis and long-term toxicity and cosmetic outcome. This trial is expected to meet its primary endpoint for all patients in June 2023.

Eligibility criteria for APBI has varied in clinical trials (Table 1). Initially, DCIS was largely excluded from APBI trials. NSABP B39, RAPID and Florence trials did include DCIS (5, 8, 9). In the current ASTRO guidelines, APBI is suitable for DCIS if it is screen detected, low-intermediate grade, ≤ 2.5 cm and margins ≥ 3 mm (13, 14). Age has also been a variable criteria. While current ASTRO guidelines consider APBI suitable for patients ≥ 50 years old and cautionary for patients 40-49 years old, Polgar et al., GEC-ESTRO trial, RAPID trial and Florence trial all included patients > 40 years old (3, 6, 8, 9, 13, 14). The size of the primary tumor, biological subtype, nodal status and definition of negative margins has also varied between trials. Given these

TABLE 4 DVH characteristics of patients treated from 2010-2019.

Parameter	Mean	Standard Deviation	Range
PTV D95% (%)	100.0	1.1	84.7-103.3
Mean Heart Dose (cGy)			
Left-Sided Tumors	23.8	0.5	0.0-81.0
Right-Sided Tumors	12.7	0.2	0.0-33.0
Heart V3Gy (%)			
Left-Sided Tumors	0.46	2.8	0.0-33.9
Right-Sided Tumors	0.0006	0.003	0.0-0.03
Ipsilateral Lung V10% (%)	1.0	2.2	0.0-22.0
Ipsilateral Lung V30% (%)	0.4	0.9	0.0-8.2
Ipsilateral Breast V50% (%)*	41.1	14.0	0.0-67.3
Ipsilateral Breast V100% (%)*	20.3	8.7	0.0-38.1

n=331 for all categories except those marked with (*), where n = 329.
DVH, dose volume histogram; PTV, planning target volume.

variations, current ASTRO guidelines are currently being revised to better define eligibility criteria for APBI.

Finally, with the publication of the UK FAST FORWARD trial and increasing use of 5-fraction WBI fractionation schemes, the accelerated nature of APBI becomes less specific to partial breast and available for whole breast regimens as well (22). Thus future trials comparing APBI to accelerated WBI are necessary and the comparison of toxicity and cosmesis between APBI and WBI may shift as WBI schemes change.

Author contributions

All authors listed have made a substantial, direct, and intellectual contribution to the work, and approved it for publication.

Conflict of interest

The authors declare that the research was conducted in the absence of any commercial or financial relationships that could be construed as a potential conflict of interest.

Publisher's note

References

1. Siegel RL, Miller KD, Fuchs HE, Jemal A. Cancer statistics, 2021. *CA Cancer J Clin* (2021) 71:7–33. doi: 10.3322/caac.21654

2. Hannoun-Levi JM, Resch A, Gal J, Kauer-Dorner D, Strnad V, Niehoff P, et al. Accelerated partial breast irradiation with interstitial brachytherapy as second conservative treatment for ipsilateral breast tumour recurrence: Multicentric study of the gec-estro breast cancer working group. *Radiother Oncol* (2013) 108:226–31. doi: 10.1016/j.radonc.2013.03.026

3. Polgár C, Fodor J, Major T, Sulyok Z, Kásler M. Breast-conserving therapy with partial or whole breast irradiation: Ten-year results of the budapest randomized trial. *Radiother Oncol* (2013) 108:197–202. doi: 10.1016/j.radonc.2013.05.008

4. Rodríguez N, Sanz X, Dengra J, Foro P, Membrive I, Reig A, et al. Five-year outcomes, cosmesis, and toxicity with 3-dimensional conformal external beam radiation therapy to deliver accelerated partial breast irradiation. *Int J Radiat Oncol Biol Phys* (2013) 87:1051–7. doi: 10.1016/j.ijrobp.2013.08.046

5. Vicini FA, Cecchini RS, White JR, Arthur DW, Julian TB, Rabinovitch RA, et al. Long-term primary results of accelerated partial breast irradiation after breast-conserving surgery for early-stage breast cancer: A randomised, phase 3, equivalence trial. *Lancet* (2019) 394:2155–64. doi: 10.1016/S0140-6736(19)32514-0

6. Ott OJ, Strnad V, Hildebrandt G, Kauer-Dorner D, Knauerhase H, Major T, et al. Gec-estro multicenter phase 3-trial: Accelerated partial breast irradiation with interstitial multicatheter brachytherapy versus external beam whole breast irradiation: Early toxicity and patient compliance. *Radiother Oncol* (2016) 120:119–23. doi: 10.1016/j.radonc.2016.06.019

7. Coles CE, Griffin CL, Kirby AM, Titley J, Agrawal RK, Alhasso A, et al. Partial-breast radiotherapy after breast conservation surgery for patients with early breast cancer (uk import low trial): 5-year results from a multicentre, randomised, controlled, phase 3, non-inferiority trial. *Lancet* (2017) 390:1048–60. doi: 10.1016/S0140-6736(17)31145-5

8. Whelan TJ, Julian JA, Berrang TS, Kim DH, Germain I, Nichol AM, et al. External beam accelerated partial breast irradiation versus whole breast irradiation after breast conserving surgery in women with ductal carcinoma *in situ* and node-negative breast cancer (rapid): A randomised controlled trial. *Lancet* (2019) 394:2165–72. doi: 10.1016/S0140-6736(19)32515-2

9. Meattini I, Marrazzo L, Saieva C, Desideri I, Scotti V, Simontacchi G, et al. Accelerated partial-breast irradiation compared with whole-breast irradiation for early breast cancer: Long-term results of the randomized phase iii apbi-imrt-florence trial. *J Clin Oncol* (2020) 38:4175–83. doi: 10.1200/JCO.20.00650

10. Veronesi U, Orecchia R, Maisonneuve P, Viale G, Rotmensz N, Sangalli C, et al. Intraoperative radiotherapy versus external radiotherapy for early breast cancer (eliot): A randomised controlled equivalence trial. *Lancet Oncol* (2013) 14:1269–77. doi: 10.1016/S1470-2045(13)70497-2

11. Orecchia R, Veronesi U, Maisonneuve P, Galimberti VE, Lazzari R, Veronesi P, et al. Intraoperative irradiation for early breast cancer (eliot): Long-term recurrence and survival outcomes from a single-centre, randomised, phase 3 equivalence trial. *Lancet Oncol* (2021) 22:597–608. doi: 10.1016/S1470-2045(21)00080-2

12. Vaidya JS, Bulsara M, Baum M, Wenz F, Massarut S, Pigorsch S, et al. Long term survival and local control outcomes from single dose targeted intraoperative radiotherapy during lumpectomy (targit-iort) for early breast cancer: Targit-a randomised clinical trial. *Bmj* (2020) 370:m2836. doi: 10.1136/bmj.m2836

13. Orecchia R, Veronesi U, Maisonneuve P, Galimberti VE, Lazzari R, Veronesi P, et al. Accelerated partial breast irradiation: Executive summary for the update of an astro evidence-based consensus statement. *Pract Radiat Oncol* (2017) 7:73–9. doi: 10.1016/j.prro.2016.09.007

14. Smith BD, Arthur DW, Buchholz TA, Haffty BG, Hahn CA, Hardenbergh PH, et al. Accelerated partial breast irradiation consensus statement from the american society for radiation oncology (astro). *Int J Radiat OncolBiolPhys* (2009) 74:987–1001. doi: 10.1016/j.ijrobp.2009.02.031

15. Formenti SC, Rosenstein B, Skinner KA, Jozsef G. T1 stage breast cancer: Adjuvant hypofractionated conformal radiation therapy to tumor bed in selected postmenopausal breast cancer patients–pilot feasibility study. *Radiology* (2002) 222:171–8. doi: 10.1148/radiol.2221010769

16. Formenti SC, Truong MT, Goldberg JD, Mukhi V, Rosenstein B, Roses D, et al. Prone accelerated partial breast irradiation after breast-conserving surgery: Preliminary clinical results and dose-volume histogram analysis. *Int J Radiat Oncol Biol Phys* (2004) 60:493–504. doi: 10.1016/j.ijrobp.2004.04.036

17. Formenti SC, Hsu H, Fenton-Kerimian M, Roses D, Guth A, Jozsef G, et al. Prone accelerated partial breast irradiation after breast-conserving surgery: Five-year results of 100 patients. *Int J Radiat Oncol Biol Phys* (2012) 84:606–11. doi: 10.1016/j.ijrobp.2012.01.039

18. Wen B, Hsu H, Formenti-Ujlaki GF, Lymberis S, Magnolfi C, Zhao X, et al. Prone accelerated partial breast irradiation after breast-conserving surgery: Compliance to the dosimetry requirements of rtog-0413. *Int J Radiat Oncol Biol Phys* (2012) 84:910–6. doi: 10.1016/j.ijrobp.2012.01.055

19. Jozsef G, DeWyngaert JK, Becker SJ, Lymberis S, Formenti SC. Prospective study of cone-beam computed tomography image-guided radiotherapy for prone accelerated partial breast irradiation. *Int J Radiat Oncol Biol Phys* (2011) 81:568–74. doi: 10.1016/j.ijrobp.2010.11.029

20. Shah BA, Xiao J, Oh C, Taneja S, Barbee D, Maisonet O, et al. Five-fraction prone accelerated partial breast irradiation: Long-term oncologic, dosimetric, and cosmetic outcome. *Pract Radiat Oncol* (2022) 12:106–12. doi: 10.1016/j.prro.2021.08.009

21. White JR, Winter K, Cecchini RS, Vicini FA, Arthur DW, Kuske RR, et al. Cosmetic outcome from post lumpectomy whole breast irradiation (wbi) versus partial breast irradiation (pbi) on the nrg oncology/nsabp b39-rtog 0413 phase iii clinical trial. *Int J Radiat OncolBiolPhys* (2019) 105:S3–4. doi: 10.1016/j.ijrobp.2019.06.384

22. Murray Brunt A, Haviland JS, Wheatley DA, Sydenham MA, Alhasso A, Bloomfield DJ, et al. Hypofractionated breast radiotherapy for 1 week versus 3 weeks (fast-forward): 5-year efficacy and late normal tissue effects results from a multicentre, non-inferiority, randomised, phase 3 trial. *Lancet (London England)* (2020) 395:1613–26. doi: 10.1016/S0140-6736(20)30932-6

frontiers | Frontiers in Oncology

TYPE Original Research
PUBLISHED 16 January 2023
DOI 10.3389/fonc.2022.1066915

OPEN ACCESS

EDITED BY
Vishruta Dumane,
Icahn School of Medicine at Mount Sinai, United States

REVIEWED BY
Udhaya Kumar S.,
Baylor College of Medicine, United States
Hidekazu Tanaka,
Yamaguchi University Graduate School of Medicine, Japan

*CORRESPONDENCE
Jessica Prunaretty
jessica.prunaretty@icm.unicancer.fr
Sophie Gourgou
sophie.gourgou@icm.unicancer.fr

†These authors have contributed equally to this work

SPECIALTY SECTION
This article was submitted to Radiation Oncology, a section of the journal Frontiers in Oncology

RECEIVED 11 October 2022
ACCEPTED 22 December 2022
PUBLISHED 16 January 2023

CITATION
Prunaretty J, Bourgier C, Gourgou S, Lemanski C, Azria D and Fenoglietto P (2023) Different meaning of the mean heart dose between 3D-CRT and IMRT for breast cancer radiotherapy. *Front. Oncol.* 12:1066915. doi: 10.3389/fonc.2022.1066915

Different meaning of the mean heart dose between 3D-CRT and IMRT for breast cancer radiotherapy

Jessica Prunaretty[1,2*†], Celine Bourgier[1,2,3†], Sophie Gourgou[4*], Claire Lemanski[1,2], David Azria[1,2,3] and Pascal Fenoglietto[1,2]

[1]Institut de Recherche en Cancérologie de Montpellier (IRCM), INSERM U1194, Montpellier, France, [2]Fédération Universitaire d'Oncologie Radiothérapie d'Occitanie Méditerranée, Institut régional du Cancer Montpellier (ICM), Montpellier, France, [3]Université Montpellier, Montpellier, France, [4]Biostatistics Department, Institut du Cancer de Montpellier, Montpellier, France

Background: Previous studies in 2D and in 3D conformal radiotherapy concludes that the maximal heart distance and the mean heart dose (MHD) are considered predictive of late cardiac toxicities. As the use of inverse-planned intensity modulated radiation therapy (IMRT) is increasing worldwide, we hypothesized that this 3D MHD might not be representative of heart exposure after IMRT for breast cancer (BC).

Methods: Patients with left-sided BC and unfavorable cardiac anatomy received IMRT. Their treatment plan was compared to a virtual treatment plan for 3D conformal radiotherapy with similar target volume coverage (study A). Then, a second 3D conformal treatment plan was generated to achieve equivalent individual MHD obtained by IMRT. Then the heart and left anterior descending (LAD) coronary artery exposures were analyzed (study B). Last, the relationship between MHD and the heart volume or LAD coronary artery volume receiving at least 30Gy, 40Gy and 45Gy in function of each additional 1Gy to the MHD was assessed (study C).

Results: A significant decrease of heart and LAD coronary artery exposure to high dose was observed with the IMRT compared with the 3D conformal radiotherapy plans that both ensured adequate target coverage (study A). The results of study B and C showed that 3D MHD was not representative of similar heart substructure exposure with IMRT, especially in the case of high dose exposure.

Conclusions: The mean heart dose is not a representative dosimetric parameter to assess heart exposure following IMRT. Equivalent MHD values following IMRT and 3DRT BC treatment do not represent the same dose distribution leading to extreme caution when using this parameter for IMRT plan validation.

KEYWORDS

breast cancer radiotherapy, heart exposure, IMRT, 3D-CRT, mean heart dose

Background

Breast-conserving surgery followed by whole breast irradiation (WBI) is the current standard of care for patients with early stage breast cancer (BC). Although WBI significantly decreases the risk of locoregional recurrences and consequently BC-related mortality, some long-term BC survivors will develop ischemic heart disease (IHD). Since the mid-90s, long-term cardiac morbidities/mortality have been reported after radiotherapy. In 2005, the EBCTCG meta-analysis showed that heart disease significantly increases mortality of patients with BC (hazard ratio: 1.27, p=0.0001) (1). From 2000, the BC radiation oncology community has focused on identifying parameter(s) that predict late cardiac toxicities. It was first reported that the maximal heart distance correlates with the percentage of irradiated heart volume (2). More than a decade later, Darby and colleagues assessed IHD risk in function of the heart exposure and the presence of cardiac risk factors (history of circulatory disease, diabetes, chronic obstructive pulmonary disease, smoking, high body mass index, regular analgesic use) in a population-based case-control study of women with BC who received radiotherapy between 1958 and 2001 and with major coronary events (i.e. myocardial infarction, coronary revascularization or death from IHD) or not (controls) (3). This study relied on real clinical data with estimated radiotherapy plans. From this study, dose-volume histograms, mean doses and equivalent doses delivered in 2Gy fractions (EQD2) were generated for the whole heart and for the left anterior descending (LAD) coronary artery. The mean heart doses (MHD) were 4.9Gy for the whole population and 6.6Gy for patients with left BC, respectively. The mean LAD coronary artery dose and mean EQD2 were 9.9Gy and 4.4Gy for the whole population. The authors concluded that MHD is the most predictive factor of developing a major coronary event, and higher MHD values significantly enhance the risk of major coronary event. Taylor and colleagues assessed MHD predictive value after the introduction of modern radiotherapy techniques (3D conformal and inverse-planned intensity modulated radiation therapy, IMRT) (4). Their treatment plans showed MHD of 9.2Gy for 3D conformal radiotherapy of left-sided BC and internal mammary chain (IMC) and of 8.6Gy for IMRT. These values decreased to 3.4Gy and 5.6Gy with 3D conformal radiotherapy and IMRT, respectively, when the IMC was not included. Furthermore, in patients with unfavorable anatomy (pectus excavatum), MHD was 14.8Gy. The estimated radiation-induced heart disease incidence rates were 1.3% and 2.5% and the cardiac-related mortality rates were 0.6% and 1.2% without and with IMC irradiation, respectively, for 50-year-old patients without any cardiac risk factor, regardless of the radiation technique.

Abbreviations: BC, breast cancer; CTV, Clinical Target Volume; IHD, ischemic heart disease; IMRT, intensity modulated radiation therapy; LAD, left anterior descending; MHD, mean heart dose; OAR, organs at risk; PTV, Planning Target Volume; RA, Rapid Arc; WBI, whole breast irradiation.

Nevertheless, several studies challenged the use of MHD as an appropriate surrogate parameter. The BACCARAT study recommended assessing the dose distribution of the cardiac substructures, in particular the LAD (5). Recently, Naimi et al. (6) studied the radiation dose distribution to cardiac subvolumes in left breast cancer radiotherapy for 50 patients treated with 3D-conformal hypofractionated radiotherapy. They showed a poor correlation between MHD and dose to cardiac substructures and suggested to define the left ventricle and the LAD as separate organ at risk.

To our knowledge, these observations have not been reported with IMRT techniques. Although the American Society for Radiation Oncology (ASTRO) does not recommend IMRT for the routine delivery of WBI following breast-conserving surgery, some studies showed that IMRT use is increasing worldwide (7–9). Pierce and colleagues recently reported that in the USA, approximately 40% of patients with BC receive IMRT (10). The present study objective was to determine whether MHD is representative of similar heart substructure exposure after 3D or IMRT for BC. To this aim, first we estimated the MHD following breast irradiation by IMRT and using an optimal strategy with a 3D technique. Then, we analyzed the heart and LAD dose distribution with an equivalent MHD (obtained from the radiotherapy plans for the two techniques) and the impact of MHD variations on these structures.

Materials and methods

After the study approval by the local Ethics Committee, ten patients with left-sided BC and unfavorable cardiac anatomy (i.e. maximum heart depth ≥1.0 cm within the tangent fields) and/or unfavorable anatomy (pectus excavatum) and their relative treatment plans were retrieved from our database (Figure S1). These patients were treated between December 2012 and March 2016. All patients had lumpectomy and sentinel node biopsy followed by adjuvant radiotherapy. Due to their unfavorable cardiac anatomy, all patients received IMRT using the RapidArc (RA) technology without breath-hold technique. All patients were on supine position, both arms over the head with personalized foam and underwent non-contrast Computed Tomography (CT)-based simulation (Optima CT580 RT, General Electric Healthcare, Waukesha, WI). CT images were acquired using a 2.5 mm slice thickness from the top of the second cervical vertebral body to the bottom of the first lumbar vertebral body.

Delineation of target and organs at risk (OAR) volumes

As the BC was removed by surgery, no gross target volume was delineated. The breast Clinical Target Volume (CTV) was

defined according to the ESTRO guidelines (11). Briefly, breast CTV encompassed the clinical (delineated by radio-opaque markers) and visible mammary gland. The tumor bed CTV included surgical clips with a 20mm-margin extension (12, 13). Heart and LAD coronary artery (including the LAD coronary artery and interventricular branch) were delineated using the atlas by Feng and colleagues (14). The Planning Target Volume (PTV) was defined as a 3D-expansion of the CTV with a margin of 7mm. All PTV and CTV were limited 5 mm under the skin. The total doses delivered to the breast and tumor bed PTV were 52.2Gy and 63.22Gy in 29 fractions, respectively.

Treatment plans

Patients were treated according to RA technique owing to their unfavorable cardiac anatomy and/or unfavorable anatomy (pectus excavatum). RA radiotherapy plans were prepared using the mono-isocentric technique with six partial rotation arcs, each with 50° gantry rotations, as described by Tsai et al. (15). Photon Optimizer (PO, v15.5) was used for RA optimization. RA radiotherapy plans were considered as completed when at least 99% of the breast CTV received a total dose of 49.6Gy (i.e. 95% of 52.2Gy) and when at least 95% of the tumor bed PTV received 95% of the total dose of 63.22Gy (SIB technique). OAR dose constraints are summarized in Table 1. Dose distributions were calculated with the analytical anisotropic algorithm (v15.5, Varian Medical Systems, Palo Alto, CA, USA) on a TrueBeam linear accelerator equipped with a Varian 120 multileaf collimator.

For dosimetric comparison, virtual 3D-conformal RT plans were generated using common tangent wedged fields (6MV photon energy; maximum 400MU/min dose rate). A total dose of 52.2Gy in 29 fractions was prescribed to breast PTV following by a boost dose of 11.02Gy in 29 fractions to the tumor bed (equivalent prescription to the RA technique).

TABLE 1 Dose constraints for the indicated organs at risk.

OAR	Constraints
Heart	$D_{1\%}$< 40 Gy
	D_{mean} < 10 Gy
Left Lung	$D_{20\%}$ < 22 Gy
	$D_{10\%}$ < 30 Gy
	$D_{80\%}$ < 5 Gy
	D_{mean} < 13 Gy
Right Lung	$D_{1\%}$ < 10 Gy
	D_{mean} < 5Gy
Right Breast	$D_{1\%}$ < 10 Gy
	D_{mean} < 5Gy

Study A: All patients had a RA radiotherapy plan to optimize the target volume coverage and to limit OAR exposure, particularly the heart (treatment performed). Then, heart and LAD coronary artery exposure were compared in function of the treatment technique (RA IMRT and virtual 3D conformal radiotherapy). For this, virtual 3D conformal radiotherapy plans were created to ensure that the target volume dose-volume histograms would be the same as those obtained with the RA radiotherapy plans. Heart exposure to high total dose were monitored by calculating the mean dose (Gy) and the volumes at 30, 40 and 45Gy (V30Gy, V40Gy and V45Gy; i.e. the percentage of heart volume in % encompassed by the 15Gy, 30Gy, 40Gy and 45Gy isodose, respectively). Concerning LAD coronary artery exposure, V15Gy, V30Gy, V40Gy and V45Gy were reported.

Study B: Based on the individual MHD obtained in the RA radiotherapy plans, virtual 3D conformal radiotherapy plans were generated to obtain similar MHD, regardless of the PTV coverage. Heart and LAD coronary artery exposure were monitored by calculating the V5Gy, V10Gy, V30Gy, V40Gy and V45Gy (percentage of heart volume and LAD coronary artery volume in cc encompassed by the 5Gy, 10Gy, 30Gy, 40Gy and 45Gy isodose, respectively). The aim of this study is to analyze the difference in dose distribution for different dose levels between the two techniques for similar MHD values.

Study C: Darby and colleagues reported in their population-based case-control study a MHD of 6.6Gy for left-sided BC (with 3D conformal radiotherapy) and an increase by 7.4% of major coronary events for each 1Gy increment in the MHD. Study C aim was to assess the relationship between the MHD, and the heart volume receiving at least 30Gy, 40Gy and 45Gy in function of each additional 1Gy to the MHD. To this aim, the individual 3D conformal radiotherapy plans from study A were used: MHD was >6.6Gy (from 7.6Gy to 29.7Gy) and <6.6Gy (from 1.4Gy to 4.3Gy) in six and four patients with unfavorable cardiac anatomy, respectively. For each patient, the 3D conformal radiotherapy plan was recalculated to obtain a MHD between 3.5Gy and 7Gy, either by decreasing or increasing the MHD (0.5Gy each time). The percentage of heart volume, and LAD coronary artery volume (in cc) encompassed by the 30Gy, 40Gy and 45Gy isodose were retrieved for each patient. The correlations between MHD and heart volume (percentage) or LAD coronary artery volume (in cc) were analyzed.

Statistical considerations

Data were described using the mean, minimal and maximal values for continuous parameters and percentages and 95% confidence interval for categorical parameters.

Continuous parameters were compared between categories using the Wilcoxon - Mann Whitney test. Correlation analyses

10.3389/fonc.2022.1066915

between continuous parameters were performed using the Spearman's rank correlation coefficient.

Results

Patients, OAR volumes

All patients had pT1N0 (n=9) or pT2N0 (n=1) left invasive ductal carcinoma BC. The mean breast CTV was 761.3 cc (min – max, 175 cc – 1642.5 cc), mean heart volume 612cc (min – max, 439 – 749cc) and mean LAD coronary artery volume 2.74 cc (min – max, 1.1 – 5.7 cc).

Significant decrease of heart and LAD exposure to high dose with RapidArc for the same target coverage (study A)

In study A, the real RA radiotherapy plan of each patient was compared to the virtual 3D conformal radiotherapy plan with the same CTV coverage (i.e. at least 99% of breast CTV encompassed by the 95% isodose; Figure 1). Concerning heart exposure, MHD was not significantly different in the RA and 3D conformal radiotherapy plans (6.4Gy and 9.4Gy). However, heart exposure to high total doses was significantly different: V45Gy, V40Gy and V30Gy were strongly reduced in the RA radiotherapy plans (V30Gy and V45Gy: 1.1% and 0.1%) (Figure 2). The mean LAD coronary artery was significantly lower with RA than with 3D conformal radiotherapy (17.1Gy and 41.1Gy; p-value=0.003) as well as the LAD coronary artery V45Gy, V40Gy,V30Gy and V15Gy (Figure 2).

The mean heart dose is not representative of heart substructure exposure when using RapidArc IMRT (Studies B and C)

Study B. The intra-patient MHD was similar with both radiotherapy techniques (MHD=6.4Gy), whereas dose distribution was significantly different. A better breast PTV coverage was observed with the RA than with the 3D conformal radiotherapy plans (V49.6Gy=99% *versus* 97.5%). Moreover, heart exposure to high doses was significantly decreased with the RA technique (<1% of heart volume for V30Gy, V40Gy and V45Gy), while it was increased for V5Gy exposure compared with the 3D conformal technique (39.6% versus 17.1%, respectively) (Figure 3). The mean LAD coronary artery dose was significantly reduced in the RA compared with the 3D conformal radiotherapy plans (17.1Gy *versus* 42.2Gy). LAD coronary artery exposure to low dose was comparable between techniques, whereas exposure to high doses was significantly reduced in the RA compared with the 3D conformal radiotherapy plans (Figure 3).

Study C. The relationship between the MHD, and the heart volume exposure was evaluated in function of each additional 0.5Gy to the MHD (Figure 4A). Study C. MHD and heart exposure (V30Gy, V40Gy and V45Gy) showed a strong linear correlation (R^2 closed to 1) (Figure 4B) whereas LAD coronary artery exposure (V30Gy, V40Gy and V45Gy) displayed a polynomial correlation with MHD (Figure 4C). When these correlations were assessed for a MHD of 6.6Gy (the reference from the article by Darby et al), the 3D conformal radiotherapy plans achieved heart V30Gy, V40Gy and V45Gy of 8.17%, 6.86% and 5.72%, respectively, whereas the RA radiotherapy plans significantly decreased the heart V30Gy, V40Gy and V45Gy (1.11%; 0.36% and 0.09%, respectively). Similar results were obtained for the LAD coronary artery V30Gy, V40Gy and V45Gy (1.98cc; 1.91cc and 1.87cc, respectively, in the 3D conformal radiotherapy plans, and 0.2cc; 0.06cc and 0.02cc, respectively, in the RA radiotherapy plans).

Discussion

The present study showed that the use of RA allow a significant better PTV coverage, a significant lesser LAD exposure than 3D-conformal technique in patients with left-sided BC and unfavorable cardiac anatomy and/or unfavorable anatomy. Regarding MHD after RA planning, our results are consistent with those reported by Taylor and colleagues (4) (MHD pectus excavatum=14.8 Gy; MHD unfavorable anatomy=7.1Gy).

The effect on the heart of dose sparing strategies, particularly the role of the deep inspiration breath hold technique, has been extensively studied, by assuming that the MHD is the appropriate dosimetric parameter to evaluate the risk of late cardiac toxicity occurrence.

The reference study by Darby and colleagues showed that the MHD in patients with left-sided BC treated by 2D or 3D conformal radiotherapy should be lower than 6.6Gy (3). The methodology used in this study is one of its limitations: MHD was estimated to be 4.9Gy for a woman with typical anatomy because no individual data was available. In a more recent study based on individual data, the MHD was 4.4Gy when only the left-sided BC was irradiated (without any node field) (16). This study on 910 patients with BC showed that the relationship between acute coronary events and the left ventricle volume receiving 5Gy was more important than MHD. Furthermore, more and more radiation oncologists use IMRT for BC treatment, and the systematic review (studies from 2003 to 2013) by Taylor et al. found that the recommended value from the study by Darby et al. could not be respected when the IMC was included in the radiotherapy prescription (MHD=9.2Gy), and when using IMRT (MHD=8.6Gy) (4).

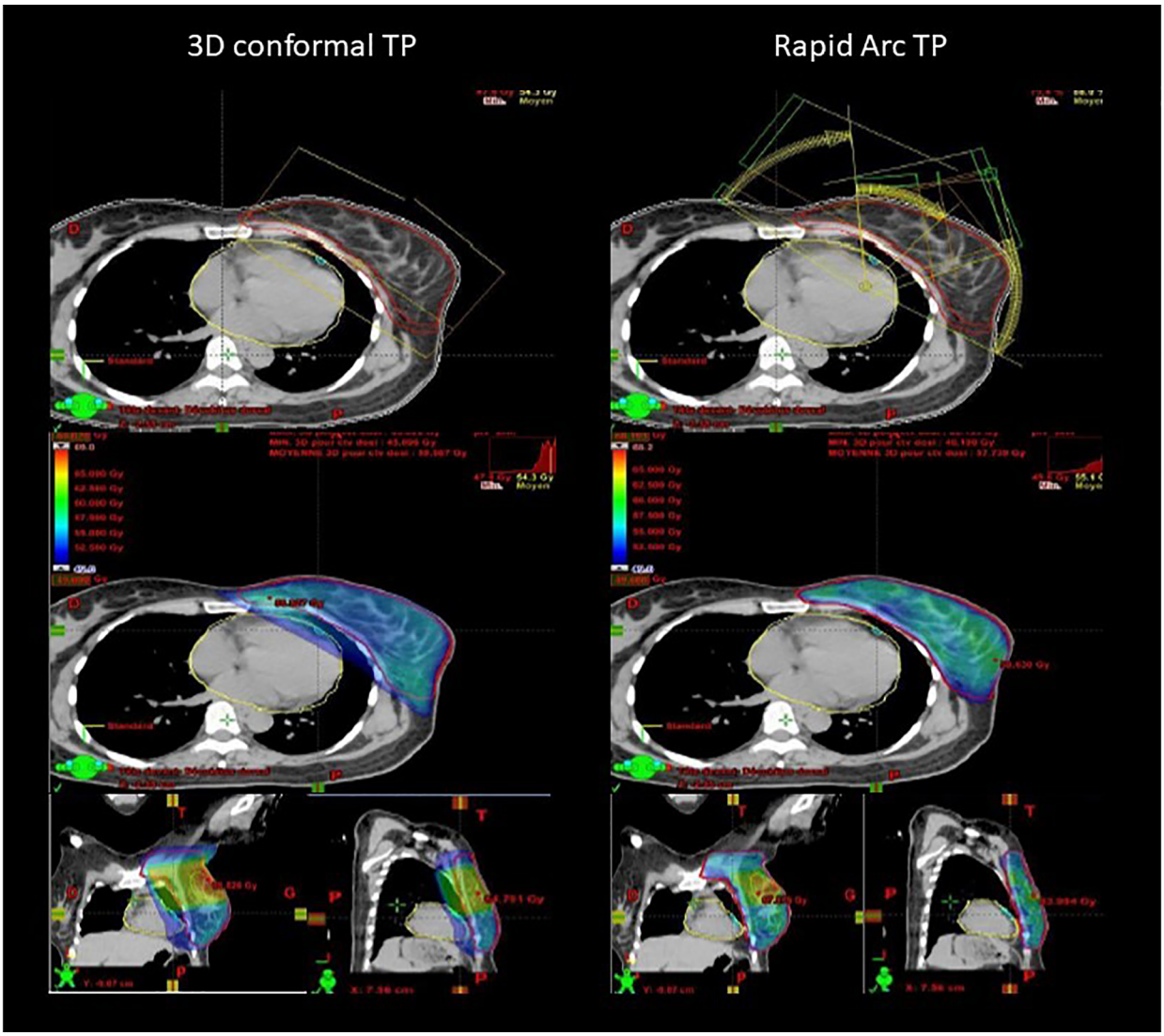

FIGURE 1
Example of comparison of 3D conformal (virtual) radiotherapy plan with tangent fields and RapidArc-based IMRT (real) plan with six partial rotation arcs to ensure the same target volume coverage (95% isodose displayed).

Our study found that the MHD is not the most appropriate dosimetric parameter for IMRT if we follow clinical rule defined for 3D CRT treatment: heart and LAD coronary artery dose distribution are significantly different in function of the radiotherapy technique (IMRT and 3D conformal radiotherapy), despite comparable MHD. In 3D technique, the MHD value is the result of a small volume receiving a high dose (upper 40Gy) combined with a very large volume of heart not irradiated. It is clear that there is a relationship between the portion of heart irradiated and the toxicity, but these last come from high dose region and the representation of a mean value is not the better way to represent it. Looking the volume of heart receiving dose upper 40 Gy is more representative to the real dose distribution and despite a generally higher D_{mean} with IMRT in clinical routine, the volume irradiated at high dose is significantly lower than in 3D CRT. This is clearly show in the study B for an equivalent MHD for the two techniques. Looking to 3D treatment in our study we try to convert a MHD value leading to clinical effects (as in Darby paper) into a portion of heart irradiated to high volume to define some limits for our optimization in inverse planning techniques (Figure 3).

Similarly results were reported by the BACCARAT study (ClinicalTrials.gov: NCT02605512) the aim of which was to determine predictive factors (circulating biomarkers and heart dosimetric parameters) of early radiation-induced subclinical cardiac dysfunction in patients with BC treated by 3D conformal radiotherapy (5). In this study, the MHD and mean LAD coronary artery dose were 2.9Gy and 15.7Gy, respectively. The authors observed that in patients with left-sided BC, the

10.3389/fonc.2022.1066915

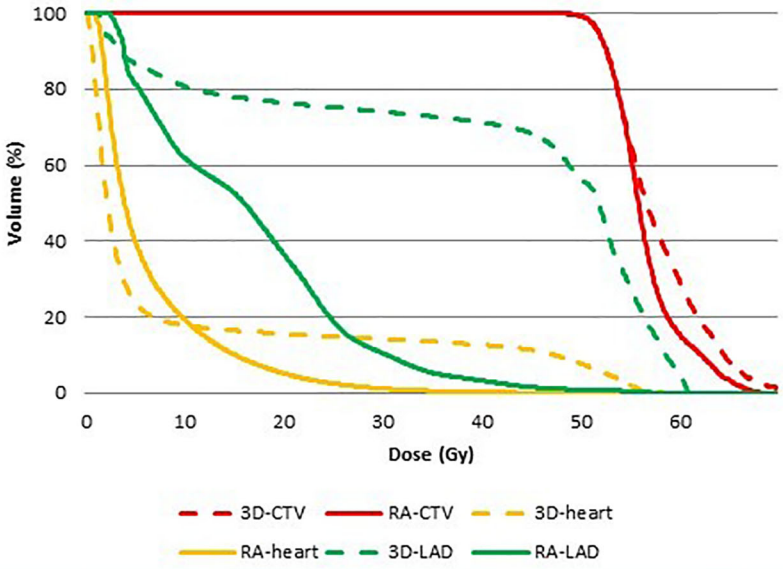

TREATMENT PLANNING		RapidArc	3D-conformal	P-value
Heart	Mean dose (Gy)	6.4	9.4	0.58
	V30Gy (%)	1.1	14.2	0.001
	V40Gy (%)	0.4	12.75	0.0005
	V45Gy (%)	0.1	11.4	0.0002
LAD	Mean dose (Gy)	17.1	41.1	0.003
	V15Gy (cc)	1.3	1.9	0.0009
	V30Gy (cc)	0.2	1.7	0.0005
	V40Gy (cc)	0.1	1.7	0.0001
	V45Gy (cc)	0	1.6	0.0001

FIGURE 2
Comparison of heart and LAD exposure in the radiotherapy plans (3D-conformal versus RapidArc-based IMRT) for similar target coverage. 3D, 3D-conformal; RA, RapidArc; CTV, clinical target volume; LAD, left anterior descending coronary artery.

correlation between MHD and left ventricle exposure was stronger (R^2 = 0.78) than between MHD and LAD coronary artery dose (R^2 = 0.67). Unlike the BACCARAT study, we found a strong polynomial (and not linear) correlation between MHD and LAD coronary artery exposure when using 3D conformal radiotherapy: with increasing doses to the heart, LAD coronary artery exposure progressively increased until it reached a threshold corresponding to the proportion of LAD within the tangent fields. To date, all studies on dosimetric parameters as predictive factors of radiation-induced cardiotoxicity used 3D conformal radiotherapy plan data. Due to the lack of long-term data on IMRT use in patients with BC and the risk of IHD occurrence in such patients, 3D-conformal radiotherapy planning constraints are routinely applied to IMRT treatment planning. The recent study by Loap and colleagues suggested similar observations (17): among the many cardiotoxicity predictive factors found in the literature (mean dose, maximum dose, V3Gy, V5Gy, V10Gy, V15Gy, D90% and D95%), IMRT MHD is not representative of the cardiac substructure exposure in the same way as 3D CRT.

Darby et al. report an increase by 7.4% of major coronary events for each 1Gy increment in the MHD, but we show in our study C that a small increase in the MHD value for 3D CRT technique is generated by a large increase of the heart volume

10.3389/fonc.2022.1066915

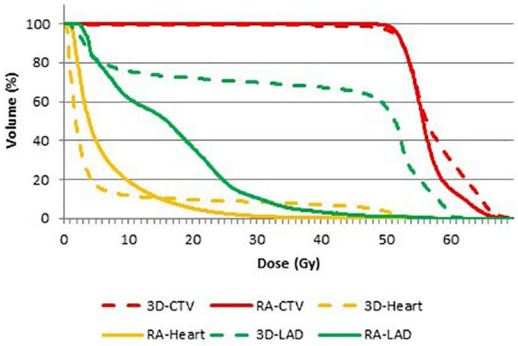

	MHD (Gy)	
	3D-TP	RA-TP
Patient 1	8.4	8.4
Patient 2	7.1	7.2
Patient 3	4.8	4.8
Patient 4	5.1	5.2
Patient 5	6.0	6.1
Patient 6	4.2	4.1
Patient 7	7.1	7.1
Patient 8	3.5	3.5
Patient 9	7.1	7.1
Patient 10	10.8	10.7

RADIOTHERAPY PLAN		RapidArc	3D conformal	P-value
Heart	Mean	6.4	6.4	-
	V5Gy (%)	39.6	17.1	0.00002
	V10Gy (%)	19.2	11.7	0.12
	V30Gy (%)	1.1	8.4	0.0006
	V40Gy (%)	0.4	7.1	0.0002
	V45Gy (%)	0.1	6.0	0.0001
LAD	Mean dose (Gy)	17.1	42.2	0.0007
	V5Gy (cc)	2.3	2.2	1
	V10Gy (cc)	1.6	2.1	0.24
	V30Gy (cc)	0.2	1.9	0.0004
	V40Gy (cc)	0.06	1.84	0.0002
	V45Gy (cc)	0.02	1.8	0.0001

FIGURE 3
Comparison of heart and LAD exposure in the radiotherapy plans (3D-conformal versus RapidArc-based IMRT) for similar intra-patient MHD. 3D, 3D-conformal; RA, RapidArc; CTV, clinical target volume; LAD, left anterior descending coronary artery; TP, treatment plan.

receiving high dose leading to the correlation between the volume of heart irradiated to *dose upper* 40 Gy with toxicity. Evolution of the mean dose in IMRT/VMAT treatment is not lead by the same dose distribution but more with low dose area.

Similar findings were recently reported for lung cancer. In a large retrospective cohort, LAD coronary artery dose exposure was related to severe adverse cardiac events, especially in patients without any history of coronary heart disease. IHD risk (HR=24.8) was significantly higher for patients with LAD coronary artery V15Gy ≥10% without but not with coronary heart disease history (18, 19). Moreover, a mean total coronary artery dose ≥7Gy increased the absolute risk of IHD in patients without coronary heart disease history by 5% in 1 year.

Here, we showed that MHD is not representative of the cardiac exposure: heart and LAD coronary artery dose distribution were significantly different in function of the radiotherapy technique, although MHD was the same, and IMRT significantly decreased heart and LAD coronary artery exposure to high dose. This indicates that using 3D conformal dosimetric constraints for IMRT is not the most appropriate strategy. Future studies are needed to correlate heart and its substructures exposure with prospective clinical data in order to generate appropriate surrogate in cardio-oncology field.

Last, a Sweden study using a national cardiac register assessed the long-term risk of IHD (defined as angina pectoris, acute myocardial infarction, complications due to myocardial infarction, and chronic IHD) after adjuvant radiotherapy, and observed that node irradiation (HR=1.46), post-mastectomy radiotherapy (HR=1.25), and the combination of endocrine therapies and chemotherapy (HR=1.35) increased the IHD risk in patients with left-sided BC (20). The authors reported high LAD coronary artery exposure (mean dose to the distal LAD coronary artery of 26.7Gy) and recommended to include LAD coronary artery radiation dose in radiotherapy plans, with the lowest possible dose. Minimizing the dose to the LAD coronary artery should decrease the risk of later radiation-induced stenosis.

Conclusion

IMRT techniques significantly reduce high dose exposure to OAR, while, in the meantime, spreading low dose to OAR compared to 3D techniques (where dose distribution is restricted

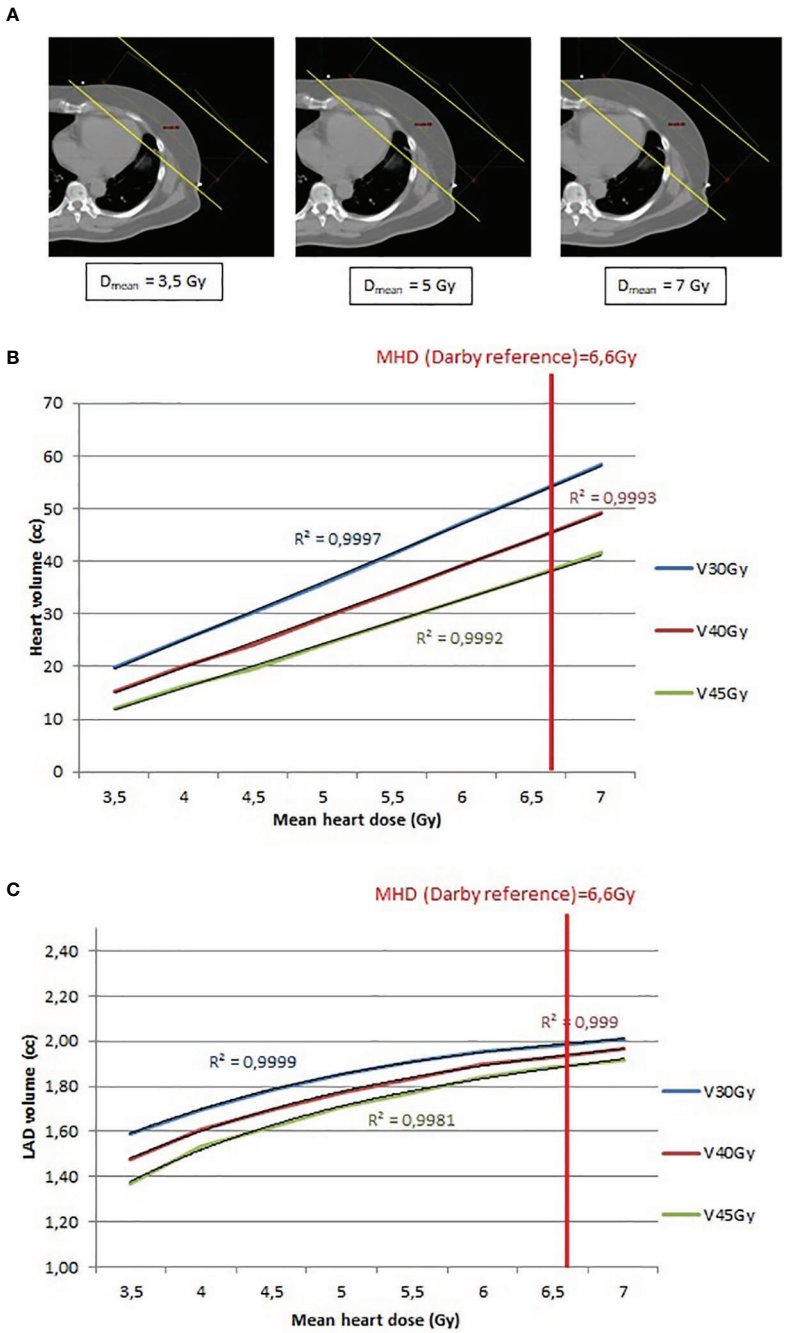

FIGURE 4
(A) Example of 3D tangent fields (yellow lines) plan recalculation to obtain a MHD between 3.5Gy and 7Gy, by step of 0.5Gy. **(B)** Relationship between heart volume (cc) and mean heart dose (Gy) and determination of the R^2 value. **(C)** Relationship between LAD coronary artery volume (cc) and mean heart dose (Gy) and determination of the R^2 value.

within treatment fields). Even though clinical heart event after BC is clearly correlated with the irradiation of the heart, we show that MHD issue from the cohort of patients irradiated with 3D technique is not directly transposable to modern radiotherapy delivery like IMRT or VMAT. Volume of heart (or substructures) receiving high dose region is certainly a better surrogate.

Data availability statement

The original contributions presented in the study are included in the article/Supplementary Material. Further inquiries can be directed to the corresponding authors.

Author contributions

CB, JP, and PF contribute to the conception, the design of the work; JP, PF, and SG to the acquisition, and analysis; CB, JP, and PF to the interpretation of data; all authors have drafted the work or substantively revised it. Each author has approved the submitted version and agreed both to be personally accountable for the author's own contributions.

Acknowledgments

Elisabetta ANDERMARCHER for English editing.

Conflict of interest

The authors declare that the research was conducted in the absence of any commercial or financial relationships that could be construed as a potential conflict of interest.

Publisher's note

Supplementary material

The Supplementary Material for this article can be found online at: https://www.frontiersin.org/articles/10.3389/fonc.2022.1066915/full#supplementary-material

SUPPLEMENTARY FIGURE 1
CT images showing the anatomy of the ten patients with left breast cancer included in this study. Patients had unfavorable cardiac anatomy (i.e. maximum heart depth ≥1.0 cm within the tangent fields; patients n=9) and/or unfavorable anatomy (pectus excavatum; patients n=1).

References

1. Clarke M, Collins R, Darby S, Davies C, Elphinstone P, Evans V, et al. Effects of radiotherapy and of differences in the extent of surgery for early breast cancer on local recurrence and 15-year survival: An overview of the randomised trials. *Lancet (London England)* (2005) 366:2087–106. doi: 10.1016/S0140-6736(05)67887-7

2. Kong F-M, Klein EE, Bradley JD, Mansur DB, Taylor ME, Perez CA, et al. The impact of central lung distance, maximal heart distance, and radiation technique on the volumetric dose of the lung and heart for intact breast radiation. *Int J Radiat Oncol Biol Phys* (2002) 54:963–71. doi: 10.1016/S0360-3016(02)03741-0

3. Darby SC, Ewertz M, Hall P. Ischemic heart disease after breast cancer radiotherapy. *N Engl J Med* (2013) 368:2527. doi: 10.1056/NEJMoa1209825

4. Taylor CW, Wang Z, Macaulay E, Jagsi R, Duane F, Darby SC, et al. Exposure of the heart in breast cancer radiation therapy: A systematic review of heart doses published during 2003 to 2013. *Int J Radiat Oncol Biol Phys* (2015) 93:845–53. doi: 10.1016/j.ijrobp.2015.07.2292

5. Jacob S, Camilleri J, Derreumaux S, Walker V, Lairez O, Lapeyre M, et al. Is mean heart dose a relevant surrogate parameter of left ventricle and coronary arteries exposure during breast cancer radiotherapy: A dosimetric evaluation based on individually-determined radiation dose (baccarat study). *Radiat Oncol* (2019) 14:29. doi: 10.1186/s13014-019-1234-z

6. Naimi Z, Moujahed R, Neji H, Yahyaoui J, Hamdoun A, Bohli M, et al. Cardiac substructures exposure in left-sided breast cancer radiotherapy: Is the mean heart dose reliable predictor of cardiac toxicity? *Cancer/Radiotherapie* (2021) 25:229–36. doi: 10.1016/j.canrad.2020.09.003

7. Huh SJ, Park W, Choi DH. Recent trends in intensity-modulated radiation therapy use in korea. *Radiat Oncol J* (2019) 37:249–53. doi: 10.3857/roj.2019.00577

8. Mayles WPM, Radiotherapy Development B. Survey of the availability and use of advanced radiotherapy technology in the uk. *Clin Oncol (Royal Coll Radiologists (Great Britain))* (2010) 22:636–42. doi: 10.1016/j.clon.2010.06.014

9. Shumway DA, Griffith KA, Pierce LJ, Feng M, Moran JM, Stenmark MH, et al. Wide variation in the diffusion of a new technology: Practice-based trends in intensity-modulated radiation therapy (imrt) use in the state of michigan, with implications for imrt use nationally. *J Oncol Pract* (2015) 11:e373–9. doi: 10.1200/JOP.2014.002568

10. Pierce LJ, Feng M, Griffith KA, Jagsi R, Boike T, Dryden D, et al. Recent time trends and predictors of heart dose from breast radiation therapy in a large quality consortium of radiation oncology practices. *Int J Radiat Oncol Biol Phys* (2017) 99:1154–61. doi: 10.1016/j.ijrobp.2017.07.022

11. Offersen BV, Boersma LJ, Kirkove C, Hol S, Aznar MC, Biete Sola A, et al. Estro consensus guideline on target volume delineation for elective radiation therapy of early stage breast cancer. *Radiotherapy Oncol J Eur Soc Ther Radiol Oncol* (2015) 114:3–10. doi: 10.1016/j.radonc.2014.11.030

12. Molina MA, Snell S, Franceschi D, Jorda M, Gomez C, Moffat FL, et al. Breast specimen orientation. *Ann Surg Oncol* (2009) 16:285–8. doi: 10.1245/s10434-008-0245-z

13. Bartelink H, Bourgier C, Elkhuizen P. Has partial breast irradiation by iort or brachytherapy been prematurely introduced into the clinic? *Radiotherapy Oncol J Eur Soc Ther Radiol Oncol* (2012) 104:139–42. doi: 10.1016/j.radonc.2012.07.010

14. Feng M, Moran JM, Koelling T, Chughtai A, Chan JL, Freedman L, et al. Development and validation of a heart atlas to study cardiac exposure to radiation following treatment for breast cancer. *Int J Radiat oncology biology Phys* (2011) 79:10–8. doi: 10.1016/j.ijrobp.2009.10.058

15. Tsai PF, Lin SM, Lee SH, Yeh CY, Huang YT, Lee CC, et al. The feasibility study of using multiple partial volumetric-modulated arcs therapy in early stage left-sided breast cancer patients. *J Appl Clin Med Phys* (2012) 13:3806. doi: 10.1120/jacmp.v13i5.3806

16. van den Bogaard VA, Ta BD, van der Schaaf A, Bouma AB, Middag AM, Bantema-Joppe EJ, et al. Validation and modification of a prediction model for acute cardiac events in patients with breast cancer treated with radiotherapy based on three-dimensional dose distributions to cardiac substructures. *J Clin Oncol Off J Am Soc Clin Oncol* (2017) 35:1171–8. doi: 10.1200/JCO.2016.69.8480

17. Loap P, Fourquet A, Kirova Y. Should we move beyond mean heart dose? *Int J Radiat oncology biology Phys* (2020) 107:386–7. doi: 10.1016/j.ijrobp.2020.02.017

18. Atkins KM, Chaunzwa TL, Lamba N, Bitterman DS, Rawal B, Bredfeldt J, et al. Association of left anterior descending coronary artery radiation dose with major adverse cardiac events and mortality in patients with non-small cell lung cancer. *JAMA Oncol* (2021) 7:206–19. doi: 10.1001/jamaoncol.2020.6332

19. Atkins KM, Bitterman DS, Chaunzwa TL, Kozono DE, Baldini EH, Aerts HJWL, et al. Mean heart dose is an inadequate surrogate for left anterior descending coronary artery dose and the risk of major adverse cardiac events in lung cancer radiation therapy. *Int J Radiat Oncol Biol Phys* (2021) 110(5):1473–147. doi: 10.1016/j.ijrobp.2021.03.005

20. Wennstig AK, Garmo H, Isacsson U, Gagliardi G, Rintelä N, Lagerqvist B, et al. The relationship between radiation doses to coronary arteries and location of coronary stenosis requiring intervention in breast cancer survivors. *Radiat Oncol* (2019) 14:40. doi: 10.1186/s13014-019-1242-z

frontiers | Frontiers in Oncology

TYPE Original Research
PUBLISHED 20 January 2023
DOI 10.3389/fonc.2023.1067500

OPEN ACCESS

EDITED BY
Mark Trombetta,
Allegheny Health Network, United States

REVIEWED BY
Samantha Dicuonzo,
European Institute of Oncology, Italy
Vishruta Dumane,
Icahn School of Medicine at Mount Sinai, United States

*CORRESPONDENCE
Mutlay Sayan
msayan@bwh.harvard.edu

SPECIALTY SECTION
This article was submitted to Radiation Oncology, a section of the journal Frontiers in Oncology

RECEIVED 11 October 2022
ACCEPTED 09 January 2023
PUBLISHED 20 January 2023

CITATION
Sayan M, Hathout L, Kilic SS, Jan I, Gilles A, Hassell N, Kowzun M, George M, Potdevin L, Kumar S, Sinkin J, Agag R, Haffty BG and Ohri N (2023) Reconstructive complications and early toxicity in breast cancer patients treated with proton-based postmastectomy radiation therapy.
Front. Oncol. 13:1067500.
doi: 10.3389/fonc.2023.1067500

Reconstructive complications and early toxicity in breast cancer patients treated with proton-based postmastectomy radiation therapy

Mutlay Sayan[1,2]*, Lara Hathout[3], Sarah S. Kilic[4], Imraan Jan[3], Ambroise Gilles[5], Natalie Hassell[5], Maria Kowzun[6], Mridula George[7], Lindsay Potdevin[6], Shicha Kumar[6], Jeremy Sinkin[5], Richard Agag[5], Bruce G. Haffty[3] and Nisha Ohri[3]

[1]Department of Radiation Oncology, Dana-Farber Cancer Institute and Harvard Medical School, Boston, MA, United States, [2]Department of Radiation Oncology, Brigham and Women's Hospital and Harvard Medical School, Boston, MA, United States, [3]Department of Radiation Oncology, Rutgers Cancer Institute of New Jersey, Rutgers University, New Brunswick, NJ, United States, [4]Department of Radiation Oncology, Taussig Cancer Institute, Cleveland Clinic, Cleveland, OH, United States, [5]Division of Plastic Surgery, Departments of Surgery, Rutgers Cancer Institute of New Jersey, Rutgers University, New Brunswick, NJ, United States, [6]Departments of Surgical Oncology, Rutgers Cancer Institute of New Jersey, Rutgers University, New Brunswick, NJ, United States, [7]Departments of Medicine, Rutgers Cancer Institute of New Jersey, Rutgers University, New Brunswick, NJ, United States

Background: Postmastectomy radiation therapy (PMRT) decreases the risk of locoregional recurrence and increases overall survival rates in patients with high-risk node positive breast cancer. While the number of breast cancer patients treated with proton-based PMRT has increased in recent years, there is limited data on the use of proton therapy in the postmastectomy with reconstruction setting. In this study, we compared acute toxicities and reconstructive complications in patients treated with proton-based and photon-based PMRT.

Methods: A retrospective review of our institutional database was performed to identify breast cancer patients treated with mastectomy with implant or autologous reconstruction followed by PMRT from 2015 to 2020. Baseline clinical, disease, and treatment related factors were compared between the photon-based and proton-based PMRT groups. Early toxicity outcomes and reconstructive complications following PMRT were graded by the treating physician.

Results: A total of 11 patients treated with proton-based PMRT and 26 patients treated with photon-based PMRT were included with a median follow-up of 7.4 months (range, 0.7-33 months). Six patients (55%) in the proton group had a history of breast cancer (3 ipsilateral and 3 contralateral) and received previous RT 38 months ago (median, range 7-85). There was no significant difference in mean PMRT (p = 0.064) and boost dose (p = 0.608) between the two groups. Grade 2 skin toxicity was the most common acute toxicity in both groups (55% and 73% in the proton and photon group, respectively) (p = 0.077). Three patients (27%) in the proton group developed grade 3 skin toxicity. No Grade 4 acute toxicity was

reported in either group. Reconstructive complications occurred in 4 patients (36%) in the proton group and 8 patients (31%) in photon group (p = 0.946).

Conclusions: Acute skin toxicity remains the most frequent adverse event in both proton- and photon-based PMRT. In our study, reconstructive complications were not significantly higher in patients treated with proton- versus photon-based PMRT. Longer follow-up is warranted to assess late toxicities.

KEYWORDS

carcinoma, mastectomy, proton, radiotherapy, breast

Introduction

The clinical indication for proton-based radiation therapy (RT) continues to grow for treatment of various cancers. This is mainly due to the dosimetric benefits of proton-based RT which includes a low to medium entrance dose and homogenous dose distribution within the target (1–3). In addition, protons have a steep fall-off to zero dose distally to the target, known as Bragg peak, resulting in a significant normal tissue sparing, which may potentially decrease the risk of toxicity. Although these unique characteristics of protons support its use, the clinical significance of proton-based RT has not been clearly demonstrated in breast cancer patients. The RADCOMP trial is currently investigating the efficacy and cardiovascular benefits of proton-based RT in patients with non-metastatic breast cancer.

Adjuvant RT is an important component in the multidisciplinary management of breast cancer patients. In the setting of post-mastectomy, patients with high-risk node positive breast cancer often receive adjuvant RT. Postmastectomy radiation therapy (PMRT) decreases the risk of locoregional recurrence and increases overall survival rates in patients with locally advanced disease as demonstrated in multiple randomized trials, as well as the Early Breast Cancer Trialists' Collaborative Group (EBCTCG) meta-analysis (4–7). More recently, with the increase in number of proton centers, the number of breast cancer patients treated with proton-based PMRT has increased. However, there is limited data on the use of proton therapy in the postmastectomy with reconstruction setting.

Given its significant impact on quality of life, identifying the risk factors for acute toxicities and reconstruction outcomes after PMRT is crucial. In this study, we compared acute toxicities and reconstructive complications in postmastectomy patients with implant or autologous reconstruction treated with proton-based PMRT and photon-based PMRT.

Materials and methods

A retrospective review of our institutional database was performed to identify breast cancer patients treated with adjuvant proton or photon therapy. Patients were eligible for this study if they had mastectomy with implant or autologous reconstruction and underwent radiation therapy. Patients who underwent breast-conserving surgery and those who had mastectomy without reconstruction were excluded.

Baseline clinical characteristics were collected and included patient age, race, body mass index (BMI), history of smoking, diabetes, history of prior breast cancer and treatment received. Disease-related characteristics including histology, hormone receptor status, AJCC T stage, and AJCC N stage were also recorded. Treatment related factors included type of breast reconstruction (implant vs. autologous), receipt of chemotherapy (neoadjuvant vs. adjuvant chemotherapy), hormonal therapy, and adjuvant radiation therapy (proton- vs. photon-based PMRT).

Early toxicity outcomes (fatigue, dermatitis, pain, and esophagitis) were graded by the treating physician during the treatment course using the National Cancer Institute Common Terminology Criteria for Adverse Events (CTCAE), version 3.0. Minor reconstruction complications included infection resolved with oral antibiotics, Baker grade ≤2 capsular contracture, or fat necrosis without need for revision. Major reconstruction complications included infection or exposure of implant requiring IV antibiotics and/or operation, Baker grade ≥3 capsular contracture or fat necrosis requiring revision.

Baseline characteristics between the two groups were compared using the Chi-squared or Fisher exact test for categorical variables and a t-test for metric variables. Statistical analyses were performed using SPSS statistical software version 25 (IBM Corp., Armonk, NY, USA).

Results

Eleven patients treated with proton therapy and 26 patients treated with photon therapy were included. Baseline patient characteristics are shown in Table 1. Median follow-up was 7.4 months (range, 0.7-33 months). There was no significant difference in age (p = 0.973), race (p = 0.405), laterality (p = 0.389), histology (p = 0.118), BMI ≥30 (p = 0.583), history of smoking (p = 0.228) and diabetes (p = 0.348) between the two groups. Six patients (55%) in the proton group had a history of breast cancer, of which 3 had ipsilateral and 3 had contralateral disease treated with radiation. For the three patients with a history of prior ipsilateral radiation therapy, all three patients had implant reconstruction in place at the time of proton radiation therapy. Each patient was treated with conventional fractionation in 1.8 Gy per fraction to a total dose of 4,320 to 5,750

TABLE 1 Baseline characteristics.

	Proton	Photon	p
Patient, n	11	26	
Age at diagnosis			
Mean, years	49.3	49.2	0.973
Race, n (%)			0.405
White	10 (91)	19 (73)	
Black or African American	1 (9)	4 (15)	
Asian	0	3 (12)	
Breast laterality, n (%)			0.389
Left	8 (73)	15 (58)	
Right	3 (27)	11 (42)	
Histology, n (%)			0.118
Invasive ductal carcinoma	11 (100)	21 (82)	
Invasive lobular carcinoma	0	5 (18)	
AJCC clinical T stage, n (%)			0.472
T1	2 (18)	4 (15)	
T2	6 (55)	8 (31)	
T3	2 (18)	11 (42)	
T4	1 (9)	3 (12)	
AJCC clinical N stage, n (%)			0.183
N0	3 (27)	2 (8)	
N1	4 (37)	15 (58)	
N2	3 (27)	3 (12)	
N3	1 (9)	6 (22)	
Receptor status, n (%)			
Estrogen receptor-positive	5 (45)	16 (62)	0.367
Progesterone receptor-positive	5 (45)	17 (65)	0.259
HER2/neu-amplified	3 (27)	6 (22)	0.267
History of smoking, n (%)	2 (18)	10 (38)	0.228
Diabetes, n (%)	2 (18)	2 (8)	0.348
BMI ≥30, n (%)	4 (37)	12 (46)	0.583
History of breast cancer, n (%)	6 (55)	0	<0.001
Ipsilateral, n (%)	3 (27)		
Treated with radiotherapy, n (%)	6 (55)	N/A	
Time since completion of radiotherapy			
Median, months (range)	38 (6.7-85.2)	N/A	
Follow-up			0.342
Median, months (range)	9.1 (2-29)	6.7 (0.7-33)	

BMI, Body mass index.

cGy. The chest wall and axilla were treated in all three patients. The patient treated to 5,750 cGy had mild late contracture; the other two patients had no late toxicity after proton radiation therapy. The median time between previous radiation and second course of RT was 38 months (range 7-85).

There was no difference in reconstruction types between the groups (p = 0.786). Treatment-related characteristics are shown in Table 2. The most common reconstruction type was implant (73% in proton and 77% in photon group). There was no significant difference in the mean PMRT dose (4797 cGy and 4986 cGy, p = 0.064) and boost dose (948 cGy vs 1033 cGy, p = 0.608) in the proton vs photon groups, respectively.

Treatment related toxicities are shown in Table 3. Grade 2 skin toxicity was the most common acute toxicity in both groups (55% in proton and 73% in photon) (p = 0.077). Three patients (27%) in the proton group developed Grade 3 skin toxicity. Grade 2-3 pain was reported by 45% of patients in the proton group while only Grade 2 pain was reported by 27% patients in the photon group (p = 0.077). Grade 2 fatigue was significantly higher in the proton group (45% vs 12%, p = 0.035). No Grade 4 acute toxicity was reported in either group. There was no significant difference in reconstructive complications between the groups (36% in proton vs 31% photon group, p = 0.946).

Discussion

Within a cohort of breast cancer patients treated with proton-based PMRT, we noted acceptable rates of acute toxicities and reconstructive complications that are not significantly higher compared to patients treated with photon-based PMRT.

Evaluation of the success of the breast reconstruction following PMRT is an important aspect of the treatment outcome. Photon-based PMRT to the reconstructed breast has a complication rate of 35%, including a Baker III or IV contracture rate of 38% in implant-based reconstructions (8, 9). Consensus guidelines regarding radiation therapy in the context of breast reconstruction provide important guidance for radiation oncologists (10). However, the data on reconstructive complications following proton-based PMRT, the subject of the present study, remains limited. Several prior small studies have investigated this topic. In a small study by Luo et al. including 27 patients treated with proton-based PMRT, reconstructive complications occurred in 27% including six patients with capsular contractures and one patient with implant infection (11). Similarly, Smith et al. reported a 39% reconstruction complication rate in 42 patients following proton-based PMRT (12). In a recent study by Naoum et al. proton-based PMRT significantly increased overall reconstruction failure when compared photon-based PMRT (53% vs 43%, p-value = 0.004) (13). In our study, the reconstruction complication rate was 36% following proton-based PMRT, which is comparable to the rates reported in prior studies, and not significantly different when compared to patients treated with photon-based PMRT.

A better understanding of the risk of complications might impact the decision on when to use proton-based therapy. Similar to the incidence of reconstruction complications, no significant difference in acute skin toxicity and pain was noted between the treatment groups. However, grade 3 skin toxicity was only reported in patients treated with proton-based PMRT. This is likely due to the increased skin

TABLE 2 Treatment-related characteristics.

	Proton (n:11)	Photon (n:26)	*p*
Type of breast reconstruction, n (%)			0.786
Implant	8 (73)	20 (77)	
Autologous	3 (27)	6 (23)	
Systemic therapy			
Chemotherapy[a]			0.033
Neoadjuvant	3 (27)	18 (69)	
Adjuvant	8 (73)	7 (27)	
Trastuzumab	4 (36)	5 (19)	0.226
Endocrine therapy	4 (36)	18 (69)	0.063
Radiation therapy parameters			
Mean dose (cGy)	4797	4986	0.064
Fraction number, mean	25	25	0.668
Boost, n (%)	4 (36)	18 (69)	0.063
Mean dose (cGy)	947.5	1033.3	0.608
Radiation Field Design			0.005
3-4 fields[b]	7 (64)	26 (100)	

[a]One patient in photon group did not receive chemotherapy.
[b]Supraclavicular field with or without a posterior axillary boost.

TABLE 3 Treatment related toxicities.

	Proton (n:11)	Photon (n:26)	p
Dermatitis, n (%)			0.077
Grade 2	6 (55)	19 (73)	
Grade 3	3 (27)	0	
Pain, n (%)			
Grade 2	3 (27)	7 (27)	0.077
Grade 3	2 (18)	0	
Fatigue, n (%)			
Grade 2	5 (45)	3 (12)	0.035
Esophagitis, n (%)			
Grade 2	1 (9)	0	
Reconstructive complication, n (%)			0.946
Minor[a]	1 (9)	2 (8)	
Major[b]	3 (27)	6 (23)	

[a]Minor = infection resolved with po antibiotic, Baker grade ≤2 capsular contracture, or fat necrosis without need for revision.
[b]Major = infection or exposure of implant requiring IV antibiotic and/or operation, Baker grade ≥3 capsular contracture or fat necrosis require revision.

surface dose with proton therapy. Better understanding the proton treatment planning and improvement in treatment delivery techniques such as pencil beam versus scattered beams can help improve the acute toxicity outcomes.

Limitations of our study include its small sample size, retrospective design, and inherent confounding factors that cannot be completely accounted for in a non-randomized study. In addition, another limitation is the lack of assessment of the cosmetic outcome which is an important part of the treatment success. An additional limitation is that the small sample size of the present study limited any meaningful analysis of the impact of implant size on toxicity. Furthermore, the definition of reconstruction complication and assessment is not universally agreed upon which limits the external validity when results are compared with published studies.

In patients with a history of thoracic irradiation, challenging anatomies, or left-sided disease requiring nodal irradiation, proton therapy can provide significant advantages. However, the benefits of proton-based PMRT must be weighed against its potential complications.

Conclusions

Our study reported similar rates of reconstructive complications and physician-reported toxicity in patients treated with proton-based and photon-based PMRT. Grade 3 skin toxicity was higher in the proton-based PMRT group. Despite being well tolerated, the benefit of proton-based PMRT is still investigational. For patients with left-side breast disease, challenging anatomies or history of previous radiation, proton-based PMRT is beneficial based on small retrospective studies while awaiting the results of the RADCOMP trial which will provide a better insight into the clinical benefits of proton therapy.

Data availability statement

The original contributions presented in the study are included in the article/supplementary material. Further inquiries can be directed to the corresponding author.

Ethics statement

The studies involving human participants were reviewed and approved by Rutgers Cancer Institute of New Jersey. Written informed consent for participation was not required for this study in accordance with the national legislation and the institutional requirements.

Author contributions

All authors listed have made a substantial, direct and intellectual contribution to the work, and approved it for publication.

Conflict of interest

The authors declare that the research was conducted in the absence of any commercial or financial relationships that could be construed as a potential conflict of interest.

Publisher's note

References

1. Pearlstein KA, Chen RC. Comparing dosimetric, morbidity, quality of life, and cancer control outcomes after 3D conformal, intensity-modulated, and proton radiation therapy for prostate cancer. *Semin Radiat Oncol* (2013) 23(3):182–90. doi: 10.1016/j.semradonc.2013.01.004

2. Bekelman JE, Lu H, Pugh S, Baker K, Berg CD, Berrington de González A, et al. Pragmatic randomised clinical trial of proton versus photon therapy for patients with non-metastatic breast cancer: the radiotherapy comparative effectiveness (RadComp) consortium trial protocol. *BMJ Open* (2019) 9(10):e025556. doi: 10.1136/bmjopen-2018-025556

3. Prasanna PG, Rawojc K, Guha C, Buchsbaum JC, Miszczyk JU, Coleman CN. Normal tissue injury induced by photon and proton therapies: Gaps and opportunities. *Int J Radiat Oncol Biol Phys* (2021) 110(5):1325–40. doi: 10.1016/j.ijrobp.2021.02.043

4. Overgaard M, Hansen PS, Overgaard J, Rose C, Andersson M, Bach F, et al. Postoperative radiotherapy in high-risk premenopausal women with breast cancer who receive adjuvant chemotherapy. Danish breast cancer cooperative group 82b trial. *N Engl J Med* (1997) 337(14):949–55. doi: 10.1056/NEJM199710023371401

5. Overgaard M, Jensen MB, Overgaard J, Hansen PS, Rose C, Andersson M, et al. Postoperative radiotherapy in high-risk postmenopausal breast-cancer patients given adjuvant tamoxifen: Danish breast cancer cooperative group DBCG 82c randomised trial. *Lancet* (1999) 353(9165):1641–8. doi: 10.1016/S0140-6736(98)09201-0

6. Felsten G, Wilcox K. Influences of stress and situation-specific mastery beliefs and satisfaction with social support on well-being and academic performance. *Psychol Rep* (1992) 70(1):291–303. doi: 10.2466/pr0.1992.70.1.291

7. Clarke M, Collins R, Darby S, Davies C, Elphinstone P, Evans V, et al. Effects of radiotherapy and of differences in the extent of surgery for early breast cancer on local recurrence and 15-year survival: An overview of the randomised trials. *Lancet* (2005) 366 (9503):2087–106. doi: 10.1016/S0140-6736(05)67887-7

8. Yun JH, Diaz R, Orman AG. Breast reconstruction and radiation therapy. *Cancer Control* (2018) 25(1):1073274818795489. doi: 10.1177/1073274818795489

9. El-Sabawi B, Sosin M, Carey JN, Nahabedian MY, Patel KM. Breast reconstruction and adjuvant therapy: A systematic review of surgical outcomes. *J Surg Oncol* (2015) 112 (5):458–64. doi: 10.1002/jso.24028

10. Meattini I, Becherini C, Bernini M, Bonzano E, Criscitiello C, De Rose F, et al. Breast reconstruction and radiation therapy: An Italian expert Delphi consensus statements and critical review. *Cancer Treat Rev* (2021) 99:102236. doi: 10.1016/j.ctrv.2021.102236

11. Luo L, Cuaron J, Braunstein L, Gillespie E, Kahn A, McCormick B, et al. Early outcomes of breast cancer patients treated with post-mastectomy uniform scanning proton therapy. *Radiother Oncol* (2019) 132:250–6. doi: 10.1016/j.radonc.2018.10.002

12. Smith NL, Jethwa KR, Viehman JK, Harmsen WS, Gonuguntla K, Elswick SM, et al. Post-mastectomy intensity modulated proton therapy after immediate breast reconstruction: Initial report of reconstruction outcomes and predictors of complications. *Radiother Oncol* (2019) 140:76–83. doi: 10.1016/j.radonc.2019.05.022

13. Naoum GE, Ioakeim MI, Shui AM, Salama L, Colwell A, Ho AY, et al. Radiation modality (Proton/Photon), timing, and complication rates in patients with breast cancer receiving 2-stages Expander/Implant reconstruction. *Pract Radiat Oncol* (2022) 12 (6):475–86. doi: 10.1016/j.prro.2022.05.017

frontiers | Frontiers in Oncology

TYPE Original Research
PUBLISHED 17 March 2023
DOI 10.3389/fonc.2023.1122093

OPEN ACCESS

EDITED BY
Nisha Ohri,
Rutgers, The State University of New Jersey, United States

REVIEWED BY
Mariacarla Valli,
Oncology Institute of Southern Switzerland (IOSI), Switzerland
Mutlay Sayan,
Dana–Farber Cancer Institute, United States

*CORRESPONDENCE
Imjai Chitapanarux
imjai@hotmail.com;
imjai.chitapanarux@cmu.ac.th

SPECIALTY SECTION
This article was submitted to Breast Cancer, a section of the journal Frontiers in Oncology

RECEIVED 23 December 2022
ACCEPTED 08 March 2023
PUBLISHED 17 March 2023

CITATION
Chitapanarux I, Nobnop W, Onchan W, Klunklin P, Nanna T, Sitathanee C, Kulpisitthicharoen S and Sripan P (2023) Hypofractionated whole breast irradiation with simultaneous integrated boost in breast cancer using helical tomotherapy with or without regional nodal irradiation: A report of acute toxicities. *Front. Oncol.* 13:1122093. doi: 10.3389/fonc.2023.1122093

Hypofractionated whole breast irradiation with simultaneous integrated boost in breast cancer using helical tomotherapy with or without regional nodal irradiation: A report of acute toxicities

Imjai Chitapanarux[1,2]*, Wannapha Nobnop[1,2], Wimrak Onchan[1,2], Pitchayaponne Klunklin[1,2], Thongtra Nanna[3], Chomporn Sitathanee[3], Sutthisak Kulpisitthicharoen[4] and Patumrat Sripan[5]

[1]Division of Radiation Oncology, Faculty of Medicine, Chiang Mai University, Chiang Mai, Thailand, [2]Northern Thai Research Group of Radiation Oncology (NTRG-RO), Faculty of Medicine, Chiang Mai University, Chiang Mai, Thailand, [3]Division of Radiation Oncology, Faculty of Medicine, Ramathibodi Hospital, Bangkok, Thailand, [4]Division of Radiation Oncology, Lopburi Cancer Hospital, Lopburi, Thailand, [5]Research Institute for Health Sciences, Chiang Mai University, Chiang Mai, Thailand

Purpose: We prospectively investigated the acute toxicities focusing on skin and hematologic function in breast cancer patients who received hypofractionated whole breast irradiation with simultaneous integrated boost (HF-WBI-SIB) with helical tomotherapy (HT), with or without regional nodal irradiation (RNI).

Methods: The dose of WBI and RNI was 42.4 Gy in 16 fractions. Tumor bed was prescribed to 49.6 Gy in 16 fractions simultaneously. The association between the worst grade of acute toxicities during treatment and receiving RNI was analyzed. The integral dose to the whole body between the two groups was also compared.

Results: Between May 2021 and May 2022, 85 patients were enrolled; 61 patients received HF-WBI-SIB only (71.8%) and 24 patients (28.2%) received HF-WBI-SIB with RNI. Grade 2 acute skin toxicity was found in 1.2%. The most frequent grade 2 or more hematologic toxicity was leukopenia, which occurred in 4.8% and 11% in the 2nd and 3rd week, respectively. Mean whole body integral dose was significantly higher in patients treated with RNI compared to patients treated without RNI: 162.8 $\pm$ 32.8 *vs*. 120.3 $\pm$ 34.7 Gy-L (p-value < 0.001). There was no statistically significant difference in acute grade 2 or more skin and hematologic toxicities between the two groups.

Conclusions: HF-WBI-SIB with or without RNI is feasible with acceptable acute skin and hematologic toxicities. RNI and whole body integral dose were not associated with these acute toxicities.

KEYWORDS

regional nodal irradiation (RNI), simultaneous integrated boost (SIB), hypofractionation, breast cancer, helical tomotherapy (HT), acute toxicities

Introduction

Radiotherapy (RT) plays an important role in the treatment of breast cancer patients undergoing breast-conserving surgery (BCS). RT improves both local control and breast cancer specific survival as shown by a meta-analysis of 17 trials, most of them using conventional fractionation (1). Phase III randomized trials investigating hypofractionated (HF) dose delivery for whole breast irradiation (WBI) demonstrated equivalence with conventional fractionation (CF) both in clinical outcomes and toxicity profiles (2, 3).

Our previous study of HF radiotherapy using Helical TomoTherapy (HT) to the chest wall/breast with/without regional nodal irradiation (RNI) demonstrated excellent 3-year locoregional failure-free survival (LRFFS) and minimal acute and late toxicities (4). HF with simultaneous integrated boost (SIB) has been studied and seems to be practical and safe (5). A phase II study using Volumetric Modulated Radiation Therapy (VMAT) for hypofractionated whole breast irradiation with simultaneous integrated boost (HF-WBI-SIB) confirmed the safety and reported good cosmetic results, even in patients who received adjuvant systemic therapy (5, 6). The latest comparative dosimetric study (7), demonstrated that HF-WBI-SIB using HT with TomoEdge offered a significantly lower mean equivalent dose in 2-Gy fractions (EQD2) to OARs and showed no significant difference between HF-SIB and sequential boost. Both HF-SIB and normally fractionated SIB (N-SIB) conformed significantly better to the breast and boost planning target volumes (PTV) than both sequential boost techniques.

HT, a fan beam intensity modulated radiotherapy (IMRT) technique, characterized by a helical movement of the beam delivery, provides satisfactory target coverage and doses to the surrounding organs at risk (OARs). However, it can cause a larger volume of normal tissue in the treated area and whole body to receive low radiation doses as a result of the longer beam on times (8). The increase in normal tissue integral dose caused by IMRT has given concern for radiation-induced secondary malignancies (9). Studies on this issue in patients treated with HT show mixed results: some have found an increase of the integral dose with HT (10, 11) while others found contradicting results with no increase of the integral dose with HT as compared to conventional IMRT techniques, and in some cases even a slight decrease (12, 13).

To our knowledge, all previous HF-WBI-SIB trials excluded patients who needed RNI. We conducted a prospective multicenter study on HF-WBI-SIB in breast cancer patients after breast conserving surgery treated by HT, to which we also added RNI when indicated. In the present report, we assess the acute toxicities and calculate the integral dose to the whole body in breast cancer patients who received HF-WBI-SIB with or without RNI using HT. The association between integral dose and acute toxicities is also explored. Treatment outcome, which includes field boost recurrence (IFBR) rate (tumor recurrence in boost area), locoregional recurrence (LRR) rate (tumor recurrent in ipsilateral breast and/or regional lymph node area), cosmetic results, and late toxicities will be reported after a longer follow-up.

Material and methods

Patients

This phase II prospective study was registered with the Thai Clinical Trials Registry (TCTR20210623004) and was approved by the institutional review board at each of the three contributing centers: Chiang Mai University (Chiang Mai), Ramathibodi Hospital (Bangkok), and Lopburi Cancer Hospital (Lopburi). All patients provided written informed consent. Eligible patients were patients who received breast conserving surgery (BCS) for a pathologically confirmed invasive ductal carcinoma, had surgical margins free from both invasive carcinoma and ductal carcinoma *in situ* (DCIS), were age ≥ 18 years, with ECOG performance status 0 or 1. All patients had an indication for tumor bed boost according to institutional protocols (age < 50 years or age > 50 years with high-risk features). The tumor bed had to be clearly identified (preferred by radiopaque clips). Patients who needed regional nodal irradiation (RNI) were allowed in this study. We excluded patients who had bilateral breast cancer, had extensive postoperative seroma at the commencement of RT, and patients who met all the following criteria: age > 70, T1, N0, ER+, low-intermediate grade, margin ≥ 2mm.

Radiotherapy

All patients underwent a three-dimensional simulation procedure in the supine position on a wing board (CIVCO, USA)

with both arms up above the head. Computed tomography (CT) was performed with a slice thickness of 5 mm, using radiopaque wires to define the scars and field borders on the patients' skin during CT-simulation. The entire mammary gland constituted the clinical target volume (CTV) of the whole breast (WB). The tumor bed plus 1 cm added to the surgical clips placed in the lumpectomy cavity constituted the CTV of the boost. A five-millimeter margin was added to form the planning target volumes (PTV) for each of these CTVs. The ribs and lung tissue were excluded from the PTV. To reduce the potential for skin reactions and dose inhomogeneity, breast PTV was restricted to a depth of 3 mm under the skin surface. We followed the Radiation Therapy Oncology Group (RTOG) atlas to contour CTV/PTV (14). We prescribed the radiation dose with the SIB technique for 16 fractions with 2.65 Gy/fraction to a total dose of 42.4 Gy for the PTV WB, and 3.1 Gy/fraction to a total dose of 49.6 Gy to the PTV boost. For the patients who received RNI, the PTV for the lymph nodes was separated and prescribed at 2.65 Gy/fraction to a total of 42.4 Gy. HT treatment plans were created using a jaw width of 5.0 cm, a pitch of 0.287, and a modulation factor of 3.0. We created a directional block to limit the entrance dose to the following OARs: the bilateral lungs, the contralateral breast, the heart, and the left anterior descending coronary artery (LAD). Plan objectives, concerning target coverage and homogeneity, were as follows: near-to-minimum dose $D_{98\%}$ >95%, near-to-maximum dose $D_{2\%}$ <107% for PTV WB and RNI (where $D_{x\%}$ was the dose delivered to at least or at most x %). The dose parameters for OARs are shown in Table 1 where Vx_{Gy} was the volume receiving at least xGy. Integral dose, which is the volume integral of the dose deposited in each patient, was explored. The whole body integral dose is defined as the mean dose in Gray (Gy) of the entire volume of all slices where PTV existed plus 2 cm superior and inferior to the PTV, multiplied by the volume of the whole body in Liter (L) (13, 15).

Radiotherapy started within 6 weeks after the last dose of chemotherapy. Clinical assessment for acute skin and hematologic toxicities were assessed once a week during RT using the RTOG/EORTC acute radiation morbidity score (16). Our endpoints of interest were the worst grade of acute skin toxicity and the nadirs of white blood cell (WBC), hemoglobin and platelets, defined as the least value occurring between the start of RT and the end of RT.

Statistical analysis

A descriptive analysis was performed to calculate proportions and frequencies of patient and treatment characteristics, while medians with interquartile ranges (IQR) were calculated for the age of patient. A mean with standard deviation (SD) was calculated for the integral dose and dosimetric characteristics. Acute skin and hematologic toxicities were assessed as frequency and percentages per grade. The association between the worst grade of acute toxicities during treatment (week 1, week 2 and week 3) and receiving RNI, considered as a binary variable was analyzed using the Fisher exact test. The Wilcoxon-Mann-Whitney test was used to compare the integral dose and dosimetric characteristics between groups of patients who received HF-WBI-SIB using HT, with or without RNI respectively. Analyses were performed using STATA software version 16 (Stata Corp, College Station, TX).

TABLE 1 Dose constraint for organ at risk (OARs) in this study.

OAR	Acceptable	
	WBI	WBI + RN
Heart (Right Breast)	D_{max} < 20 Gy V_{8Gy} < 15%	$D_{15\%}$ < 10 Gy $D_{20\%}$ < 8 Gy D_{mean} < 9 Gy
Heart (Left Breast)	$D_{5\%}$ < 20 Gy V_{8Gy} < 35%	$D_{15\%}$ < 10 Gy $D_{20\%}$ < 8 Gy D_{mean} < 9 Gy
Left anterior descending coronary artery (LAD)	–	D_{mean} < 9.7 Gy $D_{1\%:}$ < 16.1 Gy
Ipsilateral lung	V_{16Gy} < 20% V_{8Gy} < 40%	$D_{15\%}$ < 31 Gy $D_{20\%}$ < 26.4 Gy $D_{35\%}$ < 17.6 Gy $D_{50\%}$ < 13 Gy
Contralateral lung	V_{4Gy} < 15%	$D_{20\%}$ < 13 Gy $D_{35\%}$ < 10.6 Gy $D_{50\%}$ < 9 Gy
Contralateral breast	D_{max} < 2.64 Gy	$D_{15\%}$ < 17.6 Gy $D_{20\%}$ < 9 Gy $D_{35\%}$ < 6 Gy $D_{50\%}$ < 4.4 Gy
Esophagus	–	D_{max} < 15 Gy

Results

Between May 2021 and May 2022, 85 patients were enrolled from 3 radiotherapy centers: 61 patients received HF-WBI-SIB only (71.8%) and 24 patients (28.2%) received HF-WBI-SIB with RNI. The median age was 53 years (IQR: 45-59, Range: 32-73). Over 90% of patients had stage I and II disease and only 9% had stage III disease. HER2-/HR+ was the most common subtype (64.7%) followed by HER2+/HR+, HER2 enriched, and triple negative. Most of the patients in this study had received previous adjuvant chemotherapy (85.9%) with an anthracycline-based regimen. There was no statistically significant difference in the mean PTV volume between patients who received HF-WBI-SIB without RNI (824.4 ± 339.8 cm^3) and those with RNI (991.5 ± 494.1 cm^3), p= 0.12. The whole body integral dose in the group of patients receiving HF-WBI-SIB with RNI was significantly higher than the group without RNI (p- value <0.001). The patients and treatment characteristics are summarized in Table 2.

Regarding the target coverage, following the International Commission on Radiological Units and Measurements (ICRU) no. 83, all plans were approved when the near-to-maximum dose $D_{2\%}$ was less than 53.1 Gy (107% of the prescription for PTV boost) and the near-to-minimum dose $D_{98\%}$ was more than 47.1 Gy (95% of the prescription for PTV boost) and 40.3 Gy (95% of the prescription for PTV WB), respectively.

Pre-radiotherapy hematological data of our patients was recorded. All patients had no thrombocytopenia. One patient (1.2%) had grade 1 anemia, while grade 1, 2, and 3 leukopenia were found in 9 patients (10.6%), 1 patient (1.2%), and 1 patient (1.2%), respectively.

We found that the compliance of this RT scheme was very good: all patients could complete their treatment. Grade 2 acute skin toxicity was found in 1 patient (1.2%) during the 3rd week of treatment. The most frequent hematologic toxicity was leukopenia. We found grade 2 leukopenia in 4 patients (4.8%) during the 2nd week, which increased to 9.8% in the 3rd week of treatment. Grade 3 leukopenia was demonstrated in 1 patient (1.2%) at the 3rd week, for this patient the treatment needed to be delayed. Figure 1 shows the acute skin and hematologic toxicity during the 3 weeks of treatment in all patients. There was no statistically significant difference in both acute severe (grade ≥2) skin and hematologic toxicities between patients who received RNI and those who did not, as shown in Figure 2.

Discussion

Our present multicenter prospective phase II study, using HF-WB-SIB for 16 fractions with 2.65 Gy/fraction to a total dose of 42.4 Gy for the PTV WB and RNI, and 3.1 Gy/fraction to a total dose of 49.6 Gy to the PTV boost, revealed acceptable rates of acute skin and hematologic toxicities. HF-WB-SIB (without RNI) was investigated in many prospective studies and reported satisfactory result on early acute toxicities. A prospective phase III randomized controlled trial by Paelinck et al. (17) compared the acute toxicities between HF-WBI with a sequential boost (40.05 Gy/15 fractions + 10 Gy/4 fractions in negative surgical margins or 14.88 Gy/6 fractions in positive margins) or SIB (42.4/46.8 and 49.95 Gy/15 fractions in negative and positive margin, respectively) planning by VMAT and irradiated in prone position. They also reported that HF-WBI-SIB had significantly lower grade 2/3 dermatitis and pruritus. Focusing only on their SIB arm, grade 2 or 3 dermatitis was found in 24/83 patients (28%) which was much higher than in our study which reported grade 2 in only 1.2% and no grade 3 toxicity. When considering the circumstances, the PTV volume of their study did not differ from our PTV volume (in the breast without RNI group). We hypothesize that the prone position in their study could be the cause of more severe skin toxicity, compared to the supine position. However, the authors also indicated a limitation in their scoring of toxicity, which relied on subjective grading.

A phase I/II study from India (18) performed HF-WBI-SIB with 40.5 and 48 Gy in 15 fractions with VMAT in 10 patients. They reported satisfactory PTV coverage and OAR sparing. The most common acute toxicities were grade 1 dermatitis. Grade 2 skin toxicities were found in 2 patients (20%). This study had also higher grade 2 acute skin toxicity than ours. This might due to the small number of patients and the fact that the mean volume of PTV whole breast and boost was higher than in our patients (1015.08 cm^3 versus 824.4 cm^3 in our breast without RNI group). Their margin of CTV boost was an additional 1.5 cm margin from the surgical bed, whereas 1 cm was used in our study. VMAT-SIB hypofractionation was investigated by De Rose et al. (5). They reported 8% of grade 2 RTOG acute toxicity which were found in the last week of treatment, which is comparable to our findings. However, no grade 2 patient in their study had moist desquamation while we found this in 1 patient (1.2%). The latest multicenter prospective phase II study from Germany (RO-2013-04, NCT01948726) (19) reported the outcome of HF-WBI-SIB using 40/48 Gy in 16 fractions. Grade 2 or more skin toxicity was found in 14.7% which was also higher than our study. More than half of the patients (58.7%) in this study received 3D-CRT, which could be an explanation for the increased occurrence of toxicities.

As a consequence of enrolling the patients who need RNI in our study (28.2%), the percentage of patients who had prior chemotherapy before RT in our study was the highest (85.9%) when compared to 34% in a German trial (19) and 32% in a Belgian study (17). Almost of our patients (85.9%) received anthracycline-based chemotherapy which has myelosuppression as a side effect. Eleven patients (13.0%) had leukopenia and 1 patient (1.2%) had anemia before starting radiotherapy. However, we found that the number of acute grade 2 or more hematologic toxicities was still increasing during the treatment. Grade 2 anemia was demonstrated in 2.5% in the 1st week and 3.7% in the 3rd week of treatment. Grade 2 leukopenia was found in 4.8% in the 2nd week and increased to 9.8% in the 3rd week. We also had grade 3 leukopenia in 1 patient (1.2%) in the last week of treatment. The incidence of severe grade hematologic toxicities was higher in the patient group who received

TABLE 2 Patient and treatment characteristics.

Variables	N (%)
Age (years) Median = 53 (IQR: 45-59, Range: 32-73)	
<40	11 (12.9)
41-50	25 (29.4)
51-60	31 (36.5)
>60	18 (21.2)
Smoking	
YES	0 (0.0)
NO	85 (100.0)
BMI (kg/m2)	
<18.5	6 (7.0)
18.5-24.9	48 (56.5)
25-29.9	18 (21.2)
>30	13 (15.3)
Underlying cardiac disease	
YES	6 (7.0)
NO	79 (93.0)
AJCC stage	
I	37 (43.5)
II	40 (47.1)
III	8 (9.4)
Subtype	
HER2-/HR+	55 (64.7)
HER2+/HR+	14 (16.5)
HER2+/HR−	5 (5.9)
HER2−/HR−	11 (12.9)
Chemotherapy	
YES	73 (85.9)
AC4	41 (56.1)
FAC6	8 (11.0)
AC4T4	24 (32.9)
NO	12 (14.1)
Hormonal therapy	
YES	67 (78.8)
Tamoxifen	42 (62.7)
Aromatase inhibitor	25 (37.3)
NO	18 (21.2)
Regional nodal irradiation (RNI)	
YES	24 (28.2%)
NO	61 (71.8%)
PTV Volume (Mean ± SD) (cm3)	
Breast only	824.4 ± 339.8
Breast + RNI	991.5 ± 494.1
Whole body Integral dose (Mean ± SD) (Gy-L)	
Breast only	120.3 ± 34.7
Breast + RNI	162.8 ± 32.8

RNI (4.2% *vs* 3.3% for grade ≥ 2 anemia and 16.7% *vs* 8.2% for grade ≥2 leukopenia). However, no statistically significant difference was demonstrated between these two groups. Due to the lack of reports on acute hematologic toxicities in most HF-SIB breast cancer studies, we were unable to compare our results. All studies (17–19) reported the acute skin toxicities but not the hematological toxicities. However, the incidence of severe grade hematologic toxicities in our study was very low and caused a delay of treatment in only 1 patient.

The integral dose to the whole body due to the large treatment volume of HF-WBI-SIB using HT has given concern for higher rates of acute hematologic toxicity. There is limited data about regarding the whole body integral dose for hypofractionated breast treatment by HT. Karpf et al. (20) compared the normal tissue integral dose (NTID) for tangential techniques between IMRT and VMAT. The IMRT technique significantly reduced NTID by 19% (p = 0.000005). Phurailatpam et al. (21) compared the whole-body integral dose for bilateral breast treatment between VMAT and HT. The whole-body integral dose was found to be comparable with no statistically significant variation between two techniques: 289 Gy kg (VMAT) versus 299 Gy kg (HT) (p-value 0.24). Our results reported a significantly higher whole body integral dose in the group of HF-WBI-SIB with RNI compared to the group without RNI (increase by 26.1%). Nevertheless, no statistically significant difference in hematologic toxicities was found between the two groups. Even though the higher whole body integral dose did not affect the acute toxicities, late toxicities should be close monitored in a long-term follow-up. We are also waiting for the report of acute and late toxicities and long-term outcomes in a large German phase III study comparing HF-WB-SIB to normal fractionation and/or sequential boosts (NCT02474641), enrolling more than 2,000 patients.

To the extent of our knowledge, even though there are some reports on HF-WBI-SIB, ours is the first study to explore HF-WBI-SIB with RNI. Moreover, we also investigated the whole-body integral dose and its association with acute hematologic toxicity. This phase II study did not compare HF-WBI-SIB to other SIB techniques, conventional fractionation, or other HF regimens, which can be considered one of its main limitations. Due to the short follow up time, we could not report the cosmetic outcome.

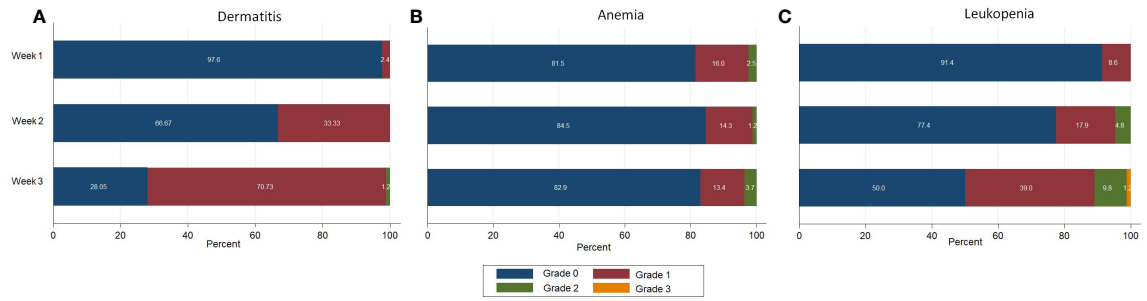

FIGURE 1
Acute toxicities during treatment in all patients. **(A)** Dermatitis **(B)** Anemia **(C)** Leukopenia.

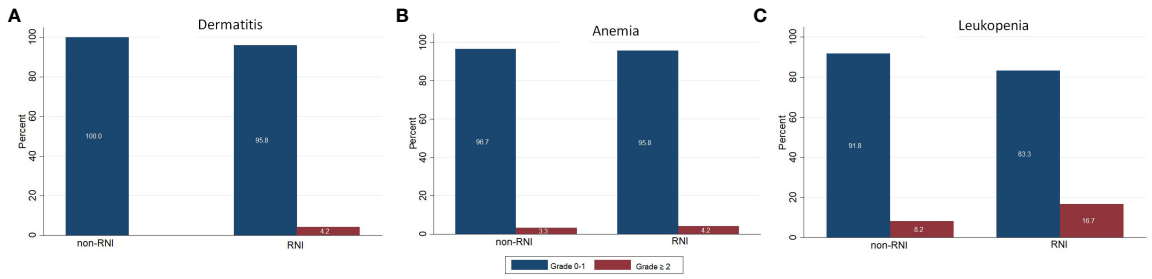

FIGURE 2
Comparing of acute toxicities between patients received and not received regional nodal irradiation. **(A)** Dermatitis **(B)** Anemia **(C)** Leukopenia.

The study is ongoing and we will address the treatment outcome, cosmesis, and late toxicities in a subsequent report.

Conclusion

Based on our data, HF-WBI-SIB with or without RNI could be offered after breast conserving surgery and adjuvant chemotherapy. This scheme was feasible with acceptable acute skin and hematologic side effects.

Data availability statement

The raw data supporting the conclusions of this article will be made available by the authors, without undue reservation.

Ethics statement

The studies involving human participants were reviewed and approved by The Research Ethics Committee of Faculty of Medicine, Chiang Mai University, Ramathibodi Hospital, and Lopburi Cancer Hospital. The patients/participants provided their written informed consent to participate in this study.

Author contributions

IC initiated and coordinated the study, interpreted the data, and wrote the manuscript. WN calculated the dose, analyzed the data, and wrote the manuscript. PS performed the statistical analysis. WO, PK, TN, CS, and SK performed clinical data acquisition. All authors contributed to the article and approved the submitted version.

Conflict of interest

The authors declare that the research was conducted in the absence of any commercial or financial relationships that could be construed as a potential conflict of interest.

Publisher's note

References

1. Darby S, McGale P. Effect of radiotherapy after breast conserving surgery on 10-year recurrence and 15-year breast cancer death: meta-analysis of individual patient data for 10,801 women in 17 randomised trials. *Lancet* (2011) 378:1707–16. doi: 10.1016/S0140-6736(11)61629-2

2. Haviland JS, Owen JR, Dewar JA, Agrawal RK, Barrett J, Barrett-Lee PJ, et al. The UK standardisation of breast radiotherapy (START) trials of radiotherapy hypofractionation for treatment of early breast cancer: 10-year follow-up results of two randomised controlled trials. *Lancet Oncol* (2013) 14:1086–94. doi: 10.1016/S1470-2045(13)70386-3

3. Whelan TJ, Pignol JP, Levine MN, Julian JA, MacKenzie R, Parpia S, et al. Long-term results of hypofractionated radiation therapy for breast cancer. *N Engl J Med* (2010) 362:513–20. doi: 10.1056/NEJMoa0906260

4. Chitapanarux I, Nobnop W, Tippanya D, Sripan P, Chakrabandhu S, Klunklin P, et al. Clinical outcomes and dosimetric study of hypofractionated helical TomoTherapy in breast cancer patients. *PLoS One* (2019) 14(1):e0211578. doi: 10.1371/journal.pone.0211578

5. De Rose F, Fogliata A, Franceschini D, Navarria P, Villa E, Iftode C, et al. Phase II trial of hypofractionated VMAT-based treatment for early stage breast cancer: 2-year toxicity and clinical results. *Radiat Oncol* (2016) 11:120. doi: 10.1186/s13014-016-0701-z

6. De Rose F, Fogliata A, Franceschini D, Iftode C, Navarria P, Comito T, et al. Hypofractionation with simultaneous boost in breast cancer patients receiving adjuvant chemotherapy: A prospective evaluation of a case series and review of the literature. *Breast* (2018) 42:31–7. doi: 10.1016/j.breast.2018.08.098

7. Zwicker F, Hoefel S, Kirchner C, Huber PE, Debus J, Schempp M. Hypofractionated radiotherapy with simultaneous-integrated boost after breast-conserving surgery compared to standard boost-applications using helical tomotherapy with TomoEdge. *Anticancer Res* (2021) 41:1909–20. doi: 10.21873/anticanres.14957

8. Yang R, Xu S, Jiang W, Xie C, Wang J. Integral dose in three-dimensional conformal radiotherapy, intensity-modulated radiotherapy and helical tomotherapy. *Clin Oncol* (2009) 21:706–12. doi: 10.1016/j.clon.2009.08.002

9. Hall EJ, Wuu CS. Radiation-induced second cancers: the impact of 3D-CRT and IMRT. *Int J Radiat Oncol Biol Phys* (2003) 56:83–8. doi: 10.1016/s0360-3016(03)00073-7

10. Pirzkall A, Carol M, Lohr F, Höss A, Wannenmacher M, Debus J. Comparison of intensity modulated radiotherapy with conventional conformal radiotherapy for complex-shaped tumors. *Int J Radiat Oncol Biol Phys* (2000) 48:1371–80. doi: 10.1016/s0360-3016(00)00772-0

11. Lian JD, Mackenzie M, Joseph K, Pervez N, Dundas G, Urtasun R, et al. Assessment of extendedfield radiotherapy for stage IIIC endometrial cancer using three dimensional conformal radiotherapy, intensity-modulated radiotherapy and helical tomotherapy. *Int J Radiat Oncol Biol Phys* (2008) 70:935–43. doi: 10.1016/j.ijrobp.2007.10.021

12. Shi CY, Penagaricano J, Papanikolaou N. Comparison of IMRT treatment plans between linac and helical tomotherapy based on integral dose and inhomogeneity index. *Med Dosim* (2008) 33:215–21. doi: 10.1016/j.meddos.2007.11.001

13. Aoyama H, Westerly DC, Mackie TR, Olivera GH, Bentzen SM, Patel RR, et al. Integral radiation dose to normal structures with conformal external beam radiation. *Int J Radiat Oncol Biol Phys* (2006) 64:962–7. doi: 10.1016/j.ijrobp.2005.11.005

14. White J, Tai A, Arthur D, Buchholz T, MacDonald S, Marks L, et al. *Breast cancer atlas for radiation therapy planning: Consensus definitions*. Available at: https://www.nrgoncology.org/Portals/0/Scientific%20Program/CIRO/Atlases/BreastCancerAtlas_corr.pdf?ver=2018-04-18-144201-270 (Accessed July 2020).

15. Ślosarek K, Osewski W, Grządziel A, Radwan M, Dolla Ł, Szlag M, et al. Integral dose: Comparison between four techniques for prostate radiotherapy. *Rep Pract Oncol Radiother* (2014) 20(2):99–103. doi: 10.1016/j.rpor.2014.10.010

16. Cox JD, Stetz JA, Pajak TF. Toxicity criteria of the radiation therapy oncology group (RTOG) and the European organization for research and treatment of cancer (EORTC). *Int J Radiat Biol Phys* (1995) 31(5):1341–6. doi: 10.1016/0360-3016(95)00060-C

17. Paelinck L, Gulyban A, Lakosi F, Vercauteren T, De Gersem W, Speleers B, et al. Does an integrated boost increase acute toxicity in prone hypofractionated breast irradiation? a randomized controlled trial. *Radiother Oncol* (2017) 122(1):30–6. doi: 10.1016/j.radonc.2016.12.023

18. Mondal D, Julka PK, Sharma DN, Jana M, Laviraj MA, Deo SV, et al. Accelerated hypofractionated adjuvant whole breast radiation with simultaneous integrated boost using volumetric modulated arc therapy for early breast cancer: A phase I/II dosimetric and clinical feasibility study from a tertiary cancer care centre of India. *J Egypt Natl Canc Inst* (2017) 29(1):39–45. doi: 10.1016/j.jnci.2017.01.005

19. Krug D, Baumann R, Krockenberger K, Vonthein R, Schreiber A, Boicev A, et al. Adjuvant hypofractionated radiotherapy with simultaneous integrated boost after breast-conserving surgery: Results of a prospective trial. *Strahlenther Onkol* (2021) 197(1):48–55. doi: 10.1007/s00066-020-01689-7

20. Karpf D, Sakka M, Metzger M, Grabenbauer GG. Left breast irradiation with tangential intensity modulated radiotherapy (t-IMRT) versus tangential volumetric modulated arc therapy (t-VMAT): trade-offs between secondary cancer induction risk and optimal target coverage. *Radiat Oncol* (2019) 14(1):156. doi: 10.1186/s13014-019-1363-4

21. Phurailatpam R, Wadasadawala T, Chauhan K, Panda S, Sarin R. Dosimetric comparison of volumetric-modulated arc therapy and helical tomotherapy for adjuvant treatment of bilateral breast cancer. *J Radiother Pract* (2022) 21:36–44. doi: 10.1017/S1460396920000795

frontiers | Frontiers in Oncology

TYPE Original Research
PUBLISHED 03 April 2023
DOI 10.3389/fonc.2023.991952

OPEN ACCESS

EDITED BY
Vishruta Dumane,
Icahn School of Medicine at Mount Sinai, United States

REVIEWED BY
Meryem Aktan,
Necmettin Erbakan University, Türkiye
Udhaya Kumar. S,
Baylor College of Medicine, United States

*CORRESPONDENCE
Reena Phurailatpam
reena.ph@gmail.com
Tabassum Wadasadawala
twadasadawala@actrec.gov.in

†These authors have contributed equally to this work and share first authorship

SPECIALTY SECTION
This article was submitted to Radiation Oncology, a section of the journal Frontiers in Oncology

RECEIVED 12 July 2022
ACCEPTED 06 March 2023
PUBLISHED 03 April 2023

CITATION
Phurailatpam R, Sah Mk, Wadasadawala T, Khan A, Palottukandy J, Gayake U, Jain J, Sarin R, Pathak R, Krishnamurthy R, Joshi K and Swamidas J (2023) Can knowledge based treatment planning of VMAT for post-mastectomy locoregional radiotherapy involving internal mammary chain and supraclavicular fossa improve performance efficiency? *Front. Oncol.* 13:991952. doi: 10.3389/fonc.2023.991952

Can knowledge based treatment planning of VMAT for post-mastectomy locoregional radiotherapy involving internal mammary chain and supraclavicular fossa improve performance efficiency?

Reena Phurailatpam[1*†], Muktar kumar Sah[1†], Tabassum Wadasadawala[1,2*], Asfiya Khan[1,2], Jithin Palottukandy[1], Umesh Gayake[1], Jeevanshu Jain[1,2], Rajiv Sarin[1,2], Rima Pathak[1,2], Revathy Krishnamurthy[1,2], Kishore Joshi[1,2] and Jamema Swamidas[1,2]

[1]Department of Radiation Oncology, Advanced Centre for Treatment, Research and Education in Cancer (ACTREC), Tata Memorial Centre, Homi Bhabha National Institute, Mumbai, India, [2]Department of Radiation Oncology, Tata Memorial Centre, Homi Bhabha National Institute, Mumbai, India

Introduction: To validate and evaluate the performance of knowledge-based treatment planning for Volumetric Modulated Arc Radiotherapy for post-mastectomy loco-regional radiotherapy.

Material and methods: Two knowledge-based planning (KBP) models for different dose prescriptions were built using the Eclipse RapidPlanTM v 16.1 (Varian Medical Systems, Palo Alto, USA) utilising the plans of previously treated patients with left-sided breast cancer who had undergone irradiation of the left chest wall, internal mammary nodal (IMN) region and supra-clavicular fossa (SCF). Plans of 60 and 73 patients were used to generate the KBP models for the prescriptions of 40 Gy in 15 fractions and 26 Gy in 5 fractions, respectively. A blinded review of all the clinical plans (CLI) and KBPs was done by two experienced radiation oncology consultants. Statistical analysis of the two groups was also done using the standard two-tailed paired t-test or Wilcoxon signed rank test, and $p<0.05$ was considered significant.

Results: A total of 20 metrics were compared. The KBPs were found to be either better (6/20) or comparable (10/20) to the CLIs for both the regimens. Dose to heart, contralateral breast,contralateral lung were either better or comparable in the KBP plans except of ipsilateral lung. Mean dose (Gy) for the ipsilateral lung are significantly ($p<0.001$) higher in KBP though the values were acceptable clinically. Plans were of similar quality as per the result of the blinded review which was

conducted by slice-by-slice evaluation of dose distribution for target coverage, overdose volume and dose to the OARs. However, it was also observed that treatment times in terms of monitoring units (MUs) and complexity indices are more in CLIs as compared with KBPs ($p<0.001$).

Discussion: KBP models for left-sided post-mastectomy loco-regional radiotherapy were developed and validated for clinical use. These models improved the efficiency of treatment delivery as well as work flow for VMAT planning involving both moderately hypo fractionated and ultra-hypo fractionated radiotherapy regimens.

KEYWORDS

knowledge-based planning, chest wall, internal mammary nodal (IMN) region and supra-clavicular fossa (SCF), validation, left-side, post-mastectomy radiotherapy

Introduction

Breast cancer is the most commonly diagnosed cancer in women (approximately 2 million cases worldwide in 2020) and it accounts for 6.9% of the total cancer-related deaths (1).

Breast cancer screening leading to early diagnosis and effective treatment strategies have led to an improvement in the prognosis and survival rates, especially in the western world. However, in low and middle income countries (LMICs), majority of women still have to undergo mastectomy as they present with a locally advanced stage, often with internal mammary nodal (IMN) involvement, which is picked up on cross-sectional imaging done for disease staging. The loco-regional radiotherapy (LRRT) in such cases encompasses Post-Mastectomy Radiation Therapy (PMRT), including the regional nodes. As generally, the axilla is addressed surgically, regional nodal irradiation (RNI) often includes targeting the internal mammary node(IMN) and the supraclavicular fossa (SCF). Internal Mammary Nodal (IMN) Irradiation, particularly in patients with left-sided primary disease, is one of the most challenging scenarios in adjuvant radiation therapy owing to the close proximity of the target to the critical organs at risk, namely the heart, left anterior descending artery (LADA), lungs, and contralateral breast.

Traditionally, 3-dimensional conformal radiotherapy (3DCRT) delivered using partially wide tangents was one of the most common techniques employed for treating the chest wall along with the internal mammary region. This technique restricts the dose to the OARs (organs at risk), especially the heart and LAD, but compromises the target coverage and dose homogeneity (2). The combination of photon beam and electron beam has also been used for IMNI but with the limitations of over or under dosing at the photon-electron junction along with a high dose to the anterior myocardium. Rotational intensity modulated radiotherapy (IMRT) provides a viable solution in such a scenario by providing better target coverage, improved dose conformity, as well as homogeneity and better sparing of the OARs (3, 4). The absence of any form of junction and ease of setup are the added advantages. Volumetric modulated arc therapy (VMAT) is a commonly used technique to deliver IMRT.

A typical VMAT plan optimization requires multiple iterations, which makes it a time-consuming process. Variation in patient anatomy, skills and experience of the planner, clinical goals, and dose constraints are some of the parameters that affect the plan quality and make treatment planning laborious. Nelms et al. have stated that inter-planner variation, even within the same institute, is very evident in planning as each planner approaches plan optimization in a different manner using different plan optimization parameters, objectives, and priorities (5). David et al. have also stated that the dependence of the radiotherapy planning process on the planner's experience has been increasing (6). Li et al. have also reported significant inconsistencies in plan quality and dose in the normal brain among VMAT brain stereotactic plans generated manually by three different institutions (7). They have, however, stated that automated planning has improved out-of-target dose and has the potential to help standardise the quality of care for patients receiving VMAT-based multi-target SRS. Knowledge-based planning has, thus, evolved as a way to efficiently create plans of uniform quality by reducing the inter-planner variability and the duration of the optimisation process. Scaggion et al. also reported that KBP can be used as a valuable tool to leverage the planning skills of less experienced planners, thereby ensuring better uniformity of treatment plan quality (8).

KBP models have been reported in the literature for multiple sites like head and neck cancer, prostate cancer, gynaecological cancer, and even breast cancer. Knowledge-based planning (KBP) models are reported in the literature for whole breast irradiation along with draining lymph nodes, bilateral breast radiotherapy, and chest wall irradiation without IMN targets. This study aims at evaluating the knowledge-based planning model, created using a commercial KBP tool RapidPlan^{TM} (RP) provided with the Eclipse treatment planning system (Varian Medical Systems, Palo Alto, USA), for postmastectomy loco-regional radiation therapy

including internal mammary nodes and supraclavicular nodes, and thereby validating it for clinical implementation. The complexity metrics of KBP plans are compared with clinical plans (9, 10). Patient specific quality assurance of KBP as well as clinical plans (CLI) is done using Arc Check phantom (Sun Nuclear Corporation, USA) and SNC patient software. To the best of our knowledge, such an investigation on dosimetric validation and deliverability check of the KBP plans for 26 Gy/5 fractions in comparison to CLI plans has not been reported though there are many papers on the conventional fractionation for 40 Gy/15 fractions.

Materials and methods

This retrospective dosimetric study is a part of the KBP project that was approved by the Institutional Ethics Committee for which consent waiver was granted. Two knowledge-based planning (KBP) models for different dose prescriptions (40 Gy in 15 fractions and 26 Gy in 5 fractions) were built using RapidPlan™ v16.1 Eclipse Treatment Planning System (Varian Medical Systems, Palo Alto, USA) based upon previously treated patients with left-sided breast primary who had undergone irradiation of the left chest wall, internal mammary nodal region and supra-clavicular fossa. All consecutive patients with left sided breast cancer treated with VMAT at our institute from 2018 to 2021 were used for making KBP models and patients treated from 2020 to 2022 were screened for the validation. Patients in whom the target volumes encompassed the left chest wall, SCF and IMN and were treated with free breathing were considered as cases for the study. Other patients, including additional targets or not irradiating IMN were excluded.

As breast cancer patients with locally advanced disease routinely undergo axillary dissection, axillary radiotherapy is avoided to minimise the risk of lymphedema. RapidPlan™ is a commercially available module with Eclipse treatment planning system which models the data from previous patients and gives the DVH estimation of the volumes of interest prior to planning based on the various geometric and dosimetric parameters extracted from the input treatment plans. The patients incorporated for KBP model training were planned using Volumetric Modulated Arc Therapy (VMAT, Photon Optimizer, Acuros-XB, Eclipse v 16.1, Varian Medical Systems, Palo Alto, USA). The standard fractionation for IMNI is 40 Gy in 15 fractions at our institute. However, during the COVID-19 pandemic, the fast forward fractionation was adopted for breast radiotherapy based on the modified UK recommendations released during the pandemic in April 2020 (11). Hence the patients with locally advanced breast cancer requiring IMNI were also treated with fast forward fractionation during the pandemic.

Contouring

Clinical Target volumes (CTV) for Left chest wall (CTV_CW), and SCF (CTV_SCF) were delineated according to the ESTRO guidelines (12). For the internal mammary nodal targets, CTV comprised of the IMN vessels (CTV_IMN) starting from the caudal limit of CTV_SCF to cover the upper three intercostal spaces (up to the fourth rib) as the most common location of the IMN was in the first intercostal space. A margin of 5 mm was given to the CTV to delineate all the PTVs. PTVs were cropped 3mm from the skin. The organs at risk that were delineated included left anterior descending artery (LAD), heart, left lung, right lung, contralateral breast (right breast), thyroid, oesophagus and spinal cord.

KBP model: training, outlier analysis and model objectives generation

The two KBP models were trained using the plans of treated patients which were made following a consistent planning protocol. Flattened 6 MV beam was used to plan the cases with 2 to 4 partial arcs of arc length between 180˚ to 220˚with the isocentre placed at the centre of PTV chest wall. The collimator angle was varied between 5˚ to 15˚.A total of 60and 73 patients were selected for generating the KBP modelsfor40 Gy in 15 fractions and 26 Gy in 5 fractions model respectively. The inclusion criteria for plans to be used in the training set were based on their compliance with the institutional dose constraints. (Table 1)

A detailed explanation of the configuration and training process of KBP models has been given by various authors (13, 14). RapidPlan Model creation is an iterative process that includes training, outlier analysis and re-training based on the outlier statistics. The RP models created were analysed for the outliers using the regression and residual plots of the OARs. Regression models created by KBP between geometric and dosimetric components can detect outliers and thereby improve the capability of KBP. The geometric outliers were retained in the training set, but the dosimetric outliers were identified for further modification. The plans of the dosimetric outliers were studied for root-cause analysis and if required, the cases were re-planned and put into the training set again.The coefficients of determination (R^2), Chi-square (χ^2), and the mean square error (MSE)are the in-built statistical tools provided with RP module.For the target volumes, suitable objective priorities established from clinical experience were used while for the OARs, optimization constraints such as 'line objectives', mean dose and upper dose constraints were used in accordance with the clinical goals. The priority values were automatically generated. Upper dose objectives were placed in addition to the line objective along the inferior DVH prediction boundary for OARs. Normal tissue objective settings were based on clinical experience so that the dose spill outside the target volumes was controlled. The priority was set similar to that of the PTVs while the distance from the target border was set as 0.5 cm with a start dose of 100%, end dose of 60% and a fall off criteria of 0.5.

Validation

Thirteen patients were used for the validation of the 26 Gy/5 fractions KBP model, while ten patients were used to validate the 40 Gy/15 fractions model. These patients were totally independent of the training set and were planned manually as well as using the

TABLE 1 Clinical Goals for the targets and Dose Constraints for the Organs at risk.

TARGET	Clinical Goals (For 26 Gy/5 # and 40 Gy/15#)	
	Desirable	Acceptable
PTV LT CW	V95% ≥ 95%	V95% ≥ 92%
PTV LT SCF	V95% ≥ 95%	V95% ≥ 92%
PTV LT IMN	V95% ≥ 95%	V95% ≥ 90%
Organs at risk	Dose Constraints	
	26Gy/5#	40Gy/15#
LAD	Dmax≤ 13 Gy ± 2 Gy	Dmax≤ 18 Gy ± 4 Gy
Heart	Dmean≤ 2.5 Gy ± 0.5 Gy	Dmean≤ 5 Gy ± 1 Gy
Contralateral Breast (Right)	Dmean≤ 2 Gy ± 0.5 Gy	Dmean≤ 3 Gy ± 0.5 Gy
Contralateral Lung (Right)	Dmean≤ 2 Gy ± 1 Gy	Dmean≤ 4 Gy ± 1 Gy
Ipsilateral Lung (Left)	Dmean≤ 7 Gy ± 1 Gy V3Gy≤ 55% ± 10% V6Gy≤ 35% ± 10%	Dmean≤ 10 Gy ± 2 Gy V5Gy ≤ 35% ± 10% V18Gy≤ 30% ± 5%
Oesophagus	Dmax≤ 26 Gy ± 1 Gy	Dmax≤ 40 Gy ± 1 Gy
Thyroid	Dmax≤ 26 Gy ± 1 Gy	Dmax≤ 40 Gy ± 1 Gy
Spinal Cord	Dmax≤ 10 Gy ± 3 Gy	Dmax≤ 18 Gy ± 4 Gy
Body	Dmax≤ 107% ± 5% V107% ≤ 2cc ± 3cc	Dmax≤ 107% ± 5% V107% ≤ 2cc ± 3cc

respective KBP models. The plan parameters, like the energy and the arc geometry, were kept exactly the same in the manual as well as in KBP plans. KBP plans were generated in a single optimization run without any manual intervention.

The CLI plans and the KBP plans were compared on the basis of various dosimetric parameters like the conformation number, homogeneity index, total MUs(monitor units), and various dose levels for OARs. Conformation number is considered as it takes into account irradiation of both target volume and healthy tissues. To check the statistical significance of the difference between CLI and KBP plans, either a two-tailed paired t-test or a Wilcoxon signed rank test was done based on the normality of the data distribution and the differences were reported with a 95% confidence interval. (Table 2). For the qualitative comparison of KBP with CLI, a visual check of axial dose distribution was done. The definitions of the various indices used for the data analysis have been reported below:

Conformation number, CN = (VT_{ref}/VT) x (VT_{ref}/V_{ref})

where VT_{ref} is the volume of target receiving a dose equal to or greater than the reference dose, VTis the total target volume, V_{ref} is the volume receiving a dose equal to or greater than the reference dose. Total Target volume (VT) is the sum of PTV_CW, PTV_SCF and PTV_IMN.

Homogeneity index, HI = (D_2 -D_{98})/Dp ×100

where D_2 = minimum dose to 2% of the target volume indicating the "maximum dose",

D_{98} = minimum dose to the 98% of the target volume, indicating the "minimum dose" and

D_p = prescribed dose.

The Ideal value for Conformation number (CN) is 1 and it ranges are from 0 to 1.Ideal value of Homogeneity index (HI) is zero.

Computation of plan complexity and the delivery quality assurance

The plan's complexity was checked by total MUs and aperture complexity metrics. The aperture complexity metric is the MU weighted sum over all control points of the perimeter by area for the aperture. The aperture complexity parameter was calculated by

$$M = \frac{1}{MU}\sum_{i=1}^{N} MUi \times \frac{yi}{Ai}$$

Where y_i is the perimeter and A_i is the area of the aperture at the control point. MU represents the total MU for the plan while MU_i is MU delivered at the i^{th} control point. The plan complexity is

TABLE 2 Mean ± standard deviation of the dose-volume parameter of clinical plans as compared to validation plans. p values are given for Clinical plan vs Predicted plan (p<0.05 considered as significant).

Organ & Dose Parameter	Clinical Plan	26 Gy/5 Fractions Predicted Plan	p value	Clinical Plan	40 Gy/5 Fractions Predicted Plan	p value
PTV LT CW V95% (%)	93.24 ± 2.41	93.2 ± 3.05	0.947	96.59 ± 1.62	95.25 ± 2.21	0.053
PTV LT SCF V95%(%)	94.95 ± 1.43	97.27 ± 1.68	0.000	98.03 ± 1.30	97.63 ± 1.72	0.301
PTV LT IMN V95%(%)	89.48 ± 2.94	91.21 ± 2.49	0.171	92.76 ± 2.12	92.57 ± 2.45	0.819
LAD Dmax(Gy	15.1 ± 3.07	13.16 ± 2.43	0.001	17.19 ± 2.70	16.27 ± 2.30	0.144
Heart Dmean(Gy)	2.92 ± 0.54	2.79 ± 0.55	0.060	3.45 ± 0.69	3.37 ± 0.73	0.426
Contralateral Breast (Right) Dmean(Gy)	2.14 ± 0.34	2.27 ± 0.24	0.162	3.14 ± 0.23	2.85 ± 0.25	<0.000
Contralateral Lung (Right)Dmean(Gy)	2.377 ± 0.39	2.162 ± 0.23	0.012	3.46 ± 1.04	3.06 ± 1.04	0.039
IpsilateralLung : Dmean(Gy) V3Gy/V5Gy (%) V6Gy/V18Gy (%)	6.67 ± 0.71 53.68 ± 3.68 35.88 ± 3.72	7.48 ± 0.39 61.49 ± 2.78 41.54 ± 2.39	<0.001 <0.001 <0.001	9.10 ± 0.85 48.04 ± 3.55 17.39 ± 2.64	9.71 ± 0.70 51.60 ± 4.45 19.29 ± 2.58	0.042 0.078 0.022
Oesophagus: Dmax(Gy)	25.65 ± 1.53	25.95 ± 1.64	0.063	39.89 ± 3.77	39.54 ± 4.24	0.173
Thyroid: Dmax(Gy)	26.35 ± 0.57	26.93± 0.21	0.005	41.09 ± 0.46	41.03 ± 0.47	0.697
Spinal cord: Dmax(Gy)	11.81± 1.79	10.97 ± 2.07	0.043	17.32 ± 3.15	13.54 ± 1.57	0.002
Body V107% (cc)	0.4 ± 0.733	0.489 ± 1.33	0.965	0.21 ± 0.35	0.53 ± 0.89	0.236
Homogeneity Index	0.121 ± 0.020	0.118 ± 0.023	0.390	0.085 ± 0.013	0.0931 ± 0.016	0.022
Conformation Number	0.931 ± 0.022	0.934 ± 0.028	0.470	0.878 ± 0.019	0.864 ± 0.018	0.009
Complexity metrices	0.14 ± 0.02	0.12 ± 0.01	0.014	0.13 ± 0.12	0.12± 0'01	0.049
Total MUs	1994.461 ± 275.249	1704.538 ± 315.274	0.013	948.1 ± 141.506	897.8 ± 149.924	0.010
Gamma	96.21(± 4.85)	96.87(± 1.77)	0.598	97.92 ± 1.39	98.36 ± 1.19	0.031

calculated using the Eclipse Application Programming Interface (Eclipse ESAPI) version 16.1 [9, 10].

The plan deliverability was checked by performing patient specific QA and calculating the gamma passing rate (GPR) using the Arc Check phantom (Sun Nuclear Corporation, USA) and SNC patient software.

Assessment of the impact of KBP implementation on clinical work flow

The impact of KBP on the clinical work flow in terms of plan uniformity and the time taken for generating a clinically acceptable plan in view of the experience of the planners was also evaluated.

Blinded review of plans

To avoid inclination towards any specific planning technique, blinded review of the CLI and KBP plans for both the models was done by experienced clinicians. The CLI and KBP plans were randomly renamed as A or B, and the clinicians were asked to select the better plan. It was slice by slice evaluation of dose distribution for coverage and overdose volume as well as dose to OARs.

Results

The CLI as well as the KBP plans could achieve all the clinical goals, and a representative dose distribution for their comparison is shown in Figures 1, 2 for 26Gy/5fractions and 40 Gy/15fractions, respectively. The mean DVH plots for each target volume and OARs are also shown in Figures 3, 4 for the 26Gy/5 fractions and 40Gy/15 fractions, respectively.

Model 1 (KBP model for 26Gy in 5 fractions)

In terms of the target coverage and dosimetric indices, clinical goals are achieved by the CLI as well as the KBP plans. KBP plans give comparable coverage to the targets when compared to CLI.Coverage of Targets (PTV left CW and PTV left IMN) coverage are not significantly different between CLI and KBPs while coverage of PTV SCF (%) is significantly better in KBP (97.27 ± 1.68) as compared to CLI (94.95 ± 1.43) with p=0.000.At the same time HI and CN are comparable. Mean Heart dose (Gy) is not significantly lesser in KBP (2.79 ± 0.55) as compared to CLI (2.92 ± 0.54) with p=0.060.Whereas the dose parameters for the contralateral lung(p=0.012), LAD(p=0.001), and spinal cord

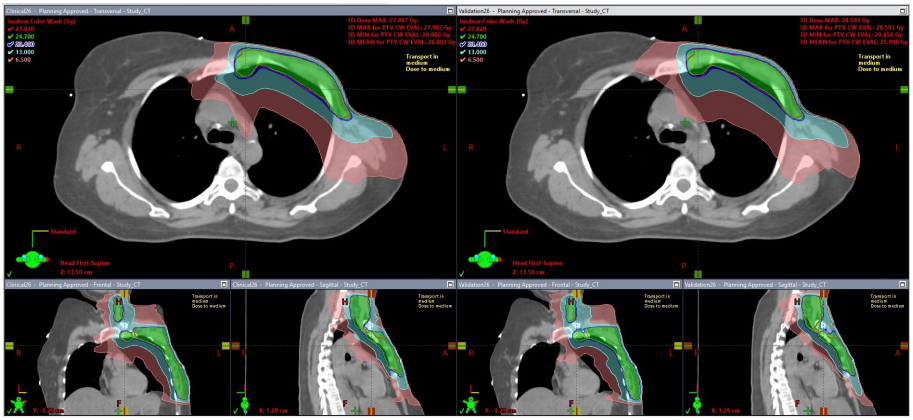

FIGURE 1
Representative dose distribution for comparison of CLI vs KBP_26Gy in 5 fractions.

(p=0.043) were significantly lower in KBP than in CLI. However, mean dose (Gy) for the ipsilateral lung are significantly higher in KBP (7.48± 0.39) than in CLI (6.67 ± 0.71) with p<0.001.Contralateral breast (p=0.162) and oesophagus (p=0.063) dose are comparable.Thyroid dose is significantly more in CLI (p=0.005).CLI plans are found to be more complex than KBPs as MUs (p=0.013) and complexity indices (p=0.014) are significantly higher. The GPR for delivery quality assurance (DQA) were comparable (p=0.598).

Model 2 (KBP model for 40 Gy in 15fractions)

KBP plans give comparable coverage to the targets when compared to CLI. For heart, LAD, thyroid and oesophagus, doses are comparable in KBP and CLI. However, the dose parameters for contralateral breast (p<000), contralateral lung (p=0.039) and spinal cord (p=0.002) are significantly less in KBP plans than in CLIs thereby favoring KBP plans. For Ipsilateral lung, mean dose (Gy)in KBP plan(9.71 ± 0.70) significantly higher than in CLI (9.10 ± 0.85)with p=0.042.However volume of ipsilateral lung getting 5Gy dose (V5) is comparable with p=0.078. Similar to the observation in model 1, CLI plans are found to be more complex than the KBP plans as MUs(p=0.01) and complexity indices(p=0.049) are significantly higher for CLI as compared to KBPs. GPR for DQA are significantly better for KBPs(p=0.031). CN (p=0.009) and HI (p=0.022) values significantly favored CLI plans.

Impact of KBP on clinical work flow

The plans used for training both the KBP models have been planned by highly experienced planners (at least 10 years' experience). The time taken for creating a manual plan is calculated to be approximately 4-5 hrs. During the manual planning, planners have to create many optimization structures to control the dose spill outside the PTVs and to create dose gradients

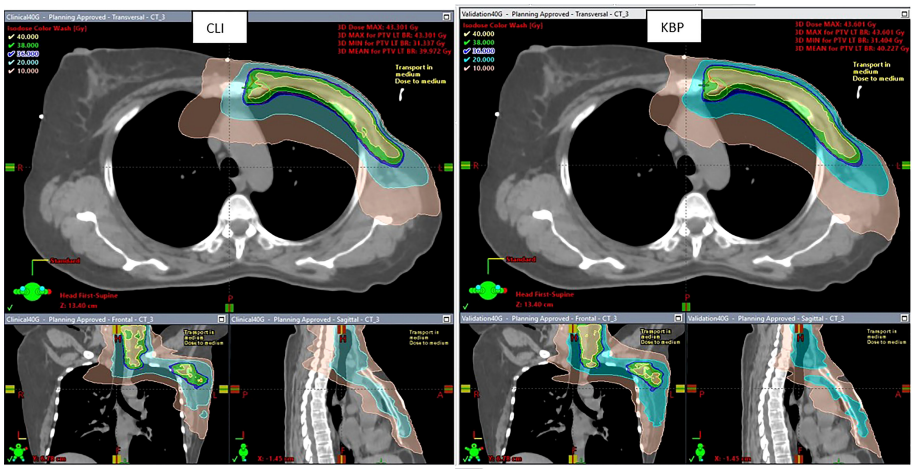

FIGURE 2
Representative dose distribution for comparison of CLI vs KBP_40 Gy in15 fractions.

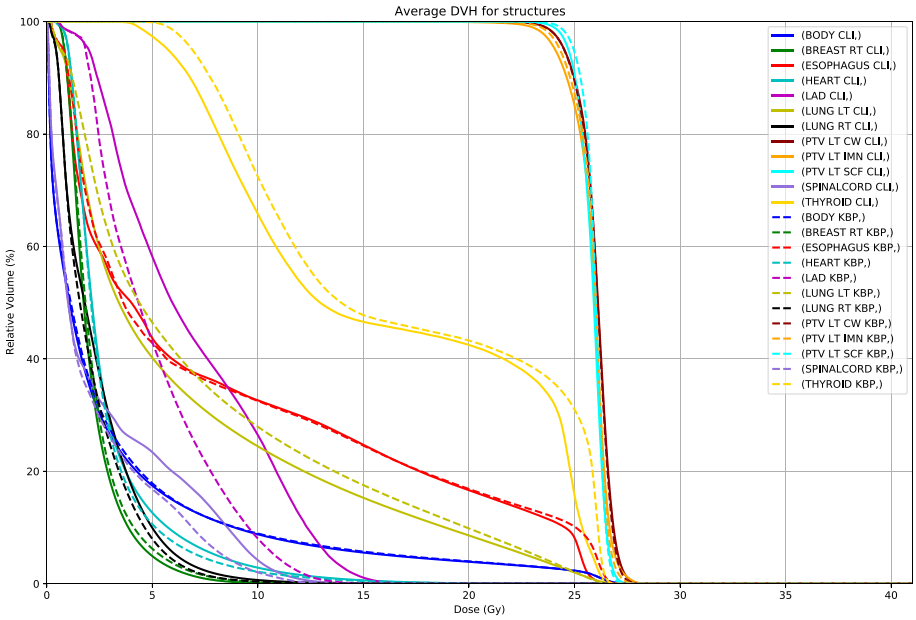

FIGURE 3
Average DVH comparison of CLI and KBP_26Gy in 5 fractions.

in the OARs. To achieve the clinical goals, the optimizer has to constantly change constraints and penalties to target volumes and OARs using the hit-and-trial method. KBP plans have been created by inexperienced planners. The optimization is done in a single run, so a clinically acceptable plan is created in 20–30 minutes. It is thus observed that the time required to achieve clinically acceptable plans has been drastically reduced.

Blinded review

For Model 1 (26Gy in 5 fractions), out of the 13 validation cases, consultant 1 found 7 CLI plans and 5 KBP plans better on comparison, while for 1 validation case, both the plans were of equal quality. Consultant 2 chose 5 CLI plans and 7 KBP plans, and in one case, both plans were of equal quality. The result is depicted in Figure 5.

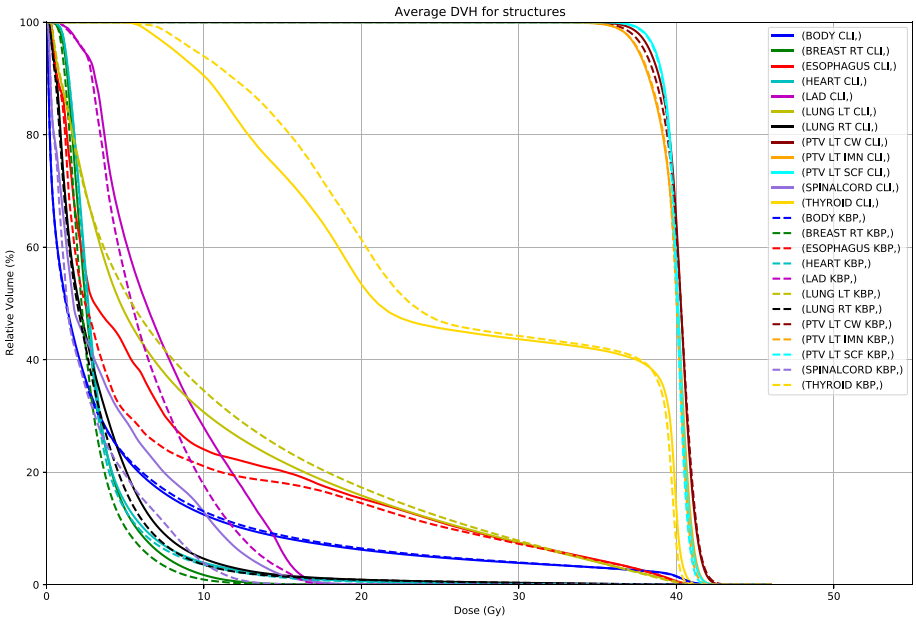

FIGURE 4
Average DVH comparison of CLI and KBP_40Gy in 15 fractions.

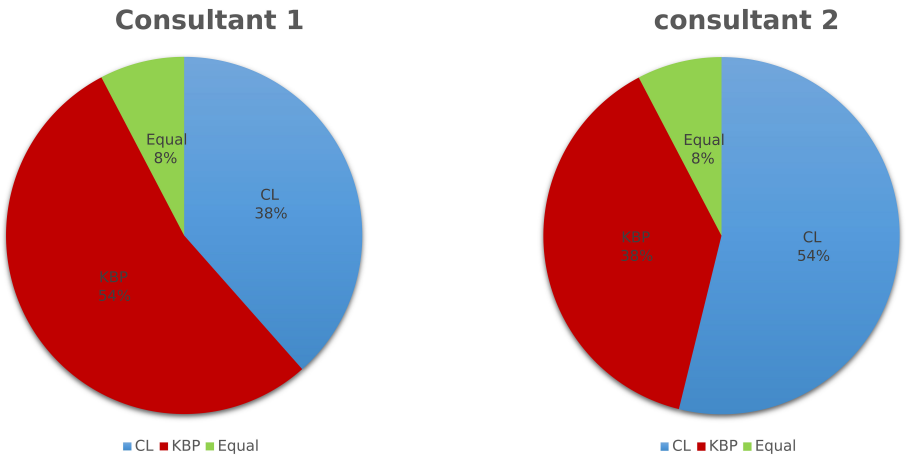

FIGURE 5
Blinded review result for 26Gy in 5 fractions.

For Model 2 (40Gy in 15 fractions), out of the 10 validation cases, 3 CLI plans and 4 KBP plans were selected, while 3 plans were found to be of equivalent quality by consultant 1. Consultant 2, on the other hand, preferred 6 CLI plans and 4 KBP plans. The result is depicted in Figure 6.

Discussion

Keeping pace with the numerous advancements in the field of radiation oncology, artificial intelligence and machine learning have proven to have great potential for impacting the patient workflow in cancer care, especially for busy radiation oncology setups providing services to treat the most prevalent disease sites like head and neck, breast, gynecological, or prostate cancers. There have been various published reports on the automated planning models for breast cancer, as summarized in Table 3 (14–21). Out of 8 papers discussed, 6 papers are on RapidPlan™ while 2 papers are on Raystaion TPS and MD Anderson Cancer Center Auto Plan (MDAP) system. Many authors have hypothesized the potential of automated radiotherapy treatment planning for increasing consistency, improving plan quality, and reducing workloads for all routinely challenging treatments involving complex anatomical sites or involving multiple dose levels (15, 19). Most of these papers reported on the conventional fractionation regime while we are reporting on the KBPs for both moderately hypo fractionated and ultra-hypo fractionated (fast forward) regimens. The model for fast forward fractionation (26 Gy in 5 fractions) has not been reported in literature. Anatomical differences amongst patients are taken into account and extrapolated in the evaluation of DVH for the treating patients. Our study is not restricted to the dosimetric validation but also includes checks on the deliverability of plans in terms of plan complexity, MU, and gamma passing rate. Patients undergoing mastectomy and presenting with N3 disease in view of an initial

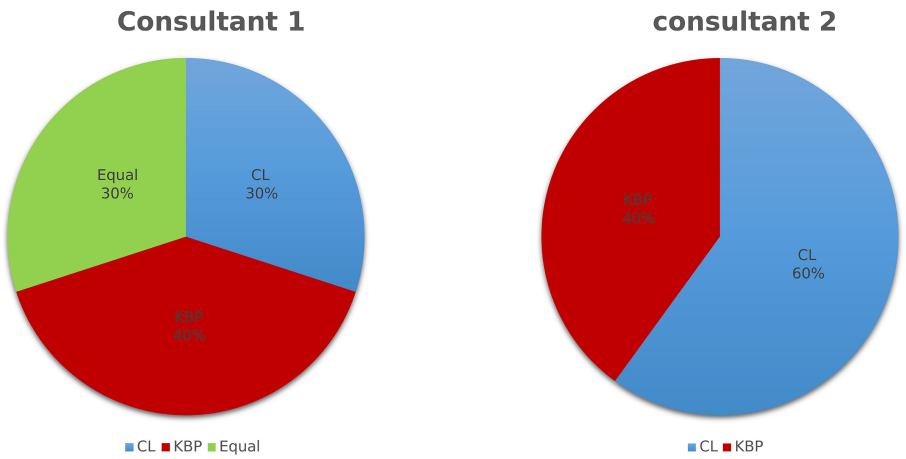

FIGURE 6
Blinded review result for 40 Gy in 5 fractions.

TABLE 3 Review of studies published on rapid planning for breast cancer.

Author	Year	N for model/validation	Laterality	Target volumes	Guidelines	Metrices compared	Dose prescription/technique	External validation	KBP performance	Time reduction
Fogliata (14)	2015	150/50	Both and bilateral	Breast and boost	In-house	18	40.5 in 15 for breast and 48 in 15 for boost, VMAT in Eclipse v 13.5	Yes	7 no difference, 11 better in KBP	Not reported
Wang (15)	2017	80/10	Left	Breast and boost	In-house	16	45 in 25 for breast and 60 in 25 for boost, VMAT in Eclipse v 13.5	No	No difference for senior planners	Not reported
Ben Archibald-Heeren (16)	2020	100/0	Both	Breast alone	RTOG/ ESTRO	39	50 in 25 and 42.4 in 16, Hybrid IMRT tangent RT in Raystation	No	23 no difference, 14 better in KBP and 2 better in CP	23 to 5 mins
Inoue (17)	2020	20/5	Left and bilateral	Breast alone	RTOG	9	50 in 25, VMAT in Eclipse v 15.6	No	7 no difference, 2 better in KBP	120 to 15 mins
Costa (18)	2021	56/20 each for Truebeam and Halcyon	Left	Breast/ SCF/AX/ IMN	ESTRO	28	40 in 15 or 50 in 25 or 50.4 in 28 for breast with 63 in 28 for boost, VMAT in Eclipse v 15.6	No	Comparison with CP not shown. Truebeam and Halcyon plans compared	Not reported
Rago (19)	2021	52-120/40	Both	Breast/ Boost/ SCF/IMN	In-house	32	40 in 15 or 50 in 25 for breast with 57.5-62.5 in 25 for boost, VMAT in Eclipse v 15.6	Yes	24 no difference, 8 better in KBP	Not reported
Apaza Blanco OA (20)	2021	50/20	Both	Breast alone	AAPM report TG-263	8	three dose levels in 20 fractions. (CTV_SIB) dose prescription of 56Gy, proximal CTV of 46 Gy and (CTV_ distal) of 43 Gy. Ecclipse,VMAT	No	6 out of 8 are better Increase in ipsilateral lung dose and contra breast for	30% for beginner
Jiang (21)	2022	20/20	both	Chest wall/ SCF/IMN	ESTRO	10	50 in 25, MD Anderson Cancer CenterAutoPlan (MDAP) system and Pinnacle treatment planning system (TPS), (v9.8, Philips Radiation Oncology Systems, Fitchburg, WI)	NO	Same or better in 5,	reported
Current	2021	133/23	Left	Chest wall/ SCF/IMN	ESTRO	20	40 in 15 or 26 in 5, VMAT in Eclipse v 16.1	No	same or better in 15, CP better in 4	4 to 5 hrs to 20 minutes

10.3389/fonc.2023.991952

positive IMN node are a common scenario in our clinical practice. Hence, the geometry of the actual clinical cases is likely to fall within the range of the constituent plan library of the model. While most of the authors have developed models specific to left-sided breast cancer, including the current one, others have developed a generalized model. Foglia et al. has developed model for patients with breast conservation requiring tumor bed boost and suggested to conduct dedicated studies for other settings (14). Though few studies have developed models for RNI, most of them are either in the setting of breast conservation or has been done using conventional fractionation in non-Varian treatment planning system viz., the MD Anderson Cancer Center Auto Plan (MDAP) system and the Pinnacle treatment planning system (TPS) (21). Hence the study methodology is not comparable with the RapidPlan™ based modelling presented here. Moreover, only 20 patients were used to develop the model though it was validated in 10 right and 10 left chest wall patients. Fewer dosimetric parameters were used for the comparative analysis. Similar to our study, they also reported that quality plans can be generated by AI-based automatic planning systems with clinical efficiency. However, in view of the above shortcomings, the results of the current study are more robust compared to the MD Anderson report.

To improve the efficiency of breast treatment planning using KBP for VMAT, it is crucial to standardise various essential steps involved in the process.

1) First and foremost is the selection of cases for the model training: Minimum number of patients required for configuring KBP models is 20, however adding more plans usually helps in creating a more robust plan (13). We have taken 60 and 73 patients selected for generating the KBP models for 40 Gy in 15 fractions and 26 Gy in 5 fractions model respectively.The robustness and accuracy depend on the quality of plans used for model training and configuration. Wang et al. has also stated that suboptimal plans when used in model configuration can degrade the KBP predicted plans. He also emphasized on the requirement of deeper analyses on the goodness of the estimation model configuration in terms of the model size, plan and anatomy homogeneity (15).
2) Uniform adoption of nomenclature for target volumes and OAR: This is a very basic requirement when selecting patients for model training. It reduces errors and also forms the basis for future validation of the model for internal and external use. Adoption of uniform nomenclature (codes) for target volumes and OARs helps in clinical workflow by automatic structure matching in DVH estimation models. To take full advantage of automatic structure matching, define a code for each plan structure of the structure template, such that all plan structures will have the same structures codes as the ones introduced in the model. If a plan structure has no code, matching is based on the structure identifier. Template structure code assignment is recommended for robust structure matching between the new cases and model structures.
3) Choice of the proper objectives and priorities: The judicious use of optimization objectives while creating a model is considered crucial for model quality. Many authors have observed that OAR doses from the CLI plans and KBP plans (plans generated using line constraints and auto-generated priorities of the KBP model) were similar (22, 23). Rago et al. have also reported that the good results of the plans generated with KBP could come from the combination of the two objectives included in the model: the generated line-objective and the mean objective, both with generated priorities (19). As difference in prescription dose and number of fractions is very large in 40Gy/15 Fr and 26Gy/5Fr, difference in mean dose to the OARs are also quite large, so we have not made a generalized model. In this study, line objectives and mean objectives with generated priorities have been used for OARs.
4) Standardization of other planning parameters: Treatment planning parameters like the number of patients, beam energy, number of arcs, etc. are directly linked to the performance of the KBP models and their prediction ability. In this study, we utilized the optimal number of clinically approved treatment plans and used a flattened 6 MV beam for VMAT plans with 2 to 4 partial arcs.

Predicted gains from model-based planning and their impact on clinical workflow: Overall, plans generated by both the models (Model 1 and Model 2) are considered clinically acceptable based on the clinical goals and comparable dose distribution. Except for the increase in the dose of the ipsilateral lung which is less than 1 Gy (table 2), most of the dosimetric parameters were either comparable or better with the KBP plans. Blanco, et al. also reported significant increase in dose of ipsilateral lung in the KBP plans favoring plans of manual plan in their study (24). Many authors accepted skilled manual interventions on the KBP plans to achieve high quality results. When there is very close proximity or overlap of OARs with PTVs, minor refinements can be considered to support clinical decisions to compromise either coverage or OAR constraints (18, 19).

So Ipsilateral lung dose can be reduced by replanning KBP plans. Swamidas et al. also suggested that dose to a particular OAR can be reduced by replanning KBP plans where the optimization objectives/ priorities were manually tweaked such that the DVH of the OAR to be at the lower border of the estimation band of DVH prediction without compromising the target coverage, with a single optimization (25). Hence, these models can be considered acceptable for clinical implementation. Model-generated plans are also likely to improve the workflow by giving consistent plans, especially in this group of post-mastectomy patients wherein complex treatment volumes are very common. In the CLI plans, many optimization structures were created to control the dose spill to the heart and lungs, and it is explained in the literature (4). However, for KBP plans, the creation of such optimization structures is not necessary with RapidPlan™ as predicted DVH objectives automatically take into account the dose spill

and control it accordingly (26). It also directly helps in reducing the planning time. The time taken for plan generation has shown a considerable reduction, from 4-5 hours to 20-30 minutes. The quality of plans generated using the model is independent of the planner. Another important gain reported in our study is the generation of treatment plans with reduced monitor units and less complexity, thereby further improving the treatment planning and delivery efficiency. Many authors reported findings similar to our results. Tamura et al. have reported that two full arcs VMAT plans generated by the KBP might decrease the MU and the modulation complexity (24). In our case also, all the plans are generated with two to four partial arcs. On the other hand, Hussein et al. also showed the MU and modulation complexity were not different between KBP and clinical plan for two full arcs VMAT plans. In his study, KBP plans for prostate cancer are with lesser MU while that for cervix,KBP plans are with higher MU compared to manual plan (26). Kubo et al. also have stated that RapidPlan™ might reduce plan complexity when appropriate objective constraints are used (27). which corroborates with our experience. Swamidas et al, also reported our institutional experience on development and validation of KBP for cervical cancer and similarly found significantly lesser monitor units in KBP plans as compared to manual plans (25).

The blinded review by the consultants helped in removing any biases towards any planning technique. The results obtained showed that both the CLI and KBP plans are clinically acceptable. The sparing of ipsilateral lung was found to be lower with KBP. However, in absolute terms, the difference was less than 1 Gy. Though it can be argued that the risk of toxicity, especially radiation induced pneumonitis, will be higher, the clinical manifestation is very rare. The incidence of pneumonitis is low at our institute and the safety of IMRT for treatment of breast cancer has been reported earlier by us (28).

Limitation

As this model was made for a selected cohort of patients, its applicability to right-sided disease, breast conservation, bilateral disease, and prescriptions with multiple dose levels has not been tested. Moreover, prospective internal and external validation of the model is strongly recommended for a larger number of patients. It would also be worthwhile to quantify the time saved by employing KBP planning in clinics.

Conclusion

Knowledge based planning models for VMAT technique for dose prescriptions of 26 Gy in 5 fractions and 40 Gy in 15 fractions have been developed and validated for breast cancer involving the left chest wall, internal mammary chain and supraclavicular fossa. This has the potential to improve the work flow for VMAT planning involving moderately hypo fractionated and ultra-hypo fractionated radiotherapy regimens.

The model generated plans were comparable with the clinical plans generated by experienced physicists in terms of dose distribution. The KBP plans were found to be less complex and passed the deliverability quality assurance tests and, hence can be clinically implemented.

Data availability statement

The original contributions presented in the study are included in the article/Supplementary Material. Further inquiries can be directed to the corresponding authors.

Author contributions

All authors listed have made a substantial, direct, and intellectual contribution to the work and approved it for publication.

Acknowledgments

Prof. Luca Cozzi PhD, Istituto Clinico Humanitas IRCCS, Humanitas, Department of Radiation Oncology, Italy for providing Varian Medical Systems for Rapid Plan research license.

Conflict of interest

The authors declare that the research was conducted in the absence of any commercial or financial relationships that could be construed as a potential conflict of interest.

Publisher's note

Supplementary material

The Supplementary Material for this article can be found online at: https://www.frontiersin.org/articles/10.3389/fonc.2023.991952/full#supplementary-material

References

1. Sung H, Ferlay J, Siegel RL, Laversanne M, Soerjomataram I, Jemal A, et al. Global cancer statistics 2020: GLOBOCAN estimates of incidence and mortality worldwide for 36 cancers in 185 countries. *CA Cancer J Clin* (2021) 71(3):209–49. doi: 10.3322/caac.21660

2. Pierce LJ, Butler JB, Martel MK, Normolle DP, Koelling T, Marsh RB, et al. Postmastectomy radiotherapy of the chest wall: dosimetric comparison of common techniques. *Int J RadiatOncolBiol Phys* (2002) 52(5):1220–30. doi: 10.1016/s0360-3016(01)02760-2

3. Ranger A, Dunlop A, Hutchinson K, Convery H, Maclennan MK, Chantler H, et al. A dosimetric comparison of breast radiotherapy techniques to treat locoregional lymph nodes including the internal mammary chain. *ClinOncol (R CollRadiol)* (2018) 30(6):346–53. doi: 10.1016/j.clon.2018.01.017

4. Phurailatpam R, Wadasadawala T, Chauhan K, Panda S, Sarin R. Dosimetric comparison of volumetric-modulated arc therapy and helical tomotherapy for adjuvant treatment of bilateral breast cancer. *J Radiotherapy Pract* (2020) 21(1):1–9. doi: 10.1017/s1460396920000795

5. Nelms BE, Robinson G, Markham J, Velasco K, Boyd S, Narayan S, et al. Variation in external beam treatment plan quality: An inter-institutional study of planners and planning systems. *PractRadiatOncol.* (2012) 2(4):296–305. doi: 10.1016/j.prro.2011.11.012

6. Fried DV, Chera BS, Das SK. Assessment of PlanIQ feasibility DVH for head and neck treatment planning. *J ApplClin Med Phys* (2017) 18(5):245–50. doi: 10.1002/acm2.12165

7. Li T, Vergalasova I, Wang C, Sheng Y, Yun Y, Liu H, et al. Significant inter-planner variability in plan quality for VMAT-based multi-target Stereotactic Radiosurgery (SRS): A multi-institution analysis. *Int J RadiatOncolBiol Phys* (2019) 105(15):E767. doi: 10.1016/j.ijrobp.2019.06.807

8. Scaggion A, Fusella M, Roggio A, Bacco S, Pivato N, Rossato MA, et al. Reducing inter- and intra-planner variability in radiotherapy plan output with a commercial knowledge-based planning solution. *Phys Med* (2018), 53:86–93. doi: 10.1016/j.ejmp.2018.08.016

9. Younge KC, Roberts D, Janes LA, Anderson C, Moran JM, Matuszak MM. Predicting deliverability of volumetric-modulated arc therapy (VMAT) plans using aperture complexity analysis. *J Appl Manual Med Phys* (2016) pp:124–31. doi: 10.1120/jacmp.v17i4.6241

10. Varian Medical Systems. Eclipse scripting API reference guide, Palo Alto, CA: Varian (2011)

11. Coles CE, Aristei C, Bliss J, Boersma L, Brunt AM, Chatterjee S, et al. International guidelines on radiation therapy for breast cancer during the COVID-19 pandemic. *ClinOncol (R CollRadiol).* (2020) 32(5):279–81. doi: 10.1016/j.clon.2020.03.006

12. Offersen BV, Boersma LJ, Kirkove C, Hol S, Aznar MC, Biete Sola A, et al. ESTRO consensus guideline on target volume delineation for elective radiation therapy of early stage breast cancer. *RadiotherOncol.* (2015) 114(1):3–10. doi: 10.1016/j.radonc.2014.11.030

13. VMS. *Eclipse photon and electron 13.6 instruction of use*. Palo Alto, CA: Varian Medical Systems, Inc (2015).

14. Fogliata A, Cozzi L, Reggiori G, Stravato A, Lobefalo F, Franzese C, et al. RapidPlan knowledge based planning: Iterative learning process and model ability to steer planning strategies. *RadiatOncol* (2019) 14:187. doi: 10.1186/s13014-019-1403-0

15. Wang J, Hu W, Yang Z, Chen X, Wu Z, Yu X, et al. Is it possible for knowledge-based planning to improve intensity modulated radiation therapy plan quality for planners with different planning experiences in left-sided breast cancer patients? *RadiatOncol* (2017) 12:85. doi: 10.1186/s13014-017-0822-z

16. Inoue E, Doi H, Monzen H, Tamura M, Inada M, Ishikawa K, et al. Dose-volume histogram analysis of knowledge-based volumetric-modulated arc therapy planning in postoperative breast cancer irradiation. *In Vivo.* (2020) 34(3):1095–101. doi: 10.21873/invivo.11880

17. Archibald-Heeren B, Byrne M, Hu Y, Liu G, Collett N, Cai M, et al. Single click automated breast planning with iterative optimization. *J ApplClin Med Phys* (2020) 21(11):88–97. doi: 10.1002/acm2.13033

18. Costa E, Richir T, Robilliard M, Bragard C, Logerot C, Kirova Y, et al. Assessment of a conventional volumetric-modulated arc therapy knowledge-based planning model applied to the new halcyon© O-ring linac in locoregional breast cancer radiotherapy. *Phys Med* (2021) 86:32–43. doi: 10.1016/j.ejmp.2021.05.022

19. Rago M, Placidi L, Polsoni M, Rambaldi G, Cusumano D, Greco F, et al. Evaluation of a generalized knowledge-based planning performance for VMAT irradiation of breast and locoregional lymph nodes–internal mammary and/or supraclavicular regions. *PloS One* (2021) 16(1):e0245305. doi: 10.1371/journal

20. Apaza Blanco OA, Almada MJ, Garcia Andino AA, Zunino S, Venencia D. Knowledge-based volumetric modulated arc therapy treatment planning for breast cancer. *J Med Phys* (2021) 46:334–40. doi: 10.4103/jmp.JMP_51_21

21. Jiang S, Xue Y, Li M, Yang C, Zhang D, Wang Q, et al. Artificial intelligence-based automated treatment PlanningofPostmastectomyVolumetricModulated arc radiotherapy. *Front Oncol* (2022) 12:871871. doi: 10.3389/fonc.2022.871871

22. Hung WM, Fung NTC, Chang ATY, Lee MCH, Ng WT. Knowledge-based planning in nasopharyngeal carcinoma. *Ann Nasopharynx Cancer* (2020) 4:6. doi: 10.21037/anpc-20-12

23. Faught AM, Olsen L, Schubert L, Rusthoven C, Castillo E, Castillo R, et al. Functional-guided radiotherapy using knowledge-based planning. *RadiotherOncol.* (2018) 129(3):494–8. doi: 10.1016/j.radonc.2018.03.025

24. Tamura M, Monzen H, Matsumoto K, Kubo K, Otsuka M, Inada M, et al. Mechanical performance of a commercial knowledge-based VMAT planning for prostate cancer. *RadiatOncol.* (2018) 13(1):163. doi: 10.1186/s13014-018-1114-y

25. Swamidas J, Pradhan S, Chopra S, Panda S, Gupta Y, Sood S, et al. Development and clinical validation of knowledge-based planning for volumetric modulated arc therapy of cervical cancer including pelvic and para aortic fields. *Phys Imaging RadiatOncol.* (2021) 18:61–7. doi: 10.1016/j.phro.2021.05.004

26. Hussein M, South CP, Barry MA, Adams EJ, Jordan TJ, Stewart AJ, et al. Clinical validation and benchmarking of knowledge-based IMRT and VMAT treatment planning in pelvic anatomy. *Radiotherapy Oncol* (2016) 120(3):473–9. doi: 10.1016/j.radonc.2016.06.022

27. Kubo K, Monzen H, Ishii K, Tamura M, Kawamorita R, Sumida I, et al. Dosimetric comparison of RapidPlan and manually optimized plans in volumetric modulated arc therapy for prostate cancer. *Phys Med* (2017) 44:199–204. doi: 10.1016/j.ejmp.2017.06.026

28. Wadasadawala T, Jain S, Paul S, Phurailatpam R, Joshi K, Popat P, et al. First clinical report of helical tomotherapy with simultaneous integrated boost for synchronous bilateral breast cancer. *Br J Radiol* (2017) 90(1077):20170152. doi: 10.1259/bjr.20170152

frontiers | Frontiers in Oncology

TYPE Original Research
PUBLISHED 18 April 2023
DOI 10.3389/fonc.2023.1124838

OPEN ACCESS

EDITED BY
Vishruta Dumane,
Icahn School of Medicine at Mount Sinai, United States

REVIEWED BY
Yannick Poirier,
University of Maryland, United States
Itzhak Orion,
Ben-Gurion University of the Negev, Israel

*CORRESPONDENCE
Manju Sharma
Manju.Sharma@ucsf.edu

SPECIALTY SECTION
This article was submitted to Radiation Oncology, a section of the journal Frontiers in Oncology

RECEIVED 15 December 2022
ACCEPTED 31 March 2023
PUBLISHED 18 April 2023

CITATION
Ramos-Méndez J, Park C and Sharma M (2023) Dosimetric characterization of single- and dual-port temporary tissue expanders for postmastectomy radiotherapy using Monte Carlo methods. *Front. Oncol.* 13:1124838. doi: 10.3389/fonc.2023.1124838

Dosimetric characterization of single- and dual-port temporary tissue expanders for postmastectomy radiotherapy using Monte Carlo methods

Jose Ramos-Méndez, Catherine Park and Manju Sharma*

Department of Radiation Oncology, University of California, San Francisco, San Francisco, CA, United States

Purpose: The aim of this work was two-fold: a) to assess two treatment planning strategies for accounting CT artifacts introduced by temporary tissue-expanders (TTEs); b) to evaluate the dosimetric impact of two commercially available and one novel TTE.

Methods: The CT artifacts were managed using two strategies. 1) Identifying the metal in the RayStation treatment planning software (TPS) using image window-level adjustments, delineate a contour enclosing the artifact, and setting the density of the surrounding voxels to unity (RS1). 2) Registering a geometry template with dimensions and materials from the TTEs (RS2). Both strategies were compared for DermaSpan, AlloX2, and AlloX2-Pro TTEs using Collapsed Cone Convolution (CCC) in RayStation TPS, Monte Carlo simulations (MC) using TOPAS, and film measurements. Wax slab phantoms with metallic ports and breast phantoms with TTEs balloons were made and irradiated with a 6 MV AP beam and partial arc, respectively. Dose values along the AP direction calculated with CCC (RS2) and TOPAS (RS1 and RS2) were compared with film measurements. The impact in dose distributions was evaluated with RS2 by comparing TOPAS simulations with and without the metal port.

Results: For the wax slab phantoms, the dose differences between RS1 and RS2 were 0.5% for DermaSpan and AlloX2 but 3% for AlloX2-Pro. From TOPAS simulations of RS2, the impact in dose distributions caused by the magnet attenuation was (6.4 $\pm$ 0.4) %, (4.9 $\pm$ 0.7)%, and (2.0 $\pm$ 0.9)% for DermaSpan, AlloX2, and AlloX2-Pro, respectively. With breast phantoms, maximum differences in DVH parameters between RS1 and RS2 were as follows. For AlloX2 at the posterior region: (2.1 $\pm$ 1.0)%, (1.9 $\pm$ 1.0)% and (1.4 $\pm$ 1.0)% for D1, D10, and average dose, respectively. For AlloX2-Pro at the anterior region (-1.0 $\pm$ 1.0)%, (-0.6 $\pm$ 1.0)% and (-0.6 $\pm$ 1.0)% for D1, D10 and average dose, respectively. The impact in D10 caused by the magnet was at most (5.5 $\pm$ 1.0)% and (-0.8 $\pm$ 1.0)% for AlloX2 and AlloX2-Pro, respectively.

Conclusion: Two strategies for accounting for CT artifacts from three breast TTEs were assessed using CCC, MC, and film measurements. This study showed that the highest differences with respect to measurements occurred with RS1 and can be mitigated if a template with the actual port geometry and materials is used.

KEYWORDS

PMRT, temporary-tissue-expanders, Monte Carlo-TOPAS, high-density metal artifacts, collapsed cone convolution algorithm, breast cancer, radiation effects

1 Introduction

Post-mastectomy radiation treatment (PMRT) is selectively recommended for patients with locally advanced and/or high-risk biologically aggressive breast cancers (1). For patients who undergo prosthetic breast reconstruction, radiation increases the risk for adverse effects including capsular contracture, scarring at the implant-tissue junction, development of the seroma and dehiscence of the skin incision (2). As such, a two-stage reconstruction using a temporary tissue expander (TTE), followed by PMRT then delayed final prosthetic reconstruction is often preferred (3). The TTEs help preserve the breast skin and organ at risk contours improving the radiotherapy treatment planning, which in turn alleviates the complication risks. Most TTEs consist of an injection port through which a saline solution is injected to expand the surrounding skin. The port consists of a central high-density magnet enclosed in an encasing to locate the injection site (4). In addition, suction drains are routinely placed to drain the seroma (5). The different TTEs such as CPX® (Mentor, Irvine, CA, USA), Natrelle® (Allergan Inc., Santa Barbara, CA, USA) and DermaSpan (Sientra, Inc., Santa Barbara, CA, USA) have a single port with a high-density magnetic disk placed in a high-density encasing. More recently, AlloX2 and AlloX2-Pro (Sientra Inc., Santa Barbara, CA, USA) breast TTEs were introduced with a dual port system. One port is used for traditional saline injection, and the second facilitates fluid drainage. This feature of dual ports enables independent management of postoperative seroma and thereby reducing the rate of infection by 7.8% as shown retrospectively for the AlloX2 TTE (6).

The PMRT is delivered in conventional 2Gy per fraction for a total dose of 50Gy over five weeks, or with more modern hypofractionation techniques over 3 weeks. The 3D CT data is used to delineate tumors and organs at risk (OAR), and the electron density information in the Hounsfield units (HU) of the CT data is used in the calculation of dose distributions. The presence of high-density magnets imposes challenges to accurate treatment planning and delivery. Some key challenges are (1) the increased scatter dose at the skin surface may lead to skin and subcutaneous toxicity varying from mild erythema to skin fibrosis or skin dyspigmentation (2). The tissue attenuation can lead to cold spots or under dosage of the planning target volume (3). The presence of an implant or other high-density materials leads to streaking artifacts that impede the accurate delineation of tumors and OARs. In addition, due to a limited value range of HU to electron density tables in standard CT systems, the density values of TTEs are not reconstructed correctly in the CT data (7), calling into question the accuracy of the computed dose distribution models.

The dosimetric impact in PMRT of single metal ports have been examined in several studies (8–11). Results largely depend on the treatment modality. For example, for 3D-CRT using single 6MV and 15 MV photon beams, the dose perturbations are reported between 5 to 30% (9, 11, 12) and 16% (11), respectively. For VMAT, differences below 6% had been reported (12); however, some studies had reported a negligible difference (13, 14).

The dual ports cover a significant amount of the treatment volume and perturb the radiation treatment field with increased scatter dose and tissue attenuation beneath the device. To the best of our knowledge, there is no literature on the dose perturbations caused by PMRT with dual metal ports. Therefore, this characterization study aims at a detailed comparison of the three TTEs: single port DermaSpan, dual port AlloX2, and the novel AlloX2-Pro. We provide a detailed comparison of the three TTEs using flat, breast phantom geometries and six clinical cases. In addition, the dose computed by the collapsed-cone convolution (CCC) algorithm v5.5 in RayStation TPS is compared with TOPAS Monte Carlo Tool calculations and experimental Gafchromic film measurements.

2 Methods

2.1 TrueBeam phase space verification

Fifty phase space files containing the positions of particles, angular momenta and kinetic energies generated by Monte Carlo simulations of a 6 MV TrueBeam Linac were obtained from MyVarian at www.myvarian.com/montecarlo. The total number of primary histories per phase space was 10^9 and was generated without any variance reduction technique. The phase spaces were scored at a plane positioned at 73.3 cm from the Linac isocenter, upstream of any moving parts of the Linac treatment head. A comparison was performed between the percentage depth-dose and lateral dose distributions at several depths calculated in water and measured data obtained at the time of commissioning for a

TrueBeam Linac at our institution. For that, two open field setups at 3 x 3 cm^2 and 10 x 10 cm^2 defined at 100 cm SSD were used. The water phantom had dimensions of 20 x 20 x 35 cm^3 with a voxel resolution of 1 x 1 x 0.5 mm^3; the highest resolution was used along the beam direction. The following linac devices were included in the simulation: jaws, base plate, 120 Millennium MLC, and mylar tray. The geometry details were obtained from the vendor. The absorbed dose averaged by primary history retrieved at 10 cm depth was used to scale the simulations to the dose calibration conditions at our institution: 1 cGy/MU at a depth of maximum dose for a 10 x 10 cm^2 field defined at 100 cm SSD. An exponential fit was adjusted to the calculated PDD between the range of 5 to 15 cm to retrieve the calculated absorbed dose at 10 cm depth.

The Monte Carlo simulations were performed with TOPAS version 3.7 (15, 16) built on top of Geant4 toolkit version 10.07 patch 3 (17). The physics list was the electromagnetic module called "g4em-standard_opt4" which was described and benchmarked for its application in radiotherapy as reported elsewhere (18). For all dose calculations, azimuthal particle redistribution with a split number of 50 (19) was used through the geometrical particle split technique available in TOPAS (20). The statistical uncertainty of the dose distributions was 0.5% or better in all simulated cases.

2.2 Breast tissue expander geometries

Breast TTEs consisted of a silicon bag filled with saline solution containing one or two draining or filling ports with a high-density magnet embedded to allow its localization. Three breast TTEs were used in this work. Two commercially available (DermaSpan™ and AlloX2®) and a novel TTE (AlloX2-Pro-Sientra, Inc). The geometry details and materials of the ports obtained from Sientra Inc. are presented in Figure 1. The DermaSpan model consisted of a single titanium (ρ=4.54 g/cm^3) port with a neodymium (ρ=7.6 g/cm^3) magnet enclosed. The AlloX2 model consisted of two titanium ports with one neodymium magnet enclosed in each port. The AlloX2-Pro model consisted of two ports made of peek material (ρ=1.3 g/cm^3), with a single neodymium magnet located between the ports. The geometry and densities from all the three ports were saved as contour templates in RayStation.

2.3 Strategies for handling metal artifacts

The CT artifacts caused by the metal-ports are managed using two density override strategies at our institution. The first strategy (hereafter called RS1) consists of identifying the metal by adjusting the image window-level to display only the brightest region, assumed occupied by the metal port. Subsequently, a contour is delineated enclosing the artifact and the density of surrounding voxels is set to unity. The second strategy (hereafter called RS2) consists of registering rigidly a geometry template with the dimensions, materials, and densities from the corresponding metal-ports obtained from the vendor; the density of voxels outside the port geometry is set to unity. Both strategies were compared using Collapsed Cone Convolution (CCC) version 5.5 in RayStation version 11A, and TOPAS Monte Carlo simulations. The resolution of the dose grid for RayStation and TOPAS calculations was 2 x 2 x 2 mm^3. Calculated results were compared with Gafchromic film (Ashland Inc.) measurements using two irradiation setups as described below.

2.4 Wax slab phantom setup

A setup consisting of a wax slab phantom irradiated by an AP field was configured to assist in the validation of TOPAS simulations for each TTE port. For each TTE, the ports were stripped off from the silicon bag and embedded in a slab phantom made of wax (ρ=0.92 g/cm^3). The phantom had

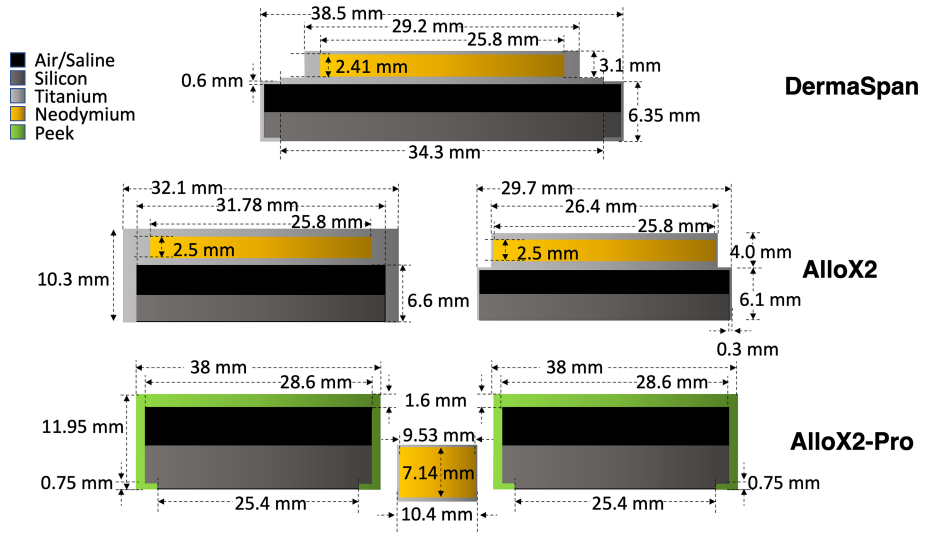

FIGURE 1
Drain/injection ports for the three temporal breast tissue expanders studied in this work.

dimensions of 30 x 30 x 1.7 cm^3. An irradiation setup was configured consisting of the slab phantom stacked between 1.5 cm thickness of plastic water and 10 cm thickness underneath, see Figure 2. An iterative metal artifact reduction (iMAR) (Siemens Medical System) algorithm was used to reduce the high-density metal artifacts. The setup was simulated and exported to RayStation TPS for planning. The plan consisted of a 6 MV field of 15 x 10 cm^2 defined at 100 SSD, 500 MU delivered in the AP direction. The remained metal artifacts were handled with the two strategies described in section 2.3. The setup was reproduced with TOPAS simulations which included the actual port geometries shown in Figure 1. The ports were aligned to the metal artifact using the RayStation contours from RS2 as a frame of reference. The overlapping of geometries was handled by the feature Layered Mass Geometry (21). Film dosimetry was performed by placing Gafchromic films at different positions as shown in Figure 2.

2.5 Breast tissue expander phantom setup

The effect of using multiple gantry angles was evaluated for AlloX2 and AlloX2-Pro TTEs. The partial arc irradiations were performed on the ports using an open field as detailed below. This setup was representative of a worst-case scenario where multiple x-ray beams interacts with the metal port for most of the irradiation time.

The AlloX2 and AlloX2-Pro TTEs were irradiated in their standard configuration during PMRT i.e., embedded in the silicon bag filled with water. The silicon bag wall (~1.1 g/cm^3) was about 1 mm of thickness and had a negligible effect on the dose distributions. In this work, water was used instead of saline solution which shown to be dosimetrically equivalent for MV radiation. However, it has a dosimetric impact by 5% for kV photons, as shown by (22). A customized breast phantom holder and bolus (5 mm thickness) were made with wax to immobilize the phantom for reproducibility. The bolus was placed on top of a thermoplastic mesh covering the breast tissue expander with the air gaps filled with superflab bolus as best as possible. CT images were obtained with iMAR algorithm (section 2.3) and exported to RayStation TPS for planning. The plan consisted of a 6 MV conformal arc (3 x 3 cm^2), gantry angles from 90 to 270 degrees in the counterclockwise direction, delivering 355 MU in a single fraction, see Figure 2. The partial arc configuration considered the contribution of parallel opposed fields at 90 and 270 deg. Contours were drawn for the analysis which included the silicon bag, an expanded wall to the silicon bag of 3 mm thickness split into four contours. These contours covered the anterior (C_Anterior), posterior (C_Posterior), left (C_Left) and right (C_Right) directions of the beam. Pieces of films were positioned at several depths as shown in Figure 2. The films for analysis were 1 x 1 cm^2 and were read at least 24 hours after the irradiation.

3 Results

3.1 TrueBeam phase space verification

In Figure 3, the measured percentage depth-dose (PDD) and crossline dose profiles are compared with the ones calculated with the Varian phase spaces for two open fields. For the crossline profiles, several curves are displayed at a depth of 1.5 cm, 10 cm, and 20 cm depths. The bottom of each panel displays the γ-index value resulting from the TOPAS and measurements comparison. As

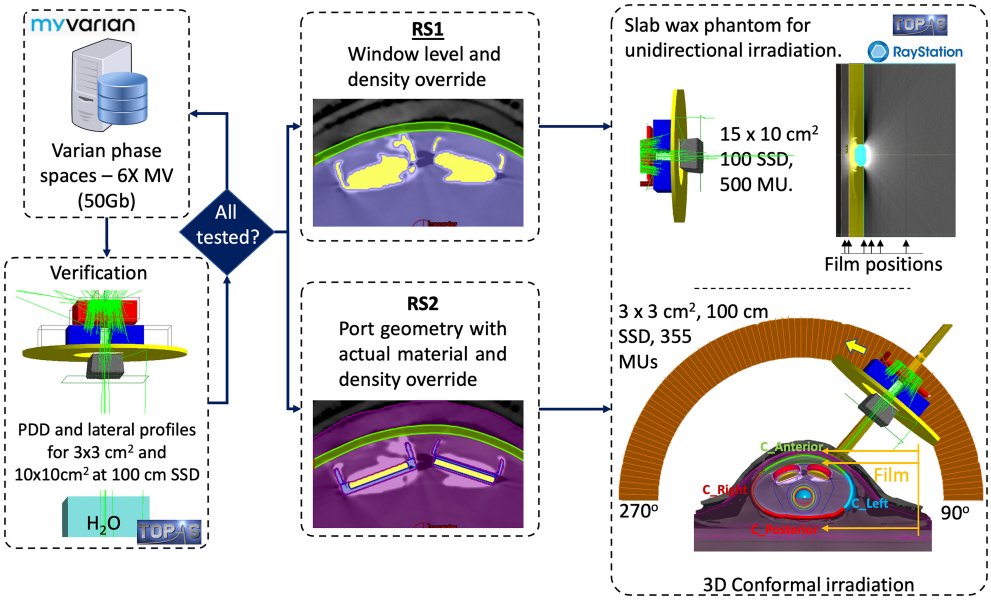

FIGURE 2
Simulation workflow. Phase space files were obtained from myVarian webpage and verified with Monte Carlo simulations of two open fields. Subsequently, two strategies were used to identify or override the metal artifact using RayStation TPS. Finally, both strategies were studied and compared with film measurements. Two irradiation setups were considered, the first using an AP beam and a slab wax phantom stacked between plastic water; the second using conformal beam irradiating the TTE filled with water embedded in a customized wax phantom.

10.3389/fonc.2023.1124838

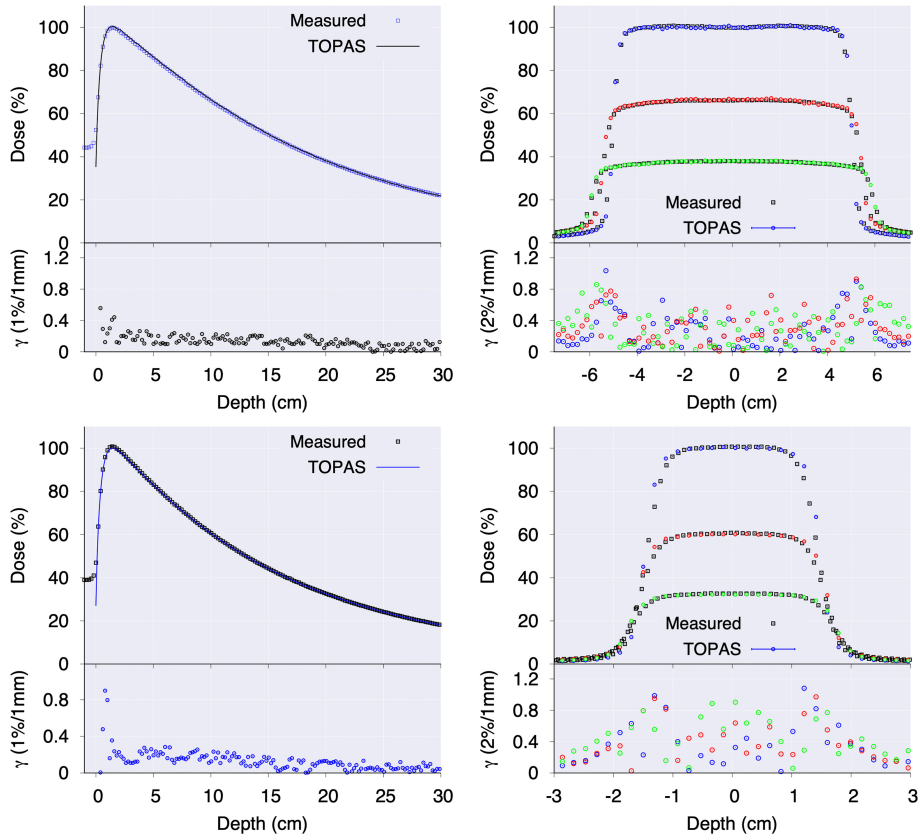

FIGURE 3
Percentage depth-dose and crossline profiles for 10 x 10 cm^2 (top row panel A and B) and 3 x 3 cm^2 (bottom row **C**, **D**) fields calculated with Varian phase spaces. Crossline profiles **(B, D)** are presented at depth of maximum dose, and at 10 cm and 20 cm depth. The γ-index values are presented at the bottom of each panel.

depicted, for all the panels the γ-index is below unity for the 1%/1mm (PDD) and 2%/1 mm (crossline) criteria.

3.2 Slab wax phantom setup

Panels of Figure 4 show depth-dose profiles for the configuration consisting of the breast tissue expander ports embedded in a wax slab phantom. For DermaSpan and AlloX2-Pro the central profiles are shown, whereas for AlloX2, the profiles crossing the injection port are shown. Film measurements are shown with symbols. At the bottom of the panels, the less restricted of percentage difference and distance-to-agreement to the measured data are shown. The vertical lines delimit the region occupied by the slab wax phantom. For the DermaSpan port (panel A), both RS1 and RS2 were within 2%/1 mm in the buildup region

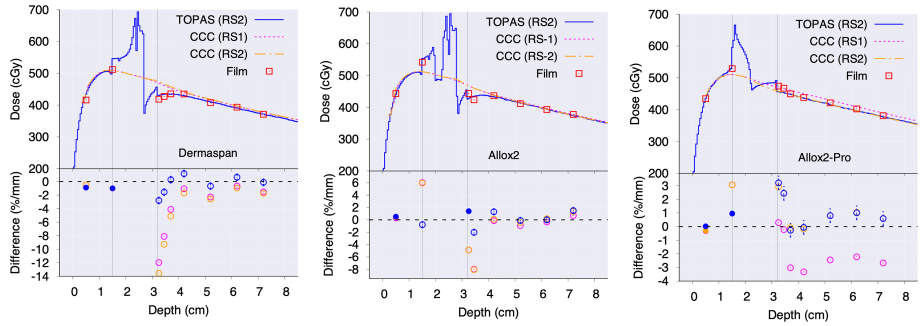

FIGURE 4
Depth-dose curves comparing the CCC (RS1 in dashed, RS2 in dotted-dashed), TOPAS (RS2 in solid) and film measurements (empty squares) for: DermaSpan **(A)**, AlloX2 **(B)** and AlloX2-Pro **(C)**. The bottom of each panel shows the least restricted between the percentage difference (empty symbols) and distance-to-agreement (filled symbols). The vertical lines limit the region occupied by the slab wax phantom.

and distal falloff. Much higher difference was seen at the region immediately at downstream the port. For the AlloX2 (panel B), both RS1 and RS2 were within 2%/1 mm at the buildup and distal falloff. Lastly, for the AlloX2-Pro (panel C), at the buildup region, both RS1 and RS2 were within 2%/1 mm from measurements. At the distal falloff, RS1 differed from the film measurements by 2.7% whereas for RS2 the differences were within 1%. For all the three ports, TOPAS simulations were within (2% ± 0.5%)/1mm in the buildup and distal falloff regions.

The effect of the port in the depth-dose distributions outside the wax phantom was calculated with TOPAS by comparing simulations with the port substituted by wax. Results are shown in the Figure 5. As depicted, the underdosages caused by the attenuation from the magnets in the ports were (6.4 ± 0.4)%, (4.9 ± 0.7)% and (2.0 ± 0.9)% for DermaSpan, AlloX2 and AlloX2-Pro, respectively. In the region proximal to the beam entrance, an overdose caused by the backscatter radiation was observed for the AlloX2-Pro. The overdose decays rapidly from about 3% ± 1% to zero within the first 5 mm.

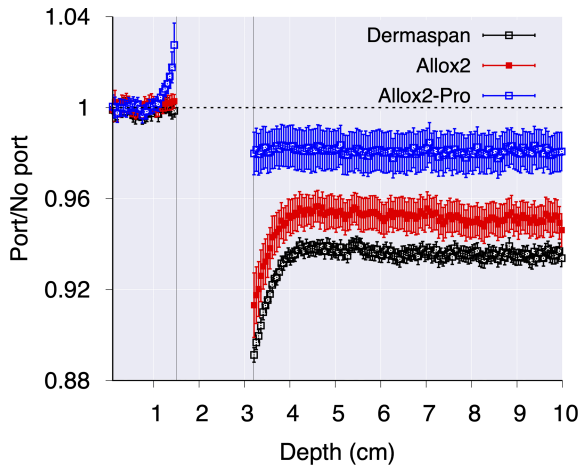

FIGURE 5
The effect of metal port calculated with MC simulations for the three breast tissue expander models.

3.3 Tissue expander phantom setup

In panels of Figure 6 the dose profiles along the anterior-posterior direction traversing the drain and central magnets are shown for the AlloX2 (panel A) and AlloX2-Pro (panel B), respectively (section 2.5 and Figure 2). Film measurements are shown with symbols at three positions. For both TTEs, RS2 calculated with CCC (CCC (RS2)) agreed reasonably well with TOPAS calculations but did not reproduce the dose perturbation near the magnet, at about the 4 cm position. RS1 (MC (RS1)) and RS2 (MC (RS2)) results calculated with TOPAS had better agreement to the film measurements, been RS2 the closer to the measured data, as shown in the bottom of each panel of Figure 6. The axial isodose distributions calculated with TOPAS for AlloX2 and AlloX2-Pro using RS-1 and RS-2 are displayed in Figure 7. As depicted, the most significant dose differences, as large as 25% ± 1.5% and 28% ± 1.5%, occur locally around the magnet region. These dose differences are almost entirely contained by the silicon bag. The dosimetric impact outside of the bag is minimal as shown for the contour volumes in Tables 1, 2.

The impact of the TTE port in the dose distribution was quantified by comparing dose volume histogram (DVH) parameters for simulations with and without the metal port, for the contours displayed in Figure 2. Results are shown in Tables 1, 2 for the AlloX2 and AlloX2-Pro, respectively. Combined statistical uncertainties were 1.0%, one standard deviation, or better. For AlloX2, the impact of the metal port calculated by RS1 and RS2 exceeded statistical uncertainties only for the contour C_Posterior located at the posterior region of the phantom, effect caused by the attenuation introduced by the metal port. In this region, RS1 produced a higher dose than using RS2, e.g., by 2.1% for D10. On the other hand, for AlloX2-Pro the impact of the metal port in the

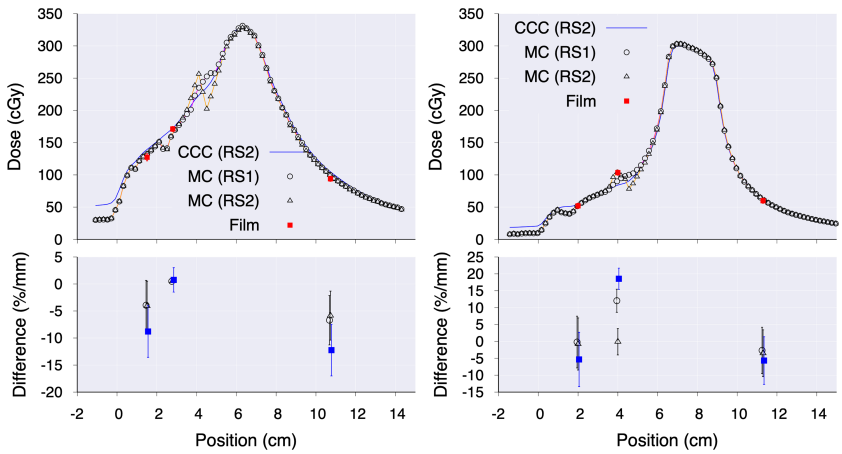

FIGURE 6
Dose profiles along the anterior-posterior direction for AlloX2 (left) and AlloX2-Pro (right). For CCC, only results using RS2 are shown. The panels at the bottom show the difference between measured and calculated data.

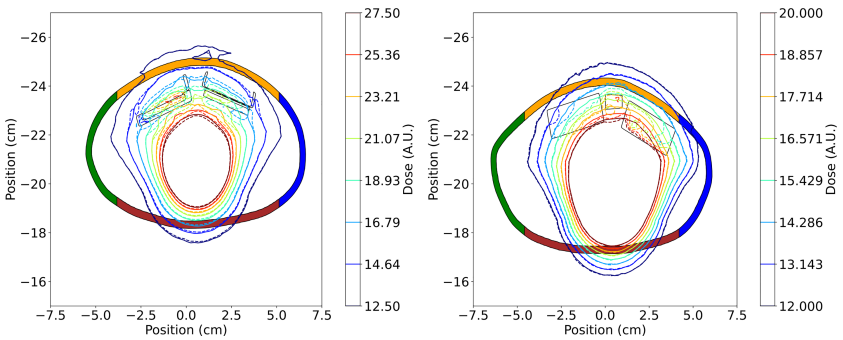

FIGURE 7
Axial isodose distributions in arbitrary units (A.U.) calculated with Monte Carlo for the AlloX2 (left) and AlloX2-Pro (right) TTEs. Solid lines correspond to RS1, and dashed lines correspond to RS2. The colored regions correspond to each contour shown in Table 2. The outer limiting frame of the metal ports are shown with solid lines.

computation of DVH parameters shown in Table 2 resulted in subpercentage differences, smaller than the combined statistical uncertainty. Furthermore, RS1 and RS2 were statistically equivalent as the percentage differences between DVH parameters fell within the combined statistical uncertainty.

4 Discussion

In this work, the dosimetric characterization of three TTEs was performed with the Monte Carlo method and CCC. Dose at selected positions in two irradiation setups, using wax slab phantom (3D-CRT) and customized breast phantom (conformal arc radiotherapy), were compared with film measurements obtaining an overall agreement within 3%. For both irradiation setups, two strategies for handling the CT artifacts produced by TTE metal ports in the calculation of dose distributions for were evaluated.

For the 3D-CRT irradiation setup, the absorbed dose for DermaSpan and AlloX2 was attenuated downstream the magnet. The thickness of each magnet was 2.41 mm and 2.5 mm for DermaSpan and AlloX2, respectively (Figure 1). Under ideal conditions neglecting scattering, the attenuation caused by the magnet (7.4 g/cm^3) irradiated with MV x-rays was expected to be ~5% approximately, the Monte Carlo calculated results also included the titanium port and resulted 6.4% and 4.9%, respectively (Figure 5). Conversely, for the AlloX2-Pro (7.14 mm thickness) the attenuation was substantially lower. This effect was caused by the magnet geometry; the physical dimensions perpendicular to the beam were about one third smaller than for the other two ports. Thus, there was more in-scatter radiation from

TABLE 1 Impact of TTE port in dose distributions for AlloX2.

ROI	Vol. cc	No port – RS1 (%)			No port – RS2 (%)			RS1–RS2 (%)		
		D1	D10	Ave.	D1	D10	Ave.	D1	D10	Ave.
C_Left	7.9	0.1	-0.1	0.4	0.0	-0.2	0.7	0.0	-0.1	0.3
C_Right	8.3	-0.1	-0.1	0.2	-0.1	0.0	0.4	0.0	0.1	0.2
C_Anterior	17.6	-0.2	-0.1	-0.2	-0.3	-0.2	-0.3	-0.1	-0.1	-0.1
C_Posterior	15.4	4.3	3.7	2.6	6.2	5.5	4.0	2.1	1.9	1.4

The impact is quantified by the percentage differences between DVH parameters calculated with Monte Carlo. The percentage difference between RS1 and RS2 are also shown. DVH parameters include the dose at 1% of the volume (D1), dose at 10% of the volume (D10) and average dose.

TABLE 2 Impact of TTE port in dose distributions for AlloX2-Pro.

ROI	Vol. cc	No port – RS1 (%)			No port – RS2 (%)			RS1–RS2 (%)		
		D1	D10	Ave.	D1	D10	Ave.	D1	D10	Ave.
C_Left	9.0	-0.1	-0.2	-0.2	-0.5	-0.4	-0.6	-0.4	-0.3	-0.4
C_Right	9.1	-0.1	0.2	-0.1	-0.6	-0.2	-0.6	-0.5	-0.4	-0.5
C_Anterior	15.8	-0.1	-0.2	-0.2	-1.0	-0.9	-0.7	-1.0	-0.6	-0.6
C_Posterior	18.1	0.0	0.4	-0.1	-0.5	-0.2	-0.6	-0.6	0.6	-0.5

The impact is quantified by the percentage differences between DVH parameters calculated with Monte Carlo. The percentage difference between RS1 and RS2 are also shown. DVH parameters include the dose at 1% of the volume (D1), dose at 10% of the volume (D10) and average dose.

the unobstructed portion of the beam for AlloX2-Pro. The in-scatter radiation compensated the attenuation of dose leading to an underdose of about 2%. On the other hand, in the buildup region backscatter dose was observed for AlloX2-Pro only. That backscatter originated by the closer position of the AlloX2-Pro magnet to the TTE surface compared to the other two models. In the literature, backscatter dose factors for 6 MV beams incident in lead (11.3 g/cm^3) had been reported to reduce from a factor of 1.03 to 1 within the first centimeter (23). The dose profile calculated with Monte Carlo in this work showed the equivalent behavior as that reported in the literature. The clinical impact of the backscatter dose is expected to be negligible as the maximum extent of the magnet dictates the diameter of the region irradiated by backscatter radiation. This diameter (10.4 mm) is smaller than the diameter stated by ICRU 50 (15 mm) for the definition of a hot spot (24).

The calculated absorbed dose using CCC for both strategies (RS1 and RS2) agreed with Monte Carlo and film measurements within 2%/1 mm for DermaSpan and AlloX2 and within 3%/1 mm for AlloX2-Pro in the buildup region and distal falloff of the depth-dose distribution (Figure 4).

The higher discrepancies occurred in the region downstream of the magnet within the first centimeter. While this discrepancy was a result of the limitations of the dose calculation algorithms and dose grid resolution, its location was expected to be within the filled TTE silicon bag region which might encompass at least 4-5 cm thickness, having minimal impact on the patient. The closer agreement between RS1 and RS2 for DermaSpan and AlloX2 at the distal falloff region was not surprising. The maximum density (2.5 g/cm^3) from the CT density tables assigned to the metal artifact for RS1 was about three times smaller than the actual magnet density (7.4 g/cm^3) used in RS2, however, the thickness of the identified metal artifact was also about three times greater than the thickness of the actual magnet geometry. Thus, the amount of attenuation in both cases was similar. On the other hand, for AlloX2-Pro the thickness of the metal artifact and the magnet were about the same dimension. Therefore, there was less attenuation using strategy RS1 that led to an overdose of about 3% compared with RS2.

The impact of the beam direction was quantified using partial arc irradiation and a customized phantom for both AlloX2 and AlloX2-Pro. Comparison between simulations with and without port were presented in Tables 1, 2. For AlloX2, the metal port attenuated the dose distribution posteriorly leading to a reduction of the D10 parameter by 5.5%, calculated with RS2. By using RS1, this value can be overestimated by ~2% as shown in Table 1. For the regions located at the lateral positions, the effect of the port was mitigated by the opposed radiation fields (23). This compensation resulted in a negligible difference in the DVH parameters as shown in Table 1. On the other hand, for AlloX2-Pro the impact of the metal port under partial arc irradiation resulted in sub-percentage differences in the DVH parameters, as shown in Table 2. This effect resulted from the small size of the magnet, which allowed more contribution from the in-scatter radiation, as shown for the slab wax phantom setup. Finally, sub-percentage differences in DVH parameters between RS1 and RS2 resulted from the comparable dimension of the metal artifact and the magnet.

In this work 6 MV beams were considered. Retrospective studies reported that 6 MV beams are mostly used for 3D planning of breast with tangents (25) while higher energy beams are often used for large breast separations to improve homogeneity. Above 10 MV, the dose distributions are highly affected by the pair production process within the first 2 cm from the surface of metal objects (23). In addition, the production of photoneutrons takes relevance. Contrary to CCC, these two interaction processes can be explicitly modeled with the Monte Carlo method so that dose differences between the two methods are expected near the metal ports. The dosimetric study of high energy beams in metal ports is out of the scope of current work as a prior validation of TOPAS for the simulation of the photoneutrons yield is needed. This task is ongoing in our research group and will be presented in future work.

In a typical IMRT treatment in VMAT mode, for example, the MLC modulation might partially or totally occlude the radiation directed to the metal port. Thus, the partial arc configuration represented the extreme scenario when the port was irradiated all the time. The highest differences found in the DVH parameters calculated with RS1 and RS2 might be mitigated by the MLC modulation.

Finally, caution must be practiced when higher saturation HU values are used, which lead to higher density values. The density assigned to the identified metal artifact in RS1 highly depended upon the CT density tables and the delineation of artifacts. Thus, we recommend using the actual port geometry and materials. Templates compatible with RayStation TPS are provided in the supplementary material of this work to reduce the delineation time for the TTEs studied in this work.

5 Conclusions

The dosimetric impact of the TTEs in PMRT depended on the geometry, artifact delineation method, and irradiation conditions. The greatest differences with respect to measurements were observed in the RS1 strategy. Using a template with the actual port geometry and materials (RS2) can alleviate the differences and reduce the artifact delineation time. Negligible dose perturbation was observed for the novel TTE under continuous partial arc irradiation conditions compared to a single beam at normal incidence.

Data availability statement

The raw data supporting the conclusions of this article will be made available by the authors, without undue reservation.

Author contributions

MS was involved in conceptualizing the research design, planning, and continued supervision of the work. MS performed and processed the experimental data and analysis and wrote on the manuscript. JM conceptualized and executed the Monte Carlo simulations, analyzed the data, and wrote the manuscript. CP aided

in interpreting the results and worked on the manuscript. All authors contributed to the article and approved the submitted version.

Funding

This work is supported in part by a sponsored grant sponsored by Sientra Inc CA0160869 and NIH/NCI U24 CA215123.

Acknowledgments

We acknowledge Peter Li from the University of California Berkely for his help in analyzing the film data, Annette Villa and Naoki Dominguez-Kondo from the University of California San Francisco for making the wax phantoms and for providing the TOPAS geometry extension for the 120 Millennium MLC, respectively; and Darren Sawkey from Varian for providing the 120 Millennium MLC geometry details. We would like to thank Joanna C Yang, Adam Melancon and Junhan Pan for the initial discussions on AlloX2 TTEs.

Conflict of interest

This work was partially supported by a research grant from Sientra Inc.

Publisher's note

References

1. Canturk NZ, Şimşek T, Guler SA. Standard mastectomy. In: Rezai M, Kocdor MA, Canturk NZ, editors. *Breast cancer essentials*. Cham: Springer International Publishing (2021). p. 331–47. doi: 10.1007/978-3-030-73147-2_31

2. Friedrich M, Krämer S, Friedrich D, Kraft C, Maass N, Rogmans C. Difficulties of breast reconstruction – problems that no one likes to face. *Anticancer Res* (2021) 41 (11):5365–75. doi: 10.21873/anticanres.15349

3. Bellini E, Pesce M, Santi P, Raposio E. Two-stage tissue-expander breast reconstruction: a focus on the surgical technique. *BioMed Res Int* (2017) 2017:1–8. doi: 10.1155/2017/1791546

4. Pacella SJ. Evolution in tissue expander design for breast reconstruction: technological innovation to optimize patient outcomes. *Plast Reconstructive Surg* (2018) 142:21S–30S. doi: 10.1097/PRS.0000000000004999

5. Degnim AC, Scow JS, Hoskin TL, Miller JP, Loprinzi M, Boughey JC, et al. Randomized controlled trial to reduce bacterial colonization of surgical drains after breast and axillary operations. *Ann Surg* (2013) 258(2):240–7. doi: 10.1097/SLA.0b013e31828c0b85

6. Franck P, Chadab T, Poveromo L, Ellison A, Simmons R, Otterburn DM. Prepectoral dual-port tissue expander placement: can this eliminate suction drain use? *Ann Plast Surg* (2020) 85(S1):S60–2. doi: 10.1097/SAP.0000000000002344

7. Mizuno N, Takahashi H, Kawamori J, Nakamura N, Ogita M, Hatanaka S, et al. Determination of the appropriate physical density of internal metallic ports in temporary tissue expanders for the treatment planning of post-mastectomy radiation therapy. *J Radiat Res* (2018) 59(2):190–7. doi: 10.1093/jrr/rrx085

8. Thompson RCA, Morgan AM. Investigation into dosimetric effect of a MAGNA-SITE™ tissue expander on post-mastectomy radiotherapy: dosimetric effect of a tissue expander. *Med Phys* (2005) 32(6Part1):1640–6. doi: 10.1118/1.1914545

9. Damast S, Beal K, Ballangrud Å, Losasso TJ, Cordeiro PG, Disa JJ, et al. Do metallic ports in tissue expanders affect postmastectomy radiation delivery? *Int J Radiat OncologyBiologyPhysics* (2006) 66(1):305–10. doi: 10.1016/j.ijrobp.2006.05.017

10. Chatzigiannis C, Lymperopoulou G, Sandilos P, Dardoufas C, Yakoumakis E, Georgiou E, et al. Dose perturbation in the radiotherapy of breast cancer patients implanted with the magna-site: a Monte Carlo study. *J Appl Clin Med Phys* (2011) 12 (2):58–70. doi: 10.1120/jacmp.v12i2.3295

11. Yoon J, Xie Y, Heins D, Zhang R. Modeling of the metallic port in breast tissue expanders for photon radiotherapy. *J Appl Clin Med Phys* (2018) 19(3):205–14. doi: 10.1002/acm2.12320

12. Park SH, Kim YS, Choi J. Dosimetric analysis of the effects of a temporary tissue expander on the radiotherapy technique. *Radiol Med* (2021) 126(3):437–44. doi: 10.1007/s11547-020-01297-6

13. Strang B, Rt KM, Seal S, Cin AD. Does the presence of an implant including expander with internal port alter radiation dose? *Ex Vivo Model* (2013) 21(1):4. doi: 10.1177/229255031302100109

14. Trombetta DM, Cardoso SC, Facure A, da Silva AX, da Rosa LAR. Influence of the presence of tissue expanders on energy deposition for post-mastectomy radiotherapy. *PloS One* (2013) 8(2):e55430. doi: 10.1371/journal.pone.0055430

15. Perl J, Shin J, Schümann J, Faddegon B, Paganetti H. TOPAS: an innovative proton Monte Carlo platform for research and clinical applications. *Med Physics.* (2012) 39(11):6818–37. doi: 10.1118/1.4758060

16. Faddegon B, Ramos-Méndez J, Schuemann J, McNamara A, Shin J, Perl J, et al. The TOPAS tool for particle simulation, a Monte Carlo simulation tool for physics, biology and clinical research. *Physica Med* (2020) 72(February):114–21. doi: 10.1016/j.ejmp.2020.03.019

17. Agostinelli S, Allison J, Amako K, Apostolakis J, Araujo H, Arce P, et al. Geant4–a simulation toolkit. *Nucl. Instrum. Methods Phys Res A* (2003) 506(3):250–303. doi: 10.1016/S0168-9002(03)01368-8

18. Arce P, Bolst D, Bordage M, Brown JMC, Cirrone P, Cortés-Giraldo MA, et al. Report on G4-med, a Geant4 benchmarking system for medical physics applications developed by the Geant4 medical simulation benchmarking group. *Med Physics* (2021) 48(1):19–56. doi: 10.1002/mp.14226

19. Bush K, Zavgorodni SF, Beckham WA. Azimuthal particle redistribution for the reduction of latent phase-space variance in Monte Carlo simulations. *Phys Med Biol* (2007) 52(14):4345–60. doi: 10.1088/0031-9155/52/14/021

20. Ramos-Méndez J, Perl J, Faddegon B, Schümann J, Paganetti H. Geometrical splitting technique to improve the computational efficiency in Monte Carlo calculations for proton therapy. *Med Physics.* (2013) 40(4):041718. doi: 10.1118/1.4795343

21. Enger SA, Landry G, D'Amours M, Verhaegen F, Beaulieu L, Asai M, et al. Layered mass geometry: a novel technique to overlay seeds and applicators onto patient geometry in Geant4 brachytherapy simulations. *Phys Med Biol* (2012) 57(19):6269–77. doi: 10.1088/0031-9155/57/19/6269

22. Redler G, Templeton A, Zhen H, Turian J, Bernard D, Chu JCH, et al. Dosimetric effects of saline- versus water-filled balloon applicators for IORT using the model S700 electronic brachytherapy source. *Brachytherapy* (2018) 17(2):500–5. doi: 10.1016/j.brachy.2017.11.003

23. Reft C, Alecu R, Das IJ, Gerbi BJ, Keall P, Lief E, et al. Dosimetric considerations for patients with HIP prostheses undergoing pelvic irradiation. report of the AAPM radiation therapy committee task group 63. *Med Phys* (2003) 30(6):1162–82. doi: 10.1118/1.1565113

24. International Commission on Radiation Units and Measurements. *Prescribing, recording, and reporting photon beam therapy* Vol. 72. . Bethesda, Md: Internat. Comm. on Radiation Units and Measurements (1993).

25. Nichol A, Narinesingh D, Wade L, Raman S, Gondara L, Speers C, et al. Breast tangent beam energy, surgical bed-to-Skin distance and local recurrence after breast-conserving treatment. *Int J Radiat Oncol Biol Phys* (2022) 112(3):671–80. doi: 10.1016/j.ijrobp.2021.10.014

frontiers | Frontiers in Oncology

TYPE Original Research
PUBLISHED 23 May 2023
DOI 10.3389/fonc.2023.1118713

OPEN ACCESS

EDITED BY
Vishruta Dumane,
Icahn School of Medicine at Mount Sinai, United States

REVIEWED BY
Hidekazu Tanaka,
Yamaguchi University Graduate School of Medicine, Japan
Christin A. Knowlton,
Yale University, United States

*CORRESPONDENCE
Ryan M. Rhome
rrhome@iuhealth.org

RECEIVED 07 December 2022
ACCEPTED 09 May 2023
PUBLISHED 23 May 2023

CITATION
Le A, Achiko FA, Boyd L, Shan M, Zellars RC and Rhome RM (2023) Patient characteristics and clinical factors affecting lumpectomy cavity volume: implications for partial breast irradiation.
Front. Oncol. 13:1118713.
doi: 10.3389/fonc.2023.1118713

Patient characteristics and clinical factors affecting lumpectomy cavity volume: implications for partial breast irradiation

Amy Le[1], Flora Amy Achiko[1], LaKeisha Boyd[2], Mu Shan[2], Richard C. Zellars[1] and Ryan M. Rhome[1]*

[1]Department of Radiation Oncology, Indiana University School of Medicine, Indianapolis, IN, United States, [2]Department of Biostatistics, Indiana University School of Medicine, Indianapolis, IN, United States

Introduction: Partial breast irradiation (PBI) has increased in utilization, with the postoperative lumpectomy cavity and clips used to guide target volumes. The ideal timing to perform computed tomography (CT)–based treatment planning for this technique is unclear. Prior studies have examined change in volume over time from surgery but not the effect of patient characteristics on lumpectomy cavity volume. We sought to investigate patient and clinical factors that may contribute to larger postsurgical lumpectomy cavities and therefore predict for larger PBI volumes.

Methods: A total of 351 consecutive women with invasive or *in situ* breast cancer underwent planning CT after breast-conserving surgery at a single institution during 2019 and 2020. Lumpectomy cavities were contoured, and volume was retrospectively computed using the treatment planning system. Univariate and multivariate analyses were performed to evaluate the associations between lumpectomy cavity volume and patient and clinical factors.

Results: Median age was 61.0 years (range, 30–91), 23.9% of patients were Black people, 52.1% had hypertension, the median body mass index (BMI) was 30.4 kg/m^2, 11.4% received neoadjuvant chemotherapy, 32.5% were treated prone, mean interval from surgery to CT simulation was 54.1 days $\pm$ 45.9, and mean lumpectomy cavity volume was 42.2 cm^3 $\pm$ 52.0. Longer interval from surgery was significantly associated with smaller lumpectomy cavity volume on univariate analysis, $p = 0.048$. Race, hypertension, BMI, the receipt of neoadjuvant chemotherapy, and prone position remained significant on multivariate analysis ($p < 0.05$ for all). Prone position vs. supine, higher BMI, the receipt of neoadjuvant chemotherapy, the presence of hypertension, and race (Black people vs. White people) were associated with larger mean lumpectomy cavity volume.

Discussion: These data may be used to select patients for which longer time to simulation may result in smaller lumpectomy cavity volumes and therefore

smaller PBI target volumes. Racial disparity in cavity size is not explained by known confounders and may reflect unmeasured systemic determinants of health. Larger datasets and prospective evaluation would be ideal to confirm these hypotheses.

KEYWORDS

partial breast irradiation (PBI), breast cancer, lumpectomy, race, hypertension, BMI, neoadjuvant chemotherapy, prone

1 Introduction

Adjuvant radiation is typically indicated after breast-conserving surgery (BCS) to improve local control, which translates on meta-analysis to survival benefits (1–6). Multiple published studies have clearly established the efficacy of the partial breast irradiation (PBI) technique for adjuvant radiation after BCS. Randomized trials comparing external beam PBI with whole breast radiation (WBRT) have shown no clinically significant difference in survival, regional recurrence, or ipsilateral breast tumor recurrence (IBTR) with median follow-up ranging from 5 to greater than 10 years (7–12). Brachytherapy options exist for PBI, but accelerated (twice daily) radiation appears to be associated with worse cosmesis, and brachytherapy has been shown to result in increased IBTR (8, 13).

Variation exists in the application of the PBI technique. For external beam PBI, the postoperative lumpectomy cavity with or without clips is generally used to guide volumes to target the postoperative tumor bed and a margin of adjacent breast tissue. The NSABP B-39/RTOG 0412 protocol specified the lumpectomy excision cavity was outlined based on clear visualization on computed tomography (CT) or with the help of surgical clips if those were placed, and the clinical target volume (CTV) was defined as a 15-mm uniform expansion of the lumpectomy cavity, while the planning target volume (PTV) was defined as a uniform 10-mm expansion of the CTV. If the lumpectomy cavity could not be delineated clearly or the lumpectomy cavity/whole breast reference volume was >30% based on postoperative CT scan, then the patient was not eligible for study participation (8). Even without potential ineligibility based on the size of the lumpectomy cavity, a larger lumpectomy cavity will lead to larger radiation field sizes. The ideal postsurgical timing to perform CT-based treatment planning for the PBI technique is unclear. Prior studies have examined change in volume over time from surgery and associated clinical factors, with expected decrease in the size of the lumpectomy cavity or seroma volume over the postoperative period (14, 15). One study by Kader et al. demonstrated that seroma volume correlated significantly with the volume of excised breast tissue but not with other clinical characteristics including tumor diameter, surgical re-excision, and chemotherapy use (14). Simulation and treatment at the optimal time for a minimum lumpectomy cavity volume that can still be clearly delineated could increase the proportion of patients eligible for PBI and/or decrease treatment volumes.

The effect of patient characteristics including comorbidities that may affect healing in the postoperative period has not been previously reported. We sought to investigate patient and clinical factors that may contribute to larger postsurgical lumpectomy cavities and therefore would predict for larger PBI volumes.

2 Materials and methods

This study involved the secondary use of private information from the electronic medical record and was approved as exempt by the institutional review board. A total of 351 consecutive women with invasive or *in situ* breast cancer underwent CT after BCS as part of the standard planning for PBI or WBRT. CT images were obtained using 5-mm slice thickness, with the scan extending from superior to the suprasternal notch to a minimum of 5 cm below the inframammary fold. The CT images were transferred to the treatment planning system (TPS) (Eclipse, Varian Medical Systems, Palo Alto, CA).

There were 357 total lumpectomy cavities that were contoured per institutional standard at a single institution with four radiation centers during the years 2019 and 2020. In general, the lumpectomy cavity delineation included all related radiopaque surgical clips when present. In addition, contouring the seroma and surgical anatomical changes in conjunction with preoperative imaging, operative note, and pathology report was the standard with or without clips. Six patients had two lumpectomies during the same surgery due to invasive or *in situ* breast cancer in bilateral breasts. One patient had two lumpectomies in separate quadrants of the ipsilateral breast. For patients with multiple lumpectomy cavities contoured, the first record in the dataset was included and the second record was excluded in order to prevent duplicate records for the analysis of patient characteristics, resulting in 351 total included lumpectomy cavities. Contoured volume was retrospectively computed from the TPS.

Clinical data extracted from the patients' medical records included age at the time of surgery, the body mass index (BMI) at the time of surgery, race, the presence of diabetes mellitus, smoking status, the presence of hypertension, the presence of coronary artery

disease, the date of last definitive BCS (including repeat excision), the date of planning CT scan, whether surgical re-excision had been performed, the pathologic maximal diameter of the primary tumor, volume excised from lumpectomy, and additional margins (total volume of excised breast tissue), whether patients had undergone oncoplastic reduction, prior surgery or prior biopsy in ipsilateral breast, neoadjuvant hormone therapy use (including aromatase inhibitor or tamoxifen), neoadjuvant chemotherapy use, and adjuvant chemotherapy use. From the CT simulation in the TPS, the position (supine or prone), the presence of surgical clips placed at time of lumpectomy, and physician-contoured lumpectomy cavity volume were extracted. The institutional preference for positioning is the prone position; however, if the patient has smaller, non-pendulous breasts and/or difficulty remaining in the prone position due to discomfort, then the supine position is used.

The change in lumpectomy cavity volume relative to interval after surgery was calculated with linear regression using the gradient estimation method with a log transform. Since the original data for lumpectomy cavity volume followed a log-normal distribution or approximately so, the log transform was performed to reduce skewness resulting in a near-normal distribution. To evaluate the associations among patient, clinical, and treatment factors on lumpectomy cavity volume, univariate analysis was performed and variates with a p-value < 0.1 were included in multivariate analysis.

3 Results

The distribution of patient, clinical, and selected treatment characteristics are summarized in Tables 1A, B. Median age was 61.0 years (range, 30–91). The median BMI was 30.4 kg/m² (first quartile [Q1] to third quartile [Q3], 25.5–35.2). There were 23.9% of patients who were Black people, 71.2% of patients were White people, and 4.8% were other. There were 52.1% of patients who had hypertension, 17.1% had diabetes mellitus, 6.0% had coronary artery disease, 12.0% were current smokers, 29.9% were former smokers, and 58.1% were never smokers. The mean tumor size was 1.3 cm (standard deviation, 1.1).

All patients underwent BCS, with 10% requiring surgical re-excision, 8.8% had oncoplastic reduction, 5.1% had prior surgery or prior biopsy in ipsilateral breast, 4.3% of patients received neoadjuvant hormone therapy (including aromatase inhibitor or tamoxifen), 11.4% received neoadjuvant chemotherapy, and 15.1% received adjuvant chemotherapy. There were 32.5% who were treated in prone position, 82.9% of patients had surgical clips placed at time of lumpectomy, mean interval from surgery to CT simulation was 54.1 ± 45.9 days, and mean lumpectomy cavity volume was 42.2 ± 52.0 cm^3.

Longer interval from surgery (as a continuous variable) was significantly associated with smaller lumpectomy cavity volume on univariate analysis (Figure 1, estimate = −0.006, p = 0.048). For each

TABLE 1A Patient, clinical, and treatment characteristics.

Characteristic	N	Mean ± SD	Median (Q1–Q3)
Age (y) **mean ± standard**	351	60.5 ± 10.6	61.0 (53.0–68.0)
BMI (kg/m^2) **mean ± standard**	332	31.1 ± 7.3	30.4 (25.5–35.2)
Days from surgery **median (Q1–Q3)**	351	54.1 ± 45.9	37.0 (28.0–57.0)
Lumpectomy volume (cm^3) **median (Q1 –Q3)**	351	42.2 ± 52.0	26.7 (14.8–53.9)
Total volume excised (cm^3) **median (Q1 –Q3)**	345	175.7 ± 322.0	89.6 (58.5–161.3)
Tumor size (max dimension of largest tumor, cm) **median (Q1–Q3)**	351	1.3 ± 1.1	1.1 (0.6–1.8)

TABLE 1B Patient, clinical, and treatment characteristics.

Surgical re-excision	Yes	35 (10.0%)
Oncoplastic reduction	Yes	31 (8.8%)
Prior breast surgery	Yes	18 (5.1%)
Neoadjuvant AI or tamoxifen	Yes	15 (4.3%)
Neoadjuvant chemotherapy	Yes	40 (11.4%)
Adjuvant chemotherapy	Yes	53 (15.1%)
Race	Black people	84 (23.9%)
	Other	17 (4.8%)
	White people	250 (71.2%)
Diabetes mellitus	Yes	60 (17.1%)
Smoking status	Current	42 (12.0%)

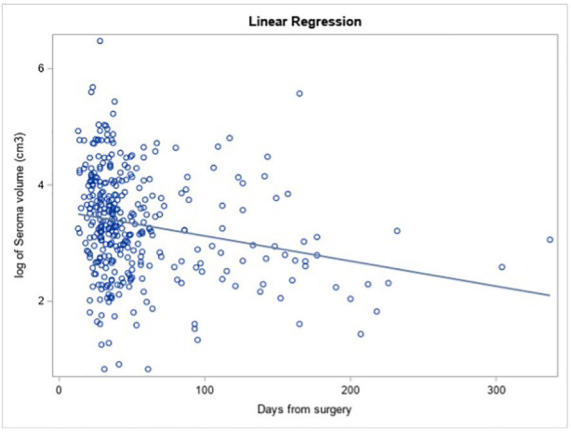

FIGURE 1
Mean lumpectomy cavity volume relative to interval after surgery.

additional day after surgery, the log of the expected mean of lumpectomy cavity volume decreased by 0.006 cm^3, meaning that a 0.6% decrease in lumpectomy cavity volume is expected per day.

On univariate analysis (Table 2), the factors that were significantly associated with lumpectomy cavity volume were interval after surgery, age, BMI, the receipt of neoadjuvant chemotherapy, race, hypertension, coronary artery disease, and position. Surgical re-excision, oncoplastic reduction, prior breast surgery, the receipt of chemotherapy, coronary artery disease, diabetes, the volume of excised breast tissue, smoking status, and the presence of clips were not significantly associated. Of note, 19 patients had missing BMI data and thus were not included in the multivariate model. On multivariate analysis (Table 3), the factors confirmed to have a significant effect on lumpectomy cavity volume ($p < 0.05$ for all) were the BMI, the receipt of neoadjuvant chemotherapy, prone position, hypertension, and race (Black people vs. White people). Higher BMI, the receipt of neoadjuvant

TABLE 2 Univariate analysis results of lumpectomy cavity volume.

Univariate analysis	Estimate	P-value
Interval after surgery	-0.006	0.048
Maximal tumor diameter	0.066	0.1633
Volume of excised breast tissue	0.000	0.8847
Age	0.014	0.0209
BMI	0.030	<0.0001
Surgical re-excision (No vs. Yes)	0.048	0.8325
Oncoplastic reduction (No vs. Yes)	0.185	0.4934
Prior breast surgery (No vs. Yes)	0.085	0.7925
Neoadjuvant AI or tamoxifen (No vs. Yes)	-0.262	0.3078
Neoadjuvant chemotherapy (No vs. Yes)	-0.401	0.0096
Adjuvant chemotherapy (No vs. Yes)	0.391	0.1115
Race		0.0178
Race (Black people vs. White people)	0.337	0.0103
Race (others vs. White people)	-0.515	0.338
Diabetes mellitus (No vs. Yes)	-0.196	0.2038
Smoking status (current, former, or never)		0.4354
Smoking (current vs. never)	0.232	0.1989
Smoking (former vs. never)	0.041	0.7837
Hypertension (No vs. Yes)	-0.417	0.003
Coronary artery disease (No vs. Yes)	-0.441	0.0206
Position (prone vs. supine)	0.296	0.0223
Clips (No vs. Yes)	-0.353	0.1155

TABLE 3 Multivariate analysis results of lumpectomy cavity volume.

Multivariate analysis (N = 332)	Estimate	P-value
Interval after surgery	-0.006	0.0795
Age	0.012	0.0627
BMI	0.020	0.004
Race		0.3215
Race (Black people vs. White people)	0.292	0.0168
Race (others vs. White people)	-0.426	0.4383
Hypertension (No vs. Yes)	-0.305	0.0316
Position (prone vs. supine)	0.256	0.0347
Coronary artery disease (No vs. Yes)	-0.209	0.2893
Neoadjuvant chemotherapy (No vs. Yes)	-0.348	0.0172

chemotherapy vs. no neoadjuvant chemotherapy, prone position vs. supine, the presence of hypertension, and race (Black people vs. White people) were associated with larger mean lumpectomy cavity volume. For example, with the absence of hypertension, the log of lumpectomy cavity volume decreased by 0.305; the log of lumpectomy cavity volume increases with the presence of hypertension. With Black people compared to White people, the log of the lumpectomy cavity volume increased by 0.292.

Sensitivity analyses were done to assess the impact of prone vs. supine position (characteristics are separated by position in Supplementary Table 1). When separated into supine (n = 237) and prone (n = 114), longer interval from surgery (as a continuous variable) was not significantly associated with decreased lumpectomy cavity volume (Supplementary Table 2). On multivariate analysis of factors with lumpectomy cavity volume for patients in the supine position (Supplementary Table 3), race (Black people vs. White people), BMI, the receipt of neoadjuvant chemotherapy, and hypertension (presence vs. absence) had a significant effect on lumpectomy cavity volume as in the main analysis that did not separate the patients by position. For prone position, the presence of hypertension was significantly associated with larger mean lumpectomy cavity volume on multivariate analysis as in the main analysis, but race, BMI, and neoadjuvant chemotherapy were not. A regression analysis was also done to determine if hypertension was associated with other factors in this population, and this revealed that hypertension was associated with increased age, increased BMI, and having diabetes (Supplementary Table 4).

An additional analysis was done to assess the association between lumpectomy volume (cm^3) and ipsilateral whole breast volume (cm^3) and the BMI (Supplementary Table 5A). Following log transformations on both the predictor and outcome variables, a univariate regression model examined the relationship between the log of ipsilateral whole breast volume (cm^3) and the log of lumpectomy volume (cm^3) with repeated measures to account for patients with multiple lumpectomies. This demonstrated a positive relationship between the variables that was significant ($p < 0.001$) (Supplementary Table 5B). A univariate regression analysis examined the relationship between BMI and the log of ipsilateral whole breast volume (cm^3) and demonstrated a positive relationship between the variables that was significant ($p < 0.001$) (Supplementary Table 5C).

4 Discussion

The growing literature discussed above on partial breast irradiation has shown overall that it is an effective and safe alternative to whole breast radiation in select patients. The ability to deliver this is predicated on reliable delineation of the lumpectomy cavity. In patients with larger lumpectomy cavities, the breast-to-target ratio is sometimes unfavorable for constraints used in major PBI trials. In those that still qualify for PBI, a geometrically larger treatment area is required for larger lumpectomy cavities. This study sought to describe factors that predict for larger lumpectomy cavity to aid in patient selection and identify modifiable changes that can optimize the target size prior to treatment planning.

Race, the presence of hypertension, higher BMI, the receipt of neoadjuvant chemotherapy, and prone position vs. supine remained significantly associated with larger mean lumpectomy cavity volume on multivariate analysis and thus were independently associated with lumpectomy cavity volume. Longer interval from surgery to simulation was associated with smaller lumpectomy cavity volume on univariate analysis and trended toward significance on multivariate analysis. The trends in lumpectomy cavity volume over time demonstrated in the present study and prior studies support the recommendation to perform the planning CT scan for PBI ideally within 8 weeks after surgery (14, 15). A study by Kader et al. showed that during weeks 3–8 after BCS, the mean lumpectomy cavity volume decreased from 47 to 30 cm^3, stabilized during weeks 9–14 (mean 21 weeks), and was involuted after 14 weeks (14). Prone positioning is thought to elongate the cavity due to the effect of gravity, congruent with the result from our study that this position was associated with larger mean lumpectomy cavity volume. Sensitivity analyses demonstrated that

the presence of hypertension remained significantly associated with larger mean lumpectomy cavity volume when separate analyses were done for prone and supine patients and that hypertension is also associated with increased age, BMI, and diabetes. An additional univariate analysis also found that lumpectomy cavity volume was associated with ipsilateral whole breast volume.

In order for a surgical cavity or wound to heal properly, adequate blood supply is necessary; therefore, conditions that impair circulation and oxygenation can delay the healing process (16). High blood pressure, diabetes, advanced age, and tobacco use may thus contribute to delayed healing. Data are lacking on the healing of the postoperative cavity or lumpectomy cavity after BCS. A study by Prendergast et al. examined the association of clinical factors for the association of volumetric change of the tumor bed before and during radiation and did not find any association with clinical factors including patient age, weight, tobacco use, re-excision, the volume of tissue removed, initial breast volume, or the use of chemotherapy (17).

Studies of breast reconstruction patients have shown postoperative complications at higher rates in patients with specific comorbidities, but the specific complications are variable between studies (18). Hypertension was found to be an independent risk factor for perioperative complications in a review of 1,170 consecutive expander/implant reconstructions, with hypertension defined as elevated blood pressure requiring medical therapy and associated with twice the risk of complications compared to patients without hypertension (19). Hypertension has also been associated with delayed surgical complications in breast reconstruction patients (5).

The significance of race predicting larger lumpectomy cavity volume is not clear. Multivariable analysis attempts to correct for imbalances in confounding variables examined here, and yet race remains a significant independent factor. Unmeasured social determinants of health may contribute to this difference, which bears further investigation. Race/ethnicity has been associated with differences in time to breast cancer diagnosis after suspicious breast abnormality first identified by a physical exam, mammogram, or ultrasound. Non-Hispanic Black people and Hispanic people were found to have a longer time to diagnosis than non-Hispanic White people, even with private health insurance (20). In this study, however, the patients all had early-stage breast cancer suitable for lumpectomy; thus, this is less likely to have been a factor. Potentially, the differences in lumpectomy cavity size could be related to differences in unexplored factors related to social determinants of health such as follow-up after surgery or differences in postoperative instructions.

Limitations of this study are related to its retrospective design. Additionally, the delineation of lumpectomy cavity can be subjective, especially in patients with dense breasts, and the analyzed dataset represented a variety of practitioners from the same institution. The delineation of lumpectomy cavity can especially be more difficult in the setting of oncoplastic reduction, which made up a small proportion of the patients in this dataset. Different surgeons were also involved in the cases that could be associated with variation in technique in addition to variation in the placement of surgical clips. Postoperative care patterns may have varied. The interpretation of results of continuous clinical variables may be harder to translate to clinical settings.

Especially relevant for patients planned to receive PBI, these data may be used to select patients for which longer time to simulation may result in smaller lumpectomy cavity volumes and therefore smaller PBI target volumes. Larger datasets and prospective evaluation would be ideal to confirm these hypotheses.

Data availability statement

The raw data supporting the conclusions of this article will be made available by the authors, without undue reservation.

Ethics statement

Consent was not required for this study. This study involved the secondary use of private information from the electronic medical record and was approved as exempt by the Indiana University institutional review board.

Author contributions

Study design: AL and RR. Data collection: AL and FA. Data analysis: AL, LB, MS, RZ and RR. Manuscript draft writing: AL and RR. Manuscript review and approval: AL, FA, LB, MS, RZ and RR. All authors contributed to the article and approved the submitted version.

Conflict of interest

The authors declare that the research was conducted in the absence of any commercial or financial relationships that could be construed as a potential conflict of interest.

Publisher's note

Supplementary material

The Supplementary Material for this article can be found online at: https://www.frontiersin.org/articles/10.3389/fonc.2023.1118713/full#supplementary-material

References

1. Spooner D, Stocken DD, Jordan S, Bathers S, JA D, Jevons C, et al. A randomised controlled trial to evaluate both the role and the optimal fractionation of radiotherapy in the conservative management of early breast cancer. *Clin Oncol (R Coll Radiol)* (2012) 24(10):697–706. doi: 10.1016/j.clon.2012.08.003

2. Forrest AP, Stewart HJ, Everington D, Prescott RJ, McArdle CS, Harnett AN, et al. Randomised controlled trial of conservation therapy for breast cancer: 6-year analysis of the Scottish trial. *Scottish Cancer Trials Breast Group Lancet* (1996) 348 (9029):708–13. doi: 10.1016/s0140-6736(96)02133-2

3. Whelan T, Clark R, Roberts R, Levine M, Foster G. Ipsilateral breast tumor recurrence postlumpectomy is predictive of subsequent mortality: results from a randomized trial. investigators of the Ontario clinical oncology group. *Int J Radiat Oncol Biol Phys* (1994) 30(1):11–6. doi: 10.1016/0360-3016(94)90513-4

4. Ford HT, Coombes RC, Gazet JC, Gray R, McConkey CC, Sutcliffe R, et al. Long-term follow-up of a randomised trial designed to determine the need for irradiation following conservative surgery for the treatment of invasive breast cancer. *Ann Oncol* (2006) 17(3):401–8. doi: 10.1093/annonc/mdj080

5. Fischer JP, Sieber B, Nelson JA, Cleveland E, Kovach SJ, Wu LC, et al. Comprehensive outcome and cost analysis of free tissue transfer for breast reconstruction: an experience with 1303 flaps. *Plast Reconstr Surg* (2013) 131(2):195–203. doi: 10.1097/PRS.0b013e318277856f

6. Darby S, McGale P, Correa C, Taylor C, Arriagada R, Clarke M, et al. Effect of radiotherapy after breast-conserving surgery on 10-year recurrence and 15-year breast cancer death: meta-analysis of individual patient data for 10,801 women in 17 randomised trials. *Lancet* (2011) 378(9804):1707–16. doi: 10.1016/s0140-6736(11)61629-2

7. Livi L, Meattini I, Marrazzo L, Simontacchi G, Pallotta S, Saieva C, et al. Accelerated partial breast irradiation using intensity-modulated radiotherapy versus whole breast irradiation: 5-year survival analysis of a phase 3 randomised controlled trial. *Eur J Cancer* (2015) 51(4):451–63. doi: 10.1016/j.ejca.2014.12.013

8. Vicini FA, Cecchini RS, White JR, Arthur DW, Julian TB, Rabinovitch RA, et al. Long-term primary results of accelerated partial breast irradiation after breast-conserving surgery for early-stage breast cancer: a randomised, phase 3, equivalence trial. *Lancet* (2019) 394(10215):2155–64. doi: 10.1016/s0140-6736(19)32514-0

9. Whelan TJ, Julian JA, Berrang TS, Kim DH, Germain I, Nichol AM, et al. External beam accelerated partial breast irradiation versus whole breast irradiation after breast conserving surgery in women with ductal carcinoma in situ and node-negative breast cancer (Rapid): a randomised controlled trial. *Lancet* (2019) 394(10215):2165–72. doi: 10.1016/s0140-6736(19)32515-2

10. Rodríguez N, Sanz X, Dengra J, Foro P, Membrive I, Reig A, et al. Five-year outcomes, cosmesis, and toxicity with 3-dimensional conformal external beam radiation therapy to deliver accelerated partial breast irradiation. *Int J Radiat Oncol Biol Phys* (2013) 87(5):1051–7. doi: 10.1016/j.ijrobp.2013.08.046

11. Polgár C, Fodor J, Major T, Németh G, Lövey K, Orosz Z, et al. Breast-conserving treatment with partial or whole breast irradiation for low-risk invasive breast carcinoma–5-Year results of a randomized trial. *Int J Radiat Oncol Biol Phys* (2007) 69(3):694–702. doi: 10.1016/j.ijrobp.2007.04.022

12. Coles CE, Griffin CL, Kirby AM, Titley J, Agrawal RK, Alhasso A, et al. Partial-breast radiotherapy after breast conservation surgery for patients with early breast cancer (Uk import low trial): 5-year results from a multicentre, randomised, controlled, phase 3, non-inferiority trial. *Lancet* (2017) 390(10099):1048–60. doi: 10.1016/s0140-6736(17)31145-5

13. Boutrus RR, El Sherif S, Abdelazim Y, Bayomy M, Gaber AS, Farahat A, et al. Once daily versus twice daily external beam accelerated partial breast irradiation: a randomized prospective study. *Int J Radiat Oncol Biol Phys* (2021) 109(5):1296–300. doi: 10.1016/j.ijrobp.2020.11.044

14. Kader HA, Truong PT, Pai R, Panades M, Jones S, Ansbacher W, et al. When is ct-based postoperative seroma most useful to plan partial breast radiotherapy? evaluation of clinical factors affecting seroma volume and clarity. *Int J Radiat Oncol Biol Phys* (2008) 72(4):1064–9. doi: 10.1016/j.ijrobp.2008.02.049

15. Truong MT, Hirsch AE, Kovalchuk N, Qureshi MM, Damato A, Schuller B, et al. Cone-beam computed tomography image guided therapy to evaluate lumpectomy cavity variation before and during breast radiotherapy. *J Appl Clin Med Phys* (2013) 14 (2):4243. doi: 10.1120/jacmp.v14i2.4243

16. Gottrup F. Oxygen in wound healing and infection. *World J Surg* (2004) 28 (3):312–5. doi: 10.1007/s00268-003-7398-5

17. Prendergast B, Indelicato DJ, Grobmyer SR, Saito AI, Lightsey JL, Snead FE, et al. The dynamic tumor bed: volumetric changes in the lumpectomy cavity during breast-conserving therapy. *Int J Radiat Oncol Biol Phys* (2009) 74(3):695–701. doi: 10.1016/j.ijrobp.2008.08.044

18. Voineskos SH, Frank SG, Cordeiro PG. Breast reconstruction following conservative mastectomies: predictors of complications and outcomes. *Gland Surg* (2015) 4(6):484–96. doi: 10.3978/j.issn.2227-684X.2015.04.13

19. Qin C, Vaca E, Lovecchio F, Ver Halen JP, Hansen NM, Kim JY. Differential impact of non-Insulin-Dependent diabetes mellitus and insulin-dependent diabetes mellitus on breast reconstruction outcomes. *Breast Cancer Res Treat* (2014) 146 (2):429–38. doi: 10.1007/s10549-014-3024-5

20. Hoffman HJ, LaVerda NL, Levine PH, Young HA, Alexander LM, Patierno SR. Having health insurance does not eliminate Race/Ethnicity-associated delays in breast cancer diagnosis in the district of Columbia. *Cancer* (2011) 117(16):3824–32. doi: 10.1002/cncr.25970

frontiers | Frontiers in Oncology

TYPE Review
PUBLISHED 26 June 2023
DOI 10.3389/fonc.2023.1151460

OPEN ACCESS

EDITED BY
Vishruta Dumane,
Icahn School of Medicine at Mount Sinai, United States

REVIEWED BY
Ryan Rhome,
Indiana University Health Methodist Hospital, United States
Ashu Gandhi,
Manchester University NHS Foundation Trust (MFT), United Kingdom

*CORRESPONDENCE
John R. Benson
john.benson7@nhs.net/john.benson@addenbrookes.nhs.uk

†These authors have contributed equally to this work and share first authorship

RECEIVED 26 January 2023
ACCEPTED 06 June 2023
PUBLISHED 26 June 2023

CITATION
Elumalai T, Jain U, Coles CE and Benson JR (2023) The role of irradiation in the management of the axilla in early breast cancer patients. *Front. Oncol.* 13:1151460. doi: 10.3389/fonc.2023.1151460

The role of irradiation in the management of the axilla in early breast cancer patients

Thiraviyam Elumalai[1†], Urvashi Jain[1†], Charlotte E. Coles[1,2] and John R. Benson[1,3*]

[1]Cambridge Breast Unit, Cambridge University Hospitals NHS Foundation Trust, Cambridge, Cambiridge, United Kingdom, [2]Department of Oncology, University of Cambridge, Cambiridge, United Kingdom, [3]School of Medicine, Anglia Ruskin University, Cambridge and Chelmsford, Cambiridge, United Kingdom

The need for axillary radiotherapy in patients with invasive breast cancer (IBC) has been a topic of great debate in the last decade. Management of the axilla has evolved significantly over the past four decades with a trend towards de-escalation of surgical interventions and the aim of reducing morbidity and enhancing QOL without compromising long-term oncology outcomes. This review article will address the role of axillary irradiation with a focus on the omission of completion axillary lymph node dissection in selected patients with sentinel lymph node (SLN) positive early breast cancer (EBC) with reference to current guidelines based on evidence to date.

KEYWORDS

axillary radiotherapy, breast cancer, sentinal lymph node biopsy, regional nodal irradiation (RNI), neoadjuvant chemotherapy

Introduction

As advances in breast cancer treatment have led to improved survival, there is a greater focus on the impact of treatment on quality of life (QOL) in the context of survivorship. Management of the axilla has evolved significantly over the past four decades with a trend towards de-escalation of surgical interventions and the aim of reducing morbidity and enhancing QOL without compromising long-term oncology outcomes. The introduction of systemic treatments has further facilitated this approach of de-escalation. A principal motivation for seeking alternatives to axillary lymph node dissection (ALND) has been to reduce rates of lymphoedema and other upper limb morbidities associated with standard forms of ALND. Lymphoedema can be severe and impair QOL substantially for patients following breast cancer treatment, both in terms of symptoms and loss of function. There has been extensive research done over the past few years to optimise axillary management and this continues to evolve (1–4). This article will address the role of axillary irradiation with a focus on omission of completion ALND in selected patients with sentinel lymph node (SLN) positive early breast cancer (EBC) with reference to current guidelines based on evidence to-date.

Evidence for axillary RT replacing ALND in sentinel node positive axilla

There are two trials (AMAROS and OTOASOR) that have directly compared axillary radiotherapy (RT) to ALND in SLN positive EBC patients and these are discussed in more detail below.

The AMAROS trial was led by the European Organisation for Research and Treatment of Cancer (EORTC) group from 2001-2010 and included 1425 patients with clinically node negative breast cancer at presentation but a subsequent positive SLN biopsy. Patients were randomised to either ALND (anatomical levels 1, 2 & 3, including at least ten nodes) or axillary RT (50Gy in 25 fractions over five weeks, including all axillary levels and medial supraclavicular fossa) (5). Of note, randomisation was performed prior to SLN biopsy, which minimised selection bias. After exclusions were applied, 744 and 681 patients in the ALND and axillary RT arms, respectively were included in the per-protocol and intention-to-treat analyses. Patient characteristics are especially important in applying the results of this trial to routine clinical practice and are highlighted in Table 1.

Within the ALND group, one-third of patients (220/672) had additional positive non-sentinel lymph nodes.

The primary intent of the AMAROS trial was to confirm non-inferiority of axillary RT compared with ALND with respect to 5-year axillary recurrence in patients with positive SLN(s). On the assumption of a 2% 5-year axillary recurrence rate in the ALND group, non-inferiority was defined as axillary recurrence no higher than 4% in the axillary RT group. A total of 52 events were required to ensure a power of 80% based on these criteria. The AMAROS trial was underpowered and did not meet its primary endpoint of non-inferiority due to a very low event rate. However, the Independent Data Monitoring Committee (IDMC) approved the decision to proceed with the final analysis.

The above results (Table 2) reveal no statistically significant difference in clinical outcomes between the two groups in terms of axillary recurrence, disease-free survival (DFS) and overall survival (OS).

Nonetheless, a notable finding was a striking difference in the incidence of lymphedema reported between the two groups with axillary RT associated with a significant reduction in rates of lymphoedema and absolute differences in arm circumference measurements (> 10%) at 5 years.

TABLE 1 Patient summary characteristics- AMAROS trial.

40% premenopausal
48% grade 2 cancer
82% had BCS
95% with 1-2 positive SLN
60% with macro metastases
90% received further systemic treatment
61% received adjuvant chemotherapy
78% received endocrine treatment

A 10-year update of the AMAROS trial was presented at the San Antonio Breast Cancer Symposium in 2018 and continued to show no differences in the aforementioned clinical endpoints. Moreover, quality-of-life scales did not differ by treatment through 5 years (6) (Table 3).

Interestingly, more cases of second primary tumors were observed following axillary RT (75/681), with one-quarter of these (n=21) in the contralateral breast. This compared with 57/744 cases in the ALND group, of which 11 were in the contralateral breast (p=0.035). Given the low overall numbers of second primary tumors and the relatively small differences in irradiated volumes between randomized groups, it is difficult to draw clear conclusions about causation, and a difference due to chance remains a possibility.

The OTOASOR trial was conducted around the same time (2002–2009) and had a similar trial design to AMAROS with the publication of results after eight years of follow-up (7).

This trial was a smaller single center, randomized controlled, non-inferiority study that recruited 525 patients with clinically node-negative tumors up to 3cm in size. SLN positive patients were randomized to either completion ALND or regional nodal irradiation (RNI) that encompassed all levels of axillary nodes together with the supraclavicular fossa- 25 fractions of 2 Gy.

No differences were observed between the groups with respect to axillary recurrence, DFS or OS (Table 4), with the caveat that the overall event rate was much lower than anticipated.

As observed in the AMAROS trial, the morbidity associated with ALND was much higher than for RNI. Combining ALND with RT for those patients with a higher nodal burden (> 4 nodes) further increased upper limb morbidity (18/57, 31.5%). However, there were not statistically significant or clinically relevant differences observed in QOL between the surgery and radiation groups.

In summary, axillary RT is an acceptable and safe alternative to ALND for clinically node negative patients with a positive SLN biopsy and otherwise similar clinical characteristics for enrolment in the AMAROS and OTOASOR trials. A key finding is the statistically and clinically significant reduction in arm morbidity for axillary RT compared to ALND.

However, there remain some outstanding clinical questions which require resolution. Firstly, there may be a cohort of patients without a high burden of axillary disease who are at lower risk and might safely be spared comprehensive axillary RT (as per AMAROS and OTOASOR protocols). There is evidence from clinical trials such as ACOSOG Z0011 and AMAROS that further axillary treatment may be unnecessary for SLN biopsy-positive patients with limited disease in sentinel nodes. It should be noted that the AMAROS trial did not include a non-intervention arm, and although axillary RT is non-inferior to ALND and associated with reduced morbidity, evidence suggests that many of these lower-risk patients may not require further definitive axillary treatment at all. Breast cancer treatments are increasingly tailored to individual patients based on disease biology and characteristics. These nuanced approaches may permit the identification of subgroups of patients who may benefit from extended irradiation with nodal fields that include the internal mammary nodes (IMN) (NCIC MA 20 and EORTC 2292) (8, 9).

TABLE 2 AMAROS: 5 years results (5).

	ALND	Axillary RT	p value	HR
AR	0.43% (4/744)	1.19 (7/681)	NS	0.00-5.27
DFS	86.9%	82.7%	NS- 0.18	1.18 (95% CI 0.93-1.51)
OS	93.3%	92.5%	NS- 0.34	1.17 (95% CI 0.85-1.62)
Lymphedema	23%	11%	0.0001	
Arm circumference > 10%	13%	5%	0.0009	

AR, Axillary recurrence; DFS, Disease Free Survival; OS, Overall survival; HR, Hazard ratio.

Evidence for omission of further axillary treatment in sentinel node positive patients

There are two seminal trials (IBCSG 23-01 and ACOSOG-Z0011) that have addressed the issue of whether any further axillary treatment (completion ALND/axillary RT) is necessary after primary surgery in SLN biopsy positive patients (10, 11).

The IBCSG 23-01 trial specifically included only patients with micro-metastases (≤2mm and >0.2mm) in the SLNs and these represented a very small "low risk" cohort within the AMAROS and OTOASOR trials (10). A total of 934 patients with micro-metastatic nodal disease were randomized to either completion ALND or observation only. The majority of patients within the no ALND group received whole breast radiotherapy (WBRT) as a component of breast conservation therapy. Of these, 80 patients (19%) received partial breast radiotherapy with intra-operative electron partial breast irradiation (ELIOT) that would be unlikely to capture lower axillary lymph nodes at levels 1 and 2. In addition within the no ALND group, 12 patients (3%) had wide local excision only and 42 patients (9%) underwent mastectomy and were not irradiated. No significant differences in DFS nor OS were observed after 5 years of follow-up. Results of this trial provides reassurance that definitive axillary treatment for this "low risk" group with micro-metastatic disease only can be safely omitted and thereby spare any additional morbidity.

The ACOSOG Z0011 study also examined omission of completion ALND in SLN biopsy positive patients presenting with clinically node negative EBC (11). This trial randomized 891 patients with no more than 2 positive sentinel nodes containing either macro-(>2mm) or micro-metastases to completion ALND or observation only with a slightly higher proportion of patients with micro metastases in the latter group (37.5% versus 44.8%; p=0.046). All patients underwent BCS and were scheduled to receive whole breast RT and adjuvant systemic treatment. Of note, about 50% of those patients (n=228) for whom detailed RT records were available received high tangent fields irrespective of treatment allocation (ALND 52.6%; SLN biopsy only 50%). Furthermore, 15% of patients with complete documentation received supraclavicular fossa irradiation (12). The study did not reach the pre-specified sample size of 1900 participants and closed early on the recommendation of the IDMC with only 50% accrual. This was due to the much lower than expected event rate making the estimated 500 deaths required for the study to have 90% power to confirm non-inferiority of SLNB alone compared with ALND unfeasible in terms of timescale. An updated analysis of this trial at 10 years was reassuring and showed continuing low rates of axillary relapse (0.5% in the completion axillary dissection arm and 1.5% in the SLN biopsy arm).There were no significant differences in outcomes for regional recurrence (p=0.28) with comparable 10-year overall survival for SLN biopsy alone (86.3%) and ALND (83.6) (HR 0.85; p=0.02) (13). Some patients had irradiation protocol variations that could potentially have resulted in small alteration of outcomes but are unlikely to have been responsible for equivalence of clinical outcomes and non-inferiority being maintained at 10 years follow up. The POSNOC trial has recently completed accrual and will provide information on outcomes in SLN biopsy positive patients with macro metastases in 1 – 2 nodes and not in receipt of breast irradiation (mastectomy group) (14).

Role of regional RT in post-operative patients

Irradiation of the axillary, supraclavicular and internal mammary lymph nodes is an integral part of adjuvant therapy for some breast cancer patients. Multiple clinical trials testify to the benefits of nodal radiation therapy in improving outcomes (8, 9). Two recent trials employing field-based planning techniques with

TABLE 3 AMAROS: 10-year update (6).

	ALND	Ax RT	p value	HR
AR	0.93% (7/744)	1.82% (11/681)		1.71 (95% CI, 0.67-4.39)
DFS	75.0% (95% CI, 71.5 to 78.2)	70.1% (95% CI, 66.2 to 73.6) i	0.11	1.19 (95% CI, 0.97-1.46)
OS	84.6% (95% CI, 81.5 to 87.1)	81.4% (95% CI, 77.9 to 84.4)	0.26	1.17 (95% CI, 0.89-1.52)
LRR	3.59%	4.07	0.69	

LRR, Loco-regional recurrence.

TABLE 4 Results of the OTOASOR trial (7).

	ALND	Axillary RT	p value
AR			
Total (%)	5 (2.0)	4 (1.7)	1.00
Isolated (%)	1 (0.4)	2 (0.8)	0.61
Survival at 8 years			
OS (%)	190 (77.9)	195 (84.8)	0.060
DFS (%)	176 (72.1)	178 (77.4)	0.51
Alive with recurrence (%)	14 (5.7)	17 (7.0)	
Died of breast cancer (%)	34 (13.9)	20 (8.7)	
Died of other cause (%)	20 (8.2)	15 (6.5)	
Morbidity at 1 year*	15.3%	4.7%	

*Clinical signs of lymphedema, paraesthesia, swelling, arm pain and shoulder mobility issues.

attention to quality assurance issues have demonstrated the benefit of regional nodal irradiation (RNI) when administered post-operatively in early-stage breast cancer patients. The NCIC Clinical Trials Group MA.20 trial evaluated the role of RNI (axilla, supraclavicular and internal mammary) amongst 1832 women with node-positive or high-risk node-negative breast cancer treated with breast-conserving surgery and adjuvant systemic therapy (8). Randomization was to whole breast irradiation (WBI) only or WBI combined with RNI (using modified wide tangent fields [14 – 18MV]). Addition of RNI to loco-regional treatment significantly increased relative DFS by 24%, with an absolute improvement of 5% at 10 years. The majority of regional treatment failures involved either the axillary (63%) or the supraclavicular nodes (27%) and hence the main treatment benefit related to reduction in rates of regional recurrence. There was no significant improvement in overall survival attributable to RNI (HR0.76; p=0.07) but marginal gains (~4%) in distant disease–free survival at 10 years (86.3% in RNI vs. 82.4% in the control group, p=0.03) (HR 0.64; p=0.002). It remains unclear which sites of nodal irradiation (internal mammary, supraclavicular, level III axillary, or all three) were responsible for improvements in DFS.

The EORTC 22922/10925 randomized 4004 patients with centrally or medially located primary tumors irrespective of whether the axillary node positive or negative (9). A total of 50Gy was delivered in 25 fractions with a mixed technique of 6MV photons (26Gy in 13 fractions) and 12MeV electrons (24Gy in 12 fractions) to medial supraclavicular and internal mammary node (RNI). At a median follow-up of 15.7 years, the RNI group showed a significant reduction in breast cancer mortality (HR 0.81; 95%CI 0.69–0.94; p = .005) and breast cancer recurrence (HR 0.87; 95%CI 0.77–0.98; p=0.024). A slight improvement in OS at five years was noted, which just reached statistical significance (HR 0.87; 95%CI 0.76–1.00; p=0.056). No difference was observed in the incidence of second malignancies, contralateral breast cancer, or cardiovascular deaths. A meta-analysis of the MA-20, EORTC and a French trial of RNI revealed a benefit for overall and metastases-free survival (HR 0.88; 95%CI 0.8–0.97; p=0.012) (15). Furthermore, the Danish Breast Cancer Cooperative Group (DBCG) registry reported outcomes for 3089 patients managed with a standard policy of internal mammary node (IMN) irradiation Right-sided breast cancer patients received IMN irradiation whereas this was omitted for left-sided cancers because of the risk of radiation-induced heart disease (16). The 15-year breast cancer mortality with IMN irradiation was 31.7% compared with 33.9% without (adjusted HR, 0.88 95%CI, 0.78-1.00; p = .05).

An overall comparison of the MA-20, EORTC and Danish trials in terms of their patient populations shows that the Danish study confined recruitment to axillary node-positive patients compared to the MA.20 and EORTC trials with 90% and 56% of node-positive patients, respectively. These differences in axillary nodal status likely contribute to observed differences in clinical outcomes. The latter may also relate to variations in chemotherapy schedules.

A large meta-analysis presented as an abstract in 2018 further evaluated the benefits of RNI based on individual patient data from randomized trials involving 13,404 patients in 14 studies (15). This analysis found no effect of RNI on breast cancer recurrence or mortality among 8 studies undertaken between 1961 and 1978. By contrast, in the six studies conducted after 1989, RNI significantly reduced not only breast cancer recurrence but also breast cancer-specific mortality. The risk of any death was reduced and there was no increase in non-breast cancer-related mortality (relative risk 0·88 (95% CI 0·82–0·95), p=0·002).

Absolute benefits were predictably greatest for patients with a higher number of involved axillary lymph nodes and hence nodal burden. The proportional benefits were similar across various tumor and treatment-related parameters and translated into a greater absolute benefit for those patients with a higher baseline risk for breast cancer-related events. It is reasonable to assume that as RT techniques become much more efficient and accurate, the corresponding proportional benefits for individual patients may be improved.

Role of regional radiotherapy in the neo-adjuvant era

The optimum axillary management and role of axillary irradiation in early breast cancer patients receiving neo-adjuvant chemotherapy (NACT) remains unclear and continues to evolve. However, there is general consensus that women who are clinically node-negative (cN0) at presentation and are found to have a negative SLN biopsy after NACT do not require any further axillary treatment (17, 18). However, axillary RT (instead of ALND) may be considered for cN0 patients who are found to have fibrosis in 1 or 2 nodes and for those found to have only micro metastases or isolated tumor cells in sentinel nodes as per some guidelines (19).But there is no robust evidence to support these latter recommendations for axillary RT. The role of axillary RT in biopsy –proven cN1 patients who are down staged and have no residual tumor in sentinel lymph nodes after NACT (ypN0) is even more controversial with lack of level 1 evidence from randomized trials at the present time.

Two retrospective national cancer database (NCDB) registry-based studies explored the role of RNI in these patient cohorts who underwent breast conserving surgery. The NCDB2003–2011 study involved more than 5000 clinically node positive patients (T1-3) undergoing NACT and found no benefit in terms of overall survival from addition of RNI to breast radiotherapy (WBI) for either ypN0 or ypN+ patients (20). An updated study from the same group (NCDB 2010–2015) involving 9474 patients similarly reported no benefit from addition of RNI to WBI, regardless of pathological nodal status (21).

A retrospective study (KROG 1 6–06) from South Korea involved 261 clinically node positive (41%) and negative patients with no residual nodal tumor (ypN0) at the time of axillary surgery post-NACT. The authors found no effect of RNI on DFS or OS, irrespective of response to NACT (22). It is conceivable that the lack of any benefit from RNI in breast conservative therapy patients might be attributed to the use of tangential beams in many of these series which can capture up to 80% of nodes at levels I and II of the axilla.

NACT results in a complete pathological response in the axillary nodes in 40-70% of patients depending on tumor phenotype. This intuitively questions the benefit of any further axillary treatment in this ypN0 group of patients (23). Current evidence suggests that core biopsy-proven node positive women with normalization of axillary nodes post-NACT can be safely considered for sentinel node biopsy alone provided at least 3 nodes are removed and dual mapping techniques employed. Alternatively, the biopsied node can be clipped and retrieved at the time of SLN biopsy – the so-called targeted ALND (24, 25). The ongoing NSABP B-51/RTOG 1304 and ATNEC trials will examine the role of RNI in ypN0 patients (26, 27). The Dutch RAPCHEM; BOOG 2020-03 registry study is the first prospective evidence for the safety of selective de-escalation of radiation therapy after NACT for biopsy-proven clinically node positive T1-2N1 early breast cancers. Patients were grouped into low, intermediate and high risk for recurrence based on pre-defined criteria and all underwent ALND post-NACT. Radiation therapy (local and/or regional) was omitted for ypN0 patients and those with residual nodal disease (ypN1) received irradiation of local tissues only. Overall 5 year rates of loco-regional recurrence were only 2.2% with this policy of response-adapted radiotherapy (28).

Concluding comments

There are several ongoing trials that aim to address some key outstanding questions in relation to the role of radiation therapy in management of early breast cancer patients. The POSNOC (POsitive Sentinel NOde: adjuvant therapy alone versus adjuvant therapy plus Clearance or axillary radiotherapy) trial is a predominantly UK-based multicenter trial that notably includes women undergoing primary surgery with either mastectomy or breast conserving therapy in conjunction with SLN biopsy (14). Women with 1 or 2 sentinel nodes containing macro metastases are eligible for randomization as well as those with extra-nodal invasion. This trial will determine whether SLN biopsy alone yields equivalent clinical outcomes to further axillary treatment (completion ALND or axillary irradiation) POSNOC has an in-built radiotherapy quality assurance programme coordinated by the UK Radiotherapy Trials Quality Assurance Group. The NSABP B-51/RTOG 1304 study will examine whether post-mastectomy radiotherapy combined with RNI or addition of RNI to breast RT following breast conserving surgery increases invasive breast cancer recurrence-free interval in cN1 patients converting to ypN0 after NACT (26). The ATNEC trial will randomize ypN0 patients to either observation only following SLN biopsy or further axillary treatment (completion ALND or axillary RT) (27). Other de-escalation studies include the ALLIANCE A011202 trial that will determine whether axillary RT combined with RNI is non-inferior to completion ALND and RNI for higher risk patients with residual nodal macro metastases after NACT followed by SLN biopsy (29). The international TAXIS (SAKK 23–16/IBCSG 57–18/ABCSG-53/GBG 101) trial has a complex study design that recruits a mixed population of clinically node positive patients undergoing NACT or upfront surgery. The trial aims to test the hypothesis that axillary RT in pathologically node-positive patients is non-inferior to ALND in terms of DFS (30). The trial incorporates methods for tailored axillary surgery such as targeted ALND. Finally, a unique feasibility study, entitled the NEONOD2 trial (NCT040196780) will evaluate the safety of omitting both ALND and RNI in patients with micro metastatic disease only in sentinel nodes (31).

Author contributions

JB is the corresponding author. TE and UJ are joint first authors. All authors contributed to the article and approved the submitted version.

Conflict of interest

CC is funded by the National Institute of Health and Social Care Research NIHR and supported by the NIHR Cambridge Biomedical Research Centre.

The remaining authors declare that the research was conducted in the absence of any commercial or financial relationships that could be construed as a potential conflict of interest.

Publisher's note

Author disclaimer

The views expressed are those of the author and not necessarily those of the NIHR or the Department of Health and Social Care.

References

1. Fisher B, Jeong JH, Anderson S, Bryant J, Fisher ER, Wolmark N, et al. Twenty-five-year follow-up of a randomized trial comparing radical mastectomy, total mastectomy, and total mastectomy followed by irradiation. *N Engl J Med* (2002) 347 (8):567–75. doi: 10.1056/NEJMoa020128

2. Deutsch M, Land S, Begovic M, Sharif S. The incidence of arm edema in women with breast cancer randomized on the national surgical adjuvant breast and bowel project study b-04 to radical mastectomy versus total mastectomy and radiotherapy versus total mastectomy alone. *Int J Radiat Oncol Biol Phys* (2008) 70(4):1020–4. doi: 10.1016/j.ijrobp.2007.07.2376

3. Krag DN, Anderson SJ, Julian TB, Brown AM, Harlow SP, Costantino JP, et al. Sentinel-lymph-node resection compared with conventional axillary-lymph-node dissection in clinically node-negative patients with breast cancer: overall survival findings from the NSABP b-32 randomised phase 3 trial. *Lancet Oncol* (2010) 11 (10):927–33. doi: 10.1016/S1470-2045(10)70207-2

4. Veronesi U, Paganelli G, Viale G, Luini A, Zurrida S, Galimberti V, et al. A randomized comparison of sentinel-node biopsy with routine axillary dissection in breast cancer. *N Engl J Med* (2003) 349:546–53. doi: 10.1056/NEJMoa012782

5. Donker M, van Tienhoven G, Straver ME, Meijnen P, van de Velde CJ, Mansel RE, et al. Radiotherapy or surgery of the axilla after a positive sentinel node in breast cancer (EORTC 10981-22023 AMAROS): a randomised, multicentre, open-label, phase 3 non-inferiority trial. *Lancet Oncol* (2014) 15:1303–10. doi: 10.1016/S1470-2045(14)70460-7

6. Bartels SAL, Donker M, Poncet C, Sauvé N, Straver ME, van de Velde CJH, et al. Radiotherapy or surgery of the axilla after a positive sentinel node in breast cancer: 10-year results of the randomized controlled EORTC 10981-22023 AMAROS trial. *J Clin Oncol* (2022) 41(12):2159–65. doi: 10.1200/JCO.22.01565

7. Sávolt Á, Péley G, Polgár C, Udvarhelyi N, Rubovszky G, Kovács E, et al. Eight-year follow up result of the OTOASOR trial: the optimal treatment of the axilla - surgery or radiotherapy after positive sentinel lymph node biopsy in early-stage breast cancer: a randomized, single centre, phase III, non-inferiority trial. *Eur J Surg Oncol* (2017) 43(4):672–9. doi: 10.1016/j.ejso.2016.12.011

8. Whelan TJ, Olivotto IA, Parulekar WR, Ackerman I, Chua BH, Nabid A, et al. Regional nodal irradiation in early-stage breast cancer. *N Engl J Med* (2015) 373:307–16. doi: 10.1056/NEJMoa1415340

9. Poortmans PM, Collette S, Kirkove C, Van Limbergen E, Budach V, Struikmans H, et al. Internal mammary and medial supraclavicular irradiation in breast cancer. *N Engl J Med* (2015) 373:317–27. doi: 10.1056/NEJMoa1415369

10. Galimberti V, Cole BF, Viale G, Veronesi P, Vicini E, Intra M, et al. International breast cancer study group trial 23-01. axillary dissection versus no axillary dissection in patients with breast cancer and sentinel-node micrometastases (IBCSG 23-01): 10-year follow-up of a randomised, controlled phase 3 trial. *Lancet Oncol* (2018) 19(10):1385–93. doi: 10.1016/S1470-2045(18)30380-2

11. Giuliano AE, Hunt KK, Ballman KV, Beitsch PD, Whitworth PW, Blumencranz PW, et al. Axillary dissection vs no axillary dissection in women with invasive breast cancer and sentinel node metastasis: a randomized clinical trial. *JAMA* (2011) 305 (6):569–75. doi: 10.1001/jama.2011.90

12. Jagsi R, Chadha M, Moni J, Ballman K, Laurie F, Buchholz TA, et al. Radiation field design in the ACOSOG Z0011 trial. *J Clin Oncol* (2014) 32(32):3600–6. doi: 10.1200/JCO.2014.56.5838

13. Giuliano AE, Ballman KV, McCall L, Beitsch PD, Brennan MB, Kelemen PR, et al. Effect of axillary dissection vs no axillary dissection on 10-year overall survival among women with invasive breast cancer and sentinel node metastasis: the ACOSOG Z0011 (Alliance) randomized clinical trial. *JAMA* (2017) 318(10):918–26. doi: 10.1001/jama.2017.11470

14. Goyal A, Mann GB, Fallowfield L, Duley L, Reed M, Dodwell D, et al. POSNOC-POsitive sentinel NOde: adjuvant therapy alone versus adjuvant therapy plus clearance or axillary radiotherapy: a randomised controlled trial of axillary treatment in women with early-stage breast cancer who have metastases in one or two sentinel nodes. *BMJ Open* (2021) 11(12):e054365. doi: 10.1136/bmjopen-2021-054365

15. Dodwell D, Taylor C, McGale P, Coles C, Duane F, Gray R, et al. Regional lymph node irradiation in early stage breast cancer: An EBCTCG meta-analysis of 13,000 women in 14 trials [abstract]. *Proceedings of the 2018 San Antonio Breast Cancer Symposium*; 2018 Dec 4-8; San Antonio, TX. Philadelphia (PA): AACR; *Cancer Res* (2019) 79(4Suppl):Abstract nr GS4-02.

16. Thorsen LBJ, Overgaard J, Matthiessen LW, Berg M, Stenbygaard L, Pedersen AN, et al. Internal mammary node irradiation in patients with node-positive early breast cancer: fifteen-year results from the Danish breast cancer group internal mammary node study. *J Clin Oncol* (2022) 40(36):4198–206. doi: 10.1200/JCO.22.00044

17. Geng C, Chen X, Pan X, Li J. The feasibility and accuracy of sentinel lymph node biopsy in initially clinically node negative breast cancer after neoadjuvant chemotherapy: a systematic review and meta-analysis. *PloS One* (2016) 11:e0162605. doi: 10.1371/journal.pone.0162605

18. Mamounas EP. Optimizing surgical management of the axilla after neoadjuvant chemotherapy: an evolving story. *Ann Surg Oncol* (2018) 25:2124e2126. doi: 10.1245/s10434-018-6537-z

19. Burstein HJ, Curigliano G, Thürlimann B, Weber WP, Poortmans P, Regan M, et al. Customizing local and systematic therapies for woment with early breast cancer: The St. Gallen international consensus guidelines for treatment of early breast cancer 2021. *Ann Oncol* (2021). doi: 10.1016/j.annonc.2021.06.023

20. Rusthoven CG, Rabinovitch RA, Jones BL, Koshy M, Amini A, Yeh N, et al. The impact of postmastectomy and regional nodal radiation after neoadjuvant chemotherapy for clinically lymph node-positive breast cancer: a national cancer database (NCDB) analysis. *Ann Oncol* (2016) 27(5):818–27. doi: 10.1093/annonc/mdw046

21. Fayanju OM, Ren Y, Suneja G, Thomas SM, Greenup RA, Plichta JK, et al. Nodal response to neoadjuvant chemotherapy predicts receipt of radiation therapy after breast cancer diagnosis. *Int J Radiat Oncol Biol Phys* (2020) 106(2):377–89. doi: 10.1016/j.ijrobp.2019.10.039

22. Cho WK, Park W, Choi DH, Kim YB, Kim JH, Kim SS, et al. Role of elective nodal irradiation in patients with ypN0 after neoadjuvant chemotherapy followed by breast-conserving surgery (KROG 16–16). *Clin Breast Cancer* (2019) 19(1):78–86. doi: 10.1016/j.clbc.2018.08.009

23. Alvarado R, Yi M, Le-Petross H, Gilcrease M, Mittendorf EA, Bedrosian I, et al. The role for sentinel lymph node dissection after neoadjuvant chemotherapy in patients who present with node-positive breast cancer. *Ann Surg Oncol* (2012) 19(10):3177–84. doi: 10.1245/s10434-012-2484-2

24. Montagna G, Lee MK, Sevilimedu V, Barrio AV, Morrow M. Is nodal clipping beneficial for node-positive breast cancer patients receiving neoadjuvant chemotherapy? *Ann Surg Oncol* (2022) 29(10):6133–9. doi: 10.1245/s10434-022-12240-6

25. Caudle AS, Yang WT, Krishnamurthy S, Mittendorf EA, Black DM, Gilcrease MZ, et al. Improved axillary evaluation following neoadjuvant therapy for patients with node-positive breast cancer using selective evaluation of clipped nodes: implementation of targeted axillary dissection. *J Clin Oncol* (2016) 34(10):1072–8. doi: 10.1200/JCO.2015.64.0094

26. Mamounas E, Bandos H, White J, Julian T, Khan A, Shaitelman S, et al. Abstract OT2-04-01: phase III trial to determine if chest wall and regional nodal radiotherapy (CWRNRT) post mastectomy (Mx) or the addition of RNRT to whole breast RT post breast-conserving surgery (BCS) reduces invasive breast cancer recurrence-free interval (IBCR-FI) in patients (pts) with pathologically positive axillary (PPAx) nodes who are ypN0 after neoadjuvant chemotherapy (NC): NRG Oncology/NSABP b-51/RTOG 1304. *Cancer Res* (2019) 79(4 Supplement):OT2-04-01-OT2-04-01. doi: 10.1158/1538-7445.sabcs18-ot2-04-01.

27. Goyal A, Cramp S, Marshall A, Hammonds N, Wheatley D, Elsberger B, et al. ATNEC: a multicenter randomised trial investigating whether axillary treatment can be avoided in patients with T1-3N1M0 breast cancer patients with no residual cancer in the lymph glands after neoadjuvant chemotherapy. *J Clin Oncol* (2022) 40:TPS615. doi: 10.1200/JCO.2022.40.16suppl.TPS615

28. Wild S, de Munck L, Simons JM, Verloop J, van Dalen T, Elkhuizen PHM, et al. De-escalation of radiotherapy after primary chemotherapy in cT1-2N1 breast cancer (RAPCHEM; BOOG 2010-03): 5-year follow-up results of a Dutch, prospective, registry study. *Lancet Oncol* (2022) 23(9):1201–10. doi: 10.1016/S1470-2045(22)00482-X

29. *Comparison of axillary lymph node dissection with axillary radiation for patients with node-positive breast cancer treated with chemotherapy (NCT01901094).*

30. Weber WP, Matrai Z, Hayoz S, Tausch C, Henke G, Zwahlen DR, et al. Tailored axillary surgery in patients with clinically node-positive breast cancer: Pre-planned feasibility substudy of TAXIS (OPBC-03, SAKK 23/16, IBCSG 57-18, ABCSG-53, GBG 101). *Breast* (2021) 60:98–110. doi: 10.1158/1538-7445.sabcs20-pd4-04

31. Tinterri C, Canavese G, Bruzzi P, Dozin B. NEONOD 2: Rationale and design of a multicenter non-inferiority trial to assess the effect of axillary surgery omission on the outcome of breast cancer patients presenting only micrometastasis in the sentinel lymph node after neoadjuvant chemotherapy. *Contemp Clin Trials Commun* (2019) 17:100496. doi: 10.1016/j.conctc.2019.100496

frontiers | Frontiers in Oncology

TYPE Original Research
PUBLISHED 12 July 2023
DOI 10.3389/fonc.2023.1146754

OPEN ACCESS

EDITED BY
Vishruta Dumane,
Icahn School of Medicine at Mount Sinai, United States

REVIEWED BY
Hidekazu Tanaka,
Yamaguchi University Graduate School of Medicine, Japan
Chenbin Liu,
Chinese Academy of Medical Sciences and Peking Union Medical College, China

*CORRESPONDENCE
Ryan Rhome
rrhome@iuhealth.org

RECEIVED 17 January 2023
ACCEPTED 06 June 2023
PUBLISHED 12 July 2023

CITATION
Rhome R, Wright J, De Souza Lawrence L, Stearns V, Wolff A and Zellars R (2023) Concurrent chemotherapy with partial breast irradiation in triple negative breast cancer patients may improve disease control compared with sequential therapy. *Front. Oncol.* 13:1146754.
doi: 10.3389/fonc.2023.1146754

Concurrent chemotherapy with partial breast irradiation in triple negative breast cancer patients may improve disease control compared with sequential therapy

Ryan Rhome[1]*, Jean Wright[2], Lana De Souza Lawrence[3], Vered Stearns[4], Antonio Wolff[4] and Richard Zellars[1]

[1]Department of Radiation Oncology, Indiana University Hospital, Indianapolis, IN, United States, [2]Department of Radiation Oncology, The Johns Hopkins Hospital, Johns Hopkins Medicine, Baltimore, MD, United States, [3]Christiana Care Health System, Wilmington, DE, United States, [4]Department of Oncology, Division of Women's Malignancies, The Johns Hopkins Hospital, Johns Hopkins Medicine, Baltimore, MD, United States

Purpose: To report outcomes on a subset of patients with triple negative breast cancer (TNBC) treated on prospective trials with post-lumpectomy partial breast irradiation and concurrent chemotherapy (PBICC) and compare them to a retrospectively assessed similar cohort treated with whole breast irradiation after adjuvant chemotherapy (WBIaC).

Methods and materials: Women with T1-2, N0-1 invasive breast cancer with ≥ 2mm lumpectomy margins were offered therapy on one of two PBICC trials. PBI consisted of 40.5 Gy in 15 daily 2.7 Gy fractions delivered concurrently with the first 2 cycles of adjuvant chemotherapy. The comparison cohort received WBI to a median dose of 60.7 Gy, (including boost, range 42.5 – 66 Gy), after completion of non-concurrent, adjuvant chemotherapy. We evaluated disease-free survival (DFS), and local/loco-regional/distant recurrence-free survival (RFS). We compared survival rates using Kaplan-Meier curves and log-rank test of statistical significance.

Results: Nineteen patients with TNBC were treated with PBICC on prospective protocol, and 49 received WBIaC. At a median follow-up of 35.5 months (range 4.8-71.9), we observed no deaths in the PBICC cohort and 2 deaths in the WBIaC cohort (one from disease recurrence). With a median time of 23.4 (range 4.8 to 47) months, there were 7 recurrences (1 nodal, 4 local, 4 distant), all in the WBIaC group. At 5 years, there was a trend towards increased local RFS (100% vs. 85.4%, p=0.17) and loco-regional RFS (100% vs. 83.5, p=0.13) favoring the PBICC cohort. There was no significant difference in distant RFS between the two groups (100%

vs. 94.4%, p=0.36). Five-year DFS was 100% with PBICC vs.78.9% (95% CI: 63.2 to 94.6%, p=0.08) with WBIaC.

Conclusion: This study suggests that PBICC may offer similar and possibly better outcomes in patients with TNBC compared to a retrospective cohort treated with WBIaC. This observation is hypothesis-generating for prospective trials.

KEYWORDS

partial breast irradiation, triple negative breast cancer, concurrent chemoradiation, breast cancer, clinical trial

Introduction

Triple negative breast cancer (TNBC) is characterized by lack of expression of estrogen (ER) and progesterone (PR) receptors and lack of overexpression of the human epidermal growth factor receptor 2 (HER2). Women with TNBC are reported to have inferior overall survival, disease free survival, and local control than their non-TNBC counterparts when treated with whole breast irradiation (WBI) (1–3).

Routine management of stage I and II TNBC usually includes mastectomy or breast conserving surgery (BCS) followed by sequential administration of chemotherapy and 3 to 6 weeks of daily WBI (with length of course predicated on nodal coverage, fractionation scheme, and use of boost) (4). In this regard, concurrent chemotherapy and radiation offers potential logistic benefits. While shortening the overall duration of therapy, both adjuvant treatments are completed sooner after surgery. Concurrency can also take advantage of potential oncologic synergy between the two modalities in improving tumor control. Concurrent chemoradiation is used in most other adenocarcinoma-based disease sites, including lung, gastrointestinal, and bladder cancers (5–9), albeit often in the definitive or pre-operative setting. However, concerns of prohibitive toxicity with concurrent administration of anthracycline-based chemotherapy regimens and others along with whole breast radiotherapy have made this approach unpopular (10). The smaller fields employed during partial breast irradiation potentially allow for mitigation of this concurrent toxicity and acceleration of the radiotherapy schedule.

We previously reported results of the first of two prospective phase I/II trials of PBI and concurrent chemotherapy (PBICC) in women with early stage breast cancer (11). Given reports of inferior oncologic outcomes in patients with TNBC and the potential of improved local control with concurrent chemotherapy and irradiation, we hypothesized that patients with TNBC treated with our novel PBICC approach will have similar or improved clinical outcomes as TNBC patients treated more traditionally with WBI after chemotherapy (WBIaC). In this report, we describe the outcome of the subset of TNBC patients enrolled in these PBICC trials. To provide an internal contemporary reference, we also retrospectively describe the outcomes of a series of patients with TNBC patients treated with WBIaC during the same time period.

Materials and methods

Study participants

We evaluated a subgroup of 19 TNBC patients treated on two prospective trials of PBICC that enrolled women with T1-2, N0-1 invasive breast cancer and ≥ 2mm lumpectomy margins between 2004-2009. Both trials were approved by the Institutional Review Board. We also retrospectively identified 51 similar patients with TNBC (T1-2, N0-1 invasive breast cancer with ≥ 2mm lumpectomy margins), treated with standard WBIaC followed by standard chemotherapy at Johns Hopkins University between 2004 and 2009 by using an Institutional Review Board-approved database and chart review. Full details on study designs and participants can be found in the original publication (11).

Radiotherapy

All patients underwent three-dimensional conformal or intensity-modulated radiation treatment planning, using five to seven non-coplanar photon beams.

WBIaC

The median dose of WBI (including boost) in the triple-negative comparison cohort was 59.89 Gy (range 42.56 – 66.60 Gy). Whole breast radiotherapy was delivered in 180-270 cGy fractions. Nodal regions were treated in 20% of the WBIaC patients.

PBICC

PBI consisted of 40.5 Gy in 15 daily 2.7 Gy fractions delivered concurrently with the first 2 of 4 cycles of chemotherapy. For the PBI trials, the clinical target volume (CTV) was defined by a uniform expansion on the lumpectomy cavity, as delineated on computed tomography (CT), by 1.5cm in all directions then cropped to 5mm from skin surface and the chest wall/lung interface. The planning target volume (PTV) was created by

uniformly expanding the CTV by 5 mm. Nodal regions did not receive directed radiotherapeutic treatment.

Chemotherapy

WBIaC and PBICC patients received cyclophosphamide +doxorubicin +/- paclitaxel (AC+T) or cyclophosphamide + docetaxel (TC), at the discretion of the treating medical oncologist.

In all WBIaC cases, radiotherapy was delivered after adjuvant chemotherapy. Decisions about additional systemic chemotherapy after completion of PBICC were made independently by the medical oncologist and the patient.

Endpoints and statistical analysis

Two patients who were lost to follow-up within 12 months of lumpectomy were excluded from the retrospective cohort, therefore 49 patients were considered evaluable. Primary endpoints were disease-free survival (DFS), local recurrence-free survival (RFS), locoregional RFS, and distant RFS which were measured from the date of lumpectomy to time of any recurrence, local failure, locoregional failure, or distant failure, respectively. Local failure was defined as a biopsy-proven recurrence in the ipsilateral breast. Locoregional failure was defined as recurrence either in the ipsilateral breast or regional nodes, including the axilla, internal mammary nodes, or supraclavicular nodes. Distant failure was defined as the development of metastatic foci other than regional lymph nodes. Only distant recurrences that occurred as a first recurrence were considered in the estimation of distant disease-free survival. Progression free survival (PFS) curves comparing treatment modalities were analyzed using the Kaplan-Meier method, and comparisons were made using log-rank χ^2 testing.

Fisher's exact and χ^2 tests were used to compare proportions between two or more groups. Nonparametric data testing consisted of the Mann-Whitney *U* test and the Kruskal-Wallis nonparametric analysis of variance test for comparison of two and three different groups. All statistics were calculated with SSPS (19.0 for Windows; SSPS, Inc., Chicago, Illinois, USA) and GraphPad Prism (5.0 for Windows; GraphPad Software Inc) software. A two-tailed *P* value of < 0.05 was considered statistically significant for all analyses.

Results

Patient characteristics

Patient characteristics are summarized in Table 1. The median follow-up was 33.9 (range 4.8 to 71.9) and 41.9 (range 17 to 68.4) months for the WBIaC and PBICC groups respectively. Median follow up time for all patients was 35.5 months (range 4.8 to 71.9).

There was no statistically significant difference between the WBIaC and PBICC groups with respect to clinical T stage, clinical N stage, median age, race, menopausal status, type of chemotherapy used, or pathologic features.

Triple negative breast cancer outcomes

Overall, seven of 49 (14.3%) of TNBC patients treated with WBIaC had disease recurrence at a median of 23.4 (range 4.8 to 47) months. Sites of recurrence included one nodal, four local, and two distant. Two WBIaC patients died (one of disease recurrence). There were no deaths or recurrences in the PBICC cohort. Patterns of treatment are summarized in Table 2.

Local recurrence

At 5 years, there was a numeric trend towards decreased local recurrence (0% vs. 14.6%, p=0.17) in the PBICC cohort compared to the WBIaC cohort. The 3 year rates of local recurrence were 0% and 7.9% for PIBCC and WBIaC cohorts, respectively. Figure 1 demonstrates Kaplan-Meier analysis comparing both groups with respect to local recurrence-free survival. The median time to initial-site local recurrence was 25.9 months (range 4.8 to 47).

Locoregional recurrence

At 5 years, there was a trend towards decreased loco-regional recurrence (0% vs. 17.8%, p=0.13) in the PBICC cohort compared to the WBIaC cohort. The 3 year locoregional recurrence rates were 0% and 13.2% for the PBICC and WBIaC cohorts, respectively. Figure 2 demonstrates Kaplan-Meier analysis comparing both groups with respect to locoregional recurrence-free survival. The time to recurrence in the single patient with initial-site nodal recurrence was 18.5 months. The median time to any locoregional recurrence was 23.4 months (range 4.8 to 47 months).

Distant recurrence

At 3 and 5 years, there was a no significant difference in the rate of distant metastasis (0% vs. 5.6%, p=0.36) between the PBICC and WBIaC cohorts. Figure 3 demonstrates Kaplan-Meier analysis comparing both groups with respect to distant recurrence-free survival. The median time to initial-site distant recurrence was 21.4 months (range 13.9 to 28.9).

Disease-free survival

Five-year DFS estimates were 78.9% (95% CI: 63.2 to 94.6%) vs. 100% in the WBIaC vs. PBICC group respectively by Kaplan-Meier survival analysis, p=0.08 (Figure 4). The 3 year DFS for the groups was 83.6% in the WBIaC group and 100% for the PBICC group. The hazard ratio for disease-free survival was 0.24, numerically in favor of the PBICC group at 5 years (95% CI: 0.05 to 1.12).

10.3389/fonc.2023.1146754

TABLE 1 Patient Characteristics.

Patient Characteristics		Triple Receptor Negative		
		WBI-SC n=49	PBI-CC *n*= 19	p
Median Age (range)		54 (36-80)	61 (40-75)	0.34
cT stage	T1	31 (63%)	11 (58%)	0.68
	T2	18 (37%)	8 (42%)	
cN stage	N0	36 (73%)	15 (79%)	0.64
	N1	13 (27%)	4 (21%)	
Menopausal Status	Pre-	16 (33%)	5 (26%)	0.61
	Post-	33 (67%)	14 (74%)	
Race	Caucasian	23 (47%)	8 (42%)	0.90
	African-American	20 (41%)	8 (42%)	
	Other/ Not specified	6 (12%)	3 (16%)	
Treatment				
Chemotherapy	AC	10 (20%)	6 (32%)	0.21
	AC+P	31 (64%)	9 (47%)	
	TC	8 (16%)	4 (21%)	
Median total RT dose incl. boost (cGy) (Range)		5989 (4256-6660)	4050 (4050-4050)	
Median RT dose per fraction (cGy) (Range)		204 (180-266)	270 (270-270)	
Pathologic Characteristics				
Mean Primary Tumor size (cm)		1.98 (SD 0.91)	1.82 (SD 0.83)	0.65
Median Number of Nodes Examined (Range)		3 (1-28)	4 (1-22)	0.47
Median Number of Nodes Positive (Range)		0 (0-4)	0 (0-2)	0.59
LVI	Present	5 (10%)	3 (16%)	0.48
	Absent	38 (78%)	12 (63%)	
	Unknown	6 (12%)	4 (21%)	
Extent of DCIS	<40%	48 (98%)	18 (95%)	0.48
	≥40%	1 (2%)	1 (5%)	

AC, doxorubicin + cyclophosphamide; AC+P, doxorubicin + cyclophosphamide followed by paclitaxel; TC, cyclophosphamide + docetaxel; LVI, lymphovascular invasion; DCIS, ductal carcinoma in situ.

Discussion

Patients with TNBC are at increased risk of breast cancer recurrence. Radiation with concurrent chemotherapy is known to improve local control *via* the radiation sensitizing effects of chemotherapy in many other disease sites (5–9). We chose to retrospectively review TNBC patients treated on 2 prospective phase I/II trials of PBI and concurrent chemotherapy, and compare their outcomes to retrospectively reviewed TNBC patients treated with WBI after adjuvant chemotherapy during the same period. The results of this study showed a trend towards improved local and loco-regional recurrence-free survival and overall disease-free survival with PBI and concurrent chemotherapy. As previously reported from the entire phase I/II cohort, this approach also has a favorable safety profile (11) in contrast with some other reports of concurrent chemoradiation for breast cancer (10). Specifically, patients in the entire cohort had an 84% rate of grade 1 dermatitis and 0% rate of grade 2+ skin toxicity. There were no incidences of pneumonitis (0%) in that report.

Increased local recurrences in women with TNBC treated with lumpectomy and whole breast irradiation are noted in several reports.

10.3389/fonc.2023.1146754

TABLE 2 Patterns of treatment Failure in Breast Cancer Patients with Triple Negative Receptor Status According to Treatment Modality.

	WBI-SC	PBI-CC	p Value
5 yr Disease-free Survival % (95% CI)	78.9 % (63.2 to 94.6%)	100%	0.08
5 yr Local Recurrence % (95% CI)	14.6 % (0.0 to 29.5%)	0%	0.17
5 yr Locoregional Recurrence % (95% CI)	16.5 % (1.4 to 31.6%)	0%	0.13
5 yr Distant Metastasis % (95% CI)	5.6% (-2.2 to 13.4%)	0%	0.36

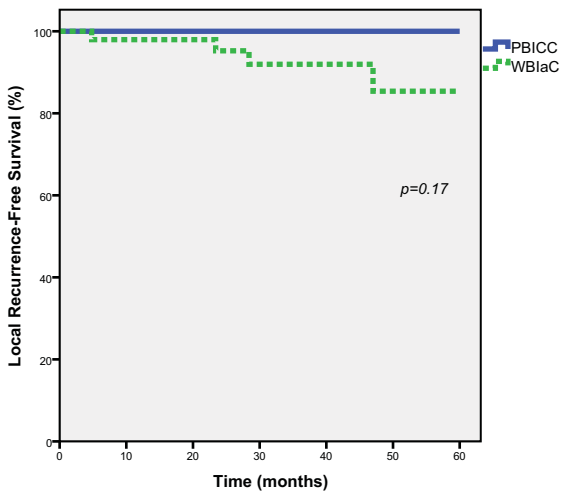

FIGURE 1
Kaplan-Meier estimates of Local Progression-Free Survival for Triple Negative Receptor Patients treated with PBICC and WBIaC.

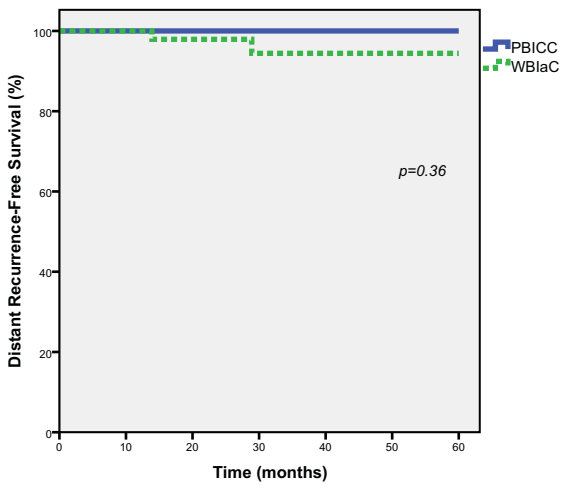

FIGURE 3
Kaplan-Meier estimates of Distant Progression-Free Survival for Triple Negative Receptor Patients treated with PBICC and WBIaC.

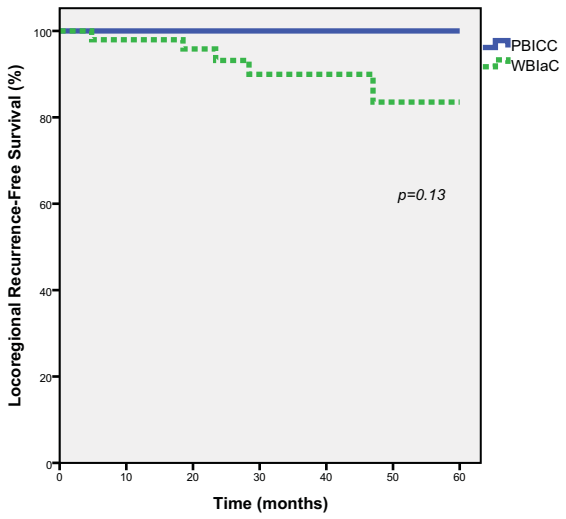

FIGURE 2
Kaplan-Meier estimates of Locoregional Progression-Free Survival for Triple Negative Receptor Patients treated with PBICC and WBIaC.

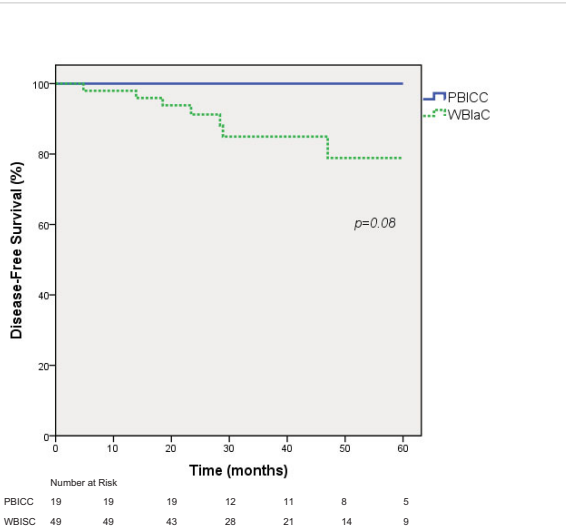

FIGURE 4
Kaplan-Meier estimates of Disease-Free survival for Triple Negative Receptor Patients treated with PBICC and WBIaC.

In a paper by Arvold et al. (12), 1434 patients treated with breast-conserving therapy were divided into standard breast cancer sub-types, 171 of whom had TNBC. With a median follow-up of 84 months, the authors reported that the TNBC sub-type was independently associated with increased local recurrence on multivariate analysis (MVA). Zaky et al. (13) reviewed 193 and 160 women with TNBC and non-TNBC respectively, all treated with BCS and WBI. With a median follow-up of 3.4 yrs, the authors reported a 12% and 4% rate of local recurrence respectively (p=0.01). On MVA, TNBC was again independently associated with local recurrence. This elevated rate of local recurrence has also been reported in patients treated with PBI. Pashtan et al. (14) recently reported a 5 year actuarial local recurrence rate of 32.5% in 9 TNBC patients treated with 3D-Accelerated partial breast irradiation. When compared to HR positive/ Her 2 negative patients, TNBC patients treated with PBI had a local recurrence hazard ratio of 15.2 (95% CI, 2.5-91). However, this increased rate of local recurrence after breast conserving therapy in TNBC patients is not a universal finding. A study by Wilkinson et al. (15), which included 20 TNBC patients and 182 receptor positive patients (almost half of whom were treated with 3D-APBI), reported a 0% actuarial rate of ipsilateral breast recurrence, nodal recurrence and distant metastases at 5 years in the TNBC cohort, which was not statistically distinct from the receptor positive patients.

There is also a suggestion of worse outcomes in patients with TNBC with regards to regional control, distant metastasis, and survival. For example, Haffty et al. (16) reported a statistically significant inferior nodal relapse-free rate (94 vs 99%), distant metastasis-free rate (68% vs. 83%) and cause-specific survival (72 vs. 85%) at 5 years with conventional breast-conserving therapy for TNBC patients compared to others. Wilder et al. (17) also demonstrated significantly inferior non-local relapse (81 vs 100%) and cause-specific survival (89 vs 100%) at 3 years for TNBC patients compared to others, when treated with PBI. Taken together with the previous discussion of local recurrences, TNBC patients are at higher risk for both local and distant recurrences.

These local and distant recurrence issues may have different solutions. One implication of the increased recurrences seen with TNBC is a relative radioresistance of this phenotype. Concurrent chemotherapy has been shown to improve response rates and overcome radioresistance to certain degrees in multiple tumor types (9). The trend towards improved outcomes with PBICC compared to WBIaC in our study may be due to the radiation sensitizing effects of concurrent chemotherapy but may also be due to the temporal proximity of radiation to surgery. Most commonly, chemotherapy is delivered after surgery and before radiation. Consequently, chemotherapy delays the start of radiation therapy. The importance of RT timing following surgery to reduce the risk of local recurrence is controversial. Bellon et al. (4) randomized 244 women to receive 12 weeks of cyclophosphamide, doxorubicin, methotrexate, fluorouracil and prednisone (CAMFP) before or after RT. At a median follow-up of 135 months, there were no significant differences between the chemotherapy-first and radiotherapy-first arms in time to any event, distant metastasis or death. Conversely, a systematic review by Huang et al. (18) of 11 studies involving 1,927 breast cancer patients demonstrated an increase in the 5-year locoregional recurrence from 6% in the RT-first group to 16% in the chemotherapy-first group (HR 2.28, 95% CI, 1.45 to 3.57). Additional evidence may possibly be seen in the study of PBI by Pashtan et al. above, in which all TNBC PBI recurrences occurred in patients who had their radiation delayed secondary to chemotherapy. How this timing is affected by the increasing use of hypofractionated (19, 20) and ultrahypofractionated (21, 22) radiation therapy is unknown. By definition, the PBICC strategy described here has a shorter interval between surgery and radiation, as the concurrent chemoradiation starts after the patient is sufficiently healed from surgery whereas the conventional standard is to complete all of adjuvant chemotherapy (several months of therapy) prior to radiation.

Our study suggests that combining concurrent chemotherapy with radiation may improve outcomes in TNBC. Concurrency in breast cancer has traditionally been avoided due to previous reports of increased toxicity (10). A recent Phase I prospective trial of concurrent carboplatin with whole breast standard fractionation radiation therapy, and found favorable safety profiles, with planned Phase II study opening thereafter (23). The patients in these trials had multiagent regimens consistent with standard recommendations for TNBC such as AC+T or TC.

We posit that the use of PBI with concurrent chemotherapy would mitigate these toxicities, and that has been supported by previous reports of these trials (11). Nonetheless, there is enough uncertainty about their propensity to recur more often, that the ASTRO guidelines for PBI stress caution in patients who are hormone-receptor-negative (24, 25). Part of the rationale in the discussion for those guidelines was a relative paucity of TNBC patients on APBI clinical trials, rather than specifically citing the recurrence propensity. For example, NSABP B39 and Florence trials had 19% and 1-2.3% of triple negative patients, respectively (22, 26). RAPID and IMPORT LOW studies had only 9-11% and 5% of ER negative patients, respectively (27, 28). One study has suggested ER negativity as a predictor of local recurrence in brachytherapy APBI (29). In contrast, Goulding et al. (30) analyzed patients on two prospective APBI trials that were treated with external beam RT, and when specifically looking at TNBC and other "high risk" patients compared with "suitable" patients, TNBC was not associated with higher in-breast recurrence risk, with no local recurrences occurring in this cohort.

There are limitations to this analysis. Although the patients treated with PBICC were participants of two prospective clinical trials, the trials were not originally designed to address this question. Thus our reported analyses of both PBICC and WBIaC cohorts are truly retrospective in nature. As a retrospective study, it is subject to limitations common with this type of analysis. Specifically there may be patient and treatment differences as well as unknown factors that may have influenced the results. We attempted to mitigate these limitations by choosing comparative cohort (WBIaC) patients with comparable stages and treated during the same time period. For instance, the doses of radiation used in the WBIaC patients were more variable and with a higher range than the PBICC group. While this is an imbalance, it does further support the trend toward control in triple negative patients with concurrent chemotherapy even at lower overall radiation doses in the concurrent cohort. An additional limitation is that our study cohorts are relatively small, likely explaining the lack of statistical significance in our findings. Nonetheless, the local recurrence rate in the WBIaC cohort is comparable to other published studies. For example, Dent et al. (3)

reported a 13% rate of local recurrence in 180 TNBC patients with clinically localized disease treated with WBIaC, with a mean time to local recurrence of 2.8 years. Conversely, the lack of local recurrences in the PBICC cohort is unexpected. As the risk of recurrence in TNBC rapidly declines after the first 3 years, we believe that the median follow-up of the TNBC patients in our study is likely to be adequate to capture a majority of recurrence events. While small, the PBICC cohort is, to the best of our knowledge, the first report of breast cancer outcomes using this approach in TNBC from prospectively collected data. Given these limitations, we consider our results hypothesis-generating.

Conclusion

The finding of extremely low recurrence rates in patients with TNBC treated with PBICC differs both from the comparison cohort of retrospectively reviewed contemporary patients treated with WBIaC, and from earlier reports of a high rate of local recurrence in TNBC patients treated with PBI. This data generates a hypothesis that the PBICC approach is associated with improved clinical outcomes, potentially due to shorter intervals from surgery to radiotherapy and/or to a synergy between radiotherapy and chemotherapy. The ongoing randomized Phase II trial (PBI 3.0, NCT01928589) currently accruing patients that will provide additional information on outcomes using PBICC.

Data availability statement

The raw data supporting the conclusions of this article will be made available by the authors, without undue reservation.

Ethics statement

The studies involving human participants were reviewed and approved by Johns Hopkins Institutional Review Board. The patients/participants provided their written informed consent to participate in this study.

Author contributions

RR: Manuscript creation, data interpretation and analysis. JW: Data interpretation and analysis, review/editing manuscript. LD: Data interpretation and analysis, review/editing manuscript. VS: Patient enrollment, review/editing manuscript, data interpretation. AW: Patient enrollment, review/editing manuscript, data interpretation. RZ: Trial design and execution, data collection, and review/editing manuscript. All authors contributed to the article and approved the submitted version.

Funding

This study was supported by the Breast Cancer Research Foundation.

Conflict of interest

The authors declare that the research was conducted in the absence of any commercial or financial relationships that could be construed as a potential conflict of interest.

Publisher's note

References

1. Rodriguez-Pinilla SM, Sarrio D, Honrado E, Hardisson D, Calero F, Benitez J, et al. Prognostic significance of basal-like phenotype and fascin expression in node-negative invasive breast carcinomas. *Clin Cancer Res* (2006) 12(5):1533–9. doi: 10.1158/1078-0432.CCR-05-2281

2. Banerjee S, Reis-Filho JS, Ashley S, Ashworth A, Lakhani SR, Smith E. Basal-like breast carcinomas: clinical outcome and response to chemotherapy. *J Clin Pathol* (2006) 59(7):729–35. doi: 10.1136/jcp.2005.033043

3. Dent R, Trudeau M, Pritchard KI, Hanna WM, Kahn HK, Sawka CA, et al. Triple-negative breast cancer: clinical features and patterns of recurrence. *Clin Cancer Res* (2007) 13(15 Pt 1):4429–34. doi: 10.1158/1078-0432.CCR-06-3045

4. Bellon JR, Come SE, Gelman RS, Henderson IC, Shulman LN, Silver BJ, et al. Sequencing of chemotherapy and radiation therapy in early-stage breast cancer: updated results of a prospective randomized trial. *J Clin Oncol* (2005) 23(9):1934–40. doi: 10.1200/JCO.2005.04.032

5. Choy H, Gerber DE, Bradley JD, Iyengar P, Monberg M, Treat J, et al. Concurrent pemetrexed and radiation therapy in the treatment of patients with inoperable stage III non-small cell lung cancer: a systematic review of completed and ongoing studies. *Lung Cancer* (2015) 87(3):232–40. doi: 10.1016/j.lungcan.2014.12.003

6. Cooper JS, Guo MD, Herskovic A, Macdonald JS, Martenson JA Jr, Al-Sarraf M, et al. Chemoradiotherapy of locally advanced esophageal cancer: long-term follow-up of a prospective randomized trial (RTOG 85-01). radiation therapy oncology group. *JAMA* (1999) 281(17):1623–7. doi: 10.1001/jama.281.17.1623

7. Gerard JP, Conroy T, Bonnetain F, Bouche O, Chapet O, Colson-Dejardin M-T, et al. Preoperative radiotherapy with or without concurrent fluorouracil and leucovorin in T3-4 rectal cancers: results of FFCD 9203. *J Clin Oncol* (2006) 24(28):4620–5. doi: 10.1200/JCO.2006.06.7629

8. Moertel CG, Childs DS Jr, Reitemeier RJ, Colby Jr MY, Holbrook MA. Combined 5-fluorouracil and supervoltage radiation therapy of locally unresectable gastrointestinal cancer. *Lancet* (1969) 2(7626):865–7. doi: 10.1016/S0140-6736(69)92326-5

9. Seiwert TY, Salama JK, Vokes EE. The concurrent chemoradiation paradigm–general principles. *Nat Clin Pract Oncol* (2007) 4(2):86–100. doi: 10.1038/ncponc0714

10. Fiets WE, van Helvoirt RP, Nortier JW, van der Tweel I, Struikmans H, et al. Acute toxicity of concurrent adjuvant radiotherapy and chemotherapy (CMF or AC) in breast cancer patients. a prospective, comparative, non-randomised study. *Eur J Cancer* (2003) 39(8):1081–8. doi: 10.1016/S0959-8049(03)00178-3

11. Zellars RC, Stearns V, Frassica D, Asrari F, Tsangaris T, Myers L, et al. Feasibility trial of partial breast irradiation with concurrent dose-dense doxorubicin and cyclophosphamide in early-stage breast cancer. *J Clin Oncol* (2009) 27(17):2816–22. doi: 10.1200/JCO.2008.20.0139

12. Arvold ND, Taghian AG, Niemierko A, Abi Raad RF, Sreedhara M, Nguyen PL, et al. Age, breast cancer subtype approximation, and local recurrence after breast-conserving therapy. *J Clin Oncol* (2011) 29(29):3885–91. doi: 10.1200/JCO.2011.36.1105

13. Zaky SS, Lund M, May KA, Godette KD, Beitler JJ, Holmes LR, et al. The negative effect of triple-negative breast cancer on outcome after breast-conserving therapy. *Ann Surg Oncol* (2011) 18(10):2858–65. doi: 10.1245/s10434-011-1669-4

14. Pashtan IM, Recht A, Ancukiewicz M, Brachtel E, Abi-Raad RF, D'Alessandro HA, et al. External beam accelerated partial-breast irradiation using 32 gy in 8 twice-daily fractions: 5-year results of a prospective study. *Int J Radiat Oncol Biol Phys* (2012) 84(3):e271–7. doi: 10.1016/j.ijrobp.2012.04.019

15. Wilkinson JB, Reid RE, Shaitelman SF, Chen PY, Mitchell CK, Wallace MF, et al. Outcomes of breast cancer patients with triple negative receptor status treated with accelerated partial breast irradiation. *Int J Radiat Oncol Biol Phys* (2011) 81(3):e159–64. doi: 10.1016/j.ijrobp.2010.12.031

16. Haffty BG, Yang Q, Reiss M, Kearney T, Higgins SA, Weidhaas J, et al. Locoregional relapse and distant metastasis in conservatively managed triple negative early-stage breast cancer. *J Clin Oncol* (2006) 24(36):5652–7. doi: 10.1200/JCO.2006.06.5664

17. Wilder RB, Curcio LD, Khanijou RK, Eisner ME, Kakkis JL, Chittenden L, et al. Results with accelerated partial breast irradiation in terms of estrogen receptor, progesterone receptor, and human growth factor receptor 2 status. *Int J Radiat Oncol Biol Phys* (2010) 78(3):799–803. doi: 10.1016/j.ijrobp.2009.08.081

18. Huang J, Barbera L, Brouwers M, Browman G, Mackillop WJ. Does delay in starting treatment affect the outcomes of radiotherapy? a systematic review. *J Clin Oncol* (2003) 21(3):555–63. doi: 10.1200/JCO.2003.04.171

19. Haviland JS, Owen JR, Dewar JA, Agrawal RK, Barrett J, Barrett-Lee PJ, et al. The UK standardisation of breast radiotherapy (START) trials of radiotherapy hypofractionation for treatment of early breast cancer: 10-year follow-up results of two randomised controlled trials. *Lancet Oncol* (2013) 14(11):1086–94. doi: 10.1016/S1470-2045(13)70386-3

20. Whelan TJ, Pignol J-P, Levine MN, Julian JA, MacKenzie R, Parpia S, et al. Long-term results of hypofractionated radiation therapy for breast cancer. *N Engl J Med* (2010) 362(6):513–20. doi: 10.1056/NEJMoa0906260

21. Brunt AM, Haviland JS, Sydenham M, Agrawal RK, Algurafi H, Alhasso A, et al. Ten-year results of FAST: a randomized controlled trial of 5-fraction whole-breast radiotherapy for early breast cancer. *J Clin Oncol* (2020) 38(28):3261–72. doi: 10.1200/JCO.19.02750

22. Meattini I, Marrazzo L, Saieva C, Desideri I, Scotti V, Simontacchi G, et al. Accelerated partial-breast irradiation compared with whole-breast irradiation for early breast cancer: long-term results of the randomized phase III APBI-IMRT-Florence trial. *J Clin Oncol* (2020) 38(35):4175–83. doi: 10.1200/JCO.20.00650

23. Bellon JR, Chen Y-H, Rees R, Taghian AG, Wong JS, Punglia RS, et al. A phase 1 dose-escalation trial of radiation therapy and concurrent cisplatin for stage II and III triple-negative breast cancer. *Int J Radiat Oncol Biol Phys* (2021) 111(1):45–52. doi: 10.1016/j.ijrobp.2021.03.002

24. Smith BD, Arthur DW, Buchholz TA, Haffty BG, Hahn CA, Hardenbergh PH, et al. Accelerated partial breast irradiation consensus statement from the American society for radiation oncology (ASTRO). *Int J Radiat Oncol Biol Phys* (2009) 74(4):987–1001. doi: 10.1016/j.ijrobp.2009.02.031

25. Correa C, Harris EE, Leonardi MC, Smith BD, Taghian AG, Thompson AM, et al. Accelerated partial breast irradiation: executive summary for the update of an ASTRO evidence-based consensus statement. *Pract Radiat Oncol* (2017) 7(2):73–9. doi: 10.1016/j.prro.2016.09.007

26. Vicini FA, Wilkinson JB, Lyden M, Beitsch P, Vicini FA. Long-term primary results of accelerated partial breast irradiation after breast-conserving surgery for early-stage breast cancer: a randomised, phase 3, equivalence trial. *Lancet* (2019) 394 (10215):2155–64. doi: 10.1016/S0140-6736(19)32514-0

27. Whelan TJ, Asmar L, Wang Y, Tole S, Barke L, Widner J, et al. External beam accelerated partial breast irradiation versus whole breast irradiation after breast conserving surgery in women with ductal carcinoma in situ and node-negative breast cancer (RAPID): a randomised controlled trial. *Lancet* (2019) 394 (10215):2165–72. doi: 10.1016/S0140-6736(19)32515-2

28. Coles CE, Cecchini RS, White JR, Arthur DW, Julian TB, Rabinovitch RA, et al. Partial-breast radiotherapy after breast conservation surgery for patients with early breast cancer (UK IMPORT LOW trial): 5-year results from a multicentre, randomised, controlled, phase 3, non-inferiority trial. *Lancet* (2017) 390(10099):1048–60. doi: 10.1016/S0140-6736(17)31145-5

29. Shah C, Julian JA, Berrang TS, Kim D-H, Germain I, Nichol AM, et al. Predictors of local recurrence following accelerated partial breast irradiation: a pooled analysis. *Int J Radiat Oncol Biol Phys* (2012) 82(5):e825–30. doi: 10.1016/j.ijrobp.2011.11.042

30. Goulding A, Haviland JS, Kirby AM, Griffin CL, Sydenham MA, Titley JC, et al. Outcomes after accelerated partial breast irradiation in women with triple negative subtype and other "High risk" variables categorized as cautionary in the ASTRO guidelines. *Front Oncol* (2021) 11:617439. doi: 10.3389/fonc.2021.617439

frontiers | Frontiers in Oncology

TYPE Original Research
PUBLISHED 13 July 2023
DOI 10.3389/fonc.2023.1147775

OPEN ACCESS

EDITED BY
Vishruta Dumane,
Icahn School of Medicine at Mount Sinai,
United States

REVIEWED BY
Dr. Udhaya Kumar. S,
Baylor College of Medicine, United States
Elizabeth M. Nichols,
University of Maryland Medical Center,
United States

*CORRESPONDENCE
Chih-Jen Huang
ccjjhh@kmu.edu.tw

RECEIVED 19 January 2023
ACCEPTED 26 June 2023
PUBLISHED 13 July 2023

CITATION
Lee H-H, Wang C-Y, Chen S-T, Lu T-Y, Chiang C-H, Huang M-Y and Huang C-J (2023) Electron stream effect in 0.35 Tesla magnetic resonance image guided radiotherapy for breast cancer.
Front. Oncol. 13:1147775.
doi: 10.3389/fonc.2023.1147775

Electron stream effect in 0.35 Tesla magnetic resonance image guided radiotherapy for breast cancer

Hsin-Hua Lee[1,2,3,4], Chun-Yen Wang[2], Shan-Tzu Chen[5], Tzu-Ying Lu[2], Cheng-Han Chiang[2], Ming-Yii Huang[1,2,3,4,6] and Chih-Jen Huang[2,3,4]*

[1]Ph.D. Program in Environmental and Occupational Medicine, Kaohsiung Medical University and National Health Research Institutes, Kaohsiung, Taiwan, [2]Department of Radiation Oncology, Kaohsiung Medical University Hospital, Kaohsiung Medical University, Kaohsiung, Taiwan, [3]Department of Radiation Oncology, Faculty of Medicine, School of Medicine, College of Medicine, Kaohsiung Medical University, Kaohsiung, Taiwan, [4]Center for Cancer Research, Kaohsiung Medical University, Kaohsiung, Taiwan, [5]Department of Medical Imaging, Kaohsiung Municipal Siaogang Hospital, Kaohsiung, Taiwan, [6]Graduate Institute of Medicine, College of Medicine, Kaohsiung Medical University, Kaohsiung, Taiwan

Purpose: This research aimed to analyze electron stream effect (ESE) during magnetic resonance image guided radiotherapy (MRgRT) for breast cancer patients on a MR-Linac (0.35 Tesla, 6MV), with a focus on the prevention of redundant radiation exposure.

Materials and methods: RANDO phantom was used with and without the breast attachment in order to represent the patients after breast conserving surgery (BCS) and those received modified radical mastectomy (MRM). The prescription dose is 40.05 Gy in fifteen fractions for whole breast irradiation (WBI) or 20 Gy single shot for partial breast irradiation (PBI). Thirteen different portals of intensity-modulated radiation therapy were created. And then we evaluated dose distribution in five areas (on the skin of the tip of the nose, the chin, the neck, the abdomen and the thyroid.) outside of the irradiated field with and without 0.35 Tesla. In addition, we added a piece of bolus with the thickness of 1cm on the skin in order to compare the ESE difference with and without a bolus. Lastly, we loaded two patients' images for PBI comparison.

Results: We found that 0.35 Tesla caused redundant doses to the skin of the chin and the neck as high as 9.79% and 5.59% of the prescription dose in the BCS RANDO model, respectively. For RANDO phantom without the breast accessory (simulating MRM), the maximal dose increase were 8.71% and 4.67% of the prescription dose to the skin of the chin and the neck, respectively. Furthermore, the bolus we added efficiently decrease the unnecessary dose caused by ESE up to 59.8%.

Conclusion: We report the first physical investigation on successful avoidance of superfluous doses on a 0.35T MR-Linac for breast cancer patients. Future studies of MRgRT on the individual body shape and its association with ESE influence is warranted.

KEYWORDS

magnetic resonance image guided radiotherapy (MRgRT), magnetic resonance imaging (MRI), electron stream effect, breast cancer, image-guided radiotherapy (IGRT), skin dose, visibility

1 Introduction

Breast cancer has replaced lung cancer as the most frequently diagnosed cancer globally in the latest report by the International Agency for Research on Cancer (1). An estimated 685,000 women died from breast cancer in 2020, corresponding to 1 in every 6 cancer deaths in women (2). Breast cancer patients nowadays often are treated by breast-conserving surgery (BCS) followed by radiation therapy (RT). RT after BCS is indicated for ductal carcinoma *in situ* (stage 0), since RT greatly lowers the risk of local recurrence (3). In early (stage I-II) invasive breast cancer, adjuvant RT followed by BCS remains a standard of care (4). Based upon high level evidence for those with stage III–IV, RT is essential for selected patients after neoadjuvant systemic treatment followed by BCS or modified radical mastectomy (MRM) (4). Since RT may be recommended for all stages, the implications of different modalities of image guided radiotherapy (IGRT) are the keys to precision treatment for patients with breast cancer after BCS or MRM as well as for those with recurrence or distant metastasis (5).

The advance of both modern on-board imaging and planning software are required for adaptive treatment planning which had long been proposed (6). It has been challenging that thoracic radiotherapy such as that for breast irradiation has large inter-fractional and intra-fractional organ movement variation causing unwanted radiation-induced complications such as cardiac and pulmonary toxicities. Some used mechanical ventilation and surface-image mapping system to reduce the within-patient variability of breathing for breast cancer patients (7). A mounting body of evidence strongly supports IGRT (8–17). Until recently, image guidance was only performed prior to radiation treatment without simultaneous tracking. Magnetic resonance imaging-guided radiotherapy (MRgRT) has lately emerged as the state-of-the-art science in precision RT. It enables Radiation Oncologists to actually see the targets in relation to surrounding normal tissue during treatment (18, 19). Immediately after inspecting anatomical changes via MR guidance, Radiation Oncologists are able to recontour, recalculate and then execute a whole new set of treatment plan according to geographical variability at that specific treatment fraction (20–23). MRgRT offers not only novel online adaptation, but specifically better IGRT due to superior soft tissue contrast.

Up till now, IGRT in the form of MRgRT has not been prevalent. Cone beam computed tomography (CBCT) and mega-voltage CT (MVCT) remain the clinical standard for volumetric localization nowadays. It was reported that low-field MR provides better anatomic visualization of radiation targets and nearby organs at risk (OAR) as compared to CBCT or MVCT (24). Besides, MRgRT avoids redundant radiation exposure inherent to IGRT via CT (25). On the other hand, the influence from electron-stream effect (ESE) during MRgRT has been reported by few and not yet fully evaluated (26). When electrons are subjected to a magnetic field, they can be deflected from their original path, leading to a phenomenon known as the Lorentz force. Interactions between the electron beam and tissue can result in the electron air stream effect (ESE), leading to radiation being deposited outside of the intended treatment area, and the electron return effect, causing increased radiation dose to the skin and at the air/tissue interface (27). Out-of-field skin dose due to spiraling contaminant electrons in a perpendicular magnetic field has been observed (28). The data are limited for the assessment of ESE, modifiers of ESE and joint effects of radiotherapy and ESE during 0.35 Tesla MRgRT. To address these issues, we designed the current study to investigate ESE for breast cancer patients.

2 Materials and methods

We conducted this study on a 0.35-T MR-Linac system (MRIdian, ViewRay Inc., Mountain View, CA, USA) and used RANDO phantom to simulate the postoperative female patients with and without breast preservation (Figure 1). The anthropomorphic RANDO phantom conforms to the standards established by the International Commission on Radiation Units and Measurements (ICRU) Report No. 44. It was scanned with a 5-mm slice thickness using a Computed Tomography (CT) simulator (Brilliance 16 Big Bore, Philips Medical Systems, Cleveland, OH, USA). Following CT-simulation, MR-simulation was performed on MRIdian. The study was approved by the Ethical and Research Committee in the University Hospital (KMUHIRB-E(I)-20220101) and it was conducted under compliance of the Institutional Review

FIGURE 1
The RANDO phantom that shows **(A)** without the breast attachment in order to represent the patients after modified radical mastectomy and **(B)** with the breast attachment in order to represent the patients underwent breast conserving surgery. **(C)** The same RANDO phantom without the breast attachment that received Computed Tomography simulation with the coil on. **(D)** The same RANDO phantom with the breast attachment that received Computed Tomography simulation with the coil on.

Board regulations in accordance with the Helsinki Declaration of 1975 as revised in 1983.

2.1 Phantom mimicking modified radical mastectomy (MRM)

As shown in Figure 1, we used the anthropomorphic RANDO phantom to simulate breast cancer patients after MRM for treatment planning (Figures 1A, C). The entire structure was contoured and expanded using a 8-cm margin anteriorly and laterally to demonstrate air with the density of 0.0012g/cm as in Figure 2. The external nose is a midline protuberance in the middle of the face. In this study we marked the nasal tip, the tip of external nose, which marks the termination of nasal ridge. The chin (a.k.a. the mental protuberance) lies in the midline of the mandible anteriorly. Figure 2C documents five selected out-of-field locations 3 mm from the surface of the tip of the nose, the chin, the thyroid, the neck, and the abdomen. We specified the skin structure as a 3 mm inner rind automatically created from the external contour (29). Figures 3B, C demonstrates the addition of 1cm-bolus. After all organs at risk (OAR) were contoured manually from axial CT images as described in our previous clinical study (30), we utilized the MRIdian to generate two intensity modulated radiation therapy (IMRT) treatment plans with and without bolus. The total prescribed dose was 40.05 Gy in 15 fractions. Thirteen spaced 6-MV IMRT beams were created and optimized to deliver the prescription dose with 95% PTV coverage as in Figure 3. The same angles with 0°, 15°, 29°, 43°, 72°, 101°, 115°, 130°, 144°, 302°, 317°, 331° and 346° were chosen with mono-isocenter and applied to all plans. Table 1 is the constraints for OAR and planning target volume (PTV). Additionally, we use the software of ADAC Pinnacle 14.0 to make IMRT treatment plans using identical parameters in Table 1. There were four computerized treatment plans made for this MRM RANDO model.

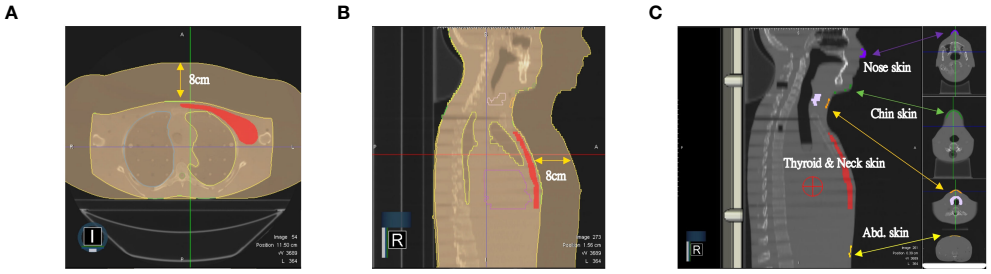

FIGURE 2
The entire structure was contoured and expanded using a 8-cm margin anteriorly and laterally to demonstrate the air as in **(A)** axial view and **(B)** sagittal view. **(C)** Five selected out-of-field locations 3 mm from the skin on the tip of the nose, the chin, the thyroid, the neck, and the abdomen.

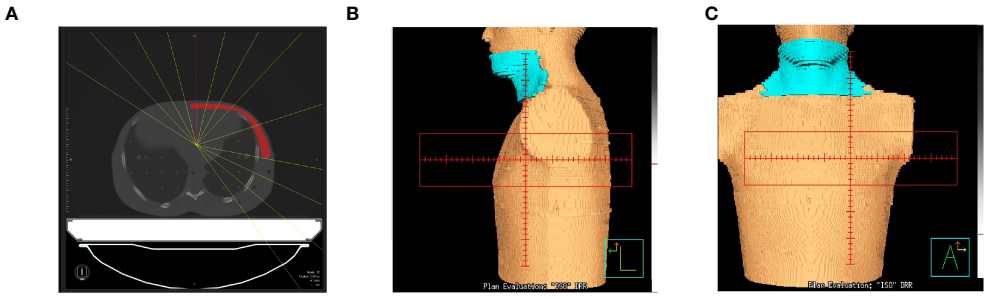

FIGURE 3
(A) Thirteen spaced 6-MV beams including 0°, 15°, 29°, 43°, 72°, 101°,115°, 130°, 144°, 302°, 317°, 331° and 346° were created and optimized to deliver the prescription dose with a mono-isocenter. The same angles were applied to all plans. The blue area denotes a 1cm-bolus in **(B)** the lateral view and **(C)** the front view.

2.2 Phantom mimicking breast conserving surgery (BCS)

The anthropomorphic RANDO phantom with the breast attachments was used to simulate breast cancer patients after BCS for treatment planning (Figures 1B, D). The same process described in 2.1 was performed again for this model of BCS RANDO. The entire structure was contoured and expanded using a 8-cm margin anteriorly and laterally to demonstrate air with the density of 0.0012g/cm as in Figure 2. Figure 2C shows five selected locations 3 mm from the surface on the tip of the nose, the chin, the thyroid, the neck, and the abdomen. Figures 3B, C shows the addition of 1cm-bolus. After all organs at risks (OAR) and region of interest were delineated manually from axial CT images as described in our earlier publication (31, 32), we utilized the MRIdian to create 2 IMRT treatment plans with and without a bolus. The total prescribed dose was 40.05 Gy in 15 fractions. Thirteen spaced 6-MV IMRT beams same as those for MRM RANDO model were fashioned and optimized to deliver the prescription dose to provide 95% PTV coverage. The same angles with 0°, 15°, 29°, 43°, 72°, 101°, 115°, 130°, 144°, 302°, 317°, 331° and 346° were chosen with one mono-isocenter and applied to all plans. Additionally, we use the ADAC Pinnacle 14.0 to make IMRT treatment plans with identical parameters in Table 1. There were four plans produced for this BCS RANDO model.

2.3 Partial breast irradiation (PBI) from 2 patients' treatment plans

Lastly, we added the images of partial breast irradiation (PBI) in two patients previously treated. Image A has right breast cancer with PVT volume of 4.4cc and image B has left breast cancer with PVT volume of 11cc. Both of them underwent BCS and received the prescribed dose of 20 Gy in one single fraction. The IMRT was performed on the Computerized Treatment Planning System of ViewRay® MRIdian.

TABLE 1 Constraints for planning target volume and organs at risk.

Structure	Constraints
planning target volume	$V_{45Gy} \leqq 1CC; V_{40.05Gy} \geqq 95\%$
spinal cord	$D_{max} \leqq 45$ Gy
right lung	$V_{16.5Gy} \leqq 950CC; V_{18Gy} \leqq 37\%$
left lung	$V_{16.5Gy} \leqq 950CC; V_{18Gy} \leqq 37\%$
heart	$V_{42Gy} \leqq 15CC$

3 Results

3.1 MRM

We found that the redundant dose was as high as 3.49 Gy in the skin of the chin and 1.87 Gy in the neck skin when simulating a patient with breast cancer after MRM (Table 2) under 0.35T with a prescribed dose of 40 Gy in 15 fractions. The maximum doses without 0.35T were 0.89 Gy for the skin of the chin and 0.89 Gy in the neck skin (both 2.22% of the prescribed dose). And the additional Pinnacle plan without 0.35T reveals 0.7 Gy for the skin of the chin and 0.97 Gy in the neck skin (1.75% and 2.42% of the prescription dose, respectively). Figure 4 illustrates the redundant doses to the skin of chin and the neck are the most prominent in MRM RANDO model: 8.71% of the prescription dose and 4.67% of the prescription dose, respectively. Figure 5A shows isodose curves deviated toward the chin as compared to that without magnetic field 0.35T (Figure 5B). Because we had expanded 8cm out of the body surface, we were able to scrutinize the dose distribution in the air near the chin and neck (Figures 5C-F). The redundant doses were obviously shown in Figure 5. However, when we added 1-cm bolus, the redundant doses dropped 55% from 3.49 Gy in the skin of the chin to 1.57 Gy; and 58.8% from 1.87 Gy in the neck skin to 0.77Gy, respectively (Figure 6). The bolus effectively avoided redundant doses.

3.2 BCS

There was noteworthy ESE observed in the sagittal planes of the dose distribution for the simulation of patients after BCS (Table 3; Figure 7). We discovered that the redundant doses from ESE were as high as 3.92 Gy in the skin of the chin, 2.24 Gy in the neck skin and 2 Gy in the abdominal skin when simulating a patient with breast cancer after BCS under 0.35T with a prescribed dose of 40 Gy in 15 fractions. Without 0.35T, the skin doses were 1.05 Gy in the skin of the chin, 1 Gy in the neck skin and 1.5 Gy in the abdominal skin when simulating a patient with breast cancer after BCS with a prescribed dose of 40 Gy in 15 fractions. And the additional Pinnacle plan without 0.35T reveals 0.49 Gy for the skin of the chin, 0.91 Gy in the neck skin and 1.09 in the abdominal skin (1.22%, 2.27% and 2.72% of the prescription dose, respectively). Figure 8 shows the redundant doses under the influence of magnetic field to the skin of chin, the neck and the abdominal skin are the most prominent in BCS RANDO model: 9.79% of the prescription dose, 5.59% of the prescription dose and 4.99% of the prescription dose, respectively. It was unique to note the unusual abdominal skin dose which has never been discovered in previous literatures. Figure 7A, C shows isodose curves deviated toward the chin as compared to that without a magnetic field of 0.35T (Figure 7B, D).

Because we had expanded 8cm out of the body surface, we were able to distinguish the dose distribution in the air near the nose, the chin, the thyroid, the neck and the abdominal skin (Figure 9). The redundant doses were noticeable and even greater than those of MRM RANDO model. When we added 1-cm bolus, the redundant doses dropped 48.2% and 59.8%, from 3.92 Gy in the skin of the chin and 2.24 Gy in the neck skin to 2.03Gy and 0.9 Gy, respectively (Figure 10). The redundant dose to abdominal skin (2Gy to 1.99Gy) was not affected by 1-cm bolus which covers only the chin and the neck (Figures 3B, C). Under the same condition, this demonstrates the beneficial effect of the coverage of 1-cm bolus.

3.3 PBI

In the experiment of PBI (Figure 11), we examined the dosimetric data from two patients previously treated with a single shot of 20Gy. The plan A disclosed maximal doses of 0.03 Gy in the skin of the chin, 0.07 Gy in the neck skin, 0.18 Gy in the abdominal skin and 0.09 Gy in the thyroid under 0.35T with a prescribed dose of 20Gy in 1 fraction. The maximum doses without 0.35T were 0.03 Gy in the skin of the chin, 0.07 Gy in the neck skin, 0.13 Gy in the abdominal skin and 0.09 Gy in the thyroid. The plan B did not cover the chin and revealed maximal doses of 0.08 Gy in the neck skin, 0.22 Gy in the abdominal skin and 0.16 Gy in the thyroid under 0.35T with a prescribed dose of 20Gy in 1 fraction. The maximum doses without 0.35T were 0.1 Gy in the neck skin, 0.23 Gy in the abdominal skin and 0.16 Gy in the thyroid. There was scant difference with or without magnetic field 0.35T in both PBI plans (Table 4). The influence from ESE was minimal for right or left PBI.

TABLE 2 Skin doses on RANDO model and the increase percentage of the presecription dose (40Gy/15fx).

	Modified radical mastectomy (MRM) / Unit: Gray															
	MRIdian 0.35T (+)				MRIdian 0.35T (-)				MRIdian 0.35T (+) + bolus				Pinnacle			
	Dmean	Dmin	Dmax		Dmean	Dmin	Dmax		Dmean	Dmin	Dmax		Dmean	Dmin	Dmax	
Nose Skin	0.13	0.05	0.22	0.55%	0.19	0.08	0.5	1.25%	0.12	0.06	0.2	0.50%	0.05	0.01	0.13	0.32%
Chin Skin	1.38	0.39	3.49	8.71%	0.56	0.28	0.89	2.22%	0.57	0.25	1.57	3.92%	0.28	0.03	0.7	1.75%
Neck Skin	0.71	0.41	1.87	4.67%	0.61	0.41	0.89	2.22%	0.53	0.42	0.77	1.92%	0.55	0.1	0.97	2.42%
Abdominal Skin	0.4	0.24	0.65	1.62%	0.38	0.18	0.57	1.42%	0.38	0.22	0.55	1.37%	0.13	0.01	0.25	0.62%
Thyroid	0.52	0.35	0.74	1.85%	0.53	0.34	0.76	1.90%	0.53	0.35	0.77	1.92%	0.42	0.25	0.68	1.70%

(+) with.
(-) without.

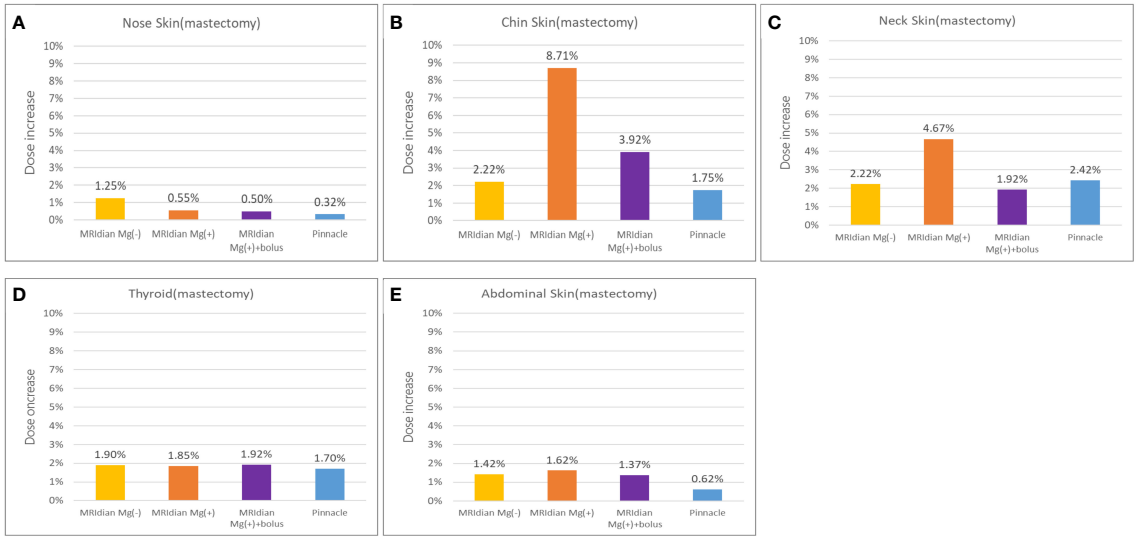

FIGURE 4
In modified radical mastectomy (MRM) model, the percentage of the redundant doses to the skin of **(A)** the nose, **(B)** the chin, **(C)** the neck, **(D)** the thyroid and **(E)** the abdomen; The dose increase in the skin of the chin **(B)** and the neck **(C)** are the most prominent in MRM RANDO model: 8.71% of the prescription dose and 4.67% of the prescription dose, respectively. When adding 1-cm bolus, the redundant dose percentages dropped from 8.71% to 3.92% and from 4.67% to 1.92% in the chin **(B)** and neck **(C)**, respectively.

4 Discussion

To the best of our knowledge, this is the first study to access redundant doses in both WBI and PBI from 0.35-Tesla MRgRT for breast cancer patients after MRM or BCS. We not only took consideration into contemporary surgical techniques of both MRM and BCS but also modern RT strategies with both WBI and PBI. MRgRT has extended a new horizon with real-time imaging tracking which monitors intra-fractional variation. With the implementation of a combination of MRI and Linear accelerator, one may ponder is RT quality transferable. Ionizing radiation can be carcinogenic. A systematic review and meta-analysis of 762,468 patients based on European or North American populations of female breast cancer patients treated in the period between 1954 and 2007 reported that radiotherapy was associated with an increased risk of secondary non-breast cancer, especially lung cancer, esophageal cancer, and sarcoma (33). CBCT generally contributes to 0.03 Gy per scan (34). MRgRT, unlike CBCT or MVCT in IGRT, has no extra radiation dose from image guidance; it utilizes magnetic field for instantaneous imaging tracking (24). However, unnecessary doses increase because the breast shape is not parallel to the magnetic field (35). It is pressing to know how much the redundant doses out of RT field under the influence of a static magnetic field can be.

The MRLinac used in the present study consists of a split-magnet low-field (0.35 Tesla) MRI scanner with a double focused multi-leaf collimator equipped 6MV linear accelerator (36). Upgrade of the technology from ^{60}Co sources to 6 MV linear accelerator improves the dose distribution and therefore reducing the low dose spread (25). Previous physics findings focused on MRLinac with ^{60}Co and were insufficient for the latest model (19, 20, 37–42). This emphasizes the need for more exploration and guidelines to be incorporated into clinical decision making (43). The influence from ESE has been the latest research topic ever since the application MRgRT in clinical world (39, 44). Lately, Liu et al. has reported that the skin dose on the chin was significantly increased due ESE under 1.5 Tesla magnetic field in their study on esophageal cancer (44). It was as high as 25.2% of the prescription dose, which was even higher than that reported by Park et al., of which the corresponding maximum dose to the patient's chin skin surface was 16.1% (39).

The purpose of the current research is to analyze ESE during RT for breast cancer patients on a MR Linac (0.35Tesla, 6MV). We discovered 9.79%, 5.59% and 4.99% of the prescription dose in the chin, neck and abdominal skin of the anthropomorphic phantom with breast attachment which was used to simulate breast cancer patients after BCS. On the other hand, 8.71% and 4.67% of the prescription dose in the chin and neck was calculated on the MRM anthropomorphic phantom model. Ten years ago, van Heijst et al. reported a pioneer study on skin dose at 0.35T and found induced effects for WBI with 2 portals or with 7 portals (35). Relative to the situation without magnetic field, the mean skin dose in WBI-2 increased by 9.5% and 12.5% at 0.35 T and 1.5 T, respectively. Although the mean skin dose in WBI with 7 portals was lower than that in WBI-2 (with 2 portals), it increased 8.2% and 6.8% at 0.35 T and 1.5 T, respectively. Though they did not investigate the effect on patients with breast cancer after MRM, they also explored PBI and concluded that the impact of the electron return effect on the

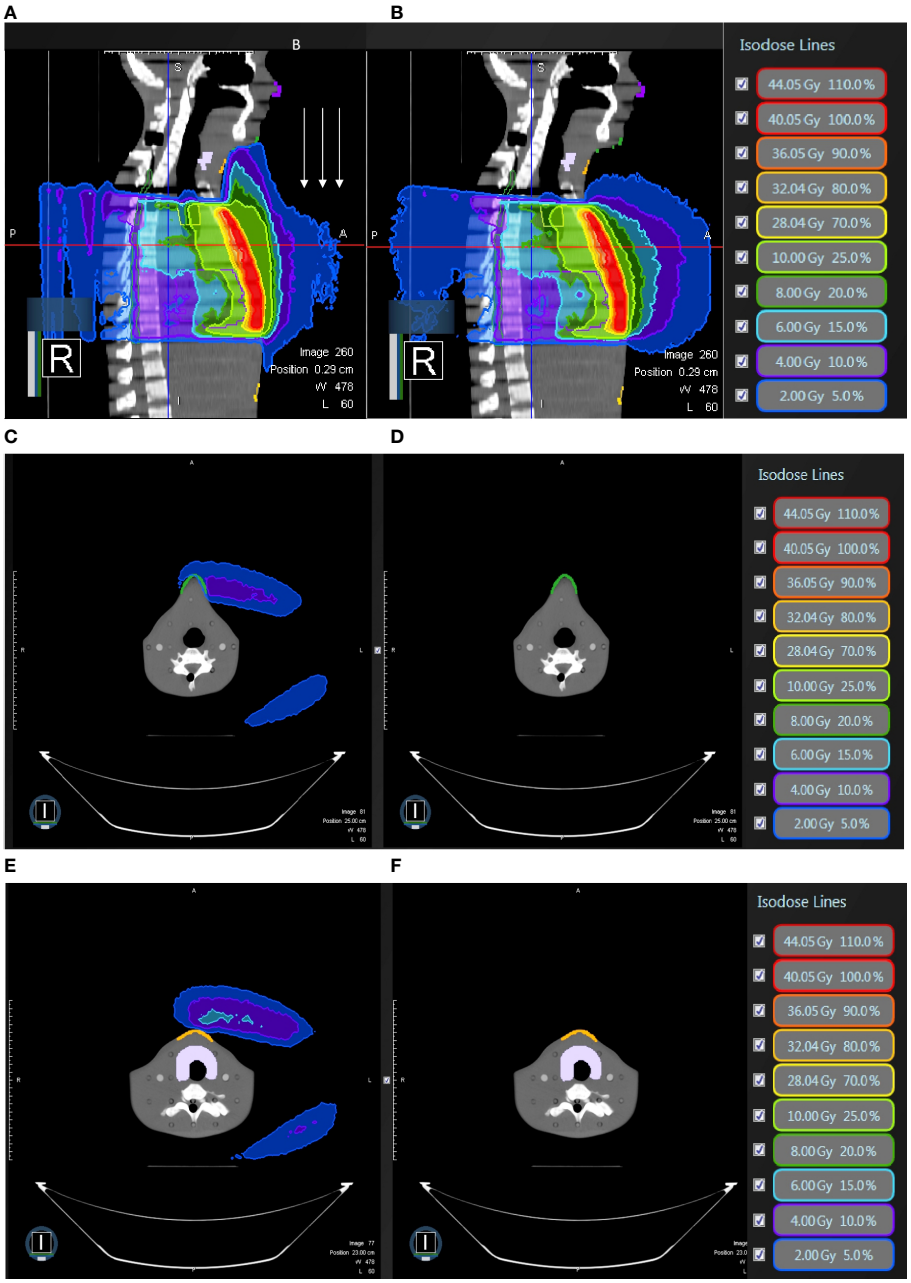

FIGURE 5
In modified radical mastectomy model, **(A)** the isodose curves under the magnetic field of 0.35T deviate toward the chin as compared to **(B)** without the magnetic field 0.35T; the dose distribution in the air near the chin with 0.35T **(C)** without 0.35T **(D)** and the neck skin with 0.35T **(E)** and without 0.35T **(F)**.

skin dose is less prominent in PBI than that in WBI (35). Such finding was also noted in our present study (Table 4). In our daily practice on MRLinac, our medical physicists often employ 12 portals or so for optimization. In the present study, we utilized 13 portals with 0°, 15°, 29°, 43°, 72°, 101°, 115°, 130°, 144°, 302°, 317°, 331° and 346° for the best result of IMRT and still the ESE was marked.

Our current study explored the redundant doses under 0.35T and probed into the prevention measures such as the use of bolus. In our present study, the redundant doses dropped 55% from 3.49 Gy in the skin of the chin to 1.57 Gy; and 58.8% from 1.87 Gy in the neck skin to 0.77Gy, respectively for MRM model with 1-cm bolus. These would be considered unnecessary and not in alignment with ALARA principles. Or for example, this would not be a technology one would want to use in a Li-Fraumeni patient. When we added 1-cm bolus, the redundant doses dropped 48.2% and 59.8%, from 3.92 Gy in the skin of the chin and 2.24 Gy in the neck skin to 2.03Gy and 0.9 Gy, respectively in the BCS model. A recent radiomics study used gradient boosting decision tree and found that SKIN_30Gy is one of the most

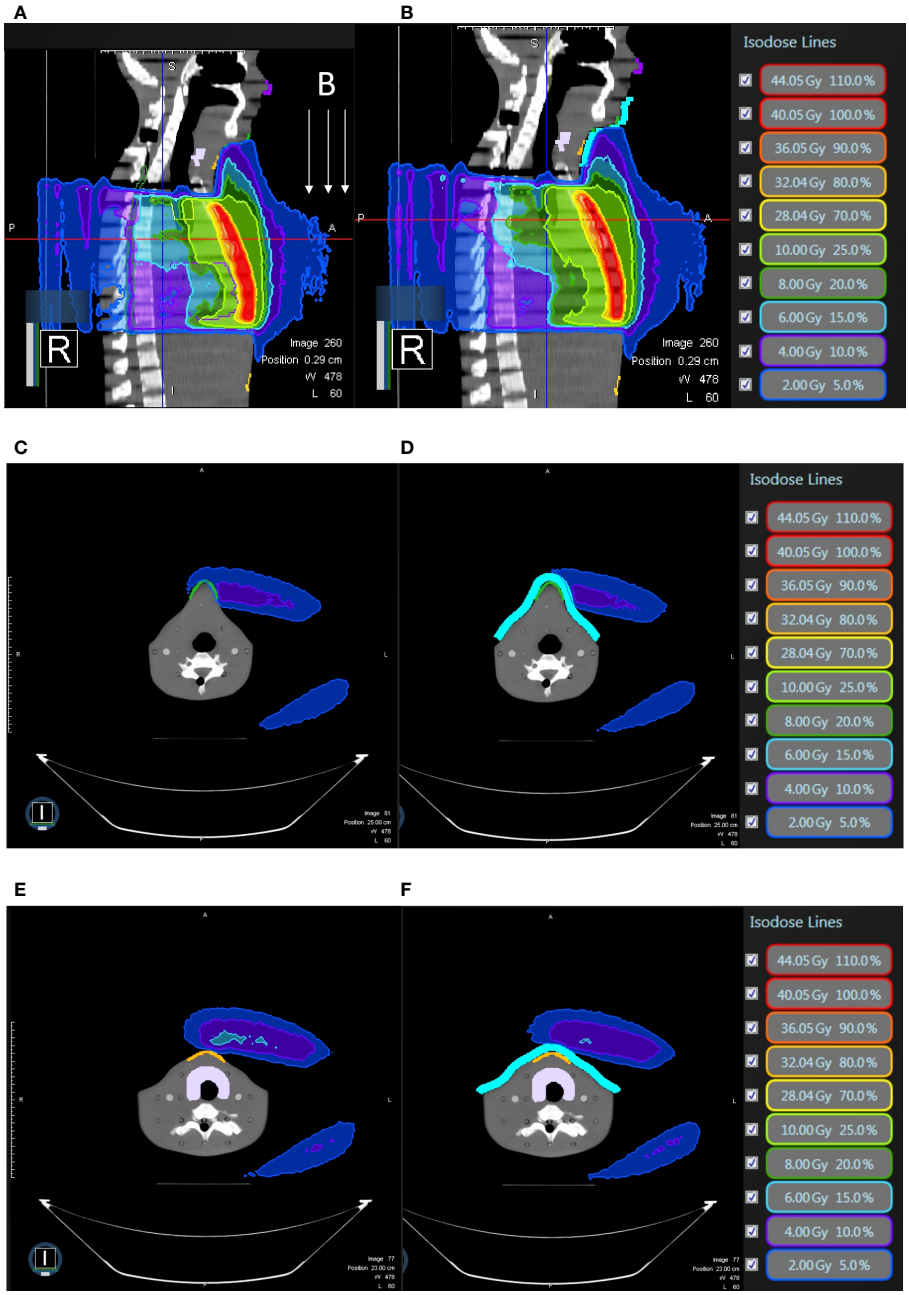

FIGURE 6
In modified radical mastectomy model, all under 0.35 T and **(A)** the isodose curves deviate toward the chin without bolus as compared to **(B)** with bolus in light blue; the dose distribution in the air near the chin without bolus **(C)** with bolus in light blue **(D)** and the neck skin without bolus **(E)** and with bolus in light blue **(F)**.

TABLE 3 Skin doses on RANDO model and the increase percentage of the presecription dose (40Gy/15fx).

	Breast conserving surgery (BCS) / Unit: Gray															
	MRIdian 0.35T (+)				MRIdian 0.35T (-)				MRIdian 0.35T (+) + bolus				Pinnacle			
	Dmean	Dmin	Dmax		Dmean	Dmin	Dmax		Dmean	Dmin	Dmax		Dmean	Dmin	Dmax	
Nose Skin	0.16	0.07	0.26	0.65%	0.26	0.09	0.61	1.52%	0.14	0.07	0.24	0.60%	0.04	0	0.11	0.27%
Chin Skin	1.66	0.51	3.92	9.79%	0.7	0.35	1.05	2.62%	0.71	0.31	2.03	5.07%	0.17	0.02	0.49	1.22%
Neck Skin	0.82	0.51	2.24	5.59%	0.73	0.56	1.00	2.50%	0.68	0.49	0.9	2.25%	0.54	0.11	0.91	2.27%
Abdominal Skin	1.02	0.56	2.00	4.99%	0.89	0.55	1.5	3.75%	0.99	0.57	1.99	4.97%	0.54	0.02	1.09	2.72%
Thyroid	0.58	0.36	0.88	2.20%	0.58	0.42	0.81	2.02%	0.57	0.35	0.8	2.00%	0.42	0.26	0.68	1.70%

(+) with.
(-) without.

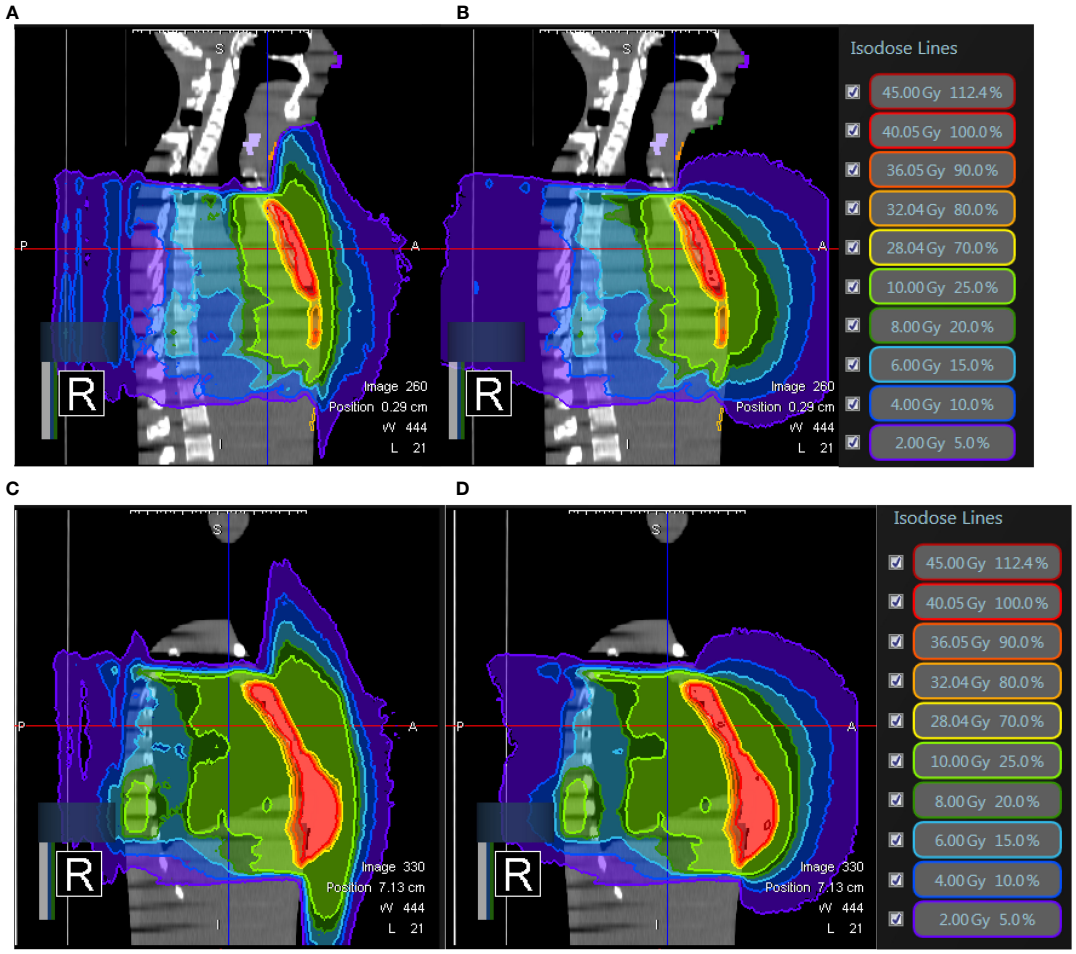

FIGURE 7
In breast-conserving surgery model, **(A)** the isodose curves under the magnetic field of 0.35T deviate toward the chin as compared to **(B)** without the magnetic field 0.35T; the dose distribution in the air in the mid-plane of the breast **(C)** with 0.35T **(D)** without 0.35T.

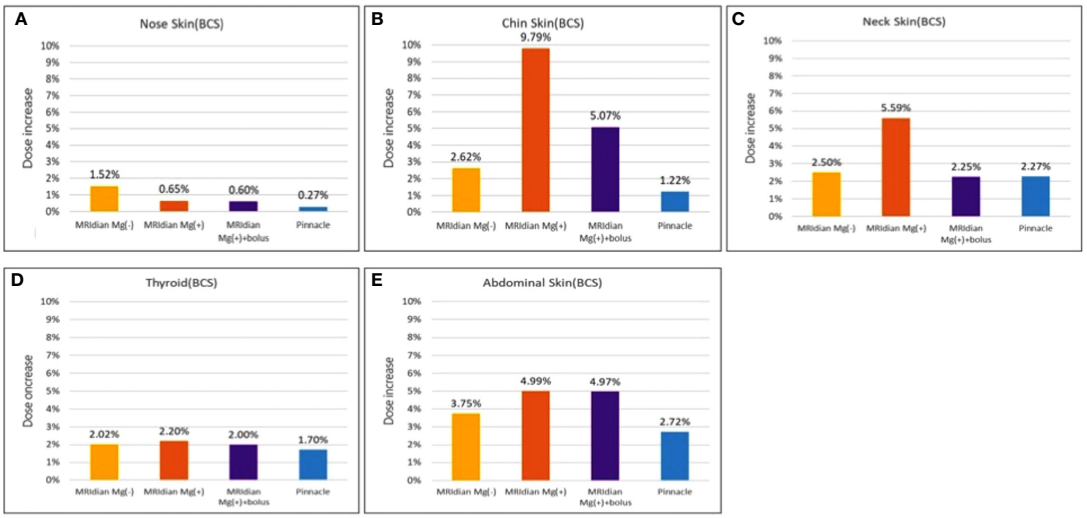

FIGURE 8
The percentage of the redundant doses to the skin of **(A)** the nose, **(B)** the chin, **(C)** the neck, **(D)** the thyroid and **(E)** the abdomen; The dose increase in the skin of the chin **(B)** and the neck **(C)** are the most prominent in breast-conserving surgery (BCS) RANDO model: 9.79% of the prescription dose and 5.59% of the prescription dose, respectively. When adding 1-cm bolus, the redundant doses dropped from 9.79% to 5.07% and from 5.59% to 2.25% in the chin **(B)** and neck **(C)**, respectively. The abdominal skin **(E)** was not affected by the bolus since the bolus covered only the chin and neck.

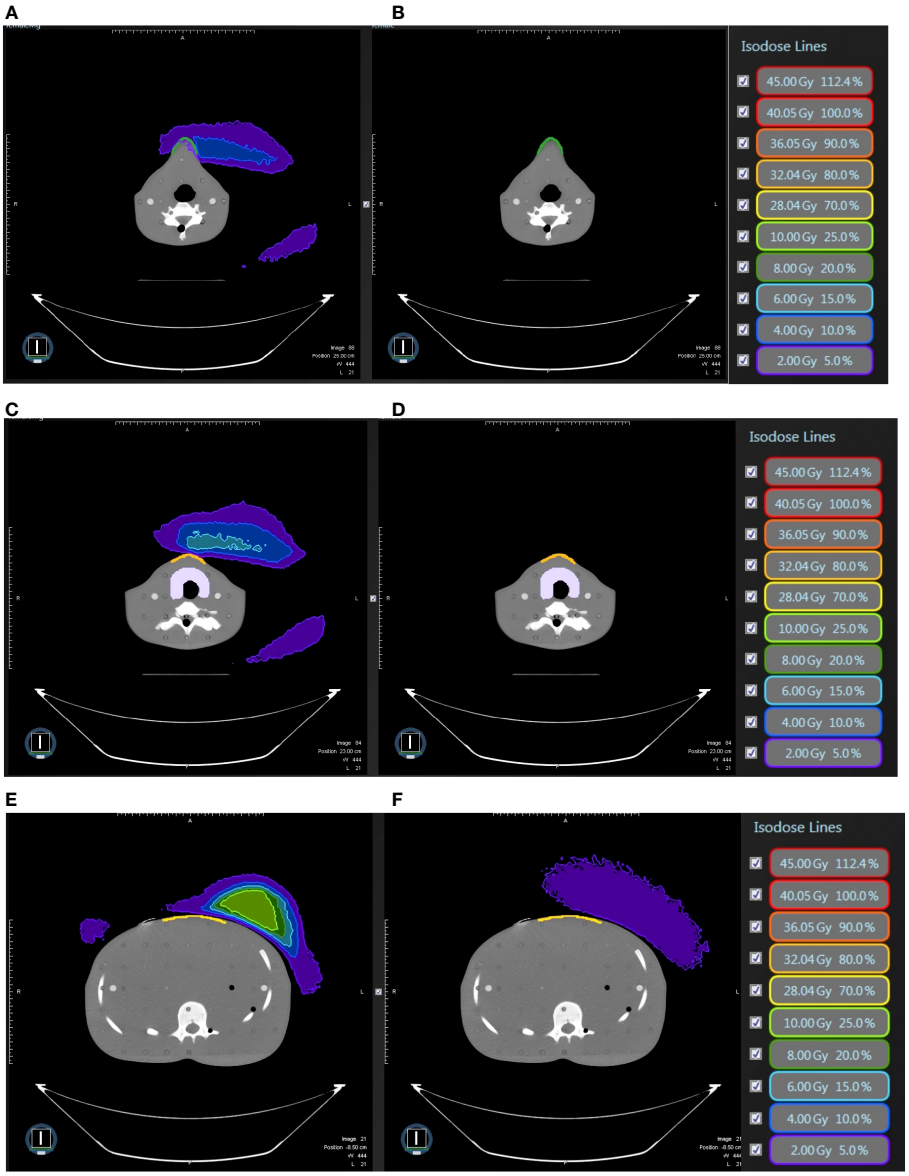

FIGURE 9
In breast-conserving surgery model, **(A)** the isodose curves deviate toward the chin as compared to **(B)** without magnetic field 0.35T; the dose distribution in the air near the neck with 0.35T **(C)** without 0.35T **(D)** and near the abdominal skin with 0.35T **(E)** and without 0.35T **(F)**. The bolus effectively avoided redundant doses.

important factors to predict radiation-induced dermatitis higher than grade 1 (45). Another study reported the volume of skin receiving a dose >35 Gy (SKIN_V35) to be one of the most significant dosimetric predictors associated with >50% probability of radiation-induced dermatitis 2+ toxicity (46). A study working on models for normal tissue complication probability reported that on multivariate analysis, the most predictive model of acute radiation-induced skin toxicity severity was a two-variable model including the skin receiving ≥30 Gy and psoriasis [Rs = 0.32, AUC = 0.84, $p < 0.001$] (47). Though the skin dose observed in the present study were relatively small, optimal MRgRT should be tailored according to diverse body shapes in each individual in order to reach precision medicine. The role of post-operative radiotherapy has been strengthened by the overall survival benefit seen in breast cancer patients (4, 5). There is unmet and urgent need to improve current treatment outcomes.

MRgRT is the new quantum leap in radiation oncology. Many researchers have found that there are significant associations between unnecessary doses during radiotherapy and cardiac toxicity (10, 48). But the new concern from MRgRT may be the ESE generated with the existence of a magnetic field that work together to increase the unwanted dose (49). Our team proposes taking ESE into consideration in the assessment of clinical

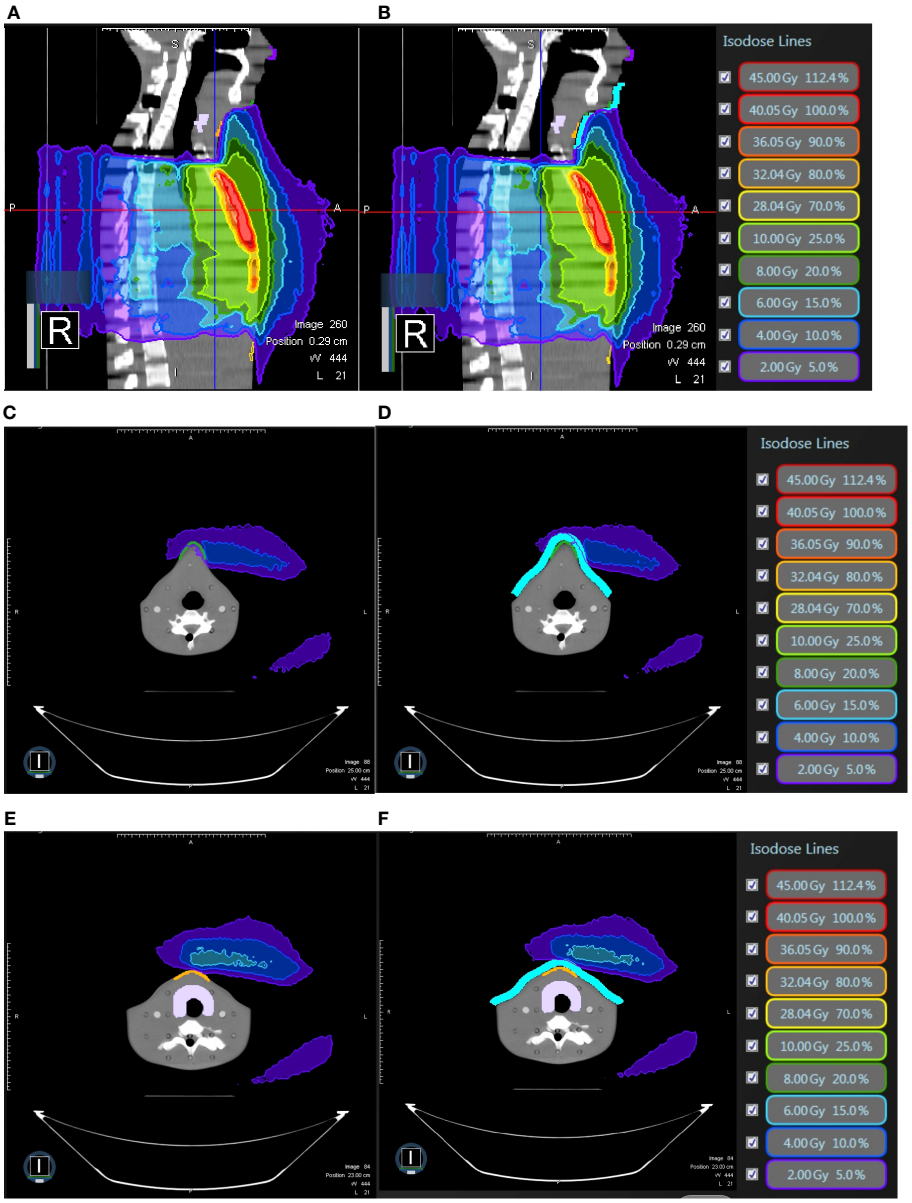

FIGURE 10
In breast-conserving surgery model, all under 0.35 T and **(A)** the isodose curves deviate toward the chin without bolus as compared to **(B)** with bolus in light blue; the dose distribution in the air near the chin without bolus **(C)** with bolus in light blue **(D)** and the neck skin without bolus **(E)** and with bolus in light blue **(F)**.

relevant complications including skin toxicity. Our previous studies demonstrated that IGRT improved acute skin toxicity with good long-term survival (32). The ultimate goal of this approach is to utilize IGRT in the most sophisticated form, namely, MRgRT, to provide more effective treatment strategies (49–51). We will design clinical trials from this aspect.

The drawbacks of this study include anthropomorphic phantoms limited to a single reference size, which may not be representative of the patient population of various body morphologies. This is a common downside of almost all dosimetric studies. Secondly, our work set out to create a method that could be used to avoid redundant doses from ESE, using 1-cm bolus has accomplished this partially, and not completely. Individually tailored radiotherapy in order to enhance accuracy and safety will minimize unintended exposures and low doses to peripheral organs. In the future, we aim to investigate the ESE effects of diverse patient sizes for better protection.

5 Conclusion

Our simulation study suggests that redundant doses from ESE during 0.35T MRgRT was more prominent in WBI for the

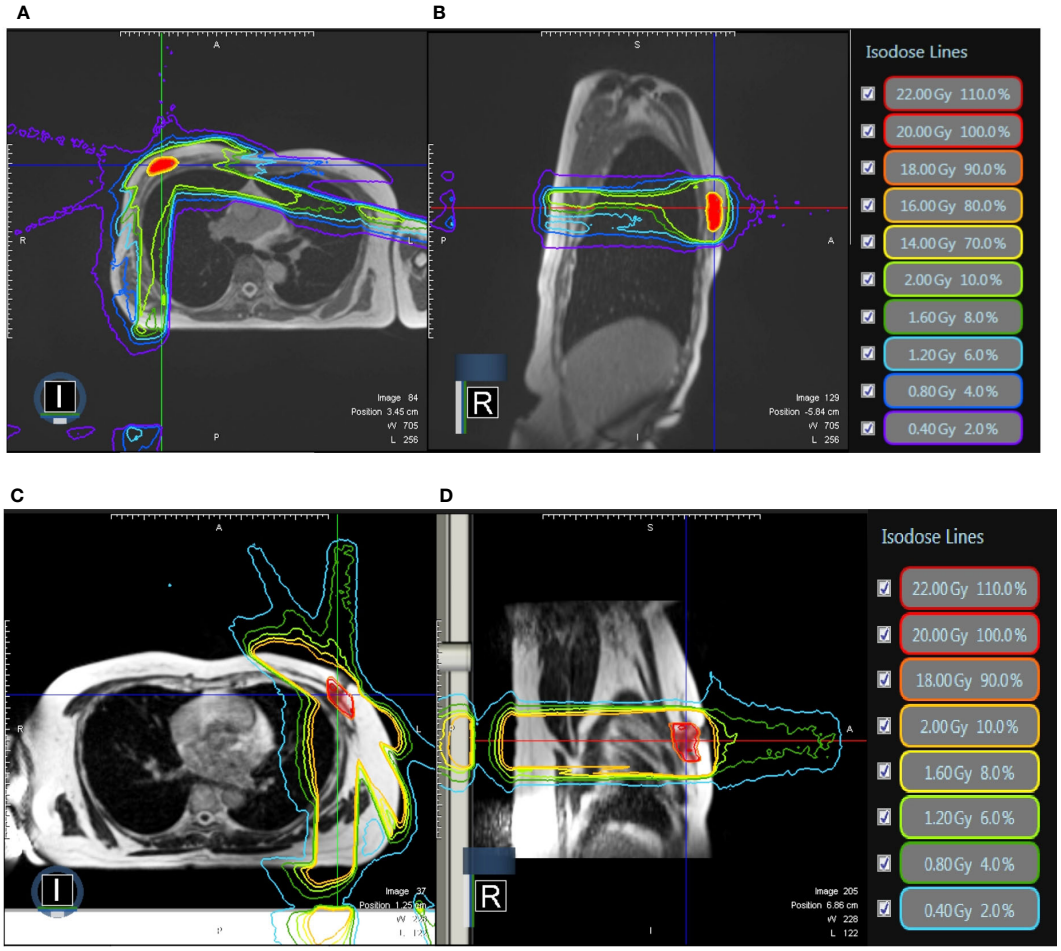

FIGURE 11
The isodose curves from two patients previously treated with a single shot of 20Gy. Both of them underwent breast-conserving surgery. **(A)** The axial view and **(B)** sagittal view of right breast cancer with a target volume of 4.4cc and **(C)** the axial view and **(D)** sagittal view of left breast cancer with a target volume of 11cc.

TABLE 4 Skin doses of 2 patient plans and the increase percentage of the presecription dose (20Gy/1fx).

	Partial breast irradiation (PBI) / Unit: Gray															
	Image A								Image B							
	MRIdian 0.35T (+)				MRIdian 0.35T (-)				MRIdian 0.35T (+)				MRIdian 0.35T (-)			
	Dmean	Dmin	Dmax		Dmean	Dmin	Dmax		Dmean	Dmin	Dmax		Dmean	Dmin	Dmax	
Chin Skin	0.01	0	0.03	0.15%	0.02	0.01	0.03	0.15%	#	#	#	#####	#	#	#	#####
Neck Skin	0.05	0.02	0.07	0.35%	0.04	0.02	0.07	0.35%	0.05	0.03	0.08	0.40%	0.05	0.02	0.1	0.50%
Abdominal Skin	0.13	0.08	0.18	0.90%	0.1	0.07	0.13	0.65%	0.16	0.11	0.22	1.10%	0.15	0.09	0.23	1.15%
Thyroid	0.06	0.04	0.09	0.45%	0.06	0.04	0.09	0.45%	0.11	0.06	0.16	0.80%	0.12	0.08	0.16	0.80%

# denotes that in Image B, there was no data for skin dose on the chin because this patient has not been scanned that high to include her chin.
(+) with.
(-) without.
#####, no data.

BCS model than that in the MRM model. Besides, ESE has minimal effect on PBI. The areas greatly under influence of 0.35T MRgRT for WBI include the chin, neck and the abdomen. Bolus with the thickness of 1cm covering the chin and neck can diminish 48.2% to 59.8% of the prescription dose. For the long term goal of breast cancer treatment, extending survival and setting our sights on a cancer-free life is imperative. In order to achieve the greatest benefit from MRgRT, doses to normal tissues in or out of field must be minimized. With the effect of ESE in mind, the workflows regarding dosimetry and medical physics will be optimized from installation and throughout the lifetime of this new technology.

Data availability statement

The original contributions presented in the study are included in the article/supplementary material. Further inquiries can be directed to the corresponding author.

Ethics statement

The studies involving human participants were reviewed and approved by Kaohsiung Medical University Hospital. The patients/participants provided their written informed consent to participate in this study.

Author contributions

H-HL and C-YW wrote the first draft of the manuscript, made the table, and contributed to image review and figure legends. S-TC, T-YL, and C-HC participated in treatment planning, dose calculation, and quality assurance. M-YH and C-JH conceived the methodology and supervised the experiment and revised the manuscript. All authors contributed to the article and approved the submitted version.

Funding

This work was supported financially by the Kaohsiung Medical University Hospital (KMUH111-1M54) in Taiwan. The funding source had no role in the study design; in the collection, the analysis or the interpretation of data; in the writing or the decision to submit the article for publication.

Conflict of interest

The authors declare that the research was conducted in the absence of any commercial or financial relationships that could be construed as a potential conflict of interest.

Publisher's note

References

1. Sung H, Ferlay J, Siegel RL, Laversanne M, Soerjomataram I, Jemal A, et al. Global cancer statistics 2020: GLOBOCAN estimates of incidence and mortality worldwide for 36 cancers in 185 countries. *CA Cancer J Clin* (2021) 71(3):209–49. doi: 10.3322/caac.21660

2. Arnold M, Morgan E, Rumgay H, Mafra A, Singh D, Laversanne M, et al. Current and future burden of breast cancer: global statistics for 2020 and 2040. *Breast* (2022) 66:15–23. doi: 10.1016/j.breast.2022.08.010

3. Stuart KE, Houssami N, Taylor R, Hayen A, Boyages J. Long-term outcomes of ductal carcinoma *in situ* of the breast: a systematic review, meta-analysis and meta-regression analysis. *BMC Cancer* (2015) 15:890. doi: 10.1186/s12885-015-1904-7

4. Polgár C, Kahán Z, Ivanov O, Chorváth M, Ligačová A, Csejtei A, et al. Radiotherapy of breast cancer-professional guideline 1st central-Eastern European professional consensus statement on breast cancer. *Pathol Oncol Res* (2022) 28:1610378. doi: 10.3389/pore.2022.1610378

5. Hennequin C, Belkacémi Y, Bourgier C, Cowen D, Cutuli B, Fourquet A, et al. Radiotherapy of breast cancer. *Cancer Radiother* (2022) 26(1-2):221–30. doi: 10.1016/j.canrad.2021.11.013

6. Yan D, Vicini F, Wong J, Martinez A. Adaptive radiation therapy. *Phys Med Biol* (1997) 42(1):123–32. doi: 10.1088/0031-9155/42/1/008

7. Parkes MJ, Green S, Stevens AM, Parveen S, Stephens R, Clutton-Brock TH. Reducing the within-patient variability of breathing for radiotherapy delivery in conscious, unsedated cancer patients using a mechanical ventilator. *Br J Radiol* (2016) 89(1062):20150741. doi: 10.1259/bjr.20150741

8. Harris EJ, Mukesh M, Jena R, Baker A, Bartelink H, Brooks C, et al. *Efficacy and mechanism evaluation. a multicentre observational study evaluating image-guided radiotherapy for more accurate partial-breast intensity-modulated radiotherapy: comparison with standard imaging technique.* Southampton (UK: NIHR Journals Library (2014).

9. Hoekstra N, Habraken S, Swaak-Kragten A, Hoogeman M, Pignol JP. Intrafraction motion during partial breast irradiation depends on treatment time. *Radiother Oncol* (2021) 159:176–82. doi: 10.1016/j.radonc.2021.03.029

10. Lemanski C, Thariat J, Ampil FL, Bose S, Vock J, Davis R, et al. Image-guided radiotherapy for cardiac sparing in patients with left-sided breast cancer. *Front Oncol* (2014) 4:257. doi: 10.3389/fonc.2014.00257

11. Liang JA, Lee PC, Ku CP, Chen WT, Chung CY, Kuo YC, et al. Effectiveness of image-guided radiotherapy in adjuvant radiotherapy on survival for localized breast cancer: a population-based analysis. *Cancer Manag Res* (2021) 13:3465–72. doi: 10.2147/CMAR.S299975

12. Pfeffer RM. Radiotherapy for breast cancer: curing the cancer while protecting the heart. *Isr Med Assoc J* (2018) 20(9):582–3.

13. Piruzan E, Vosoughi N, Mahdavi SR, Khalafi L, Mahani H. Target motion management in breast cancer radiation therapy. *Radiol Oncol* (2021) 55(4):393–408. doi: 10.2478/raon-2021-0040

14. Postma EL, van Hillegersberg R, Daniel BL, Merckel LG, Verkooijen HM, van den Bosch MA. MRI-Guided ablation of breast cancer: where do we stand today? *J Magn Reson Imaging* (2011) 34(2):254–61. doi: 10.1002/jmri.22599

15. Ricotti R, Miglietta E, Leonardi MC, Cattani F, Dicuonzo S, Rojas DP, et al. Workload of breast image-guided intensity-modulated radiotherapy delivered with TomoTherapy. *Tumori* (2020) 106(6):518–23. doi: 10.1177/0300891619868014

16. Van Limbergen E, Weltens C. New trends in radiotherapy for breast cancer. *Curr Opin Oncol* (2006) 18(6):555–62. doi: 10.1097/01.cco.0000245327.42281.9f

17. Yoo S, O'Daniel J, Blitzblau R, Yin FF, Horton JK. Accuracy and efficiency of image-guided radiation therapy (IGRT) for preoperative partial breast radiosurgery. *J Radiosurg SBRT* (2020) 6(4):295–301.

18. Charaghvandi RK, den Hartogh MD, van Ommen AM, de Vries WJ, Scholten V, Moerland MA, et al. MRI-Guided single fraction ablative radiotherapy for early-stage breast cancer: a brachytherapy versus volumetric modulated arc therapy dosimetry study. *Radiother Oncol* (2015) 117(3):477–82. doi: 10.1016/j.radonc.2015.09.023

19. Acharya S, Fischer-Valuck BW, Mazur TR, Curcuru A, Sona K, Kashani R, et al. Magnetic resonance image guided radiation therapy for external beam accelerated partial-breast irradiation: evaluation of delivered dose and intrafractional cavity motion. *Int J Radiat Oncol Biol Phys* (2016) 96(4):785–92. doi: 10.1016/j.ijrobp.2016.08.006

20. Henke LE, Contreras JA, Green OL, Cai B, Kim H, Roach MC, et al. Magnetic resonance image-guided radiotherapy (MRIgRT): a 4.5-year clinical experience. *Clin Oncol (R Coll Radiol)* (2018) 30(11):720–7. doi: 10.1016/j.clon.2018.08.010

21. Kumar S, Holloway L, Roach D, Pogson E, Veera J, Batumalai V, et al. The impact of a radiologist-led workshop on MRI target volume delineation for radiotherapy. *J Med Radiat Sci* (2018) 65(4):300–10. doi: 10.1002/jmrs.298

22. Guidolin K, Yaremko B, Lynn K, Gaede S, Kornecki A, Muscedere G, et al. Stereotactic image-guided neoadjuvant ablative single-dose radiation, then lumpectomy, for early breast cancer: the SIGNAL prospective single-arm trial of

single-dose radiation therapy. *Curr Oncol* (2019) 26(3):e334–e40. doi: 10.3747/co.26.4479

23. Whiteside L, McDaid L, Hales RB, Rodgers J, Dubec M, Huddart RA, et al. To see or not to see: evaluation of magnetic resonance imaging sequences for use in MR linac-based radiotherapy treatment. *J Med Imaging Radiat Sci* (2022) 53(3):362–73. doi: 10.1016/j.jmir.2022.06.005

24. Noel CE, Parikh PJ, Spencer CR, Green OL, Hu Y, Mutic S, et al. Comparison of onboard low-field magnetic resonance imaging versus onboard computed tomography for anatomy visualization in radiotherapy. *Acta Oncologica* (2015) 54(9):1474–82. doi: 10.3109/0284186X.2015.1062541

25. Chiloiro G, Boldrini L, Meldolesi E, Re A, Cellini F, Cusumano D, et al. MR-guided radiotherapy in rectal cancer: first clinical experience of an innovative technology. *Clin Trans Radiat Oncol* (2019) 18:80–6. doi: 10.1016/j.ctro.2019.04.006

26. Raaijmakers AJ, Raaymakers BW, van der Meer S, Lagendijk JJ. Integrating a MRI scanner with a 6 MV radiotherapy accelerator: impact of the surface orientation on the entrance and exit dose due to the transverse magnetic field. *Phys Med Biol* (2007) 52(4):929–39. doi: 10.1088/0031-9155/52/4/005

27. Nachbar M, Mönnich D, Boeke S, Gani C, Weidner N, Heinrich V, et al. Partial breast irradiation with the 1.5 T MR-linac: first patient treatment and analysis of electron return and stream effects. *Radiother Oncol* (2020) 145:30–5. doi: 10.1016/j.radonc.2019.11.025

28. Malkov VN, Hackett SL, van Asselen B, Raaymakers BW, Wolthaus JWH. Monte Carlo Simulations of out-of-field skin dose due to spiralling contaminant electrons in a perpendicular magnetic field. *Med Phys* (2019) 46(3):1467–77. doi: 10.1002/mp.13392

29. Eekers DB, In 't Ven L, Roelofs E, Postma A, Alapetite C, Burnet NG, et al. The EPTN consensus-based atlas for CT- and MR-based contouring in neuro-oncology. *Radiother Oncol* (2018) 128(1):37–43. doi: 10.1016/j.radonc.2017.12.013

30. Lee H-H, Hou M-F, Wei S-Y, Lin S-D, Luo K-H, Huang M-Y, et al. Comparison of long-term outcomes of postmastectomy radiotherapy between breast cancer patients with and without immediate flap reconstruction. *PloS One* (2016) 11(2):e0148318. doi: 10.1371/journal.pone.0148318

31. Lee H-H, Hou M-F, Chuang H-Y, Huang M-Y, Tsuei L-P, Chen F-M, et al. Intensity modulated radiotherapy with simultaneous integrated boost vs. conventional radiotherapy with sequential boost for breast cancer – a preliminary result. *Breast* (2015) 24(5):656–60. doi: 10.1016/j.breast.2015.08.002

32. Lee H-H, Chen C-H, Luo K-H, Chuang H-Y, Huang C-J, Cheng Y-K, et al. Five-year survival outcomes of intensity-modulated radiotherapy with simultaneous integrated boost (IMRT-SIB) using forward IMRT or tomotherapy for breast cancer. *Sci Rep* (2020) 10(1):4342. doi: 10.1038/s41598-020-61403-6

33. Grantzau T, Overgaard J. Risk of second non-breast cancer after radiotherapy for breast cancer: a systematic review and meta-analysis of 762,468 patients. *Radiother Oncol* (2015) 114(1):56–65. doi: 10.1016/j.radonc.2014.10.004

34. White EA, Cho J, Vallis KA, Sharpe MB, Lee G, Blackburn H, et al. Cone beam computed tomography guidance for setup of patients receiving accelerated partial breast irradiation. *Int J Radiat Oncol Biol Phys* (2007) 68(2):547–54. doi: 10.1016/j.ijrobp.2007.01.048

35. Van Heijst TC, Den Hartogh MD, Lagendijk JJ, van den Bongard HD, Van Asselen B. MR-guided breast radiotherapy: feasibility and magnetic-field impact on skin dose. *Phys Med Biol* (2013) 58(17):5917. doi: 10.1088/0031-9155/58/17/5917

36. Sahin B, Zoto Mustafayev T, Gungor G, Aydin G, Yapici B, Atalar B, et al. First 500 fractions delivered with a magnetic resonance-guided radiotherapy system: initial experience. *Cureus* (2019) 11(12):e6457. doi: 10.7759/cureus.6457

37. Groot Koerkamp ML, Vasmel JE, Russell NS, Shaitelman SF, Anandadas CN, Currey A, et al. Optimizing MR-guided radiotherapy for breast cancer patients. *Front Oncol* (2020) 10:1107. doi: 10.3389/fonc.2020.01107

38. An HJ, Kim JI, Park JM. Electron streams in air during magnetic-resonance image-guided radiation therapy. *PloS One* (2019) 14(5):e0216965. doi: 10.1371/journal.pone.0216965

39. Park JM, Shin KH, J-i K, Park S-Y, SH J, Choi N, et al. Air–electron stream interactions during magnetic resonance IGRT. *Strahlentherapie und Onkologie* (2018) 194(1):50–9. doi: 10.1007/s00066-017-1212-z

40. Jeon SH, Shin KH, Park SY, Kim JI, Park JM, Kim JH, et al. Seroma change during magnetic resonance imaging-guided partial breast irradiation and its clinical implications. *Radiat Oncol* (2017) 12(1):103. doi: 10.1186/s13014-017-0843-7

41. Fischer-Valuck BW, Henke L, Green O, Kashani R, Acharya S, Bradley JD, et al. Two-and-a-half-year clinical experience with the world's first magnetic resonance image guided radiation therapy system. *Adv Radiat Oncol* (2017) 2(3):485–93. doi: 10.1016/j.adro.2017.05.006

42. Kim J-i, Park S-Y, Lee Y, Shin K, Wu H-G, Park JM. Effect of low magnetic field on dose distribution in the partial-breast irradiation. *Prog Med Physics* (2015) 26:208. doi: 10.14316/pmp.2015.26.4.208

43. Verkooijen HM, Henke LE. Sensible introduction of MR-guided radiotherapy: a warm plea for the RCT. *Front Oncol* (2021) 11(872). doi: 10.3389/fonc.2021.652889

44. Liu H, Ding S, Wang B, Li Y, Sun Y, Huang X. In-air electron streaming effect for esophageal cancer radiotherapy with a 1.5 T perpendicular magnetic field: a treatment planning study. *Front Oncol* (2020) 10:607061. doi: 10.3389/fonc.2020.607061

45. Feng H, Wang H, Xu L, Ren Y, Ni Q, Yang Z, et al. Prediction of radiation-induced acute skin toxicity in breast cancer patients using data encapsulation screening and dose-gradient-based multi-region radiomics technique: a multicenter study. *Front Oncol* (2022) 12. doi: 10.3389/fonc.2022.1017435

46. Lee T-F, Sung K-C, Chao P-J, Huang Y-J, Lan J-H, Wu H-Y, et al. Relationships among patient characteristics, irradiation treatment planning parameters, and treatment toxicity of acute radiation dermatitis after breast hybrid intensity modulation radiation therapy. *PloS One* (2018) 13(7):e0200192. doi: 10.1371/journal.pone.0200192

47. Pastore F, Conson M, D'Avino V, Palma G, Liuzzi R, Solla R, et al. Dose-surface analysis for prediction of severe acute radio-induced skin toxicity in breast cancer patients. *Acta Oncol* (2016) 55(4):466–73. doi: 10.3109/0284186X.2015.1110253

48. Crockett CB, Samson P, Chuter R, Dubec M, Faivre-Finn C, Green OL, et al. Initial clinical experience of MR-guided radiotherapy for non-small cell lung cancer. *Front Oncol* (2021) 11:617681. doi: 10.3389/fonc.2021.617681

49. Park JM, Shin KH, Kim JI, Park SY, Jeon SH, Choi N, et al. Air-electron stream interactions during magnetic resonance IGRT : skin irradiation outside the treatment field during accelerated partial breast irradiation. *Strahlenther Onkol* (2018) 194(1):50–9. doi: 10.1007/s00066-017-1212-z

50. De-Colle C, Nachbar M, Mönnich D, Boeke S, Gani C, Weidner N, et al. Analysis of the electron-stream effect in patients treated with partial breast irradiation using the 1.5 T MR-linear accelerator. *Clin Transl Radiat Oncol* (2021) 27:103–8. doi: 10.1016/j.ctro.2020.12.005

51. Berlangieri A, Elliott S, Wasiak J, Chao M, Foroudi F. Use of magnetic resonance image-guided radiotherapy for breast cancer: a scoping review. *J Med Radiat Sci* (2022) 69(1):122–33. doi: 10.1002/jmrs.545

frontiers | Frontiers in Oncology

TYPE Case Report
PUBLISHED 27 July 2023
DOI 10.3389/fonc.2023.1132178

OPEN ACCESS

EDITED BY
Tsair-Fwu Lee,
National Kaohsiung University of Science and Technology, Taiwan

REVIEWED BY
Anna L. Petoukhova,
Haaglanden Medical Center, Netherlands
Meryem Aktan,
Necmettin Erbakan University, Türkiye
Itzhak Orion,
Ben-Gurion University of the Negev, Israel

*CORRESPONDENCE
Chin-Cheng Chen
chen.ccc@gmail.com

†These authors have contributed equally to this work

RECEIVED 27 December 2022
ACCEPTED 21 June 2023
PUBLISHED 27 July 2023

CITATION
Chen CC, Liu J, Park P, Shim A, Huang S, Wong S, Tsai P, Lin H and Choi JI (2023) Case Report: Cumulative proton dose reconstruction using CBCT-based synthetic CT for interfraction metallic port variability in breast tissue expanders. *Front. Oncol.* 13:1132178. doi: 10.3389/fonc.2023.1132178

Case Report: Cumulative proton dose reconstruction using CBCT-based synthetic CT for interfraction metallic port variability in breast tissue expanders

Chin-Cheng Chen[1,2*†], Jiayi Liu[1†], Peter Park[1], Andy Shim[1], Sheng Huang[1], Sarah Wong[1], Pingfang Tsai[1], Haibo Lin[1,3,4] and J. Isabelle Choi[1,3]

[1]New York Proton Center, New York, NY, United States, [2]Institute of Nuclear Engineering and Science, National Tsing Hua University, Hsinchu, Taiwan, [3]Memorial Sloan-Kettering Cancer Center, New York, NY, United States, [4]Department of Radiation Oncology, Montefiore Medical Center and Albert Einstein College of Medicine, Bronx, NY, United States

Introduction: Dose perturbation of spot-scanning proton beams passing through a dislocated metallic port (MP) of a breast tissue expander may degrade target dose coverage or deliver excess dose to the ipsilateral lung and heart. The feasibility of utilizing daily cone-beam computed tomography (CBCT)–based synthetic CTs (synCTs) for dose reconstruction was evaluated, and the fractional and cumulative dosimetric impact due to daily MP dislocation is reported.

Methods: The synCT was generated by deforming the simulation CT to daily CBCT. The MP structure template was mapped onto all CTs on the basis of daily MP position. Proton treatment plans were generated with two and three fields on the planned CT (pCT, Plan A) and the first verification CT (vCT, Plan B), respectively, for a fractional dose of 1.8 Gy(RBE). Plan A and Plan B were used alternatively, as determined by the daily MP position. The reconstructed fractional doses were calculated with corresponding plans and synCTs, and the cumulative doses were summed with the rigid or deformed fractional doses on pCT and vCT.

Results: The planned and reconstructed fractional dose demonstrated a low-dose socket around the planned MP position due to the use of field-specific targets (FSTs). Dose hot spots with >120% of the prescription due to MP dislocation were found behind the planned MP position on most reconstructed fractional doses. The reconstructed cumulative dose shows two low-dose sockets around the two planned MP positions reflecting the two plans used. The doses at the hot spots behind the planned MPs averaged out to 114% of the prescription. The cumulative $D_{95\%}$ of the CTV_Chest Wall decreased by up to 2.4% and 4.0%, and the cumulative $V_{20Gy(RBE)}$ of the left lung decreased to 16.1% and 16.8% on pCT and vCT, respectively. The cumulative D_{mean} of the heart

decreased to as low as 0.7 Gy(RBE) on pCT but increased to as high as 1.6 Gy (RBE) on vCT.

Conclusion: The robustness of proton plans using FSTs around the magnet in the MP of the tissue expander can be improved by applying multiple fields and plans, which provides forgiveness of dose heterogeneity incurred from dislocation of high-Z materials in this single case.

KEYWORDS

proton, tissue expander, CBCT-based synthetic CT, breast cancer, dose reconstruction and dosimetric impact

Introduction

Proton therapy used for breast cancer treatments is becoming more prevalent as access to proton centers increases globally (1). The *en face* beams used in most proton treatment plans for breast cancers provide a homogeneous and conformal dose to the clinical target volume (CTV) while sparing the heart and lung beyond the sharp dose falloff at Bragg peaks. Patients with breast cancer with tissue expanders who have undergone mastectomy with plan for two-stage reconstruction could be also treated with proton beams (2–6). In this approach, a saline-filled tissue expander with an embedded metallic port (MP) for fluid injection is placed at the time of mastectomy. The MP is usually constructed of a magnet enclosed in a metal case that acts as a needle guard (3).

Different planning techniques for patients with breast cancer with tissue expanders using spot-scanning proton beams have been reported (2–6). Spot-scanning proton beams can be used to shoot through the MP in the tissue expander with accurate Monte Carlo dose calculation (2) or pencil-beam convolution algorithm with well modeled and validated geometries and materials of MP (3). Spot-scanning proton beams can also be used to shoot around the MP in tissue expanders (4–7). Kirk et al. (4) and Zhu et al. (5) reported on the application of field-specific targets (FSTs) to avoid spot placements inside and beyond the MP. Two to three proton fields are used in either technique to achieve a proton treatment plan with maximal robustness.

The MP in the tissue expander requires careful delineation on computed tomography (CT) images, and the stopping power of the MP materials should be assigned accurately. Although metal artifact reduction algorithms can be used to reduce artifacts significantly, streak artifact caused by the magnet remains visible. Fortunately, both the physical geometries and materials of the MP can be provided by major manufacturers. A template of the MP can be constructed on the basis of manufacturer's specifications and mapped on patients' CT images. MP displacement during treatment should also be considered. Mutter et al. reported that MP location is within a 1-cm difference from the planned CT (pCT) position for >95% of treatment fractions and that the dosimetric impact was clinically acceptable considering both CTV coverage and normal tissue (heart and ipsilateral lung) sparing with a 1-cm offset in the worst-case scenarios (2). However, the dosimetric impact of MP dislocations larger than 1 cm from its planned position is rarely reported in publications. Dose delivery of proton beams passing through a dislocated MP may either degrade target dose coverage or overdose the ipsilateral lung and heart.

A left-sided postmastectomy patient with Allergan Natrelle® 133 tissue expander (Allergan, Inc., Dublin, Ireland) was planned with a two-field beam arrangement with FSTs (Plan A) around the MP for a prescription of 50.4 Gy(RBE) in 28 fractions. The MP was found dislocated on the first day of treatment, and a verification CT (vCT) scan was performed for plan revision (Plan B). However, the MP on subsequent fractions was found to be relocated daily with more than 5-mm displacements compared with the planned positions of either Plan A or Plan B. The patient was then treated with Plan A or Plan B alternatively, as determined by the daily MP position shown on X-ray images, which left the daily and cumulative doses unknown due to the daily variations in the MP position.

Veiga et al. first proposed the "dose of the day" reconstruction using CT–to–cone-beam CT (CBCT) for head and neck patients treated with photon intensity modulated radiation therapy by deforming a pCT to match a daily CBCT (7). They later demonstrated the proton dose calculation on virtual CT by deforming the pCT onto the daily CBCT for adaptive proton therapy of lung cancer, in which the virtual CT was also corrected for anatomy change such as pleural effusion and tumor regression (8). The daily CBCTs of the breast patient could represent the real-time position and the anatomy change including the MP dislocation during daily treatments. The deformed reference CT onto the daily CBCT, or CBCT-based synthetic CT (synCT), with manual correction of the MP position, can be used for daily and cumulative dose reconstruction.

In this study, the feasibility of utilizing daily CBCT-based synCTs for proton dose reconstructions was evaluated. The CBCT-based synCTs for 28 fractions were generated with the dislocated MP. The reconstructed fractional doses were calculated with corresponding plans and synCTs, and the cumulative doses were summed with rigid or deformed fraction doses to evaluate the dosimetric impact due to daily MP dislocations.

Methods

Patient selection

A 33-year-old female patient diagnosed with left breast cancer, clinical stage T2N0, underwent bilateral mastectomy with immediate tissue expander (Natrelle® Allergan 133) reconstruction, with surgical pathology demonstrating pathologic stage T2N1 disease (2.4-cm primary tumor, 2/4 involved sentinel lymph nodes), grade 3; with lymphovascular invasion, estrogen receptor positive, progesterone receptor positive, and human epidermal growth factor receptor 2 (HER-2) negative; and with negative surgical margins. She received spot-scanning proton therapy for her adjuvant radiation therapy with a prescription of 50.4 Gy(RBE) in 28 fractions to the left reconstructed chest wall and comprehensive regional lymph nodes. This retrospective study is approved (NYPC ERC# 2020-026) by the Western Institutional Review Board, Inc. (Puyallup, WA, USA).

Simulated Planned CT and verification CT

The patient was positioned head-first supine, with head turned to the right and both arms placed above the head, immobilized with VacQfix™ Vacuum Cushions (Qfix, Avondale, PA, USA). The pCT was acquired 2 weeks prior to the first patient treatment, and the vCT was acquired on the first day of patient treatment with the same patient set up when the MP was found dislocated. Both pCT and vCT were acquired by SIEMENS SOMATOM Definition Edge CT scanner (Siemens Healthcare GmbH, Germany) with slice thickness of 2 mm in a scanning range from bottom of orbits to L2 spine.

CBCT-based synthetic CT

The CBCT-based synCT was generated in the Velocity™ Oncology Imaging Informatics System (Varian Medical Systems, Palo Alto, CA, USA) by deforming either the pCT or vCT to daily CBCT. Limited by the field-of-view (FOV) of the image panel used, only 20 cm length in patient's superior-to-inferior direction around the treatment isocenter of the pCT and vCT can be deformed to CBCT. The CTs combining the CBCT-based synCTs in the FOV and the reference CTs outside the FOVs were then used for dose reconstruction.

Metallic port template inserted on CTs

An MP structure template including the magnet and metal case as the needle guard on high-resolution CT images was delineated on the basis of the manufacturer's specifications and is used in our clinics routinely for patients with breast cancer with Natrelle® Allergan 133 tissue expander. The MP structure template on a high-resolution CT image is shown in Figure 1. The magnet in the Natrelle® 133 is Samarium Cobalt alloy with a mass density of 8.4 g/cm^3 per manufacturer, which is identical with the mass density of brass. The relative linear stopping power (RLSP) of the brass is 5.71, which is also close to the RLSP of 5.5 measured by the Mayo group (2). A Hounsfield unit (HU) of 9,316 was assigned to the magnet using our institutional calibration curve, converting the HU to RSLP. The needle guard encapsulating the magnet is made by titanium alloy with an RLSP of 3.17, and a HU of 4,540 was assigned. The water-equivalent thickness (WET) of the magnet and base of the needle guard are 13.8 mm and 3.17 mm respectively. The outline of saline-filled tissue expander was also contoured, and the HU of saline inside the tissue expander was overridden with the RLSP of 1.0. The MP structure was copied onto all CTs (pCT, vCT, and CBCT-based synCT) after the templated CT was rigid registered with the target CT images.

Treatment plans

The CTV was delineated using the RadComp contouring atlas and included the left chest wall and regional nodes (axilla, internal mammary, and supraclavicular nodes) (9). The proton spot-scanning treatment plans were generated with two (G0° and G45°) and three (G0°, G25°, and G50°) fields on the pCT (Plan A) and the first vCT (Plan B), respectively, for the fractional dose of 1.8 Gy(RBE) using Eclipse treatment planning system (TPS) (Varian Medical System, Palo Alto, CA, USA, version 15.6). Additional fields and different gantry angles were used in Plan B to improve the overall robustness of Plan A (a total four different gantry angles using five different FSTs). Figure 1 shows the FSTs with 5-mm geometrical margin from the magnet to avoid heavily weighted protons passing through the high-Z material in Plan B. The FSTs were also expanded with a 5-mm geometrical margin outwardly and cropped the patient body. It allows some spots placed at the peripheral dose falloff around the CTV and provides more flexibility for the optimizer to avoid hot spots at the edge of CTV. Another 1 mm in WET was applied in the axial margin at the distal end of all FSTs, which serves the same purpose to avoid the dose spike at the distal end of the spread-out Bragg peaks, especially at the rib cage. The FSTs for larger gantry angles such as 45° (Plan A) and 50° (Plan B) were cropped superiorly to avoid the proton beam shooting through the left arm. Both Plan A and Plan B were generated with multi-field optimization and robust optimization with ±5-mm setup and ±3.5% range uncertainties. As determined by the daily position of the MP, the patient received 17 fractions from Plan A and 11 fractions from Plan B.

Patient treatments and dose reconstructions

The patient was treated with either Plan A or Plan B, as determined by the MP positions on 2D kilovolt (kV) images taken prior to the CBCT. The fractional doses were forward calculated with Plan A (17 fractional doses) or Plan B (11 fractional doses) on the CBCT-based synCT generated using pCT or vCT correspondingly. The cumulative doses were generated with

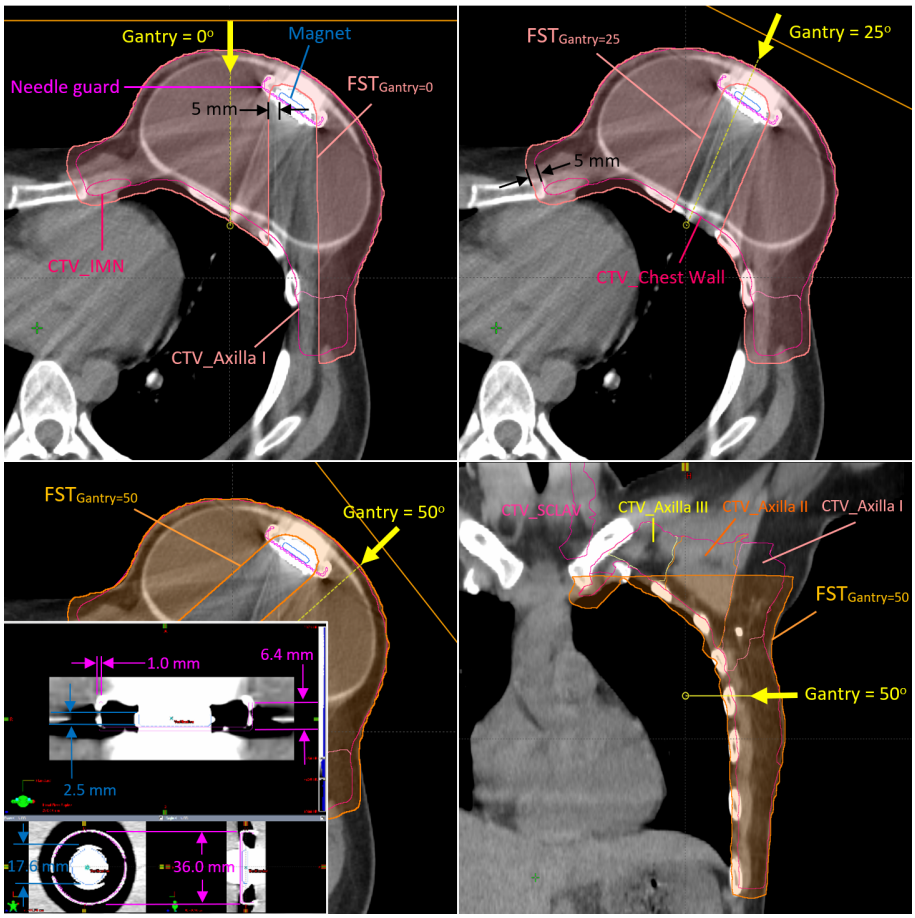

FIGURE 1
Clinical target volumes (CTVs) and the field-specific targets used for the fields at gantry angles of 0°, 25°, and 45° in Plan B The metallic port template in high-resolution CT image is also shown at the left-bottom corner of the figure.

rigid or deformable dose sum. The rigid dose sum was the direct sum of the reconstructed fractional doses using daily CBCT registration vector in Eclipse TPS. The rigid dose sum was then projected on either pCT or vCT for further evaluation. All reconstructed fractional doses were also deformed onto pCT and vCT using MIM Software (version 7.2.7, MIM Software, Inc., OH), respectively. The deformed fractional doses were then summed as the cumulative doses on pCT and vCT.

Results

Fractional doses

Figure 2 shows the planned MP contours projected on the kV X-ray and CBCT images with the displaced MP on 19 July 2021 when the patient was treated with Plan A and the reconstructed fractional dose on the synCT. The MP artifact shown at Z = 13.0 cm could not be removed when the pCT was deformed to CBCT. Consequently, the artifact around and including the planned MP with high HU was then assigned as saline (RLSP = 1.0) in the forward calculation. The treated MP inserted as described in Methods and shown at Z = 11.0 cm and X = 7.9 cm in Figure 2 was calculated. The low-dose socket around the planned MP due to the use of FSTs is distorted slightly, and the protons at the edge of FSTs around the planned MP were over-ranged due to the absence of the MP from its planned position. A significant dose hot spot of 220.9 cGy(RBE) (123% of the prescribed fractional dose) was found close to the rib cage (Z = 13.0 cm). The displaced MP at Z = 11.0 cm moved into FSTs and pulled back the proton ranges, which caused some small cold spots [yellow circle for doses <180 cGy(RBE)] inside the CTV. In addition to the MP displacement, the shape of the tissue expander changed slightly, and some setup discrepancies were found at the discontinuity of the limited synCT FOV edge. Consequently, small cold spots (<100% of the prescribed fractional dose) were found in the superior and inferior part of the CTV.

Cumulative doses

Figure 3 shows the reconstructed cumulative doses as the sum of deformed fractional doses on pCT. The low-dose socket on

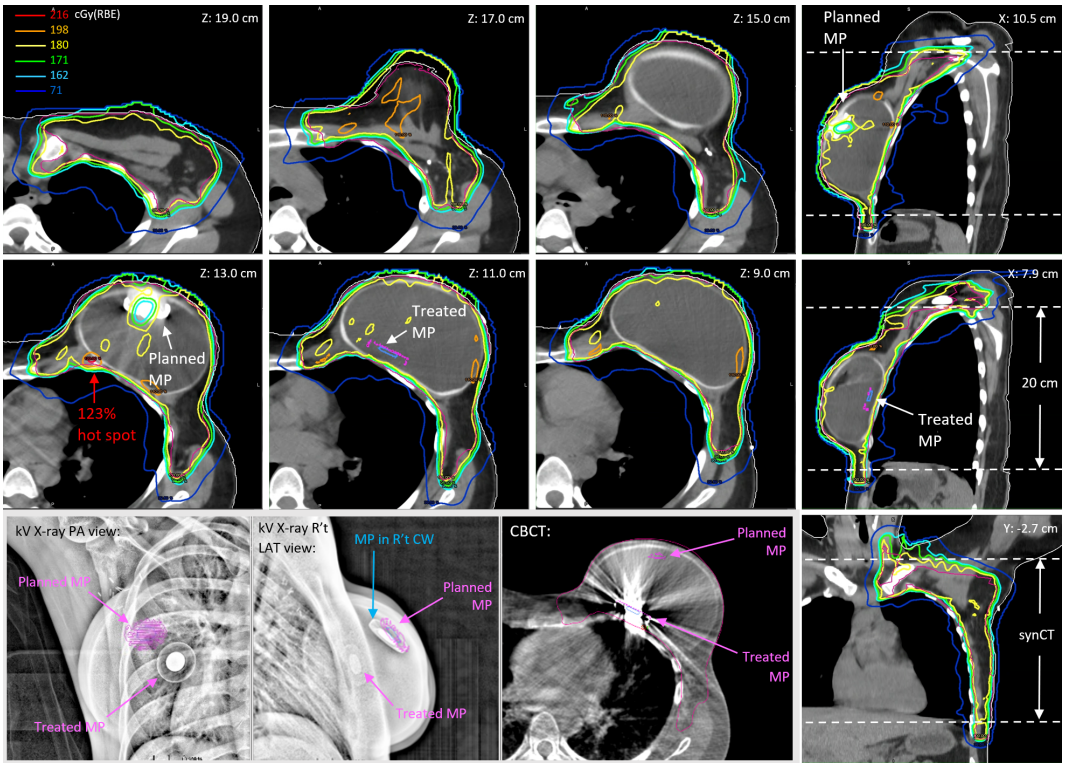

FIGURE 2
The reconstructed fractional doses on the day of 19 July 2021 for a prescription of 180 cGy(RBE) per fraction. The kV X-ray images and CBCT show the dislocation of the treated MP versus the planned MP.

fractional dose maintained when the MP moved away from the planned positions. Consequently, there were two low-dose sockets around the two planned MP positions on the reconstructed cumulative doses (Z = 13.0 cm and Z = 8.4 cm). Hot spots due to the absence of planned MP on fractional doses were also averaged out because of the two planned MP positions in the cumulative doses. The 114% global hot spot was found at Z = 13.0 cm behind the planned MP position in Plan A, in which 17 of the 28 fractions were used.

The dose–volume histogram metrics of planned and reconstructed cumulative doses on pCT and vCT are listed in Table 1. The cumulative $D_{95\%}$ of the CTV_Chest Wall decreased by up to 2.4% (rigid) and 4.0% (deformed) on pCT and vCT, respectively, from 98.8% in the nominal plans, due to the two low-dose sockets in two plans. The low-dose sockets were around the planned magnets and inside the tissue expander where no tumor cells were involved. As mentioned in the reconstructed fractional doses, the MP moved into the FSTs and then pulled back the proton ranges, which also pulled back the 20 Gy(RBE) isodose lines in the left lung. The relative volume of the left lung receiving at least 20 Gy (RBE) decreased by 3%–4% in reconstructed cumulative doses. The $V_{20Gy(RBE)}$ of left lung were to 16.1% (deformed) and 16.8% (rigid) on pCT and vCT, respectively, compared with 19.8% and 19.4% in the planned doses. The cumulative D_{mean} of the heart decreased to as low as 0.7 Gy(RBE) on pCT but increased to as high as 1.6 Gy (RBE) on vCT when the rigid plan sums were considered.

Discussion

Dose reconstruction using daily CBCT-based synCTs was demonstrated in this study. The synCT is the deformation of the referenced CT on to the daily CBCT with on-line image registration, which represents the most realistic patient setup during beam delivery.

The high-Z materials and resultant artifacts with high HU values on the referenced CT (pCT and vCT) cannot be deformed correctly onto daily CBCT. Consequently, the planned MP and artifact on synCT require removal by assigning appropriate RLSPs, and the MP structure template had to be manually inserted onto the synCT based on the daily MP location on CBCT as shown on Figure 2 (Z = 11.0 cm). The MP template insertion was the most time-consuming step. All the structure delineations and HU overrides were checked carefully before forward calculating the fractional doses.

Because of the physical limitation of the image panels on the treatment nozzle, only 20-cm FOV can be acquired in a single scan of CBCT. The treatment isocenter is selected as the geometrical isocenter of the whole CTV (chest wall and all regional nodes) in our current practice, and the FOV captures majority of CTV_Chest Wall, where the tissue expander is located. A small part of the regional node CTVs and inferior lungs were missed on the CBCT as shown in Figure 2 (coronal view). The reconstructed fractional doses in the missed regions would be identical with the planned

10.3389/fonc.2023.1132178

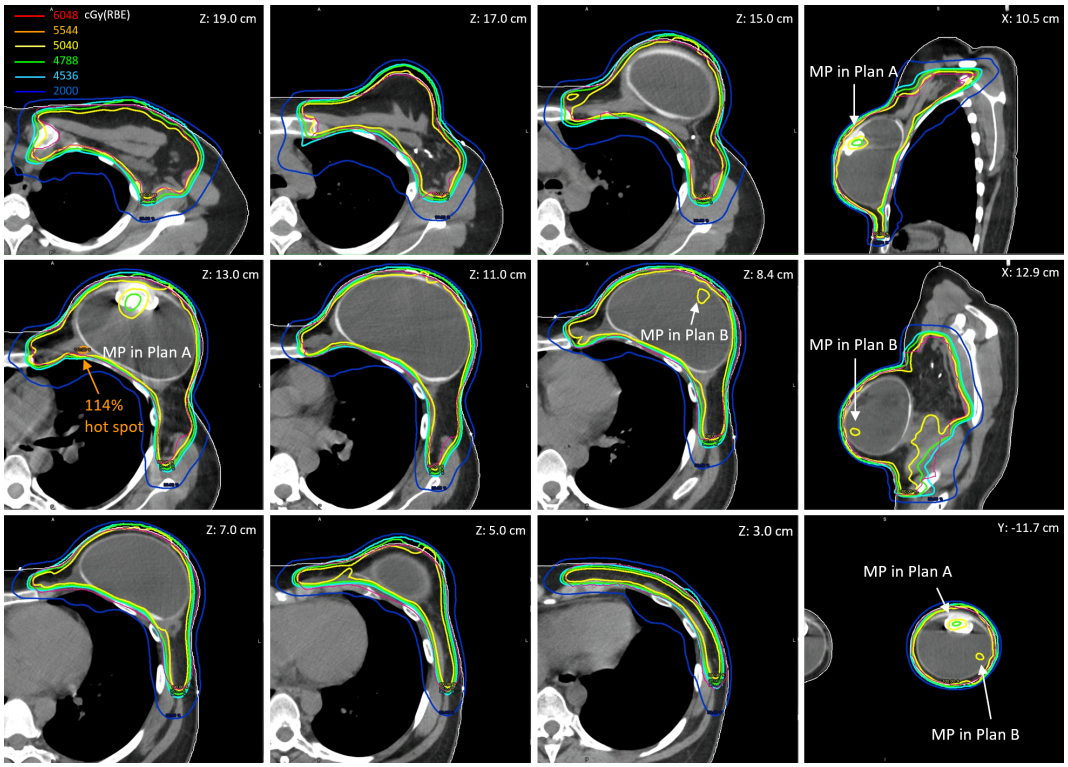

FIGURE 3
The reconstructed cumulative doses as the sum of deformed fractional doses (17 fractions from Plan A and 11 fractions from Plan B) on pCT.

doses and thus underestimate the dosimetric impact of patient setup in dose delivery.

The reconstructed fractional dose shows the most realistic daily dose delivery but in a single fraction. The $D_{95\%}$ of the CTV_Chest Wall ranged from 90.5% to 97.6% with an average of 95.5% for 28 fractions. The highest heart mean dose [equivalent to 1.43 Gy(RBE) with 28 fractions] was found on the very first day of patient treatment when the MP was found displaced and the revised plan (Plan B) was not ready. The $V_{71cGy(RBE)}$ of left lung [equivalent to $V_{20Gy(RBE)}$ with 28 fractions] could be as low as 12.9% or as high as 20.8% with an

TABLE 1 Comparisons of dose metrics of the planned and reconstructed (rigid or deformed) cumulative doses.

Structure	Dose Metric	Dose on pCT			Dose on vCT		
		Planned	Rigid	Deformed	Planned	Rigid	Deformed
CTV_50.4	$D_{95\%}$ (%)	99.2	96.3	96.7	99.1	95.2	96.4
	D_{max} (%)	113.7	115.1	113.7	113.9	115.3	113.2
CTV_Chest Wall	$D_{95\%}$ (%)	98.7	96.8	96.3	98.8	94.8	96.0
	D_{max} (%)	113.2	115.1	113.7	113.9	115.3	113.2
CTV_Axilla I L	$D_{95\%}$ (%)	100.9	97.0	98.8	100.7	97.7	98.3
CTV_Axilla II L	$D_{95\%}$ (%)	101.1	96.9	96.4	101.0	98.7	97.1
CTV_Axilla II L	$D_{95\%}$ (%)	101.4	98.5	99.8	101.2	101.1	100.8
CTV_SCLAV L	$D_{95\%}$ (%)	100.2	92.4	99.7	99.3	92.4	99.7
CTV_IMN	$D_{95\%}$ [Gy(RBE)]	50.2	44.9	46.9	49.8	49.9	48.2
Left Lung	$V_{20Gy(RBE)}$ (%)	19.8	15.3	16.1	19.4	16.8	16.0
Heart	D_{mean} [Gy(RBE)]	1.0	0.7	1.0	1.0	1.6	0.9
Esophagus	D_{max}[(Gy(RBE)]	33.8	31.2	32.9	38.2	37.9	35.9
Spinal Cord	D_{max} [Gy(RBE)]	7.1	5.6	7.7	5.9	6.2	5.6

average of 16.4%. The fractional dose sums were projected on either pCT or vCT to evaluate the cumulative dose impact due to the MP variability in position. However, the analysis of dose–volume histogram metrics relied on the patient anatomy on a single CT. The lowest $D_{95\%}$ of the CTV_Chest Wall was 94.8% with rigid dose sum on vCT, which was comparable with the average $D_{95\%}$ from the fractional dose distribution. The results of the delivered $V_{20Gy(RBE)}$ of the left lung are lower than the planned value because the displaced MP pulled back the proton range in the beam path unexpectedly. The heart D_{mean} of 1.6 Gy(RBE) was found in the cumulative dose with rigid plan sum on vCT. The vCT shows a lower tissue expander and an increased contact between the heart and chest wall. However, the deformed plan sum on pCT and vCT show heart D_{mean} equal or less than 1.0 Gy(RBE). A rigid plan sum projected on an unfavorable anatomy could overestimate the dosimetric impact.

A total of four gantry angles with five FSTs in two plans provided robust dose coverage of the CTV regardless of MP displacement. Dose coverage did not degrade significantly behind the unexpected MP position. The global D_{max} up to >120% found on the most reconstructed fractional doses behind the planned MP positions was averaged out in cumulative doses with two plans.

Conclusion

CBCT-based synCT can be used to reduce the frequency of verification CTs, especially for patients with breast cancer who will likely not experience significant toxicity-related weight loss or change in tumor size compared with other treatment sites. Dose reconstruction using synCTs associated with online image registration represents daily dose delivery on the most realistic patient setup. However, because of the physical limitation of the FOV of the CBCT, only the doses of targets and normal tissues inside the FOV can be evaluated. Robustness of proton plans using FSTs around the magnet in the MP of tissue expanders can be improved with multiple fields and plans, which provides forgiveness of dose heterogeneity incurred from dislocation of high-Z materials.

Author's note

Presented in part at American Association of Physicists in Medicine, Spring Clinical Meeting, March 26-29, 2022, New Orleans, LA.

Data availability statement

The original contributions presented in the study are included in the article/supplementary material. Further inquiries can be directed to the corresponding author.

Ethics statement

The studies involving human participants were reviewed and approved by Western Institutional Review Board, Inc. (NYPC ERC# 2020-026). Written informed consent was obtained from the participant/patient(s) for the publication of this case report.

Author contributions

Conceptualization, C-CC and JL; methodology, C-CC and JL; software, C-CC, PP, JL, SH and PT; patient treatment, SW; resources, AS and HL; writing—original draft preparation, C-CC; writing—review and editing, JC. C-CC and JL contributed equally to this manuscript. All authors have read and agreed to the published version of the manuscript.

Conflict of interest

The authors declare that the research was conducted in the absence of any commercial or financial relationships that could be construed as a potential conflict of interest.

Publisher's note

All claims expressed in this article are solely those of the authors and do not necessarily represent those of their affiliated organizations, or those of the publisher, the editors and the reviewers. Any product that may be evaluated in this article, or claim that may be made by its manufacturer, is not guaranteed or endorsed by the publisher.

References

1. Mutter RW, Choi JI, Jimenez RB, Kirova YM, Fagundes M, Haffty BG, et al. Proton therapy for breast cancer: a consensus statement from the particle therapy cooperative group breast cancer subcommittee. *Int J Radiat Oncol Biol Phys* (2021) 111 (2):337–59. doi: 10.1016/j.ijrobp.2021.05.110

2. Mutter RW, Remmes NB, Kahila MM, Hoeft KA, Pafundi DH, Zhang Y, et al. Initial clinical experience of postmastectomy intensity modulated proton therapy in patients with breast expanders with metallic ports. *Pract Radiat Oncol* (2017) 7(4): e243–52. doi: 10.1016/j.prro.2016.12.002

3. Kang Y, Shen J, Bues M, Hu Y, Liu W, Ding X. Technical note: clinical modeling and validation of breast tissue expander metallic ports in a commercial treatment planning system for proton therapy. *Med Phys* (2021) 48(11):7512–25. doi: 10.1002/mp.15225

4. Kirk M, Freedman G, Ostrander T, Dong L. Field-specific intensity-modulated proton therapy optimization technique for breast cancer patients with tissue expanders containing metal ports. *Cureus* (2017) 9(9):e1698. doi: 10.7759/cureus.1698

5. Zhu M, Langen K, Nichols EM, Lin Y, Flampouri S, Godette KD, et al. Intensity modulated proton therapy treatment planning for postmastectomy patients with metallic port tissue expanders. *Adv Radiat Oncol* (2022) 7(1):100825. doi: 10.1016/j.adro.2021.100825

6. DeCesaris CM, Mossahebi S, Jatczak J, Rao AD, Zhu M, Mishra MV, et al. Outcomes of and treatment planning considerations for a hybrid technique delivering proton pencil-beam scanning radiation to women with metal-containing tissue expanders undergoing post-mastectomy radiation. *Radiother Oncol* (2021) 164:289–98. doi: 10.1016/j.radonc.2021.07.012

7. Veiga C, McClelland J, Moinuddin S, Lourenço A, Ricketts K, Annkah J, et al. Toward adaptive radiotherapy for head and neck patients: feasibility study on using CT-to-CBCT deformable registration for "dose of the day" calculations. *Med Phys* (2014) 41(3):031703. doi: 10.1118/1.4864240

8. Veiga C, Janssens G, Teng CL, Baudier T, Hotoiu L, McClelland JR, et al. First clinical investigation of cone beam computed tomography and deformable registration for adaptive proton therapy for lung cancer. *Int J Radiat Oncol Biol Phys* (2016) 95 (1):549–59. doi: 10.1016/j.ijrobp.2016.01.055

9. MacDonald S, Choonsik L, Fagundes M, Feigenberg S, Ho A, Jimenez R, et al. *Breast contouring RADCOMP consortium v.3* (2016). Available at: https://www.nrgoncology.org/About-Us/Center-for-Innovation-in-Radiation-Oncology/Breast-Cancer/RADCOMP-Breast-Atlas (Accessed 23, 2021).

frontiers | Frontiers in Oncology

TYPE Original Research
PUBLISHED 18 August 2023
DOI 10.3389/fonc.2023.1145332

OPEN ACCESS

EDITED BY
Haibo Lin,
New York Proton Center, United States

REVIEWED BY
Ning Yue,
The State University of New Jersey, United States
Jiajian Shen,
Mayo Clinic Arizona, United States

*CORRESPONDENCE
Weijun Chen
chenweijun@hmc.edu.cn

RECEIVED 16 January 2023
ACCEPTED 31 July 2023
PUBLISHED 18 August 2023

CITATION
Li Y, Zhan W, Jia Y, Xiong H, Lin B, Li Q, Liu H, Qiu L, Zhang Y, Ding J, Fu C and Chen W (2023) Application of tangent-arc technology for deep inspiration breath-hold radiotherapy in left-sided breast cancer.
Front. Oncol. 13:1145332.
doi: 10.3389/fonc.2023.1145332

Application of tangent-arc technology for deep inspiration breath-hold radiotherapy in left-sided breast cancer

Yucheng Li[1], Wenming Zhan[1], Yongshi Jia[1], Hanchu Xiong[1], Baihua Lin[1], Qiang Li[1], Huaxin Liu[1], Lingyun Qiu[1], Yinghao Zhang[1], Jieni Ding[1], Chao Fu[2] and Weijun Chen[1]*

[1]Cancer Center, Department of Radiation Oncology, Zhejiang Provincial People's Hospital, Affiliated People's Hospital, Hangzhou Medical College, Hangzhou, Zhejiang, China, [2]Department of Tumor Radiochemotherapy, Second Affiliated Hospital of Wenzhou Medical University, Wenzhou, Zhejiang, China

Objective: To explore the advantages of dosimetry and the treatment efficiency of tangent-arc technology in deep inspiration breath-hold radiotherapy for breast cancer.

Methods: Forty patients with left-sided breast cancer who were treated in our hospital from May 2020 to June 2021 were randomly selected and divided into two groups. The first group's plan was a continuous semi-arc that started at 145° (± 5°) and stopped at 325° (± 5°). The other group's plan, defined as the tangent-arc plan, had two arcs: the first arc started at 145° (± 5°) and stopped at 85° (± 5°), and the second arc started at 25° (± 5°) and stopped at 325° (± 5°). We compared the target dose, dose in organs at risk (OARs), and treatment time between the two groups.

Results: The target dose was similar between the continuous semiarc and tangent-arc groups. The V_5 of the right lung was significantly different between the two groups (Dif 5.52, 95% confidence interval 1.92-9.13, t=3.10, P=0.004), with the patients in the continuous semi-arc and tangent-arc groups having lung V_5 values of (9.16 ± 1.62)%, and (3.64 ± 0.73)%, respectively. The maximum dose to the spinal cord was (1835.88 ± 222.17) cGy in the continuous semi-arc group and (599.42 ± 153.91) cGy in the tangent-arc group, yielding a significant difference between the two groups (Dif 1236.46, 95% confidence interval 689.32-1783.6, t=4.57, P<0.001). The treatment times was (311.70 ± 60.45) s for patients in the continuous semi-arc group and (254.66 ± 40.73) s for patients in the tangent-arc group, and there was a significant difference in the mean number of treatment times between the two groups (Dif 57.04, 95% confidence interval 24.05-90.03, t=3.5, P=0.001).

Conclusion: Both the continuous semi-arc and tangent-arc plans met the clinical prescription dose requirements. The OARs received less radiation with the tangent-arc plan than the continuous semi-arc plan, especially for the lung

(measured as V_5) and the spinal cord (measured as the maximum dose). Tangent-arc plan took significantly less time than the continuous semi-arc, which can greatly improve treatment efficiency. Therefore, tangent-arc plans are superior continuous semi-arc plans for all cases.

KEYWORDS

deep inspiration breath-hold, left breast cancer, dosimetry, organ of risk, continuous semi-arc, tangent-arc

Introduction

In women, breast cancer is the most common malignant tumor and has the highest mortality and morbidity among all malignant tumors worldwide (1–4). Recently, radiation therapy coupled with breast-conserving surgery has become the standard treatment for many patients with breast cancer (5, 6). For patients with breast cancer on the left side, the radiation dose to the heart should be taken into account during radiation therapy because the tumor is relatively close to the heart. Although no studies have demonstrated that the minimum exposure dose causes radiation-induced cardiac injury, increased cardiac doses are associated with increased rates of cardiac and coronary events. Furthermore, cardiac damage is correlated with the mean cardiac dose, with an increase of 4%-16% in the rate of acute coronary events per 1 Gy (7–11). To reduce the dose to organs at risk (OARs) as much as possible, some scholars have proposed new improvements in imaging techniques and treatment planning systems and have introduced new irradiation techniques, such as deep inspiration breath hold (DIBH) and respiratory gating (RG) (12–16). The main techniques used in breast cancer radiotherapy are three-dimensional conformal radiation therapy (3D-CRT), intensity modulated radiation therapy (IMRT), and volumetric modulated arc therapy (VMAT). Compared to 3D-CRT, both IMRT and VMAT can improve the target volume's conformity index (CI) and homogeneity index (HI) while reducing the dose to OARs (17–19). The difference between IMRT and VMAT is that, when treating patients, the IMRT gantry has a fixed angle during irradiation, whereas in VMAT, the gantry rotates while the beam is on. Therefore, VMAT technology can increase the CI of the target. In recent years, the application of VMAT combined with DIBH technology has further reduced the dose of OARs (20–22). The focus of medical physicists is the optimization of treatment efficiency and design of the X-ray angle in the radiotherapy plan such that the dose to the OARs can be reduced as much as possible while ensuring that the target volume receives a sufficient dose.

This study aims to explore a new tangent-arc irradiation technique based on DIBH. It is expected that this technique will allow patients with left-sided breast cancer to receive adequate doses of radiotherapy in the target region while further reducing the dose of OARs, especially the heart, lungs, and other organs that affect the quality of life of patients. It is also expected to reduce patients' DIBH time which can effectively improve the efficiency of treatment time while improving patient cooperation. Thus, a high-quality and efficient plan design scheme is provided for patients with left breast cancer using the DIBH technique.

Methods and materials

Patient selection

Forty patients with left-sided breast cancer who were treated in our hospital from May 2020 to June 2021 were randomly enrolled in this study and divided into two groups, one continuous semi-arc plan group and the other tangent-arc plan group. The continuous semi-arc plan had only one arc that rotated counterclockwise from 145° (± 5°) to 325° (± 5°). The tangent-arc plan had two arcs: the first arc rotated counterclockwise with a start angle of 145° (± 5°) and a stop angle of 85° (± 5°), and the second arc rotated counterclockwise from 25 (± 5)°to 325° (± 5°). The angles of the two plans are shown in Figure 1. Among them, the mean age of the 20 patients treated with continuous semi-arc technology was 47.1 (range 33-58) years, and the mean age of the 20 patients treated with tangent-arc technology was 45.7 (range 29-60) years. The inclusion criteria were left-sided breast cancer, no contraindications to radiotherapy, KPS> 70, age younger than 60 years old, ability to fully understand the process of DIBH, and ability to breath-hold for more than 30 s. All patients completed simulated positioning and surface-guided radiation therapy (SGRT) using Catalyst Systems v5.4.2 SP3 (C-RAD Positioning AB, Uppsala, Sweden) with DIBH to reduce localization uncertainty during treatment delivery. The exclusion criteria were a breath-holding time of fewer than 30 s, communication disorders, and other underlying diseases affecting radiotherapy.

CT simulation positioning, target contour, planning design

All patients were laid in a supine position with both arms fully abducted and externally rotated on a vacuum cushion on the all-in-one board. Treatment planning CT scans at 5-mm intervals from the ear to

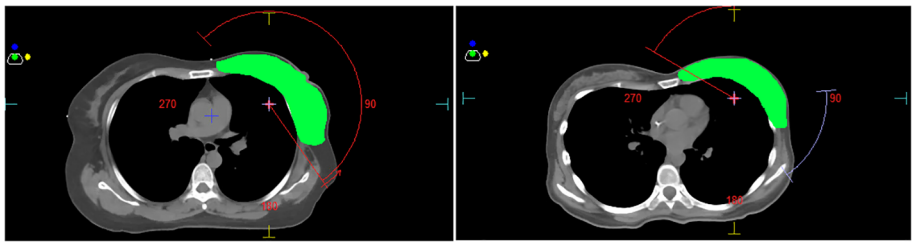

FIGURE 1
(The left is the continuous semi-arc, the right is the tangent-arc, and green represents PTV).

2 cm below the diaphragm were obtained for each patient with a CT simulator (Discovery CT590, GE, Wisconsin, USA). The target and OARs of this study were delineated following the Radiation Therapy Oncology Group (RTOG) and the International Commission Radiological Units (ICRU) (23, 24). The two groups of patients were treated with continuous semi-arc technology and tangent-arc technology. Both plans were generated using the MonacoV5.11 (Elekta AB, Stockholm, Sweden) three-dimensional treatment planning system by the same senior medical physicist. The "Dual Arc" function provided by the treatment planning system was used to generate clockwise and counterclockwise dual arcs for each plan. The doses were normalized such that the dose to 95% of the planning target volume (PTV) was the same for all plans.

Dose evaluation

All plans were compared and evaluated. The near maximum dose covering 2% of the PTV ($D_{2\%}$), near minimum dose covering 98% of the PTV ($D_{98\%}$), and mean dose (D_{mean}) to the PTV was determined. The volume of the left lung receiving dose greater than 5, 20, and 30 Gy (V_5, V_{20}, and V_{30}, respectively) and the D_{mean} of the left lung were considered as well as the V_5 and D_{mean} of the right lung, D_{mean} of the heart and left ventricle, maximum dose (D_{max}) of the spinal cord, beam-on time, CI and HI. The CI was calculated from the formula: $CI=(TV_{95}/TV)\times(TV_{95}/V_{95})$, where V_{95} is the target volume receiving 95% of the prescription dose, TV is the target volume, and V_{95} is the volume receiving 95% of the prescription dose. HI was calculated according to $HI=(D_{5\%})/(D_{95\%})$ where $D_{5\%}$ and $D_{95\%}$ represent doses received by 5% and 95% of PTV, respectively). The closer the CI and HI values are to 1, the better the quality of the plan. The treatment time of all patients was recorded by the catalyst software.

Statistical analysis

All patient data were statistically analyzed using SPSS software (version 20, SPSS Inc., Chicago, IL, USA). The independent sample t-test was used to analyze parameters with homogeneous variance and normal distribution; otherwise, the nonparametric Wilcoxon signed-rank test was used. Data with a normal distribution are expressed as x ± s and were analyzed with the independent sample t-test, while those with a nonnormal distribution are presented as M (Q1, Q3) and were analyzed with the Mann-Whitney U test. A value of $\boldsymbol{P}< 0.05$ was considered statistically significant.

Results

Details of the dosimetry, treatment time, and beam-on-time comparisons are presented in Tables 1 and 2. The dose constraints were defined for OARs as follows: left lung: $V_5<50\%$, $V_{20}< 26\%$, $V_{30}< 20\%$; right lung: $V_5<12\%$; heart: $D_{mean}<7$ Gy; left ventricle: $D_{mean}<7$ Gy; spinal cord: $D_{max}< 40$ Gy. The right lung V_5 of the patients in the continuous semi-arc group and the tangent-arc group were (9.16 ± 1.62)% and (3.64 ± 0.73)%, respectively, with a significant difference between the two groups (Dif 5.52, 95% confidence interval 1.92-9.13, t=3.10, P=0.004). The maximum dose in the spinal cord was (1835.88 ± 222.17) cGy in the continuous semi-arc group and (599.42 ± 153.91) cGy in the tangent-arc group, and there was a significant difference between the two groups (Dif 1236.46, 95% confidence interval 689.32-1783.6, t=4.57, P<0.001). The treatment time was (311.70 ± 60.45) s for patients in the continuous semi-arc group and (254.66 ± 40.73) s for patients in the tangent-arc group, with a significant difference between the two groups (Dif 57.04, 95% confidence interval 24.05-90.03, t=3.5, P=0.001).

Discussion

Recently, with developments in radiotherapy physics and computing technologies, VMAT has become one of the mainstream technologies of radiotherapy. In particular, VMAT combined with DIBH can greatly reduce the dose of OARs while ensuring a sufficient dose to the target (20–22). Currently, the 5-year survival rate for stage I breast cancer is >85% worldwide and the majority of breast cancer patients can be cured with a combination of chemotherapy and radiotherapy (25–27). However, to our knowledge, there is no evidence proving that the minimum dose does not cause radiation-induced heart and lung injuries. Therefore, to improve the patient's quality of life, medical physicists ensure that normal tissues are treated at as low a dose as possible while maintaining adequate target coverage. Comparing the time and dosimetry of two different VMAT techniques, This study showed that the tangent-arc technique was shown to reduce

TABLE 1 Comparison of parameters between continuous semi-arc and tangent-arc ($\bar{\chi} \pm s$).

parameters	continuous semi-arc	tangent-arc	Dif&95%confidence interval	*t*	*P*
$PTVD_{2\%}$(cGy)	5840.74 ± 470.47	5495.91 ± 704.10	344.84(-38.49-728.16)	1.82	0.076
$PTVD_{98\%}$(cGy)	4823.06 ± 185.46	4687.95 ± 336.43	135.11(-38.79-309.01)	1.57	0.124
CI	0.80 ± 0.06	0.81 ± 0.06	-0.01(0.05-0.02)	0.72	0.478
HI	1.18 ± 0.09	1.14 ± 0.08	0.04(-0.02-0.1)	1.42	0.163
L-Lung V_5(%)	44.67 ± 6.03	42.28 ± 5.61	2.38(-1.35-6.11)	1.29	0.204
L-Lung V_{20}(%)	20.25 ± 3.93	19.91 ± 3.89	0.09(-2.5-2.67)	0.273	0.786
L-Lung V_{30}(%)	13.81 ± 3.62	14.21 ± 3.69	-0.41(-2.75-1.93)	-0.35	0.726
R-Lung V_5(%)	9.16 ± 7.26	3.64 ± 3.28	5.52(1.92-9.13)	3.10	0.004
Heart D_{mean}(cGy)	377.66 ± 73.89	379.92 ± 108.27	-2.27(-61.6-57.07)	-0.08	0.939
Left-ventricle D_{mean}(cGy)	354.66 ± 89.61	389.31 ± 131.24	-34.64(-114.86-45.57)	-0.88	0.386
Spinal Cord D_{max}(cGy)	1835.88 ± 993.57	599.42 ± 688.32	1236.46(689.32-1783.6)	4.57	0.000
Treatment time(s)	311.70 ± 60.45	254.66 ± 40.73	57.04(24.05-90.03)	3.50	0.001

the dose to OARs and the treatment time compared to the continuous semi-arc plan.

The analysis showed that the maximum and minimum doses to the PTV increased by 5.9% and 2.8%, respectively, in the continuous semi-arc group compared with the tangent-arc group, but these increases were not statistically significant. The CI and HI of the two plans were also not significantly different. The reason for this lack of statistical difference may be that the dose of the target area was normalized to 95% for both the continuous semi-arc and tangent-arc plan designs.

Related studies have shown that V_5, $V_{20,}$ and V_{30} of the lung, especially V_{20}, play important roles in radiation-induced pulmonary injury and fibrosis. When lung V_{20}>20%, the probability of radiation pneumonitis is 28.4%, and when $V_{20} \leq$ 20%, the incidence of radiation pneumonitis is 12.5% (28–31). Here, the average V_{20} of the left lung of the continuous semi-arc plan was 20.25%, and that of the tangent-arc plan was 19.91%. Therefore, the tangent-arc plan may reduce the incidence of radiation pneumonitis. Additionally, the low-dose volume effect of the bilateral lung must be taken seriously in the clinical practice of breast cancer radiotherapy. Novakova-Jiresova et al. (32) conducted radiation-induced lung injury animal experiments, and showed that animals receiving low-dose and large-volume irradiation showed had greater lung function damage. John et al. (33) believed that larger lung volumes receiving low-dose irradiation would cause more severe radiation-induced lung damage. With the development of radiotherapy technology, the long-term survival rate of breast cancer has improved significantly. Some scholars have shown that low-dose radiation increases the risk and toxicity of secondary cancer (34, 35). Our results showed that the mean V_5 value of the left and right lungs was reduced by approximately 5.4% and 60.26%, respectively, in the tangent-arc group compared with the continuous semi-arc group. Therefore, the V_5 lung benefited from the use of tangent-arc (Table 1).

The results of this study showed that the mean cardiac doses of 377.66 cGy (continuous semi-arc group) and 379.92 cGy (tangent-arc group) in patients with breast cancer were lower than the 403 cGy value reported by Karpf et al. (36). The difference may result from the sample size and the volumes of the tumors. The author believe that this small difference would not affect the clinical benefit. Regarding the spinal cord, the maximum dose in the continuous semi-arc plan was approximately three times that of the tangent arc plan, possibly because the tangent-arc plan does not contribute any dosage to the spinal cord at 85°~25°, which is exactly the direction of vertical irradiation of the spinal cord, causing the spinal cord dose to drop significantly. Although the spinal cord doses of the two plans met the clinical dose requirement, the tangent-arc technique is more in line with the principle of being as low as reasonably achievable (37, 38).

The tangent-arc plan had shorter treatment time and X-ray beam-on time than the continuous semi-arc plan, and that the patient's breath-hold interval was an important factor in the efficiency of treatment in the delivery treatment process. During the CT simulation, the patient must hold breath longer than 30 s. Then, in the continuous semi-arc plan, the beam-on time is 82~130 s, during

TABLE 2 Comparison of the beam-on-time between continuous semi-arc and tangent-arc plans with different field angles.

plan	continuous semi-arc	tangent-arc		
degree	145°(± 5°)~325°(± 5°)	145°(± 5°)~85°(± 5°)	25°(± 5°)~325°(± 5°)	Total range time
Time(s)	82~130	41~57	38~60	81~110

which the patients can suffer from too little rest time which restricts their breathing, ultimately affecting the efficiency of treatment. However, in the tangent-arc plan, two small arcs are designed, with respective beam-on time of each arc is 41~57s and 38~60s, so the patient can complete each therapeutic arc in 1-2 breath-hold cycles. During the gantry rotation of the LINAC in between the two treatment fields, all patients were able to rest enough to maintain a stable breath-hold during the subsequent treatment field.

Conclusions

Both continuous semi-arc and tangent-arc plans met the clinical prescription dose requirements. After comparing the radiation dose to OARs and the treatment time of patients, we believe that when left-sided breast cancer patients are treated with VMAT radiotherapy combined with DIBH, tangent-arc plans can be more effective. Tangent-arc plans can reduce the radiation dose to the patient's OARs, such as the lung and spinal cord, and the treatment time can be faster. Therefore, the plan quality is superior for tangent-arc plans compared to continuous semi-arc plans for all cases. A limitation of this study is that there was no discussion of patient staging. The authors will further explore the advantages and disadvantages of using the two technical schemes in different stages.

Data availability statement

The raw data supporting the conclusions of this article will be made available by the authors, without undue reservation.

Ethics statement

The ethics institutional review board of Zhejiang Provincial People's Hospital (Hangzhou, China) approved this study (project approval number QT2023020) and waived informed consent for this retrospective study.

Author contributions

Manuscript drafting, editing, and statistical analysis: YL. Design, supervision, data interpretation, and critical review: WC. Patient surveillance and data acquisition:WZ, YJ, HX, CF, BL, and LQ. Literature search: QL, HL, and YZ, JD. All authors read and approved the final manuscript. All authors contributed to the article.

Funding

This research was partially supported by the National Natural Science Foundation of China (82102814), this research was supported by Zhejiang Provincial Natural Science Foundation of China under Grant No. GF21H180053, and the Medical and Health Research Project of Zhejiang Province (2021PY002).

Acknowledgments

Our thanks to AJE American Journal Experts for help with language editing.

Conflict of interest

The authors declare that the research was conducted in the absence of any commercial or financial relationships that could be construed as a potential conflict of interest.

Publisher's note

References

1. Ferlay J, Colombet M, Soerjomataram I, Parkin DM, Piñeros M, Znaor A, et al. Cancer statistics for the year 2020: an overview. *Int J Cancer* (2021).

2. Bray F, Ferlay J, Soerjomataram I, Siegel RL, Torre LA, Jemal A. Global cancer statistics 2018: GLOBOCAN estimates of incidence and mortality worldwide for 36 cancers in 185 countries. *CA Cancer J Clin* (2020) 68(6):394–424. doi: 10.3322/caac.21492

3. Hegde P, Pande J, Adly HH, Shetty P, Jayakumari A. Breast Cancer Risk factor awareness and utilization of screening program: A cross-sectional study among women in the Northern Emirates. *Gulf J Oncolog* (2018) 1(27):24–30.

4. Patra S, Young V, Llewellyn L, Senapati JN, Mathew J. BRAF, KRAS and PIK3CA mutation and sensitivity to trastuzumab in breast cancer cell line model. *Asian Pac J Cancer Prev* (2017) 18(8):2209–13. doi: 10.22034/APJCP.2017.18.8.2209

5. Hu S, Xie D, Zhou P, Liu X, Yin X, Huang B, et al. LINCS gene expression signature analysis revealed bosutinib as a radiosensitizer of breast cancer cells by targeting eIF4G1. *Int J Mol Med* (2021) 47(5):72.

6. Nunez A, Jones V, Schulz-Costello K, Schmolze D. Accuracy of gross intraoperative margin assessment for breast cancer: experience since the SSO-ASTRO margin consensus guidelines. *Sci Rep* (2020) 10(1):17344.

7. Darby S, McGale P, Taylor C, Peto R. Long-term mortality from heart disease and lung cancer after radiotherapy for early breast cancer. Prospective cohort study of about 300 000 women in US SEER cancer registries. *LancetOncol* (2005) 6(8):557–65.

8. Sardaro A, Petruzzelli MF, D'Errico MP, Grimaldi L, Pili G, Portaluri M. Radiation-induced cardiac damage in early left breast cancer patients. Risk factors, biological mechanisms, radiobiology, and dosimetric constraints. *Radiother Oncol* (2012) 103(2):133–42.

9. Darby SC, Ewertz M, McGale P, Bennet AM, Blom-Goldman U, Brønnum D, et al. Risk of ischemic heart disease in women after radiotherapy for breast cancer. *N Engl J Med* (2013) 368(11):987–98.

10. Van den Bogaard VAB, Ta BDP, van der Schaaf A, Bouma AB, Middag AM, Bantema-Joppe EJ, et al. Validation and modification of a prediction model for acute cardiac events in patients with breast cancer treated with radiotherapy based on three-dimensional dose distributions to cardiac substructures. *J Clin Oncol* (2017) 35:1171–8.

11. Taylor C, Correa C, Duane FK, Aznar MC, Anderson SJ, Bergh J, et al. Estimating the risks of breast cancer radiotherapy: evidence from modern radiation

doses to the lungs and heart and from previous randomized trials. *J Clin Oncol* (2017) 35:1641–9.

12. Waissi W, Amé JC, Mura C, Noël G, Burckel H. Gemcitabine-based chemoradiotherapy enhanced by a PARP inhibitor in pancreatic cancer cell lines. *Int J Mol Sci* (2021) 22(13):6825.

13. Bergom C, Currey A, Desai N, Tai A, Strauss JB. Deep inspiration breath hold: techniques and advantages for cardiac sparing during breast cancer irradiation. *Front Oncol* (2018) 8:87.

14. Reitz D, Carl G, Schönecker S, Pazos M, Freislederer P, Niyazi M, et al. Real-time intra-fraction motion management in breast cancer radiotherapy: analysis of 2028 treatment sessions. *Radiat Oncol* (2018) 13(1):128.

15. Falco M, Masojć B, Macała A, Łukowiak M, Woźniak P, Malicki J. Deep inspiration breath hold reduces the mean heart dose in left breast cancer radiotherapy. *Radiol Oncol* (2021) 55(2):212–20.

16. Pandeli C, Smyth LML, David S, See AW. Dose reduction to organs at risk with deep-inspiration breath-hold during right breast radiotherapy: a treatment planning study. *Radiat Oncol* (2019) 14(1):223.

17. Mansouri S, Naim A, Glaria L, Marsiglia H. Dosimetric evaluation of 3-D conformal and intensity-modulated radiotherapy for breast Cancer after conservative surgery. *Asian Pac J Cancer Prev* (2014) 15(11):4727–32.

18. Fong A, Bromley R, Beat M, Vien D, Dineley J, Morgan G. Dosimetric comparison of intensity modulated radiotherapy techniques and standard wedged tangents for whole breast radiotherapy. *J Med Imaging Radiat Oncol* (2009) 53(1):92–9.

19. Mo JC, Huang J, Gu WD, Gao M, Ning ZH, Mu JM, et al. A dosimetric comparison of double-arc volumetric arc therapy, step-shoot intensity-modulated radiotherapy and 3D-CRT for left-sided breast cancer radiotherapy after breast-conserving surgery. *Technol Health Care* (2017) 25(5):851–8. doi: 10.3233/THC-160746

20. Tang L, Ishikawa Y, Ito K, Yamamoto T, Umezawa R, Jingu K. Evaluation of DIBH and VMAT in hypofractionated radiotherapy for left-sided breast cancers after breast-conserving surgery: A planning study. *Technol Cancer Res Treat* (2021) 20:15330338211048706.

21. Corradini S, Ballhausen H, Weingandt H, Freislederer P, Schönecker S, Niyazi , et al. Left-sided breast cancer and risks of secondary lung cancer and ischemic heart disease: Effects of modern radiotherapy techniques. *Strahlenther Onkol* (2018) 194 (3):196–205.

22. Jensen CA, Roa AMA, Johansen M, Lund JÅ, Frengen J. Robustness ofVMATand3DCRTplanstowardsetuperrorsinradiationtherapyoflocallyadvancedleft-sidedbreastcancerwithDIBH. *Phys Med* (2020) 45:198–204. doi: 10.3322/caac.21492

23. Oncology N R G. Breast Cancer Atlases, Templates, & Tools,NRG Protocol Radiation Therapy Template (Whole Breast Photon and Proton Therapy).[Internet]. Philadelphia: NRG Oncology. Available at: https://www.nrgoncology.org/ciro-breast.

24. Prescribing I. recording, and reporting photon-beam intensity-modulated radiation therapy (IMRT)[J]. *ICRU Rep* (2010) 83(10):27–40.

25. Bijker N, Meijnen P, Peterse JL, Bogaerts J, Van Hoorebeeck I, Julien JP, et al. Breast-conserving treatment with or without radiotherapy in ductal carcinoma-in-situ: Ten-year results of European Organization for research and treatment of cancer randomized phase III trial 10853-a study by the EORTC breast cancer cooperative group and EORTC radiotherapy group. *J Clin Oncol* (2006) 24:3381–7.

26. Early Breast Cancer Trialists' Collaborative Group (EBCTCG), Darby S, McGale P, Correa C, Taylor C, Arriagada R, et al. Effect of radiotherapy after breast-conserving surgery on 10-year recurrence and 15-year breast cancer death: meta-analysis of individual patient data for 10,801 women in 17 randomized trials. *Lancet* (2011) 378:1707–16.

27. Salmon R, Garbey M, Moore LW, Bass BL. Interrogating a multifactorial model of breast conserving therapy with clinical data. *PloS One* (2015) 10:e0125006.

28. NSABP B-39. RTOG 0413: A Randomized Phase III Study of conventional whole breast irradiation versus partial breast irradiation for women with stage 0, I, or II breast cancer. *Clin Adv Hematol Oncol* (2006) 4(10):719–21.

29. Lind PA, Marks LB, Hardenbergh PH, Clough R, Fan M, Hollis D, et al. Technical factors associated with radiation pneumonitis after local +/- regional radiation therapy for breast cancer. *Int J Radiat Oncol Biol Phys* (2002) 52 (1):137–43.

30. Jain AK, Vallow LA, Gale AA, Buskirk SJ. Does three-dimensional external beam partial breast irradiation spare lung tissue compared with standard whole breast irradiation? *Int J Radiat Oncol Biol Phys* (2009) 75(1):82–8. doi: 10.1016/j.ijrobp.2008.10.041

31. Blom Goldman U, Wennberg B, Svane G, Bylund H, Lind P. Reduction of radiation pneumonitis by V20-constraints in breast cancer. *Radiat Oncol* (2010) 5:99.

32. Novakova-Jiresova A, van Luijk P, van Goor H, Kampinga HH, Coppes RP. Changes in expression of injury after irradiation of increasing volumes in rat lung. *Int J Radiat Oncol Biol Phys* (2007) 67(5):1510–8.

33. Schallenkamp JM, Miller RC, Brinkmann DH, Foote T, Garces YI. Incidence of radiation pneumonitis after thoracic irradiation: Dose-volume correlates. *Int J Radiat Oncol Biol Phys* (2007) 67(2):410–6.

34. Hall EJ. Intensity modulated radiation therapy, protons and the risk of second cancers. *Int J.Rad Oncol Biol Phys* (2006) 65(1):1–7.3.

35. Hall EJ, Wuu C-S. Radiation-induced second cancers : the impact of 3D-CRT and IMRT. *Int J.Rad Oncol Biol Phys* (2003) 56:83–8.

36. Karpf D, Sakka M, Metzger M, Grabenbauer GG. Left breast irradiation with tangential intensity modulated radiotherapy (t-IMRT) versus tangential volumetric modulated arc therapy (t-VMAT): trade-offs between secondary cancer induction risk and optimal target coverage. *Radiat Oncol* (2019) 14(1):156.

37. Fihn SD, Gardin JM, Abrams J, Berra K, Blankenship JC, Dallas AP, et al. American College of Cardiology Foundation/American Heart Association Task Force. 2012 ACCF/AHA/ACP/AATS/PCNA/SCAI/STS guideline for the diagnosis and management of patients with stable ischemic heart disease: a report of the American College of Cardiology Foundation/American Heart Association task force on practice guidelines, and the American College of Physicians, American Association for Thoracic Surgery, Preventive Cardiovascular Nurses Association, Society for Cardiovascular Angiography and Interventions, and Society of Thoracic Surgeons. *Circulation* (2012) 126(25):e354–471.

38. Wolk MJ, Bailey SR, Doherty JU, Douglas PS, Hendel RC, Kramer CM, et al. American College of Cardiology Foundation Appropriate Use Criteria Task Force. ACCF/AHA/ASE/ASNC/HFSA/HRS/SCAI/SCCT/SCMR/STS 2013 multimodality appropriate use criteria for the detection and risk assessment of stable ischemic heart disease: a report of the American College of Cardiology Foundation Appropriate Use Criteria Task Force, American Heart Association, American Society of Echocardiography, American Society of Nuclear Cardiology, Heart Failure Society of America, Heart Rhythm Society, Society for Cardiovascular Angiography and Interventions, Society of Cardiovascular Computed Tomography, Society for Cardiovascular Magnetic Resonance, and Society of Thoracic Surgeons. *J Am Coll Cardiol* (2014) 63(4):380–406.

Frontiers in Oncology

Advances knowledge of carcinogenesis and tumor progression for better treatment and management

The third most-cited oncology journal, which highlights research in carcinogenesis and tumor progression, bridging the gap between basic research and applications to imrpove diagnosis, therapeutics and management strategies.

Discover the latest Research Topics

See more →

Frontiers

Avenue du Tribunal-Fédéral 34
1005 Lausanne, Switzerland
frontiersin.org

Contact us

+41 (0)21 510 17 00
frontiersin.org/about/contact